Characterisation of *Foxp1* in striatal development and the adult brain

This dissertation is submitted for the degree of Doctor of Philosophy at Cardiff University

Amy Elizabeth Evans

Supervisors:

Professor Anne E. Rosser

Dr Michael V. Taylor

September 2013

Submission of thesis declaration and statements

DECLARATION

This work has not been submitted in substance for any other degree or award at this or any other university or place of learning, nor is being submitted concurrently in candidature for any degree or other award.

Signed ………………………………………… (candidate)   Date …………………………

STATEMENT 1

This thesis is being submitted in partial fulfilment of the requirements for the degree of …………………………(insert MCh, MD, MPhil, PhD etc, as appropriate)

Signed ………………………………………… (candidate)   Date …………………………

STATEMENT 2

This thesis is the result of my own independent work/investigation, except where otherwise stated. Other sources are acknowledged by explicit references. The views expressed are my own.

Signed ………………………………………… (candidate)   Date …………………………

STATEMENT 3

I hereby give consent for my thesis, if accepted, to be available for photocopying and for inter-library loan, and for the title and summary to be made available to outside organisations.

Signed ………………………………………… (candidate)   Date …………………………

STATEMENT 4: PREVIOUSLY APPROVED BAR ON ACCESS

I hereby give consent for my thesis, if accepted, to be available for photocopying and for inter-library loans after expiry of a bar on access previously approved by the Academic Standards & Quality Committee.

Signed ………………………………………… (candidate)   Date …………………………

Summary

The aim of the research presented in this Thesis was twofold; firstly to further understand the role of *Foxp1* in the development of striatal medium spiny neurons (MSN) and secondly its role the adult brain. Understanding the role of *Foxp1* in MSN development may allow more accurate *in vitro* protocols to be generated for use in directing renewable cell sources for use in cell replacement therapies for diseases such as Huntington's disease (HD). Additionally, its functional role in MSN development may not be exclusive, and thus have a more generalised role transferable to other neuronal processes. Thus what is learnt about its function can possibly be applied to cell transplantation protocols in general, as well as be useful in the drug discovery field.

In mice, the transcription factors (TF) *Foxp1* and *Mef2c* were shown to be significantly up-regulated during peak MNS development (embryonic day (E) E12-16) in a genetic screen carried out in the host lab in 2004. Consequently the majority of work in this thesis was focused on the characterisation of the most significantly up-regulated gene, *Foxp1*. Experiments initially focused on a *Foxp1* knock out (KO) line, both *in vitro* and following transplantation into the quinolinic acid (QA) lesioned adult mouse brain. Additionally, owing to embryonic lethality at E14, a conditional *Foxp1* KO (CKO) line was also developed to study the effects of the loss of *Foxp1* in the adult brain with a focus on the loss of *Foxp1* from the cortex. Owing to lethality at E9 a *Mef2c* CKO line was also developed and initial *in vitro* findings from this line are presented in Appendix 8 of this Thesis.

Chapter 3 characterised the wild type (WT) expression pattern of FOXP1 from E10 to P7 through the co-localisation of FOXP1 with the established MSN markers CTIP2 and DARPP-32. *In vitro* characterisation of cultures generated from striate of $Foxp1^{-/-}$ mice showed a decrease in the number of CTIP2 and DARPP-32 positive cells compared to littermate controls but that there were no differences in the proliferation of these cells between groups. Finally, results from immunohistochemistry on selected striatal KO brain sections suggested that *Foxp1* may function downstream of *Ascl1* and *Gsh2* in striatal development.

In **Chapter 4** E14 or E12 striatal tissue from all three genotypes was grafted into an adult QA-lesion mouse model. Such experiments allowed striatal neurons from *Foxp1*$^{-/-}$ mice to survive for much longer periods than was possible *in vitro* and provided them with the opportunity to make some of their normal connections. Results showed that there were fewer DARPP-32 positive cells in grafts from *Foxp1*$^{-/-}$ compared to controls, as with in Chapter 3. Moreover, FOXP1 was identified as a novel maker of P-zones in grafts derived from whole ganglionic eminence.

Chapter 5 addressed the generation of a *Foxp1* CKO mouse model under the control of an hGFAP-Cre line (*Foxp1* CKO). Histology showed that FOXP1 was lost from all layers of the cortex, but expression was maintained in the striatum. Mice appeared hyperactive in the home cage compared to littermate controls, and as mutations in FOXP1 have been associated with autism spectrum disorders, of which ADHD falls under, led to directed behavioural analysis targeting the symptoms of ADHD. Analysis revealed *Foxp1* CKO mice were significantly hyperactive (activity boxe and open-field data) and inattentive (5 choice serial reaction time task) but had no anxiety problems (elevated plus maze and marble burying task). These symptoms were shown to be reduced following the administration of atomoxetine, a drug prescirbed to patients with ADHD. Results collectively suggested that the *Foxp1* CKO line is a new mouse model of ADHD.

Acknowledgements

"When life gives you lemons make lemonade" (Elbert Hubbard, 1915).

I heard this at a conference and I think it reflects the work outlined in this thesis well!

Firstly a big thank you to my supervisors, Anne Rosser and Michael Taylor. Thanks for all your supervision over the last 4 years. Anne, I don't know how you manage to fit in being a wife, mum, researcher, clinician and P.I on a daily basis, you are a real life superwoman, and all that you have accomplished is an inspiration to me!

Thanks to the AER group past and present: Anne, Rike, Claire, Sophie, Susannah, Ngoc-Nga, Nan and Vicky, for all your advice, help and importantly laughs and cake! I have thoroughly enjoyed Friday AER meetings. Claire and Soph, you are both great scientists and now both beautiful mothers! Thank you both for all your support and encouragement over the years. Ngoc-Nga, I am so grateful for all your help and advice, I would not have completed this thesis without your molecular and dissection expertise, and secondly, for opening my eyes to the world of expensive handbags and shoes; Sam will never forgive you!

Thanks to my past officemates, Gaynor, Zubeyde and Andreas. Gayn and Zubs it was a pleasure sharing an office with two brilliant scientists. Andreas thanks for always listening and for the continuous encouragement- ich danke Ihnen sehr für Ihre Hilfe! And to my current officemates; Nan, Harri, Emma and Vicky. It is a pleasure sharing an office with so many fun people, thanks for your support and for the continuous laughs, sweets and above all for your patience for when I "lose" things! I do apologise for rendering the white board useless! Nan, you are one of the most generous and smiley people I have met,good luck with finishing! Em, keep up the enthusiasm for the rest of your PhD and I have no doubts you'll do brilliantly! Harold thanks so much for your continued help with all things behaviour, Excel and general precision, and for having to put up with an office full of excitable, loud ladies! Good luck with the rest of your PhD!

Victoria (Vic, Vicky, Toria, VicoiR) what can I say? You are one of the cleverest and hard working people I know. I would not have got here without your continued help in the lab, or our shopping, pub and dinner jaunts, and not forgetting conference trips! Thank you for your help with everything, it has been a pleasure working with and getting to know you! Good luck with finishing- you're nearly there!

Thanks to my two undergraduate students James and Aimee, for all their hard work and to Becca for all your help -good luck with your thoroughly deserved PhD!

Anne-Marie thanks for our laughs running, I will not forget "evil road" or "evil pig!"

A big thank you to the rest of the BRG; Steve, Simon, Mariah, Jane, Claris, Marija, Damla, Kate, Yat, Lu, Jess and Ed.

This thesis would not be possible without my friends and family. Mam and dad you have always encouraged me and I am very grateful to you both for your continued support and love (and food!) throughout my PhD, and in everything I have done. Thanks also to Granny Ad and little bro Dave and recently Lisa, I am finally done to come visit the calves and lambs! Also a big thanks to the Reddingtons *et al* for their encouragement over the past 7 years, it has been a pleasure joining such a welcoming and loving family.

And finally Sam, my wonderful fiancé, thank you so much for everything and above all your patience! Without your calming influence, trust me when I say I would not have made it this far without you! A massive well done on becoming a Dr (even though you beat me!), I am very proud of everything you have achieved -we can finally get back to normality and I cannot wait until May 17th 2014!

Abbreviations List

5-CSRTT	5 choice serial reaction time task
AchE	Acetylcholinesterase
ADHD	Attention Deficit Hyperactivity Disorder
AMPA	Amino-3-hydroxy-5 methylisoxazole-4-propionic acid hydrate
ANOVA	Analysis of Variance
AP	Anterior-Posterior
ASDs	Autism Spectrum Disorders
BDNF	Brain Derived Neurotrophic Factor
bHLH	Basic helix-loop-helix
BMP	Brain Morphogenic protein
BP	Base Pair
BrdU	Bromodeoxyuridine
BSA	Bovine Serum Albumin
CAG	Glutamate
CKO	Conditional knock out
CNS	Central nervous system
CTIP2	COUP TF1-interacting protein 2
DA	Dopamine
DAB	Diaminobenzidine
DARPP-32	Dopamine and cyclic AMP-regulated phosphoprotein
DBD	DNA binding domain
DIV	Days *in vitro*
DMEM	Dulbecco's modified eagle's medium
DNA	Deoxyribonucleic acid
Dsh	Dishevelled
E	Embryonic Day
EPM	Elevated Plus Maze
ESC	Embryonic stem cells
FCS	Foetal calf serum
FOXP1	Forkhead Transcription Factor 1

FGF	Fibroblast growth factor
GABA	γ-Aminobutyric acid
GSK-3β	Glycogen synthase kinase 3β
GPi/e	Globus pallidus (internal/external)
HD	Huntington's disease
HDACs	Histone Deacetylases
hGFAP	human Glial Fibrillary Acid Protein
Htt	Huntingtin gene
HTT	Huntingtin Protein
ICM	Inner cell mass
IM	Intra-muscular
IP	Intra-peritoneal
iPSC	Induced pluripotent stem cells
ITI	Inter Trial Interval
Kainate	Kainic acid monohydrate
KO	Knock out experiment
L	Lateral
LGE	Lateral Ganglionic Eminence
MBT	Marble burying task
MEF2C	Myocyte Enhancer Factor 2C
MGE	Medial Ganglionic Eminence
MOR1	μ-opioid receptor 1
MSNs	Medium Spiny Neurons
MZ	Mantle Zone
NeuN	Neuronal nuceli
NLS	Nuclear localisation signal
NMDA	N-Methyl-D-aspartic acid
O/N	Overnight
P	Post-natal day
P19 cells	embryonic carcinoma cell line as a model system
PBS	Phosphate saline buffer
PCR	Polymerase Chain Reaction
PFA	Paraformaldehyde
PLL	Poly-L-Lysine

QA	Quinolinic acid
QPCR	Semi-quantitative RT-PCR
RA	Retinoic Acid
RALDH	Retinaldehyde dehydrogenase 2
RAR	Retanoic Acid Receptor
RNA	Ribonucleic Acid
RNAi	RNA interference
RT	Room Temperature
RT-PCR	Reverse transcription PCR
RXR	Retinoic X receptor
SHH	Sonic Hedgehog
ShRNA	Short hairpin RNA
SNc/r	Substantia Nigra (pars compacta/pars reticulate)
SNP	Short Nucleotide Repeat
STN	Sub Thalamic Nucleus
SVZ	Sub-Ventricular Zone
TBS	Tris Buffered Saline
TBST/TxTBS	Triton X-100 TBS
TF	Transcription Factor
TG	Transgenic
TNS	Tris Non Saline
VZ	Ventricualr Zone
WGE	Whole Ganglionic Eminence
Wnt	Wingless
WT	Wild Type

<u>Disclaimer</u>

Miss Ngoc Nga Vinh assisted with striatal dissections in Chapters 3 and 4.

Calcium imaging studies in Chapter 3 were largely undertaken by Dr Alex Harrison.

Aimee Leadbetter, an undergraduate project student, conducted the stereology outlined in Chapter 5.

Original publications achieved during course of PhD

Evans AE, Precious SV, Kelly CM and Rosser AE. Molecular Regulation of Striatal Development: A Review Anatomy Research International Volume 2012 (2012), Article ID 106529

Roberton, V. H., **Evans, A. E.,** Harrison, D. J., Precious, S. V., Dunnett, S. B., Kelly, C. M. and Rosser, A. E. (2013). Is the adult mouse striatum a hostile host for neural transplant survival? *Neuroreport* **24:**1010-1015.

Previous SV, Kelly, CM, Vinh, NN, **Evans AE** , Pekarik, V., Scherf, C, Jeyasingham, R, Glasbey J, Holeiter M, Jones L, Taylor MV, Rosser AE[¶] *Foxp1* in MSN differentiation *Submitted to BRAIN September 2013*

Deletion of murine cortical *Foxp1* induces a behavioural phenotype resembling ADHD. **Amy E Evans**, David J Harrison, Rebeccca Openshaw ,Victoria H Roberton, Aimee E Leadbetter, Stephen B Dunnett, Simon P Brooks and Anne E Rosser.
(Currently in preparation)

Grants awarded during the course of PhD

Charles Cole Scholarship - Work in Professor Josep Canals Lab at the University of Barcelona

MRC Centenary Award- Microarray analysis on the *Foxp1*$^{-/-}$ mouse line at E14

Wellcome Trust Seedcorn Award - Microarray analysis on *Foxp1* CKO mouse model

Contents

1 <u>*Introduction*</u>

Foxp1 is a transcription factor (TF) that is implicated in many aspects of development and primarily functions as a transcriptional repressor. As of yet the function of Foxp1 in the brain is unknown, however mutations in the human FOXP1gene have been linked to some cases of autism spectrum disorder (ASD), a disease which is thought to primarily affect the cortex. It has been extensively shown that Foxp1 is expressed in the developing and adult striatum where it co-localises with markers of medium spiny neurons (MSNs), the main projection neurons of the striatum. Foxp1 is also expressed in the cortex, preferentially being associated with projection neurons located in layers 111-V1. Therefore it is anticipated that Foxp1 has an important role in neuronal development.

Huntington's disease (HD) is an autosomal, dominantly inherited disorder leading to the loss of MSNs in the striatum, as well as neuronal loss in the cortex. There is no known cure for HD but the specificity of cell loss seen in the disease makes cell transplantation an attractive therapeutic option. The use of human foetal striatal cells has shown 'proof of principle' in clinical trials; however, the practical and ethical difficulties associated with this approach demand the need for an alternative donor cell source. The requirement of an alternative cell source is that it has the means to generate the mature phenotype of the cells lost in the disease and therefore needs to be "directed" along a specific lineage. Understanding the genetics of the MSN differentiation pathway is therefore crucial for the generation of accurate protocols and thus understanding more about Foxp1 will b be important for such protocols. Moreover, DARPP-32 is the most commonly used marker of MSNs but its expression is restricted to terminally differentiated MSNs; thus differentiation protocols would be greatly improved by having a battery of MSN markers that can be used throughout the protocol, of which Foxp1 would be an obvious candidate as is known to be expressed in the developing striatum in mice from E12. Additionally understanding more about Foxp1 in the adult brain will be useful in understanding more about disorders it is known to be associated with such as ASDs and other similar diseases that fall under this umbrella terminology.

This thesis attempts to further characterise the expression of Foxp1, with the addition of understanding its functional role in both the developing mouse striatum and adult mouse cortex, through in vitro and in vivo approaches, mainly through the use knocking out Foxp1 in mice.

1.1 <u>**Foxp1**</u>

1.1.1 <u>**Why Forkhead Box Protein 1 (Foxp1)?**</u>

MSNs are the main output projection neurons of the striatum and constitute approximately 95% of all of the striatal neurons in the rodent (Gerfen 1992). The remaining 5% of neurons are aspiny interneurons (Freeman *et al.* 1995). In addition to the characteristic morphology such as size and spine density, MSNs express the dopamine and cyclic adenosine 3', 5'-monophosphate-regualted phosphoprotein, 32kDa (DARPP-32). Understanding how and when MSNs are born was a specific interest to the host lab, and to enhance what was already known from the literature, an affymetrix screen (*Affymetrix technology, MAS5.0*) was carried out in 2004 to look at gene expression changes during the development of the mouse striatum.

Specifically, the screen used whole ganglionic eminence (WGE) tissue (the region in which the striatum arises from) to compare differential gene expression changes between embryonic day (E) 12- E16 and between E14-E16, ages coincident with striatal neurogenesis. The WGE was dissected according to Dunnett et al (Dunnett 1996) and dissections were carried out at the same time of day to minimize variation and were validated using reverse transcription polymerase chain reactions (RT-PCRs) to ensure no cortical tissue had been included in the dissections and thus analysis. RNA was extracted from three replicates for use in the array and the fold changes between E12 and E16 and between E14 and E16 were looked at. Results were analysed and 175 genes were significantly up regulated (p<0.05) between E12 and E16.

The results of the gene array analysis appeared in line with existing literature and public databases (e.g. Allen Brain Bank) on striatal development, with up-regulation of known striatal-associated developmental genes, such as *Ctip2* (*Bcl11b*), *Drd2*, *Ebf1* and *Foxp2* as well as those associated with general neuronal functions such as neuroblast migration and neurite outgrowth. As expected multiple genes associated with pluripotency and cell proliferation were down regulated and were not chosen for further study.

More stringent statistical analysis revealed that the transcription factor *Foxp1* was the most significantly up-regulated gene between E12-E16 and between E14-E16

(p<0.0001). This result was confirmed through *in situ* hybridisation and qPCR and was shown to be consistent with published data that shows that *Foxp1* is expressed in the developing and adult striatum (Ferland *et al.* 2003; Tamura *et al.* 2003) where it co-localises with DARPP-32 positive projection neurons in the striatum (Tamura *et al.* 2004). These results are presented in a paper that is currently being submitted (Precious et al., 2013). From these findings *Foxp1* was selected for further study with an initial focus on its functional role in striatal development.

It is evident that *Foxp1* is involved in many developmental processes and therefore its functional role is likely not restricted to MSN development. As mutations in the human Foxp1 gene have been linked with autism spectrum disorders (ASDs) (Hamdan *et al.* 2010; Horn *et al.* 2010; Palumbo *et al.* 2013), a disease thought to preferentially the cortex, the role of *Foxp1* in the adult mouse cortex will also be looked at. Another gene, *Mef2c*, was also significantly up regulated between E12-16 (p<0.05) and was also considered for further study and preliminary data is shown in Appendix 8.

1.2 **The Foxp family**

1.2.1 **Background, Structure and Function**

The Forkhead (Fox) family of transcription factors are a large family of proteins that can commonly be identified by a winged helix/forkhead DNA-binding domain. The *forkhead* gene, the founder member of the group was first identified in drosophila (Kaufmann and Knochel 1996) and several *Fox* genes have since been identified of which examples include *Foxa1*, *Foxa2, Foxf1* and *Foxj1* (Shu *et al.* 2001). *Foxp1* (first cloned from the BCL1 leukaemia cell line), and *Foxp2* are two distinct members of the Fox family and were discovered for their interacting roles in proximal epithelial cell differentiation in mouse lung development where they were shown to restrict expression of CC10 via binding to its promoter (Shu *et al.* 2001). On-going research has further shown that these genes are crucial regulators of lung airway morphogenesis and differentiation through direct repression of *T1alpha*, specifically by binding Foxp consensus sites (common region TTATTTRT) in its promoter region. Moreover, *Foxp1* and *Foxp4* similarly associate to control epithelial cell fate in lung development through

regulation of *Arg2* (Li *et al.* 2012). *Foxp1* and *2* also interact in oesophageal muscle development (Shu *et al.* 2007).

It was initially thought that there were three possible Foxp1 isoforms in the mouse (Shu *et al.* 2001), but subsequent analysis has shown there to be four (Wang *et al.* 2003), whereas there have been at least nine alternatively spliced transcripts identified for the human Foxp1 gene (Banham *et al.* 2001; Brown *et al.* 2008a; Brown *et al.* 2008b), with more likely as cloning has not yet been exhausted.

The longest and original isoform in mice FOXP1A (705 aa protein, ~75kDa), in addition to the forkhead domain contains in the N-terminus of the protein a glutamine (Q) rich region and a zinc (Zn) finger and leucine zipper motif (allows Foxp1 homodimerization) (Shu *et al.* 2001; Wang *et al.* 2003) (A schematic of this isoform is shown in Figure 1.1). These features are also found on the human FOXP1 gene (Wang *et al.* 2003). Importantly all isoforms retain the Zn finger and leucine zipper motifs and experiments using the GAL4 heterologous DNA binding domain fusion protein system exposed these domains as being responsible for the repressive function of FOXP proteins (Shu *et al.* 2001). Interestingly further experiments have shown that FOXP1 isoforms that lack the polyQ regions (FOXP1C and D) have a higher repressive activity (monitored by luciferase activity) than those isoforms with, thus suggesting this region is a modulator of repressive activity by the Foxp1 family in mice (Wang *et al.* 2003). Further deletion analyses have also shown that the forkhead DNA binding region is also capable of repressing *c-fms* in macrophage development, offering a further level of repression by this protein family (Shi *et al.* 2004). In order to bind DNA the Foxp family require homo/heterodimeriztion thus the repressive activity of Foxp1 will be a direct result of which of the specific isoforms bind (Li *et al.* 2004).
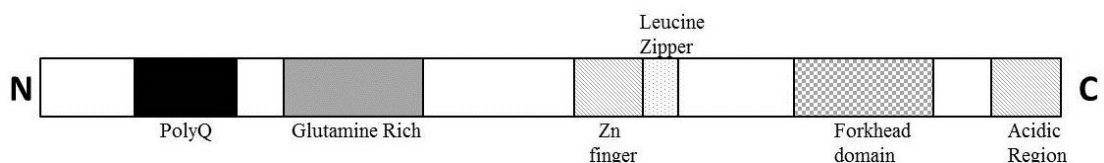

Figure 1.1- Protein structure of FOXP1A, the longest FOXP1 isoform in mice, which is 705 amino acids (aa) in total. It contains polygluatamine rich domains, a Zinc finger and leucine zipper motifs that facilliate homo/heterodimerization in its N terminal and a winged helix/forkhead domain in the C-terminus.

1.2.2 **Foxp1- Interactions, Function and Expression in Cancer**

Concurrently to the finding that *Foxp1* had a role in lung development another group showed that at a protein level it also contained motifs capable of binding CDK2 (Banham *et al.* 2001), a gene implicated in cell cycle regulation, and that FOXP1 directly represses interleukin 2 (IL2) and SV40 (Wang *et al.* 2003) by directly binding to specific consensus sequences in their promoters. Subsequent to this the first physiological gene target for *Foxp1* was identified through retroviral overexpression in HL60 cells. As mentioned *c-fms* was directly repressed by Foxp1 (expression regulated by *Mac-1*) leading to aberrant macrophage adhesion and phagocytosis (Shi *et al.* 2004). This research also suggested that the NF-Kβ pathway might offer a level of regulation on the *Foxp1* gene as the repressive activity of *Foxp1* was reduced when this pathway was blocked (Shi *et al.* 2004).

To first understand the functional role of *Foxp1*, Philip Tucker and colleagues created a *Foxp1* null mouse (*Foxp1$^{-/-}$*), which revealed that the loss of *Foxp1* caused embryonic lethality at E14.5, thus restricting analysis to this age. This group showed that *Foxp1* was needed to ensure the correct development of aspects of the cardiac system including outflow tract development and septation, cardiac cushion development, and myocardial maturation and differentiation (Wang *et al.* 2004a). Advanced research has further showed that *Foxp1* interacts with *Smrt*, and that both are needed for correct myocardial development as the deletion of either causes the same phenotype (Jepsen *et al.* 2008). Further knock out (KO) studies have also shown that *Foxp1* promotes early cardiomyocyte proliferation in a non-direct way through regulating the expression of *Fgf16* and *Fgf20* in the endocardium via inhibition of *Sox17,* but at a later time point restricts proliferation by directly repressing *Nkx2.5* (Zhang *et al.* 2010)*,* therefore emphasising the importance of temporal and spatial expression of gene function. It is not yet known if *Smrt* interacts with *Foxp1* to repress *Nk2.5* expression, further research is needed to investigate this link.

As a TF, *Foxp1* is normally localised to the nucleus, however cytoplasmic mis-localization is commonly characteristic of malignant tissues, for example in types of endometrium cancers (Banham *et al.* 2001; Giatromanolaki *et al.* 2006). In humans the *Foxp1* gene is located on chromosome 3p14.1 (in mice chromosome 6), a region that

commonly shows mutations in a wide range of tumours, and thus *Foxp1* is also closely associated with cancer. For example, *Foxp1* is reduced in colon tumour samples but alternatively is increased in stomach tumour samples (Banham *et al.* 2001).

Extensive research has been carried out, and is ongoing to study the role of *Foxp1* in B-cell development and associated cancers. Specifically *Foxp1* is expressed in normal activated B-cells, and its overexpression has been associated with B-cell like prognosis subtype of diffuse large B-cell lymphomas (DLBCL) (Banham *et al.* 2001; Banham *et al.* 2005). Genetic alterations, including chromosomal breakpoints and translocations affecting the *FOXP1* gene have also been linked to specific cases of B-cell related lymphomas as well as mucosa-associated lymphoid tissue (MALT) lymphomas (Haralambieva *et al.* 2006; Sagaert *et al.* 2006; Streubel *et al.* 2005; Wlodarska *et al.* 2005). Specifically, analysis from biopsies of patients with a subtype of *de novo* DLBCL showed those with an increased number of FOXP1 positive cells had a decrease in overall survival (Banham *et al.* 2005), advocating the presence of Foxp1 was linked with the cancer, and was not, as first supposed a tumour suppressor gene (Banham et al. 2001). Advanced research has since suggested that smaller FOXP1 isoforms (N-truncated versions) may be the prominent isoform in lymphomas and thus oncogenic, whereas the longer isoform may still act as a tumor suppressor (Brown *et al.* 2008a; Goatly *et al.* 2008), but further work is needed to refute or confirm this.

FOXP1 has also been linked to breast cancer where expression correlated with both the alpha and beta oestrogen receptors (ERα/β) in the familiar subtype, notably with nuclear ERβ. Subsequently it has been thought that in familiar breast cancers FOXP1 expression is associated with improved survival i.e. it does function as a tumour suppressor gene, therefore opening up Foxp1 as a possible therapeutic treatment option (Fox *et al.* 2004; Rayoo *et al.* 2009). Nevertheless, further work needs to be carried out to look the role of FOXP1 in sporadic breast cancer.

Foxp1 and B-cell development

To further understand the functional roles of *Foxp1* additional transgenic (TG) mouse models have been created. A similar *Foxp1*$^{-/-}$ model to Philip Tucker's was developed (also lethal at E14) to look more closely at the role of *Foxp1* in B-cell development given its prominence in lymphomas. Specifically liver cells from either E14 *Foxp1*$^{-/+}$ or

Foxp1$^{-/-}$ mice were removed and injected intravenously (i.v) into a *RAG2$^{-/-}$* mouse and analyzed in the thymus, lymph nodes, spleen and bone marrow 8 weeks post transplantation. Cells from the *Foxp1$^{-/-}$* mouse had less mature B-cells in the lymph nodes and spleens than those from *Foxp1$^{-/+}$* mice, and RT-PCR also showed that there was a decrease in B-cell lineage genes, notably *Tcfe2a* and *Ebf1*. Further analysis showed that *Foxp1* was needed to ensure the correct proB-pre-B-cell transition in the bone marrow through binding of the *Erag* enhancer, thereby regulating *Rag1/2* and subsequent V(D)J recombination (Hu et al., 2006). Additionally a *Foxp1* conditional knock out (CKO) model has been created by Feng et al (2010) to look at the role of *Foxp1* in T-cell development. This model concluded that *Foxp1* is an essential transcriptional regulator for thymocyte development and the generation of quiescent naïve t cells (Feng *et al.* 2010).

Owing to its functional role in B-cell development the role of *Foxp1* in mature B-cells was also investigated by the creation of another transgenic (Tg) mouse that expresses human *Foxp1* in lymphoid cells (Sagardoy *et al.* 2013). Activated B-cells can either become antibody-secreting plasma cells or migrate inside lymphoid follicles and become germinal centers (GCs); the genetics that control such decisions are not fully known. Results showed that unlike *Bcl6*, which is needed to ensure the correct formation of GC cells, aberrant expression of *Foxp1* impaired this formation, which the authors suggest could contribute to B-cell lymphomagenesis (Sagardoy *et al.* 2013). It has also been shown that overexpression of human FOXP1 protein impaired monocyte-macrophage maturation in the spleen and reduced selected macrophage functions (Shi *et al.* 2008). Taken together this research shows that the right levels and spatial expression of *Foxp1* during development are crucial.

Foxp1 and the CNS

In addition to their co-operative roles in lung development *Foxp1* and *Foxp2* show overlapping cortico-striatal expression patterns in songbirds, of which a similar expression pattern has been observed in the associated areas of the human brain (Teramitsu *et al.* 2004). A unique FOXP1 isoform has also been identified in human and mouse embryonic stem cells (ESCs) (includes exon 18b, FOXP1-ES), which enhances the expression of pluripotent genes such as *Oct4* and *Nanog* by directly binding to their promoters whilst simultaneously repressing the genes that control differentiation (Gabut

et al. 2011). What controls the FOXP1-FOXP1-ES switch is unknown but when understood will be important for on-going work that looks at directing ESCs to functional neurons.

Foxp1 has also been implicated in an aspect of CNS development; it has been shown to be an essential accessory factor in Hox transcriptional output, whereby it regulates motor neuron diversity and connectivity to target muscles in a dose dependant manor with expression levels being gated by upstream Hox factors such as *Hoxc6* and *Hox10* (Dasen *et al.* 2008; Rousso *et al.* 2008). Furthermore it has also been shown that the microRNA, miR-9, is important in fine-tuning the regulation of *Foxp1* expression in motor neuron specification, which importantly may be useful for applying to stem-cell based therapies for motor neuron injuries (Otaegi *et al.* 2011). Genetic studies have also revealed that certain *Foxp1* mutations in humans can persist in speech and language deficits (Hamdan *et al.* 2010; Horn *et al.* 2010) and as mentioned links with Foxp1 and ASDs have been reported (discussed in 1.7) (Hamdan *et al.* 2010; Palumbo *et al.* 2013).

1.2.3 **The Role of *Foxp1* in the Developing Brain**

*Foxp1 e*xpression has been detected from E12.5 in the developing telencephalon and expression persists into the adult (Ferland *et al.* 2003). In addition to the striatum and cortex *Foxp1* expression is also evident in the CA1 neurons of the hippocampus (Ferland *et al.* 2003) from E17.5 and is seen in the hypothalamus, the deep cerebellar nuclei, the anterior olfactory nucleus, the olfactory tubercle and sporadically in the amygdala (Ferland *et al.* 2003). However, the developmental timings of *Foxp1* expression in these areas are largely unknown.

Expression of *Foxp1* in the adult striatum is restricted to the projection neurons with no expression detected in striatal interneurons (Ferland *et al.* 2003; Tamura *et al.* 2004). It has been shown that FOXP1 is also expressed in the developing human striatum over an equivalent gestational window, and with a similar anatomical distribution to that seen in the mouse and rat, and that it co-localises with DARPP-32 and CTIP2 (Precious et al., submitted 2013). Recent work by a group in Milan have also shown comparable levels of *Foxp1* expression in the developing human striatum (Carri *et al.*

2013). *Foxp1* expression is also shown in the monkey striatum and cortex (Takahashi *et al.* 2008).

From E12, *Foxp1* is expressed in the SVZ of the developing striatum and expression at an mRNA and protein level is detectable in the SVZ and MZ of the striatum from E14 (Tamura *et al.* 2003). *Foxp1* expression was largely observed in the ventral region of the LGE and therefore has been associated with post migratory, differentiating neurons of the striatum rather than with the earlier proliferating neurons in the VZ or the SVZ (Ferland *et al.* 2003; Tamura *et al.* 2004). Specifically, it is thought that *Foxp1* is associated with the projection neurons of the matrix region of the striatum as patch projection neurons are specified by E12.5 (Tamura *et al.* 2004). It has also been suggested that *Foxp1* acts downstream of the TFs *Dlx5/6* as both genes have overlapping expression profiles (Tamura *et al.* 2004). However, it is also plausible that *Foxp1* could act upstream to these genes and more research is needed to fully understand the role of this gene in the context of MSN development.

To date, no functional analysis of *Foxp1* in the developing or adult brain has been carried out *in vivo* or *in vitro,* although recent *in vitro* work using mESCs has shown that *Foxp1* is a novel marker of midbrain dopamine neurons and has hinted at *Foxp1* having a functional role in their development. It was shown that the addition of *Foxp1* to ESCs activates the expression of *Pitx3*, a homeobox protein that is exclusively expressed in midbrain dopaminergic neurons and is vital for their differentiation and survival during development both *in vitro* and *in vivo* (Konstantoulas *et al.* 2010). Chromatin immunoprecipitation (IP) and electrophoretic mobility shift assays showed that *Foxp1* binds upstream of the Pitx3 promoter to induce transcription. This study demonstrates for the first time a transcription regulatory role for *Foxp1* on the *Pitx3* gene in mammalian stem cells (Konstantoulas *et al.* 2010). It is therefore possible that *Foxp1* has a similar role in regulating the differentiation of MSNs.

1.3   **Organisation of the Adult Striatum and Cortex**

1.3.1 **The Adult striatum**

The adult striatum is composed of two histologically identical nuclei, the caudate and putamen, that are separated by the internal capsule (this is not found in rodents) and together, with other core nuclei, make up the basal ganglia (Jain *et al.* 2001). The core nuclei in the basal ganglia in addition to the striatum are the sub thalamic nuclei (STN), the internal and external segments of the globus pallidus (GP*i/e* respectively) and the substantia nigra (SN) pars compacta and pars reticulata (SNc and SNr) (Jain *et al.* 2001). This is shown in Figure 1.2. Specifically, the striatum plays a vital role in the co-ordination of movement (primary motor control), emotions, and cognition (Jain *et al.* 2001) and forms links with widespread areas of the cortex, the thalamus and the brainstem through independent pathways (Jain *et al.* 2001).
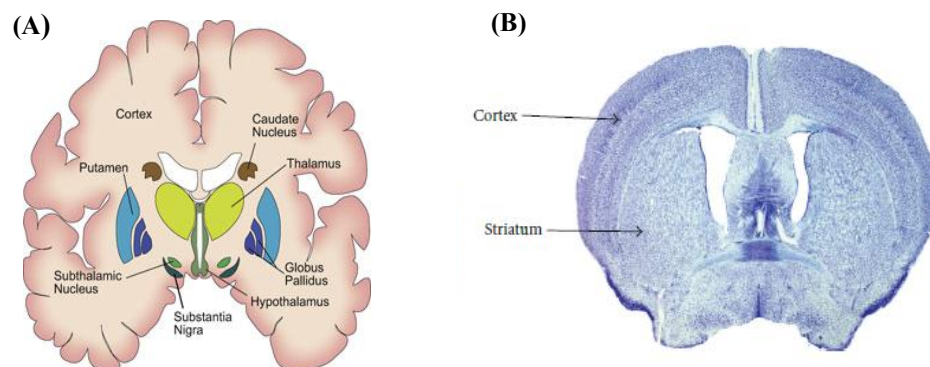
Figure 1.2(A) Coronal schematic of the human basal ganglia showing the associated nuclei (kin450-neurophysiology.wikispaces.com; accessed 19th April 2013). **(B)** Coronal section of a mouse brain stained with cresyl violet showing the striatum as one structure and the cortex (Evans *et al.* 2012).

1.3.2 **Striatal Neurons**

Striatal neurons are heterogeneous and can be subdivided according to size, density of spines, and utility of neurotransmitters and neuropeptides. MSNs are the main output projection neurons of the striatum and principally utilise the inhibitory transmitter gamma-amino butyric acid (GABA). MSNs constitute approximately 95% of all of the striatal neurons in the rodent (Gerfen 1992), an example MSN is shown in Figure 1.3A. The remaining 5% of neurons are aspiny interneurons (Freeman *et al.* 1995).

In addition to the characteristic morphology such as size and spine density, MSNs express the dopamine and cyclic adenosine 3', 5'-monophosphate-regualted phosphoprotein 32kDa (DARPP-32) which is absent from aspiny neurons as shown in Figure 1.3B. DARPP-32 is the most commonly used phenotypic marker of MSNs in the adult striatum and expression is seen in nearly all projection neurons. However, DARPP-32 expression is not detectable until late in development (Anderson and Reiner 1991). In the developing mouse brain, DARPP-32 mRNA is undetectable at E14.5, and at P0 both DARPP-32 mRNA and protein are present but in very small amounts (Ehrlich *et al.* 1990). The levels of DARPP-32 increase considerably throughout the first 3-4 postnatal weeks in mice with mRNA reaching adult levels before protein levels. During human development the difficulty in accessing foetal tissue sufficiently early in development means that it is still unclear when DARPP-32 is initially expressed.

Figure 1.3 (A) A medium spiny neuron (MSN) showing characteristic branched spiny dendrites (courtesy of P. Harper Institute of medical genetics, Cardiff University). **(B)** The white arrow shows a MSN co-stained for DARPP-32 (Green) and the neuronal marker β111Tubulin (Red) and the nuclear marker Hoechst (Blue), the yellow arrow head shows an aspiny neuron in which DARPP-32 is absent.

In addition to differences in size and shape, striatal projection neurons can be further grouped based on specific neuroch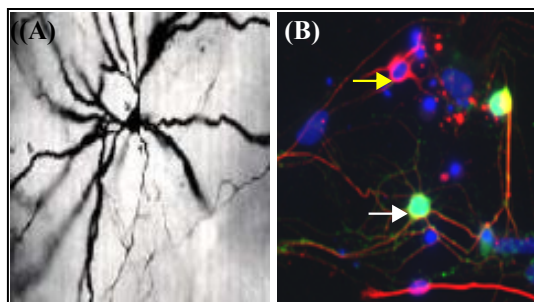emical markers and their underlying connections. This distinction results in a mosaic-like organisation in which neurons are defined into patches (also known as striosomes) (15-20%) or complementary to this, the matrix (80-85% neurons) that have been well characterised in rats, primates and cats (Gerfen 1992). Specifically striatal neurons born between E11 and E13 populate the patches (Mason *et al.* 2005), whereas those born later, between E13-E16, reside in the matrix (Van der Kooy and Fishell 1987). Although patch neurons are born first, as yet it is not possible to distinguish whether a neuron resides in the patch or matrix until late in development (~E18)/early post-natally. In the rat adult striatum the first hint of patch-matrix regions was shown through the presence of distinct patches of enriched μ-opiate receptors (Pert *et al.* 1976) and areas of weakly stained acetylchlolinesterase (AchE) labelling (Graybiel and Ragsdale 1978), whereas the matrix is rich in AchE, the 28 kD calcium-binding protein (calbindin) and somatostain fibres (Gerfen *et al.* 1985). These markers show a reliable and complementary design in the rat throughout the majority of the dorsal and ventral striatum. Briefly retrograde axonal tracing studies in rats have shown that both patch and matrix neurons project to the SN. Specifically patch neurons provide inputs to the dopaminergic neurons in the SNc and dopaminergic cell islands in the SNr whereas matrix neurons provide inputs to the location of the GABAergic neurons in the SNr (Gerfen 1984; Gerfen *et al.* 1985)

More recent research has also shown that at E18.5 in the mouse the patchy regions can be identified by DARPP-32 (Foster *et al.* 1987) and the matrix by transcription factors (TF) such as IKAROS (Martın-Ibanez *et al.* 2010). However, it should be stressed that after birth DARPP-32 does label both patch and matrix neurons (co-labels with calbindin), and it is only at E18 and P0, that it is exclusively a patch marker because DARPP-32 is only expressed in mature neurons that were born earlier and have efferent and afferent signalling apparent. Having genes that could distinguish the patch/matrix regions before E18 would be useful as it would allow a better understanding of MSN development and subsequent differentiation.

1.3.3 **Adult Cortex**

The cerebral cortex forms the outer layer of the cerebral hemisphere and comprises over three quarters of the human brain (Figure 1.2) and is the centre for conscious thought, memory and intellect (Finlay and Darlington 1995). It is the highest level at which motor functions are represented, and is the area where sensory modalities are interpreted. The cortex consists of six layers (layers I-VI, with layer VI being the innermost layer), each containing specific subtypes of neurons, characterised by their distinct projection and gene expression patterns (Molyneaux *et al.* 2007). The two major types of neurons present in the cortex are the interneurons and the projection neurons. Inhibitory γ-aminobutyric acid (GABA)-ergic interneurons make local connections within the cortex, whereas projection neurons, which are excitatory (glutamatergic), extend to form connections with other regions within the cortex and to other regions of the brain including the basal ganglia (Molyneaux *et al.* 2007).

1.3.4 **The Direct and Indirect Pathways- Linking the Cortex and the Striatum**

The cortex, striatum and associated basal ganglia nuclei are all inextricably linked to ensure the correct regulation of two key pathways needed for processing everyday tasks such as movement, these are the- the direct and indirect pathways (Kita and Kitai 1988). Both pathways comprise separate, but equal, numbers of striatal projection neurons that have received excitatory input from the cortex and can be grouped depending on their targets. Striatonigral neurons are implicated in the direct pathway and project to the SNc and SNr whereas striatopallidal neurons project to the GPi and GPe and are concerned with the indirect pathway (Gerfen 1992). Striatal neurons can also be classified into groups based on expression of different neuropeptides. The majority of striatopallidal neurons express enkephalin, whereas striatonigral neurons express substance P and dynorphin (Gerfen and Young 1988); both pathways are shown in Figure 1.4.

Differences in the physiological activity of striatal output pathways modulate the GABAergic neurons in the SN. Striatal output neurons are physiologically quiescent at rest whereas nigral GABAergic neurons are tonically active (Gerfen 1992). In the direct pathway, gluatmatergic input from the cortex to the striatum promotes activity in the quiescent neurons, which phasically inhibit the tonic action of the nigral GABAergic

neurons, causing excitatory input to the cortex via modulation of the GPi and the thalamus; this is outlined in Figure 1.4. Alternatively, in the indirect pathway, corticostriatal input onto striatopallidal neurons leads to the disinhibition of the STN increasing the activity of the GABAergic nigral neurons (Kita and Kitai 1987), therefore repressing the excitatory signals from the thalamus to the cortex; again this is shown in Figure 1.4. Additionally, the indirect pathway can decrease nigral output activity by direct pallidal (GPe) GABAergic input onto the SNr. Therefore the responsiveness of either striatonigral or striatopallidal neurons to corticostriatal input has a direct effect on output neurons of the basal ganglia to the SN.

Striatal inputs from the SN are dopaminergic whereas neurons projecting from the cortex and thalamus express glutamate and provide excitatory input to the MSNs. Dopaminergic projections from the SNc act on either dopamine receptor 1 or 2 (D_1 or D_2) of the GABAergic MSNs. Projections on to the D1 receptors results in activation of the direct pathway, whereas projections on to the D2 receptors activates the indirect pathway (Gerfen and Young 1988; Jimenez-Castellanos and Graybiel 1987). Although neurons normally contain either D_1 or D_2 receptors there may be a subtype of neurons that express both (Gerfen 1992).
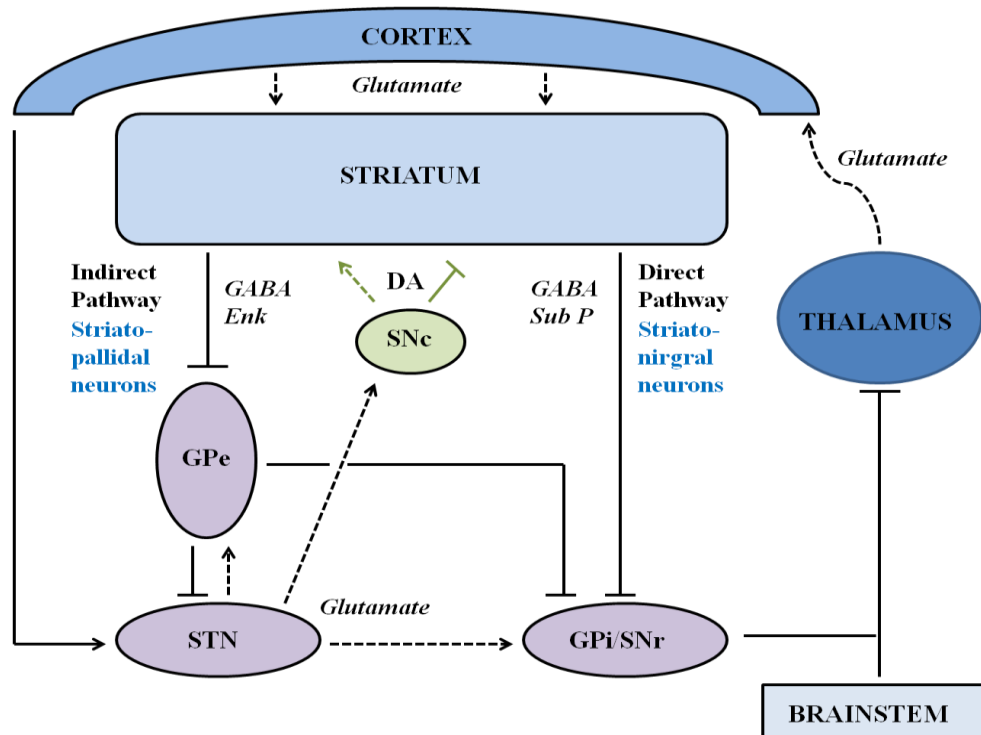
Figure 1.4-Indirect and direct pathways of the basal ganglia. The direct pathway provides direct input to the SNr through striatonigral neurons which regulate the thalamus, in turn, activating the cortex. In the indirect pathway, the striatopallidal neurons directly target the STN, which releases glutamate to the SNr and indirectly though projection onto to the SNr through inputs to the GPe, which release GABAergic inhibitory signals. Dopamine innervations from the midbrain modulate the striatal output neurons. *Abbreviations: STN-subthalamic nucleus, GPe/GPi-globus pallidus external/internal, SNr/SNc Substantia Nigra pars reticulata/compacta, Enk- Enkephelin, Sub P- Substance P. D1/D2 -Dopamine Receptor Dashed lines represent excitatory projections, solid lines represent inhibitory neurons and green arrows represent dopamine release.*

1.4 **Telencephalon Development**

1.4.1 **The nervous system**

Precise transcriptional control of neuronal development is critical for generating diversity and regional specificity in the brain, and the defined orchestration of genetic interactions needed to ensure correct striatal development and associated neurons is crucial to prevent neuronal disorders. Understanding the roles of genes involved in striatal development and, in particular, the role of genes implicated in MSN development is an area of interest to our laboratory and my PhD. The multitude of genetic tools now available has helped to establish novel genes involved in MSN development as well as elucidating more precise genetic pathways involved in striatal development.

Development of the nervous system starts with neural induction, followed by neurulation that gives rise to the neural tube, and finally, patterning of this tube along the anterior-posterior (AP) axis. Subsequent to AP patterning, the neural tube folds and is subdivided into the prosencephalon (forebrain), the most anterior (rostral) part of the neural tube, which consists of the telencephalon and diencephalon, the mesencephalon (midbrain), and the rhombencephalon (hindbrain) (Rubenstein *et al.* 1998). These major subdivisions are shown in Figure 1.5. Regional patterning of the putative brain regions is then governed by a series of interacting gene networks, of which the ones controlling telencephalic development are the most complex.
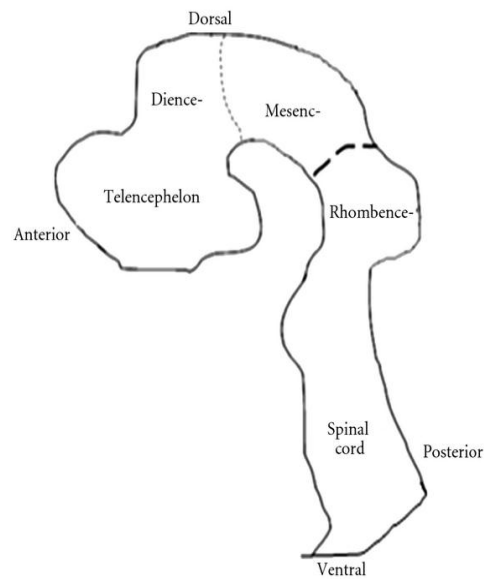
Figure 1.5 Patterning of the Neural Tube. The neural plate folds to form the neural tube, which comprises developing areas of the CNS. The prosencephalon is split into the telencephelon and diencephalon and mesencephalon and rhombencephalon.

1.4.2 <u>Regional Pattering of the Developing Telencephalon</u>

Following neural induction, the embryonic telencephalon, is divided into the dorsal telencephalon (also called pallium), which gives rise to the neocortex, and the ventral telencephalon (also called the subpallium) which forms the striatum, and is the origin of cells that populate the olfactory bulb, GP, and a small population of cortical cells (Jain *et al.* 2001). Even though the adult striatum is diverse between mammalian species, the initial subdivisions observed in the telencephalon are similar (Puelles *et al.* 2000; Rubenstein *et al.* 1998). Due to the rapid migration of post mitotic neurons from the proliferative zones in the subpallium, prominent intra-ventricular bulges form the medial and lateral ganglionic eminences (MGE/LGE), collectively referred to as the whole ganglionic eminence (WGE), shown in Figure 1.6. The MGE, the most ventral eminence, gives rise to the amygdaloid body and the GP, whilst the LGE, which is situated more dorsally, gives rise to the caudate and putamen (Deacon *et al.* 1994; Sturrock 1980). The LGE is further divided into the dorsal LGE (dLGE) and the ventral LGE (vLGE) on the basis of regional gene expression, which is discussed later.

Within the surrounding neural epithelium of the developing telencephalon, there are two proliferative zones, the ventricular zone (VZ), which is positioned on the perimeter of

the lateral ventricles, and the subventricular zone (SVZ) (unique to the telencephalon), which extends from the basal region of the VZ. Both are shown in Figure 1.6 (Campbell 2003). Striatal projection neurons are born primarily in the VZ and SVZ of the ventral LGE and make up nearly 90% of LGE neurons (Olsson *et al.* 1995; Stenman *et al.* 2003; Wichterle *et al.* 2001), whereas the dorsal LGE is mainly associated with the production of striatal, cortical and olfactory bulb interneurons (Corbin *et al.* 2000; Toresson *et al.* 2000). Interneurons are also born from the MGE and migrate to the cortex, GP, and striatum (Anderson *et al.* 1997; Campbell *et al.* 1995; Olsson *et al.* 1998). Subsequent to proliferation, neurons migrate to the mantle zone (MZ) of the developing striatum where they differentiate, shown in Figure 1.6.
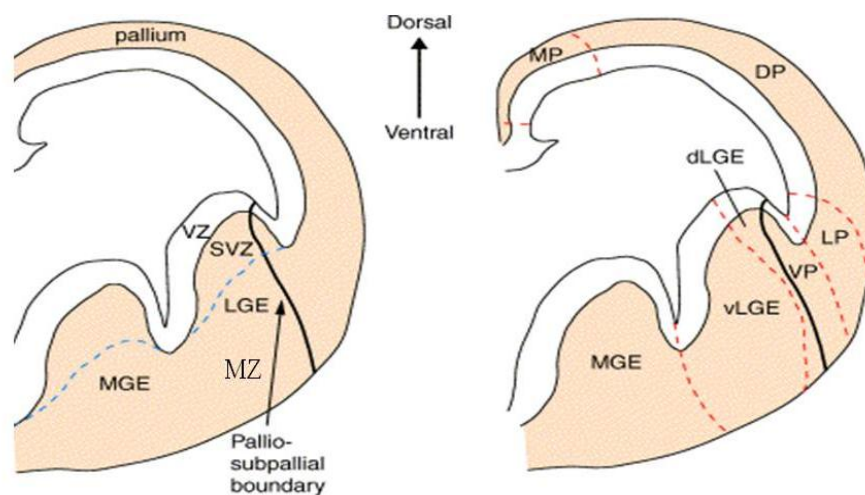
Figure 1.6 Coronal hemi sections of the mouse telencephalon at E12.5 showing morphologically defined structures and the progenitor subdomains. The VZ extends along the DV axis and contains proliferative neuronal precursor cells. The SVZ (shown by the blue dashed lines) also contains precursor cells. Progenitor cells migrate radially and tangentially from these zones to populate the MZ, an area associated with post-mitotic neurons. The dashed red lines indicate the approximate boundaries between distinct telencephalon progenitor domains. *Abbreviations: MP- medial pallium, DP- Dorsal Pallium LP- Lateral pallium, VP-ventral pallium Picture adapted from (Campbell 2003).*

1.4.3 **Radial Glia (RG)**

Although it is known where in the developing telencephalon striatal and cortical neurons arise, it is also important to know which specific cell type the neurons arise from, especially if a CKO model is to be considered. Since 2000, it has widely been accepted that RG can act as progenitor cells for over 80% of neurons, in addition to glia in the CNS (Malatesta and Gotz 2013; Malatesta *et al.* 2000; Noctor *et al.* 2002). RG express the hallmarks of astrocytes, GFAP, glial high affinity glutamate transporter (GLAST), and brain lipid binding protein (BLBP), and this latter marker can be used to distinguish the switch of neuroepithelial cells to RG, and furthermore, the onset of RG neurogenesis, which occurs concurrently around E10.5-E11 (Anthony *et al.* 2004).

It has been suggested by Anthony et al (2004) that RG can give rise to neurons through one of two routes as outlined in Figure 1.7 (Anthony *et al.* 2004). Either RG can directly give rise to heterogeneous progeny; RG and a post mitotic neuron in the VZ, as is the case in cortical neurogenesis (Noctor *et al.* 2002) or alternatively, RG produce neuroblasts which migrate to secondary proliferative layers, i.e. the SVZ where division then occurs to produce neurons, the latter is the case in the ventral telencephalon, shown in Figure 1.7. Precursors within the SVZ are normally devoid of BLBP staining. However, fate mapping using a TG mouse for a BLBP-Cre crossed to a ROSA- LacZ (R26R) mouse showed X-Gal staining in the adult striatum, suggesting these neurons were derivates of RG. As striatal neurons are known to be born principally from the SVZ of GEs (Anderson *et al.* 1997), it was believed that these SVZ precursors were indirectly produced from RG (Anthony *et al.* 2004). Numerous lineage tracing experiments have been carried out to exactly determine what areas of the CNS are populated by neurons that originate from RG, and these experiments have presented differing results in the question of whether MSNs are derived from these cells or not; this is discussed below (Anthony *et al.* 2004; Malatesta *et al.* 2003; Malatesta *et al.* 2000).

(A) RG

RG   Post-mitotic
            Neuron

(B) RG

Neuroblasts

Secondary proliferative layers
(e.g. Cells in the SVZ)

Neurons
            Happens in the ventral
            telencephelon
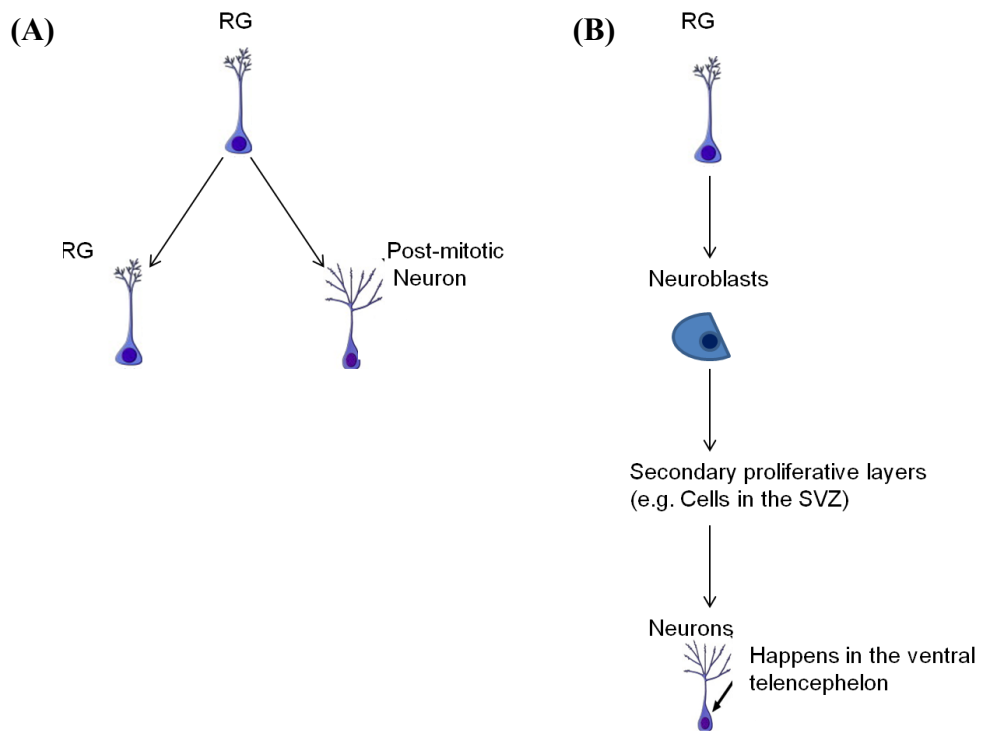
Figure 1.7 The two different routes in which radial glia (RG) can give rise to neurons in the CNS. (A) RG can divide to produce another RG and a post-mitotic neuron as seen in cortical development or **(B)** to produce a neuroblast which in turn migrates to secondary proliferative zones such as the SVZ where it gives rise to neurons, as is the case for striatal neurons.

When the human GFAP (hGFAP)-Cre was crossed with R26R mice to trace progeny it was shown that the adult striatum and layers 1 and V1 of the cortex were mainly devoid of X-Gal staining. Out of the positive striatal X-Gal cells, the majority co-stained with glia markers. Of the few that were identified as neurons only 10% co-stained with DARPP-32, 3% with calretinin and 1% stained with calbinidn (Malatesta *et al.* 2003). However, within the cortex, Er81 and Parvalbumin interneurons did co-stain with X-Gal. These cortical neurons arise from the dorsal VZ where neurogenesis is known to occur at a later stage than striatal neurons born from the GE's, which is from E11 (Mason et al., 2005). Results from these tracing experiments therefore suggested that striatal neurons are born independent of a RG phase. Or alternatively, as suggested by Anthony et al, that the majority of striatal neurons pass through a RG phase but before appreciable recombination of the hGFAP-Cre has occurred which is at E15.5 (Anthony and Heintz 2008).

It has been proposed that the heterogeneity observed in RG by the hGFAP-Cre tracing studies reflects temporal aspects of RG development rather than an underlying difference in potential (Anthony *et al.* 2004). As a means of validating this both the BLBP-Cre (Anthony and Heintz 2008; Anthony *et al.* 2004) and the GLAST-Cre lines (Anthony and Heintz 2008) also expressed in RG, but from E10.5, were crossed with R262 mice to trace neuronal progeny in the adult CNS. These experiments showed extensive X-Gal staining in the postnatal (PO) and adult striatum (Anthony and Heintz 2008; Anthony *et al.* 2004). In addition S100, a glia marker, showed that by E16.5 gliogenesis was occurring in the LGE, but expression was absent in the dorsal telencephalon until P0. Therefore the recombination patterns of X-gal using these two different Cre lines strongly suggested that MSNs do arise from RG, but at an earlier time point than when hGFAP-Cre is active, i.e. between E11.5 and E12.5. Therefore, it has been suggested that RG go through two phases:

- an early (before E12) neurogeneic BLBP +ve, GLAST +ve and GFAP- ve phase and a
- later (after E13) gliogenic BLBP +ve, GLAST +ve and GFAP + ve phase

Anthony and Heinz suggest that a BLBP-Cre is the best line to use in order to trace all progeny arising from RG in the CNS. They argue that using the hGFAP-cre to trace or knock out striatal neurons is inadvisable, as it does not accurately reflect the normal developmental pattern of RG in mice (Anthony and Heintz 2008). However, the exact timings of striatal neurogenesis, especially in the mouse, are not fully understood and it is possible that reporter lines or subsequent staining protocols are not identifying all recombined cells. Specifically, caution should be taken when inferring negative tracing results using any Cre-line as results could be recognized as weak promoter activity rather than restricted potential. Recombination efficiency can be directly linked to promoter strength and it has been shown that doubling the copy number of the promoter, i.e. two copies instead of one, can result in an increase in recombination (Anthony and Heintz 2008). For example, tracing studies carried out by Casper and McCarthy utilised the same and different hGFAP lines to Malatesta and colleagues showed higher reporter expression in the adult striatum; 54% of striatal neurons displayed X-Gal and NeuN expression (Casper and McCarthy 2006). However, of the 54% of striatal neurons that were positively stained for X-Gal, the majority co-localised with interneuron makers (Casper and McCarthy 2006).

It can be concluded from all the described tracing experiments that RG housed in the ventral telencephalon are directly or indirectly responsible for approximately 80% of neurons found in the adult striatum (Anthony *et al.* 2004). The remaining 20% are not likely to be descendants of RG, and are instead directly born from basal progenitors descended from nestin positive neuroepithelial cells (Anthony *et al.* 2004; Gotz and Huttner 2005), shown in Figure 1.8.
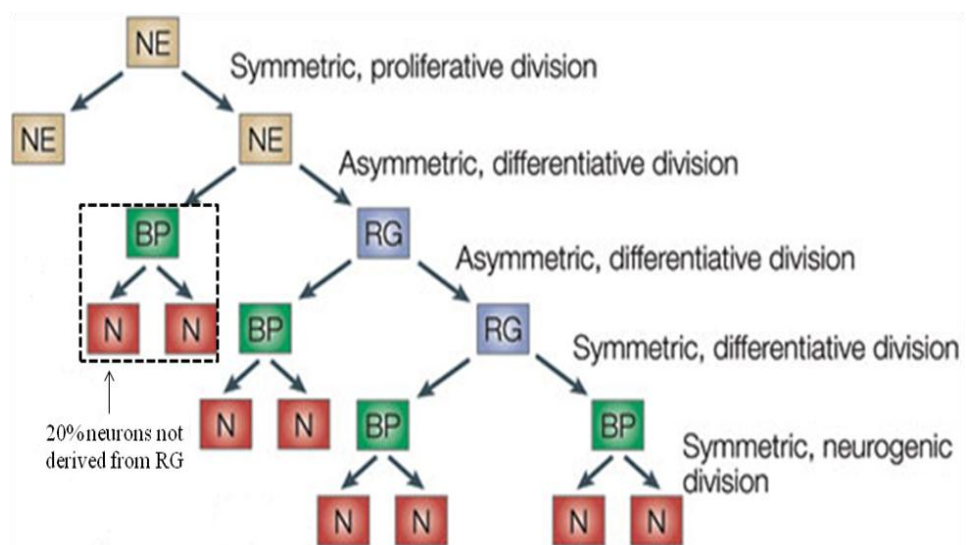
Figure 1.8 Neurogenesis Diagram shows that neurons are all born from basal progenitors (BP) that all arise from neuroepitehlial cells (NE). The majority of neurons are then born from BP descended from radial glia (RG) but there is a lineage born independent of RG as shown by the dotted box on the diagram. Figure adapted from (Gotz and Huttner 2005).

1.4.4 **Early Signals involved in Telencephalic Development**

As described above, the developing striatum and associated MSNs arise from the telencephalon; thus understanding telencephalic development is important. The telencephalon is the most complex region of the mammalian brain and shows substantial heterogeneity in terms of its neuronal populations, structures, and function. Several gene families are involved in coordinating the initial events (E8-E12) for telencephalon patterning: principally fibroblast growth factors (FGFs), bone morphogenic proteins (BMPs), *Wnts* (originated from the drosophila gene *wingless*), retinoic acid (RA), and sonic hedgehog (*Shh*). These are highlighted in Figure 1.9. These signals are responsible for activating downstream factors that enable signalling cascades to be initiated, allowing cells to gain a positional and molecular identity (Manuel *et al.* 2010). It is likely that only a proportion of the factors required for neuronal identity have been identified, and the precise way in which such factors interact to specify the timing and terminal differentiation of particular neuronal subpopulations is not yet defined. Table 1.1 (page 19) summarises the key roles known to date of the genes known to be involved in early telencephalon development. This list is not exhaustive and the need to gain a better understanding of this early stage in striatal development is paramount for improvement of *in vitro* protocols aiming to direct renewable cell sources to a functional MSN phenotype.
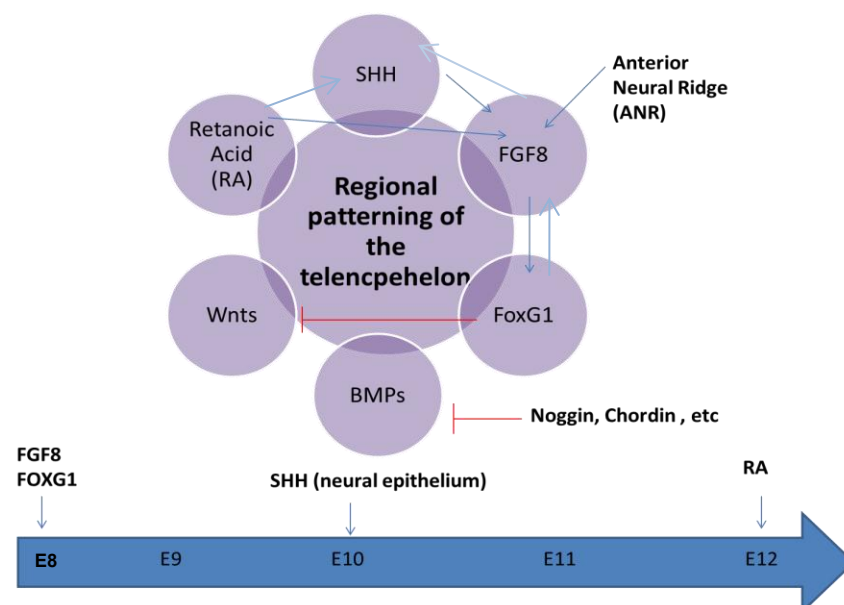
Figure 1.9 Key factors involved in early telencephalon development and timeline for onset of gene expression. *Arrows denote positive interactions; T-bars denote repressive function.*

1.4.5 **FGF8**

FGFs are growth factors that can activate several different pathways once bound to their appropriate receptors. For example, binding of FGFs to FGF receptor (FGFR) 1, 2 or 3 can activate the Ras Map Kinase (MAPK) pathway, initiating a signalling cascade to start (Mason 2007). *Fgf8* is expressed rostrally from the anterior neural ridge (ANR) in mammals from ~E8 and has roles in proliferation and cell survival. In addition, it has been shown that *Fgf8* regulates the expression of forkhead box protein G1 (*Foxg1*; previously *Bf1*), a rostral forebrain marker that is also expressed in the ANR at ~E8. These genes function through a tightly linked feedback loop (Shimamura and Rubenstein 1997). It was shown that *Fgf8* could renew *Foxg1* expression in mouse explants that had the ANR removed. Furthermore inhibitors of *Fgf*8 reduced *Foxg1* expression in neural plate explants (Shimamura and Rubenstein 1997; Ye *et al.* 1998). In addition, reduction in *Fgf8* leads to rostral truncations and midline defects in the developing forebrain (Shanmugalingam *et al.* 2000). In *Fgf8* knock out (KO) mice (*Fgf8*$^{-/-}$) the telencephalon was smaller than in littermate controls and exhibited patterning abnormalities (Shanmugalingam *et al.* 2000; Storm *et al.* 2006; Wilson and Rubenstein 2000). In particular, the MGE and LGE were absent and there was loss of genes that are typically found in the ventral region, e.g. *Dlx2* and *Nkx2.1*, but an expansion of the dorsal marker *Pax6* (Storm *et al.* 2006). These results suggested a role for *Fgf8* in ventralisation of the telencephalon.

Regulation of development at this early stage is vague; FGF8 is implicated but it would appear other factors are also implicated due to the continued presence of the telencephalon in *Fgf8*$^{-/-}$ or FGFR null mutants (Shanmugalingam *et al.* 2000). One suggestion for the telencephalon remaining in these mutants is through compensation of other *Fgfs* expressed at the same time. Nevertheless, some in the field are of the opinion that overlapping *Fgf* expression profiles do not exist and that each *Fgf* has exclusive roles in telencephalon development (Borello *et al.* 2008; Cholfin and Rubenstein 2007). They would postulate that the reason the telencephalon is not lost completely in the *Fgf8* mutant is not due to compensatory mechanisms by other family members, but because *Fgf8* is not essential for telencephalon generation and that other genetic families and ligands are also needed (Borello *et al.* 2008; Cholfin and Rubenstein 2007). Nevertheless, the fact that beads soaked in FGF8 that were added to anterior neural

explants lacking an ANR promoted expression of *Foxg1* suggests FGFs are necessary for telencephalon induction (Shimamura and Rubenstein 1997) .

Recently, work supporting gain of function studies has allowed greater insight into the role of FGFs and FGFRs in telencephalon development. Triple FGFR KOs have shown that at E10.5 embryos showed abnormalities in the anterior structures and, by E12.5, a time at which the telencephalic structures are morphologically distinguishable, mutants lacked all anterior head structures and had no visible telencephalon except for the dorsal midline (Paek *et al.* 2009). In addition, *Foxg1* was not expressed, together with complete absence of the ventral markers (*Dlx2* and *Nkx2.1*). Unexpectedly, the dorsal marker *Emx1* was also absent, suggesting that FGF has a role in forming the dorsal telencephalon in addition to the ventral telencephalon (Paek *et al.* 2009).

The phenotype of the FGFR triple KO was much more severe than the phenotype observed in single or double receptor mutants (Mason 2007), thus supporting the argument that different FGFs compensate for each other and do not have exclusive roles. However, this compensation is not absolute, given that a mild phenotype was still evident in single or double mutants. This suggests the compensating ligands and corresponding receptors can function, but are not optimum and therefore, the signalling cascades are less efficient (Paek *et al.* 2009). Subtractive results suggest that FGFR1 is responsible for the majority of signalling in early telencephalon development, and that it is the overall levels of FGF signalling that operate to initiate, pattern and sustain development as a whole, rather than specific ligands patterning different areas (Paek *et al.* 2009).

1.4.6 <u>**SHH**</u>

SHH is a member of the hedgehog (Hh) family of secreted proteins and typically acts as a morphogen during development, therefore signalling is by means of a concentration gradient. During telencephalon development SHH spans the dorsal ventral (DV) axis at different embryonic time points to promote different neuronal phenotypes; the highest concentration is seen ventrally. SHH is initially secreted from the notochord, following which, expression is from the overlying neural plate (Echelard *et al.* 1993; Roelink *et al.* 1995; Rubenstein *et al.* 1998). By E9.5 *Shh* is expressed in the neural epithelium of the

ventral telencephalon (Shimamura *et al.* 1995), and expression is seen in the MZ of the ventral telencephalon from E11.5 (Jessell 2000; Kohtz *et al.* 1998). SHH expression directs neural progenitors to a ventral fate, is both necessary and sufficient to induce specific ventral forebrain markers (Chiang *et al.* 1996; Ericson *et al.* 1995; Kohtz *et al.* 1998), and is thought to maintain *Fgf8* expression (Chiang *et al.* 1996; Ericson *et al.* 1995; Kohtz *et al.* 1998; Ohkubo *et al.* 2002). Specifically, SHH activates several transcription factors (TFs) including the telencephalic factors *Nkx2.1* (Sussel *et al.* 1999), *Gsx2* (formely *Gsh2*) (Corbin *et al.* 2000; Toresson *et al.* 2000; Yun *et al.* 2001) and *Pax6* (Stoykova *et al.* 2000).

SHH functions as a ligand for a pathway involving two trans-membrane proteins, patched (Ptc) and smoothened (Smo). Normally, Ptc is bound to Smo and the pathway is inactive as Smo is unable to activate the Glioma-associated oncogene (*Gli*). This is illustrated in Figure 1.10A. However, when SHH binds Ptc, Smo is de-repressed which results in the Gli repressor (GliR) becoming activated (GliA) and being able to translocate to the nucleus and activate gene expression, as shown in Figure 1.10B.
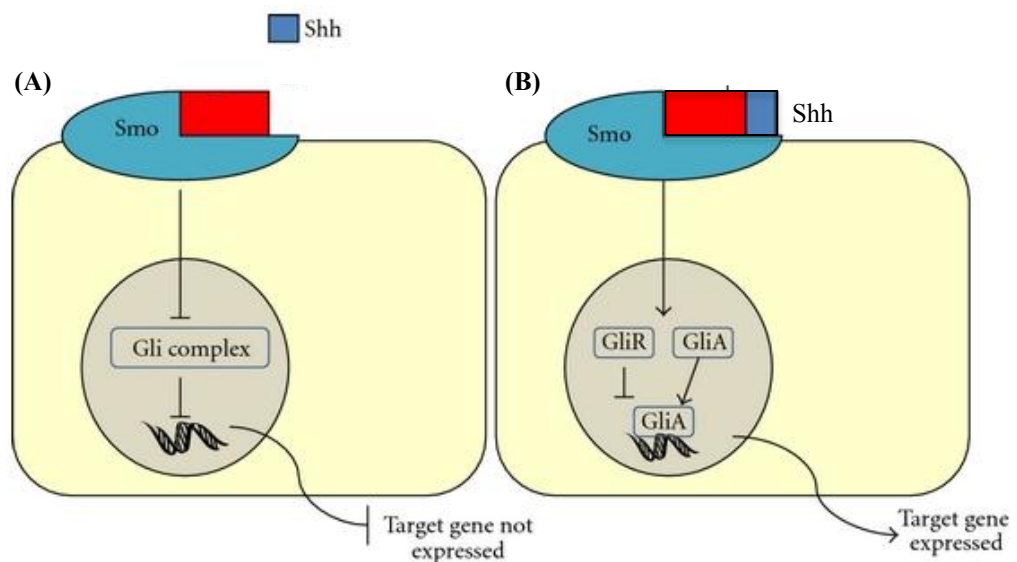
Figure 1.10 The *Shh* pathway for target gene expression (A) Repressed pathway- when SHH cannot bind Ptc, Ptc represses gene expression by being bound to Smo. Smo cannot then activate the Gli complex meaning the target gene is repressed. **(B) Induction pathway**- when SHH binds Ptc, Smo is released which allows GliA to bind the DNA and activate gene expression. *Abbreviations: SHH-sonic hedgehog, Ptc-patched, Smo-smoothened, GliA-Gli Activator, GliR-Gli Repressor (Evans et al. 2012).*

There are three members of the Gli family of zinc-finger TFs: *Gli1*, *Gli2* and *Gli3,* and all three have been shown to regulate *Shh* dependant gene expression. Gli proteins have both activator and repressor properties, the N-terminal region has a repressor function whereas the C-terminal region is required for activation (Rallu *et al.* 2002). It is believed that *Gli3* functions principally in its repressor form and that its activity is negatively regulated by *Shh* (Marigo *et al.* 1996; Wang *et al.* 2000), whereas Gli1 and 2 function primarily as transcriptional activators (Bai and Joyner 2001; Dai *et al.* 1999).

Analysis of mouse KOs for each of the Gli genes (*Gli1*$^{-/-}$,*Gli2*$^{-/-}$, and *Gli3*$^{-/-}$) has revealed that mice lacking *Gli1* or *Gli2* show only slight defects in telencephalon development (Park *et al.* 2000), whereas mice lacking *Gli3* have strong defects in dorsal telencephalon patterning (Grove *et al.* 1998; Theil *et al.* 1999; Tole *et al.* 2000). At the dorsal region of the telencephalon, where the concentration of SHH is restricted, the Gli3 protein is cleaved into a repressor form and promotes dorsal patterning (Rallu *et al.* 2002). It is the inhibition of the Gli3 repressor complex in the ventral telencephalic region that facilities correct development; therefore, one of the functions of *Shh* is to prevent the translation of Gli3 to its repressor form.

The relationship between *Shh* and Gli3 has been shown functionally through varying combinations of mutants. For example, in *Shh*$^{-/-}$ KO mice the expression of the ventral markers *Dlx2* and *Gsx2* was reduced, whereas in *Gli3*$^{-/-}$ KO mice the expression pattern of these genes was extended into dorsal regions (Rallu *et al.* 2002). In accordance with the loss of ventral markers in the *Shh*$^{-/-}$ mouse, there is a loss of ventral telencephalic cells leading to an altered morphology of the ventral telencephalon together with the ectopic expression of dorsal forebrain markers (Chiang *et al.* 1996; Ericson *et al.* 1995; Ohkubo *et al.* 2002). Complementary gain-of-function experiments carried out in zebrafish and mice has shown that SHH promotes the ventral identity of dorsal telencephalic cells *in vivo* with subsequent expression of the ventral forebrain markers *Gsx2, Dlx2* and *Nkx2.1* (Sussel *et al.* 1999). Moreover, conditional *Shh* KO mice under the control of a *Foxg1*-Cre revealed the optimal window of *Shh* signalling in telencephalon development. If *Shh* is knocked out at E8.5 there are severe defects of all ventral telencephalic regions (Fuccillo *et al.* 2004), whereas, when *Shh* is knocked out in mice from E10 using a Nestin-Cre, there are only partial defects in ventral telencephalic patterning (Xu *et al.* 2005).

In the Shh^{-/-} and *Gli3*^{-/+} KO mice telencephalon morphology is largely restored to that of the wild type (WT), but regional gene expression is not fully restored. The expression of the ventral markers *Nkx2.1, Dlx2 and Gsx2* was not restored to a WT level unless both copies of *Gli3* were lost, suggesting these genes are highly receptive to the antagonism between *Shh* and *Gli3* (Wilson and Houart 2004). In summary, between E9 and E12.5, *Shh* acts mainly by inhibiting the formation of the *Gli3* repressor (Rallu *et al.* 2002) and contributes to the establishment of DV patterning (Chiang *et al.* 1996; Fuccillo *et al.* 2004). Secondly, SHH signalling also supports the expansion of progenitors of the ventral telencephalon by inducing and maintaining the expression of *Nkx2.1* until at least E14 and later into neurogenesis (Xu *et al.* 2005). However, the fact that in the Shh KO mice ventral gene expression was reduced rather than lost suggests that other genes and signalling pathways, independent to Shh signalling, have a role in regional DV patterning of the telencephalon (Rallu *et al.* 2002).

1.4.7 **Retinoic Acid (RA)**

RA is the biologically active form of vitamin A and has been implicated in survival, specification, proliferation, and differentiation during forebrain development (Haskell and LaMantia 2005; Marklund *et al.* 2004; Schneider *et al.* 2001). For RA to function correctly, and to bind and activate its associated RA receptors (RARs) (RARα, RARβ and RARγ (RARβ is preferentially expressed in LGE)) or retinoid X receptors (RXRα, RXRβ, and RXRγ), two oxidation events occur (Mark *et al.* 2006). Initially, retinol dehydrogenases oxidise retinols to retinaldehyde before the rate-limiting enzymes, retinaldehyde dehydrogenases (Raldh), are required to oxidate retinaldehyde to RA (Duester 2008).

The first known source of RA in the developing striatum, specifically in the LGE, is at E12.5 and is produced from reactions mainly catalysed by Raldh3 (Molotkova *et al.* 2007), but, it is not until E14 that RA and Raldh3 are noticeably expressed. At this stage, RA initiates GABAergic neuronal differentiation by inducing Gad67, an enzyme needed for GABA synthesis (Chatzi *et al.* 2011). GABAergic differentiation is ongoing at E18.5, and RA continues to be expressed into adulthood (Chatzi *et al.* 2011). Notably, in RAR$\beta^{-/-}$ mutant mice there is a loss of striatal-enriched tyrosine phosphatase mRNA, and a reduction of DARPP-32 positive neurons compared to WT

mice (Mark *et al.* 2006; Schneider *et al.* 2001). RA in the LGE is not solely obtainable from Raldh3-mediated reactions as Raldh3$^{-/-}$ mutant mice do not show an obvious telencephalic phenotype (Dupe *et al.* 2003). Retinoids secreted from radial glia (RG) in the LGE are also a known source of RA (Toresson *et al.* 1999) and ensure that differentiating neurons do not lose a source of RA when migrating out of the proliferative VZ and SVZ.

The role of RA in early striatal neuronal development has been shown *in vivo* and *in vitro*. In *Raldh3$^{-/-}$* mouse embryos, LGE progenitors fail to differentiate into GABAergic striatal projection neurons whereas *in vitro*, addition of RA to the media has been shown to induce GABAerigc differentiation in both mouse LGE-derived neurospheres and human ESC cultures (Chatzi *et al.* 2011). Additionally, supplementation of RA to mouse LGE cultures showed an increase in DARPP-32 positive neurons, independent of an increase in the overall number of neurons, therefore showing that RA specifically enhances the striatal neuron phenotype (Toresson *et al.* 1999). There was no difference seen in MGE cultures despite increasing doses of RA (Toresson *et al.* 1999). It has also been shown that when chick LGE explants are treated with RAR antagonists, LGE specification is prevented (Marklund *et al.* 2004). The complementary experiment showed that when exogenous RA was added to dorsal explants, an LGE phenotype was evident (Marklund *et al.* 2004). Moreover, blocking RA in chick embryos prevents the expression of *Meis2*, the earliest known marker of striatal precursors (Toresson *et al.* 1999). Taken together, these results confirm the importance of RA in LGE specification.

As well as being important in embryonic development, RA expression remains in the forebrain throughout adult life and has been shown to maintain the expression of *Fgf8* and *Shh* in this region, as when RA is removed, *Fgf8* and *Shh* expression is lost (Haskell and LaMantia 2005; Schneider *et al.* 2001). It has recently been proposed that *Nolz1*, a zinc finger TF that is expressed in the SVZ of LGE precursor cells, is implicated in RA signalling (Urban *et al.* 2010). At E12.5 *Nolz1*-induced neurogenesis partially depends on RA signalling. It has been shown that *Nolz1* activates the RARβ receptor in LGE-derived neural precursor cells and that this effect was inhibited when RA was removed (Urban *et al.* 2010). However, *Nolz1* expression was not affected in *Raldh3* KO mice (*Raldh3$^{-/-}$*), which lack RA in the LGE, nor when a vitamin A deficient diet was fed to

the mothers (Molotkova *et al.* 2007; Verma *et al.* 1992), suggesting RA is not essential to *Nolz1* expression throughout development and that it is only needed to induce early expression. In summary RA activates *Nolz1* to induce initial neurogenesis during peak striatal development at E12.5 but is not required for its maintenance beyond this time (Urban *et al.* 2010). It has also been shown that *Nolz1* contributes to later striatal development by working downstream of *Gsx2* to activate the RAR*β* receptor.

1.4.8 <u>**Wnt Signalling**</u>

Wnts belong to the wingless protein family and are a class of ligands that are crucial in embryogenesis, and have been implicated in CNS development and can signal through three different pathways: the canonical pathway, the planar cell polarity pathway, and the calcium pathway. It is the canonical pathway that is important in telencephalon development (reviewed in *Evans et al. 2012*).

Wnts are part of the cohort of caudalizing factors that are involved in the initial anterior posterior (AP) orientation of the neural plate and are crucial for the generation of the dorsal telencephalon (Houart *et al.* 2002). WNT signalling is active in the pallium at E11.5 and E16.5 but not in the subpallium (Backman *et al.* 2005; Maretto *et al.* 2003) and is needed to further refine regional patterning and to induce the expression of *Pax6*, a dorsal telencephalon marker (Gunhaga *et al.* 2003). In the absence of canonical signalling in mice, there was ectopic expression of *Gsx2, Dlx2,* and *Ascl1* (formerly *Mash1*) in the dorsal telencephalon together with down-regulation of the dorsal markers *Emx1, 2* and *3* (Backman *et al.* 2005). This ectopic expression of ventral genes led to cells of the dorsal telencephalon adopting a ventral fate with the potential to adopt a GABAergic fate (Backman *et al.* 2005). Furthermore, using chick explant cultures, Gunhaga et al. (Gunhaga *et al.* 2003) showed that the addition of Wnt3 or Wnt8 expression can convert the ventral telencephalic cells into *Pax6* and *Ngn2* positive cells at the expense of *Ascl1* and *Nkx2.1*. Thus, WNT signalling is necessary for ensuring the correct molecular characterisation and morphology of the dorsal telencephalon and that inhibition of WNT signalling is necessary for subpallidal development (Backman *et al.* 2005).

1.4.9 **BMPs**

BMPs belong to the TGFβ family of secreted proteins and it is thought that BMPs are also needed to dorsalize the telencephalon and restrict ventral telencephalic development. When exogenous BMPs were added to mouse forebrain explant cultures ventral forebrain patterning was repressed and the expression of *Foxg1, Nkx2.1*, and *Dlx2* was inhibited (Furuta *et al.* 1997). Similarly, beads soaked in BMP4 or BMP5 that were implanted into the neural tube of a chick forebrain induced dorsal markers, for example, *Wnt4* and repressed ventral markers (Golden *et al.* 1999). Additionally, when the telencephalic roof plate (a source of BMPs) was ablated, there was a reduction in cortical size and a decrease of one of the most dorsal cortical markers, *Lhx2* (Monuki *et al.* 2001). BMPs are inhibited by several factors including chordin and noggin. In mice that lacked both copies of the chordin gene (*Chordin$^{-/-}$*) and one copy of the noggin gene (*Noggin$^{+/-}$*), a dorsal, rather than ventral telencephalon was evident. However, this effect may not be directly because of an increase in BMP and may be in part due to the decreased levels of Shh and *Fgf8* expression in the forebrain caused by increased BMP levels (Anderson *et al.* 2002). Therefore, as with WNT signalling, BMPs are needed to induce a dorsal telencephalic identity and need to be inhibited to establish ventralisation.

1.4.10 **Foxg1**

Foxg1 is a member of the winged helix family of TFs first discovered in rats and is the earliest and only exclusive, recognised marker of the telencephalon (Tao and Lai 1992). At E8.5 *Foxg1* is expressed in the neural tube, specifically in the anterior plate cells that are fated to contribute to the telencephalon (Hebert and McConnell 2000; Shimamura and Rubenstein 1997), where its role is to establish and subdivide the telencephalon. At E10.5, *Foxg1$^{-/-}$* mice show no morphological differences in the size of the developing telencephalon. However, the ventral markers *Ascl1, Nkx2.1, Gsx2*, and *Dlx1/2* are absent, and instead the dorsal markers, *Emx2* and *Pax6*, are expressed throughout the telencephalon (Martynoga *et al.* 2005; Xuan *et al.* 1995). It has also been shown that *Fgf8* was reduced at E10.5 (Martynoga *et al.* 2005). By E12.5, there were widespread morphological differences in the ventral telencephalon of the mutant when compared to WT; notably the GEs were absent but there were no obvious differences in the dorsal region (Martynoga *et al.* 2005; Xuan *et al.* 1995). 5-bromo-2'-deoxyuridine (BrdU)

staining showed that there was a loss of proliferating cells in the ventral region which could be a direct consequence of the lack of *Foxg1* expression or could be due to downstream effectors of *Foxg1* not functioning optimally (Xuan *et al.* 1995).

It has also been shown that *Foxg1* coordinates signalling pathways of SHH and WNTs, which as mentioned, are required for the development of the subpallial and pallial telencephalon, respectively (Danesin *et al.* 2009). Manuel et al. (Manuel *et al.* 2010) cultured cells from *Foxg1*$^{-/-}$ mice and showed that they were specified abnormally with loss of ventral markers which could not be restored by the addition of SHH and FGF8 alone (Manuel *et al.* 2010). Manuel et al. (Manuel *et al.* 2011) have suggested that the reason for *Foxg1*$^{-/-}$ cells behaving abnormally is due to an increase in cell cycle activity which was initially suggested by Martynoga et al. (Martynoga *et al.* 2005). Specifically, Manuel and colleagues have shown that this is due to a decrease in *Pax6* expression, a cell cycle organiser. Upon addition of *Pax6* to *Foxg1*$^{-/-}$ cells, the mutant phenotype was partially rescued (Manuel *et al.* 2011). This work suggests that *Foxg1* not only promotes ventralising cues, but has a cell autonomous role in regulating *Pax6* (Manuel *et al.* 2011). *Foxg1* is therefore crucial in forebrain development and is absolutely required for the regulation of telencephalic identity.

Gene	Summary of expression patterns and knock out phenotypes	Key References
Fgf8	• Expressed from ~E8 from the anterior neural ridge (ANR) • In *Fgf8*^{-/-} mice there is a loss of the MGE and LGE together with patterning abnormalities. • Key role in ventralisation and activates *Foxg1* • Recent work has suggested other FGFs can partially compensate in the absence of FGF8	(Shanmugalingam *et al.* 2000) (Storm *et al.* 2006; Wilson 2000) (Shimamura and Rubenstein 1997) (Paek *et al.* 2009)
Shh	• Morphogen, strongest concentration in ventral telencephalon, lowest in the dorsal region, expression from ~E9.5 • Negatively regulates *Gli3* to ensure that the repressive form is activated in dorsal and not ventral regions • In *Shh*^{-/-} mice there is an overall loss of ventralisation with reduced expression of the ventral markers *Dlx1* and *Gsx2* • Early *Shh* expression is important. If *Shh* is knocked out at E8 there is a loss of telencephalon patterning, KO of *Shh* mice after E10 only affects cortical interneuron development • Thought to maintain FGF8 expression	(Rallu *et al.* 2002) (Yu *et al.* 2009)
RA	• Expressed noticeable in the LGE from E14.5 and expression remains in the forebrain throughout life • Expressed mainly through reactions catalysed by Raldh3 but also from surrounding glia • Supplementation of RA to LGE cultures showed an increase in DARPP-32 positive neurons, whilst there was no effect seen when added to MGE cultures • RA is crucial for the correct specification of the LGE • RA activates *Nolz1* at E12.5 to induce initial neurogenesis but is not sufficient for its maintenance after this.	(Molotkova *et al.* 2007) (Chatzi *et al.* 2011) (Toresson *et al.* 1999) (Schneider *et al.* 2001) (Urban *et al.* 2010)
WNTs	• WNT signalling is necessary for dorsalisation of the telencephalon, expression from ~E11.5 • Inhibition of WNT signalling is necessary for ventralisation of the telencephalon	(Backman *et al.* 2005)
BMPs	• BMP signalling is necessary for dorsalisation of the telencephalon, expression from ~E11.5 • • Inhibition of BMP signalling is needed for ventralisation of the telencephelon	(Golden *et al.* 1999)
Foxg1	• Earliest recognised marker of the telencephalon, expressed from ~E10.5 • Crucial in forebrain development and required for the regulation of telencephalic identity • In *Foxg1*^{-/-} mice the MGE and LGE are not formed	(Tao and Lai 1992) (Xuan *et al.* 1995) (Martynoga *et al.* 2005)

Table 1.1. Summary of the key genes and signalling molecules implicated in early telencephalon development. The main roles of these genes/ molecules are highlighted and associated phenotypic consequences of when a copy/copies are removed.

1.4.11 **Dorsal Ventral Patterning of the Developing Striatum**

As discussed, the developing telencephalon is divided into dorsal and ventral regions that can be defined on a morphological and genetic basis; these genes are shown in figure Figure 1.11. At the early stages (from E8), the dorsal telencephalon can be identified by the expression of *Pax6, Neurogenin* (*Ngn*)*1/2* and *Emx1/2*, whereas the ventral telencephalon can be defined by *Gsx2, Asc1, Dlx1/2*, and *Nkx2.1* expression, as shown in Figure 1.12. Later in development, additional genes aid identification of these two regions.

Emx1/2 expression profiles are restricted to the most dorsal region of the cortex with no expression seen in the ventral cortical region. *Ngn 1* and *2* are basic helix loop helix (bHLH) TFs, which are expressed throughout the cortex together with *Pax6*. In the absence of *Ngn* expression, *Ascl1* is ectopically expressed in the dorsal telencephalon, thus priming these cells to adopt a ventral fate and becoming GABAergic rather than glutamatergic neurons. Subsequently, the roles of *Ngn1* and *2* are to maintain the DV boundary in the developing telencephalon and to inhibit ventral gene expression (Fode *et al.* 2000; Wilson and Rubenstein 2000).
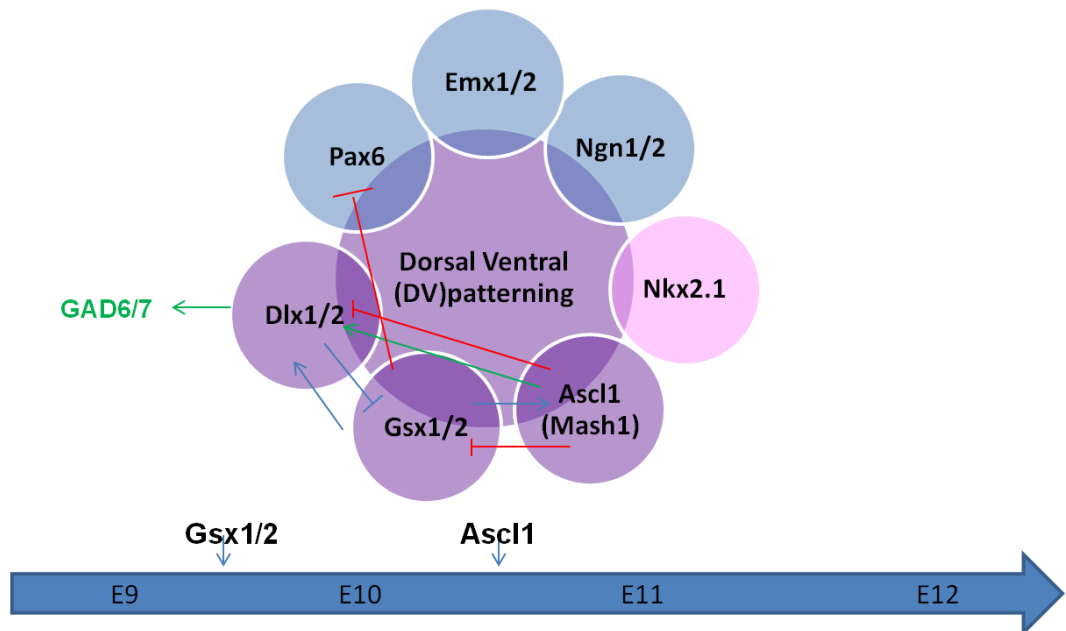
Figure 1.11 Key genes and factors involved in dorsal-ventral patterning of the striatum together with onset of expression *Arrows denote positive interactions; T-bars denote* repressive function
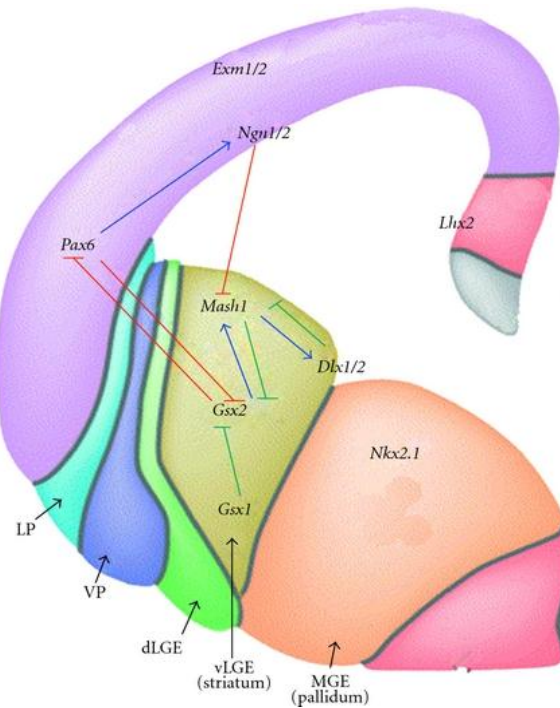
Figure 1.12 Schematic coronal section through the developing telencephalon at E12.5. The dorsal and ventral subdomains are shown and defined by unique gene expression patterns. Dorsal telencephalic markers shown are *Emx1/2, Ngn1*/2 and *Pax6.* The ventral telencephalic markers shown can be split into identifying the LGE or MGE. *Mash1 (Aslc1), Gsx1/2* and *Dlx1/2* are associated with the ventral LGE and Nkx2.1 labels the MGE. The key gene interactions are shown on the diagram. *Arrows denote positive interactions, T-bars denote inhibitory control. The green T-Bars represent recent interactions discovered. Figure adapted from (Schuurmans and Guillemot 2002)*

1.4.12 <u>**Introducing the Homeobox Genes-Pax6 and Gsx1/2**</u>

Homeobox genes, first identified in *Drosophila,* are TFs that code for proteins that have a homeodomain fold capable of binding to RNA or DNA. Homeodomain protein interactions are crucial in mediating DV patterning and importantly, in setting up regional subdivisions within the developing telencephalon, and are principally regulated through *Shh* (Corbin *et al.* 2000; Kimura *et al.* 1996; Sussel *et al.* 1999; Toresson *et al.* 2000; Yun *et al.* 2001). *Pax6* and *Gsx2* are both homeobox genes (Hsieh-Li *et al.* 1995) with overlapping, complementary expression profiles to ensure that the dorso-ventral border is maintained (Toresson *et al.* 2000). *Pax6* is expressed in a dorsal (high) to ventral (low) gradient and *Gsx2* is expressed in a ventral (high) to dorsal (low) gradient (Hebert and Fishell 2008).

The embryonic patterning role of *Pax6* was initially identified through genetic mapping of the classical "small eye" (*sey*) mouse mutant (Hill *et al.* 1991). *Pax6* is initially detected in the developing forebrain at E8 and is crucial for cortical development and as mentioned, to establish the dorsal-ventral border (Stoykova and Gruss 1994). Within the neural tube, *Pax6* expression is down regulated in ventral regions, simultaneous with the up regulation of *Nkx2.1* in this region, thus instantaneously setting up the DV border on the basis of differential gene expression (Crossley *et al.* 2001; Sussel *et al.* 1999; Toresson *et al.* 2000). In *Pax6* KO mice (*Pax6$^{-/-}$*)*,* there is a shift in the cortical-striatal boundary (Stoykova *et al.* 1997), the cortical markers *Ngn1/2* and *Emx1* are down regulated at the expense of ectopic expression of the ventral markers, *Dlx1/2*, *Ascl1* and *Gsx2* in dorsal regions of the telencephalon (Stoykova *et al.* 1996; Stoykova *et al.* 2000; Toresson *et al.* 2000). *Nkx2.1* also expands dorsally into the LGE shifting the LGE-MGE border (Stoykova *et al.* 2000).

Gsx2 is first detected in the developing forebrain between E9 and E10 and is expressed in the vLGE. *Gsx2* KO mice (*Gsx2$^{-/-}$*) have the opposite phenotype to *Pax6* KO mice; there is ectopic expression of *Pax6* and *Ngn2* in the LGE together with the subsequent loss of *Ascl1* and *Dlx2* from this region (Corbin *et al.* 2000; Toresson *et al.* 2000; Yun *et al.* 2001). There was a reduction in the size of the LGE at E12 (Szucsik *et al.* 1997), which by E18.5 led to a reduction in the size of the striatum and a decrease in striatal projection neurons, which was confirmed through a decrease of DARPP-32 32 and the

earlier MSN marker, *Foxp1* (Corbin *et al.* 2000; Toresson *et al.* 2000; Yun *et al.* 2001). However, there was a slight increase in the striatal-matrix marker calbindin. These results suggest that *Gsx2* is a crucial inducer of *Ascl1, Dlx1,* and *Dlx2,* genes associated with the development of patch neurons. However, in mice that lack both *Gsx2* and *Pax6* ($Gsx2^{-/-}$ and $Pax6^{-/-}$), the phenotype observed was more subtle than either single mutation, as in the in $Shh^{-/-}Gli3^{-/-}$ double KO mice (Corbin *et al.* 2000).

Gsx1, a gene closely related to *Gsx2*, is also expressed in the ventral telencephalon, where its expression is restricted to the ventral most region of the LGE (Toresson and Campbell 2001; Valerius *et al.* 1995; Yun *et al.* 2003). Expression is also evident in the MGE (Long *et al.* 2009). It is thought that *Gsx1* can partially compensate for the phenotype observed in $Gsx2^{-/-}$ mice (Toresson and Campbell 2001; Yun *et al.* 2003). In the $Gsx2^{-/-}$ KO mice, *Gsx1* expression expands throughout the LGE between E11 and E14.5 and shows a similar expression pattern to *Ascl1*. Until recently, the role of *Gsx1* has remained elusive as no phenotype has been discovered through using genetic KO mice. Pei et al. (Pei *et al.* 2011) have shown that *Gsx1* and *Gsx2* differentially regulate the maturation of LGE progenitors. Gain-of-function experiments revealed that Gsx2 maintains LGE progenitors in an undifferentiated position before *Gsx1*, in part through the down regulation of *Gsx2,* directs the progenitors to acquire a mature neuronal phenotype (Pei *et al.* 2011). This is shown in Figure 1.12. These novel results indicate that the Gsx genes regulate LGE patterning through a controlled balance of signalling allowing proliferation and differentiation of neuronal progenitors.

1.4.13 **Ascl1**

Ascl1 is a basic helix loop helix (bHLH) TF that has a primary role in the correct development of the ventral telencephalon and relies on *Gsx2* for normal expression (Casarosa *et al.* 1999; Corbin *et al.* 2000; Toresson *et al.* 2000; Yun *et al.* 2001). *Ascl1* is expressed throughout the ventral telencephalon but its associated protein, ASCL1, is only present in the VZ and SVZ, the area where neuronal precursor cells reside (Porteus *et al.* 1994). When *Ascl1* was ectopically expressed in the dorsal telencephalon, it was able to induce neurons to express *Dlx1/2* at the expense of cortical markers (Wilson and Rubenstein 2000). It was concluded that *Ascl1* can interact with *Dlx1/2,* that in turn activates GAD/67, the rate-limiting enzyme for

GABAergic synthesis, and the two combined, function to facilitate aspects of GABAergic differentiation in the telencephalon (Casarosa *et al.* 1999; Fode *et al.* 2000). However, in *Ascl1* KO mice (*Ascl1*$^{-/-}$), *Dlx1/2* and Gad/67 are still expressed in the ventral telencephalon (Casarosa *et al.* 1999). Together with the fact that these developing neurons can still acquire a GABAergic phenotype, it seems that there is an element of redundancy in this signalling pathway and/or the involvement of other genes not yet identified. Expression of *Gsx2* in *Ascl1*$^{-/-}$ KO mice is unchanged at E12.5, but by E18.5 there is an increase in *Gsx2* expressing cells suggesting that *Ascl*1 has the additional role of repressing *Gsx2* later in development (Wang *et al.* 2009). This suggested interaction is shown in Figure 1.12.

Ascl1$^{-/-}$ KO mice also show a reduction in the number of early born striatal (cholinergic) and cortical (GABAergic) interneurons and a reduction in size of the MGE (Casarosa *et al.* 1999). This phenotype can be explained by the initial loss of precursor cells in the SVZ, which subsequently leads to a decrease in neurons populating the MZ (Casarosa *et al.* 1999; Marin *et al.* 2000). Expectantly, tyrosine hydroxylase (TH), DR2 and enkephalin positive neurons were only slightly reduced in the mutants (Marin *et al.* 2000). From these experiments, it can be concluded that *Ascl1* has the dual role of specifying precursors and controlling the timing of their differentiation, principally in the MGE, and possibly has a role in the LGE, although it is not crucial in this later eminence (Marin *et al.* 2000; Yun *et al.* 2003).

Recent experiments by Castro and colleagues have looked more closely at the precise mechanisms by which *Ascl1* controls proliferation of neuronal precursors (Castro *et al.* 2011). Gene expression analysis from mouse primary tissue and neural stem cell cultures showed that *Ascl1* had a role in regulating cell cycle progression and that there was a direct association between neural progenitor expansion and the corresponding phases of cell cycle exit and neuronal differentiation (Castro *et al.* 2011). In summary, *Ascl1* is autonomously involved in patterning of early telencephalic progenitors (~E10.5) and non-autonomously involved in repressing the differentiation of adjacent progenitors (Casarosa *et al.* 1999). Following *Ascl1* aiding neurogenesis, *Dlx1* and *2* repress *Ascl1* and to promote terminal neuronal differentiation (Yun *et al.* 2002). The relationship between these TFs is crucial for MSN development and triple KO mice have shown aberrant MSN differentiation (Long *et al.* 2009).

1.4.14 **The Dlx Family**

The *Dlx* family bears homology to the drosophila distal less-homeobox gene family of which there are 6 murine members, 4 of which are expressed in the developing MGE and LGE (Liu *et al.* 1997). *Dlx1* and *Dlx2* are expressed by subsets of progenitor cells in the VZ by E10.5 and by the majority of cells in the SVZ with expression switching off as cells start to migrate and differentiate in the MZ. (Nery *et al.* 2003; Porteus *et al.* 1994; Yun *et al.* 2002). *Dlx5* and *Dlx6* are expressed in the SVZ and MZ only (Anderson *et al.* 1997). Single *Dlx1* or *Dlx2* KO mice show no noticeable forebrain defects; although in the absence of both genes there is arrested migration of matrix-born neurons within the SVZ, yet striatal development is not stopped completely, and this phenotype suggests other genes are involved in neuronal differentiation and migration. (Anderson *et al.* 1997; Nery *et al.* 2003).

Dlx1 and *2* activate GAD67, an enzyme needed for GABA synthesis which is found in neuronal precursors of the SVZ, and in differentiating neurons of the MZ of the ventral telencephalon (Casarosa *et al.* 1999). In *Dlx1/2$^{-/-}$* KO mice there are decreased levels of GAD67 in the dLGE (Long *et al.* 2007). It is has been suggested that *Dlx1/2* indirectly activate GAD67 and that cooperation with other proteins is needed to promote a GABA neuronal phenotype (Kuwajima *et al.* 2006).

1.4.15 **Nkx2.1**

Nkx2.1 is expressed exclusively in the MGE and is another homeodomain protein. *Nkx2.1* is needed for ventral specification of the telencephalon where it acts to repress LGE identity, and it is also important in the development of striatal interneurons (Jain *et al.* 2001; Sussel *et al.* 1999). *Nkx2.1* is induced by Shh at E8 (Ericson *et al.* 1995), and as earlier mentioned, inhibition of *Shh* leads to reduced expression of *Nkx2.1* and dorsalisation of the ventral embryo (Chiang *et al.* 1996). In the *Nkx2.1* KO mouse (*Nkx2.1$^{-/-}$*)*,* the MGE is poorly formed and a DV switch is evident; the aberrant MGE shows properties similar to the LGE rather than the MGE, for example some cells have been shown to express DARPP-32 (Sussel *et al.* 1999). The loss of *Nkx2.1* also showed a reduction of GABA and calbindin positive neurons from the cortex (Sussel *et al.* 1999) as well as loss of early migration of *Dlx2*-expressing progenitors (Nery *et al.* 2003).

Gene	Summary of expression patterns and knock out phenotypes	Key References
Pax6	*Pax6* is expressed in a dorsal (high) to ventral (low) gradient and is initially detected in the developing forebrain at E8 - Pax6 is crucial for cortical development and to establish the dorsal-ventral border - In *Pax6*$^{-/-}$ mice, there is a shift in the cortical-striatal boundary, the cortical markers *Ngn1/2* and *Emx1* are down regulated and the ventral markers, *Dlx1/2*, *Ascl1* and *Gsx2* are expressed in dorsal regions of the telencephalon	(Stoykova and Gruss 1994) (Stoykova *et al.* 1997) (Stoykova *et al.* 2000) (Toresson *et al.* 2000)
Gsx1/Gsx2	- Expressed from ~E9.5 in the LGE - In *Gsx2*$^{-/-}$ mice dorsalisation of the ventral telencephalon is apparent with a loss of *Ascl1* and *Dlx2* and a reduction in the size of the LGE at E12 that leads to a reduction in the striatum by E18.5 - In the *Gsx2*$^{-/-}$ mice there is a decrease in the number of DARPP-32 positive neurons *Gsx2* is an inducer of *Ascl1*, *Dlx1* and *2* and represses dorsal character in the vLGE partially through inhibition of *Pax6* *Gsx2* maintains LGE progenitors in a un-differentiated position *Gsx1*, in part through the down regulation of Gsx2, directs progenitors to a mature phenotype	(Corbin *et al.* 2000) (Yun *et al.* 2003) (Toresson *et al.* 2000) (Pei *et al.* 2011)
Ascl1	- Expressed in the VZ and SVZ of the telencephalon - When *Ascl1* is ectopically expressed in the dorsal telencephalon neurons express *Dlx1/2* at the expense of cortical markers (e.g. *Pax6*) *Ascl1* specifies neuronal precursors and controls the timing of their differentiation *Ascl1* interacts with *Dlx1/2* to activate GAD67 to facilitate GABAergic differentiation in the telencephalon - Inhibits *Gsx2*	(Casarosa *et al.* 1999) (Wang *et al.* 2009) (Marin *et al.* 2000) (Castro *et al.* 2011)
Dlx1/2	- Expressed in the VZ and SVZ and is switched off as cells start to differentiate - Single mutations of *Dlx1* or *2* show no forebrain defects; in double KO mice there is an abnormal SVZ leading to arrested migration of matrix neurons, but striatal development is not stopped completely - Loss of FOXP1 and DARPP-32 expression in *Dlx1/2* double KO mice	**(Anderson *et al.* 1997)** (Nery *et al.* 2003) (Long *et al.* 2009)
Nkx2.1	*Nkx2.1* is expressed exclusively in the MGE, where it acts to repress LGE identity - Induced by *Shh* at E8 - In *Nkx2.1*$^{-/-}$ mice the MGE is not properly formed and LGE markers are expressed	(Chiang *et al.* 1996) (Sussel *et al.* 1999)

Table 1.2 Summary of key genes implicated in dorsal ventral patterning. The main roles of these genes are highlighted together with the phenotypic consequences of what happens when a copy/copies are removed.

It is apparent that DV patterning of the telencephalon requires the precise orchestration of several genes and TFs that work in synergy to ensure the correct development of the striatum. The genes outlined below are largely expressed later in striatal development, and are downstream of the genes previously described.

1.4.16 **Nolz1 (*Znf503*)**

Nolz1 (Znf503) is a zinc finger TF that has been shown to be exclusively expressed in the ventral LGE and is absent from the MGE and the developing pallium (Urban *et al.* 2010). This TF has RA response elements (RARE) in its promoter region, and, as mentioned, is a downstream target of this morphogen. It is also reduced in *Gsx2* KO mice suggesting that it is downstream of this TF (Urban *et al.* 2010). *In situ* hybridisations showed that *Nolz1* expression was high in the SVZ and VZ with limited expression in the MZ. Expression in mice was highest throughout embryonic stages in proliferating neurons only, peaking at E14.5, with expression decreasing upon neuronal differentiation. Therefore, it can be concluded that *Nolz1* indirectly contributes to striatal neurogenesis by promoting RA signalling in the LGE (Urban *et al.* 2010). Expression is still seen in adulthood but is greatly reduced. This pathway is shown in Figure 1.13.

1.4.17 **Ctip2 (*Bcl11b*)**

Ctip2 (B cell leukemia/lymphoma 11B) is a TF that is expressed in the developing striatum and cortex and its expression persists throughout adulthood. CTIP2 has been used as a marker of MSNs as it co-localizes with DARPP-32 in the adult striatum (Arlotta *et al.* 2008). Additionally it is used to label layer V of the cortex (Arlotta *et al.* 2005). At E14.5 in the *Ctip2* $^{-/-}$ KO mice, there was no difference in the expression of *Nolz1* but there was a decrease in *Foxp1,*thus implying neuronal birth is not affected in the KO mice but migration and differentiation of MSNs are (Arlotta *et al.* 2008). This result is consistent with the understanding that in the developing striatum *Ctip2* is expressed in the MZ and is therefore associated with early post-mitotic MSNs (Arlotta *et al.* 2008). At P0 in the *Ctip2*$^{-/-}$ KO mice, MSNs failed to differentiate and mature into MSNs when compared with WT littermates. Specifically, the MSNs failed to form into patches leading to disrupted patch-matrix organization (Arlotta *et al.* 2008). CTIP2 expression has not been associated with interneurons and thus neuronal subtype was not

affected in the *Ctip*2$^{-/-}$ KO mice. In summary, *Ctip2* is an important regulator of MSN differentiation, striatal patch development, and the organization of the correct cellular architecture of the striatum.

1.4.18 **Ebf1 (*Olf1*)**

Ebf1 (*Olf1*) is a TF that is expressed in the MGE and LGE from E11 to E17.5; expression in the MGE is down regulated at the later stage (Garel *et al.* 1999). At E17.5 *Ebf1* expression is seen throughout the MZ of the LGE, and also in a few post mitotic cells in the SVZ. This expression is maintained at birth (P0) with the exception of groups of cells that resemble striatal "patches" which was confirmed through TH staining (Garel *et al.* 1999). In the *Ebf1* KO (*Ebf1*$^{-/-}$), cell proliferation in the VZ or SVZ was not affected, but there was rostro-caudal expansion of the SVZ markers such as *SCIP/OCT6, RARα, EphA4* and *Dlx5* into the MZ at the expense of two MZ markers, *CRAPB1* and *cadherin-8* (Garel *et al.* 1999). These results show that *Ebf1* is an important gene needed for the correct transition and differentiation of neurons from the SVZ to the MZ during development. Furthermore, in the KO mice from E18.5 there is a decrease in the size of the striatum; this phenotype continues to P20 where it is very profound and the cells appear less dense than in controls which was attributed to an increase in cell death at E18.5.

At birth, TH and DARPP-32 (patch markers) were not altered in the *Ebf1*$^{-/-}$ when compared to controls; however, calbindin (CaBP) a matrix marker was reduced in the *Ebf1*$^{-/-}$ mutant when compared to controls. Interneurons were not affected. Therefore, the role of *Ebf1* is to ensure the correct migration and differentiation of matrix neurons from the SVZ to the MZ. As the *Dlx1/2* double mutant also affects the matrix compartment (Anderson *et al.* 1997) of the developing striatum, it is thought perhaps that *Ebf1* is downstream of these genes. This proposed pathway is shown in Figure 1.13.

1.4.19 **Helios (*Ikzf2*)**

Recently the Canals' group in Barcelona detected a novel marker of MSNs. Helios (*Ikzf2*) is a member of the Ikaros (*Ikzf*) family of TFs, which is expressed in the LGE from E14.5 with expression peaking at E18.5 before disappearing during post natal development (Martin-Ibanez *et al.* 2012). It was shown that Helios is associated with

immature neurons in the SVZ and MZ as it co-stains with NESTIN. At P3, Helios did not co-localise with NEUN or DARPP-32, suggesting that it was associated with later born matrix neurons as opposed to earlier born patch neurons; the authors suggest co-localisation with CTIP2 and FOXP1 confirmed this (Martin-Ibanez *et al.* 2012). Helios expression was not detected in *Dlx1/2* and *Gsx2* KO mice but its expression was maintained in *Ascl1* mutants, suggesting it is involved in a MSN lineage independent of *Ascl1* (Martin-Ibanez *et al.* 2012). This proposed pathway is shown in Figure 1.13.
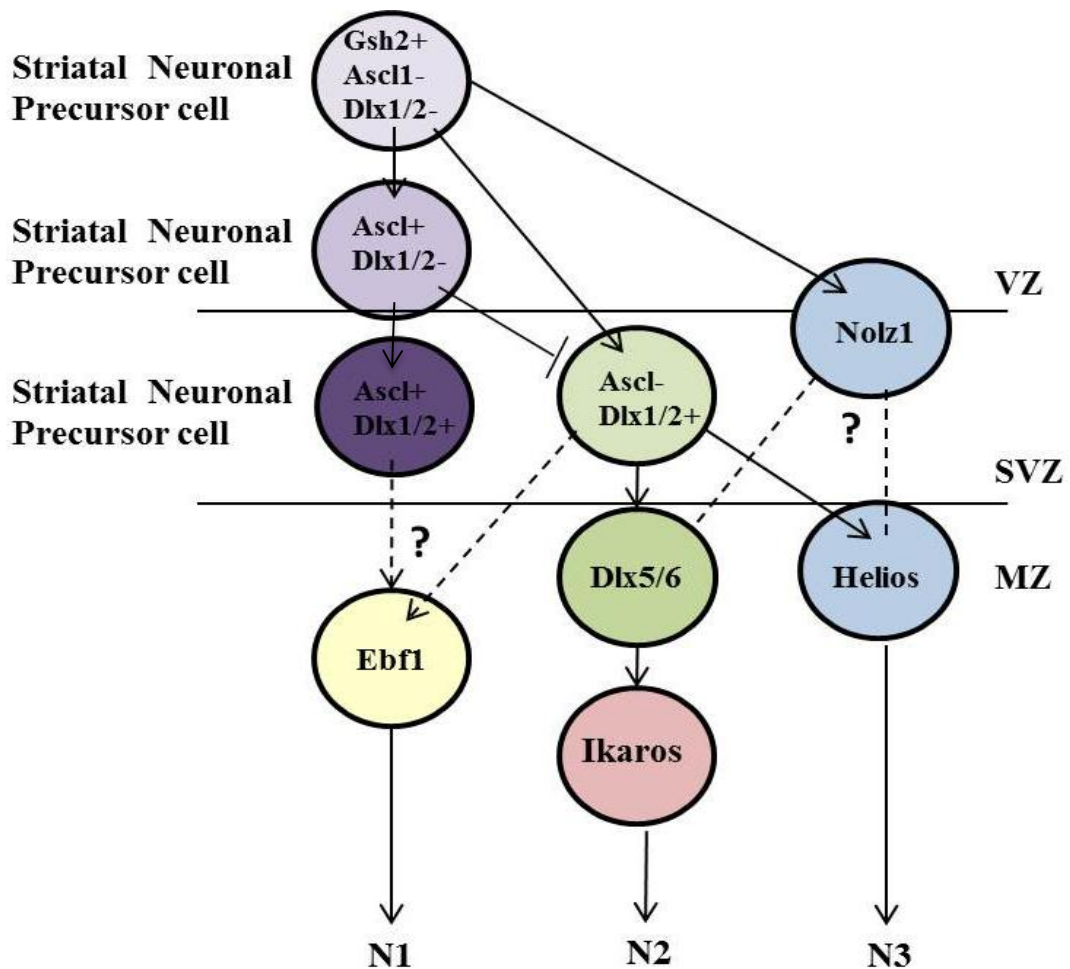
Figure 1.13 Proposed model of the different genetic lineages contributing to striatal development. These genetic interactions are based on a model by (Martin-Ibanez *et al.* 2012) which is largely based on the information learnt from genetic knock out models in mice. The dashed lines represent possible downstream targets of genes but have not be proven yet. *Abbreviations: VZ- Ventricular zone, SVZ- sub-ventricular zone, MZ-Mantle zone, N- Neuronal lineage. Figure adapted from (Martin-Ibanez et al. 2012)*

1.5   **Huntington's** Disease

The main aim for studying the function of *Foxp1* was to look at its role in striatal development so that new knowledge could be applied to protocols that aim to replace the MSNs lost in Huntington's disease (HD). HD is an inherited, autosomal dominant neurodegenerative disorder, which at a macroscopic level is characterised by the loss of MSNs in the head of the caudate and putamen, collectively termed the "neostriatum", shown in Figure 1.14. As the disease progresses and neuronal loss is increased, the atrophy of the caudate and putamen worsen and there is expansion of the lateral ventricles and shrinkage of the cortex. The adult onset of the disease is characterised by neurological and psychiatric symptoms with the most obvious motor impairment in HD presenting as chorea. As the disease progresses, motor symptoms worsen and walking becomes difficult, as does speaking and eating (Craufurd and Snowden 2002). Psychiatric disturbances are also common and often manifest before the onset of motor disturbances. Depression, anxiety, irritability, and reduced motivation and attention are commonly seen and, taken together these symptoms, can make patients feel vulnerable and depressed, leading to a compromised quality of life, and consequently suicide is a high risk factor associated with HD (Craufurd and Snowden 2002). Cognitive impairment is also seen and the disease ultimately induces dementia in patients. As HD progresses, all the associated symptoms deteriorate and the most common cause of death in HD patients is pneumonia; others include choking and nutritional deficiencies (Harris and Barraclough 1994; Lanska *et al.* 1998).

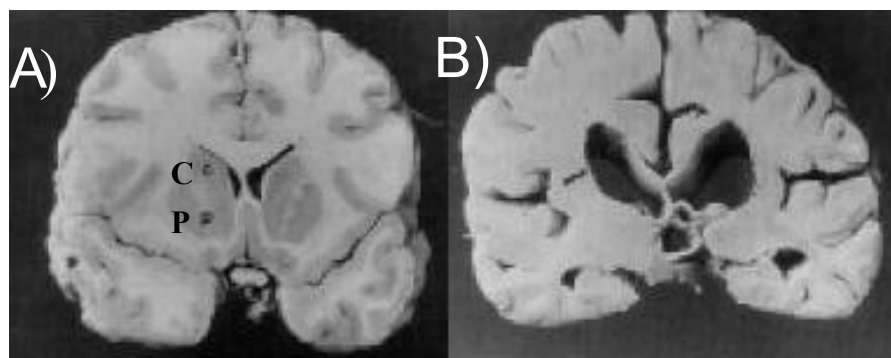**Figure 1.14 Coronal brain sections of the adult brain (A)** Normal brain showing the caudate nucleus (C) and the putamen (P). **(B)** An HD brain showing atrophy in the caudate and putamen and enlarged vesicles (Permission of Peter Harper).

1.6   <u>**HD genetics**</u>

HD was first characterised by George Huntington in 1872. Over one hundred years following his initial discovery a considerably amount more is known about the disease and its genetic cause. It is believed that the disease affects approximately 5-8 people per 100,000 in the Caucasian community with no gender preference (Harper 1997) and commonly becomes prevalent in the third and fourth decades of life with death occurring approximately 20 years following the onset of motor symptoms (Ross and Margolis 2001).

In 1993 the *Huntington's Disease Collaborative Research Group (1993)* isolated and cloned a novel gene found on the short arm of chromosome 4 (4p16.3) that today is known as Huntingtin *(Htt)*. In exon 1 of the normal *Htt* gene there is a repeated tri-nucleotide CAG (glutamine), which on average has 10-29 (median 18) consecutive repeats. HD patients have a mutation in this exon and have an expanded number of CAG repeats, ranging from 36-121 (median 44), which results in a longer protein being translated (Craufurd and Snowden 2002). Those with an intermediate repeat length (27-35 repeats) are unlikely to manifest the disease but their children have an increased risk of inheriting HD (Squitieri and Jankovic 2012). There are reports of late onset disease patients with intermediate repeat lengths (Groen *et al.* 2010); however, not all people in this range will present with the disease suggesting that other factors may be contributing to disease onset. Longer repeats, normally over 70, are associated with juvenile onset of the disease. Although the age of onset cannot be directly correlated to the number of repeats for an individual, on a population basis the number of repeats is inversely correlated with age of onset (Kremer *et al.* 1994). Currently, there are some symptomatic treatments for patients with severe chorea such as tetrabenezine (Walker 2007) but there are no disease modifying drugs.

One possible therapeutic being explored is cell transplantation, the aim of which is to replace the neurons lost in the disease with donor cells that will develop new connections and thus reform the circuitry within the host brain to alleviate disease symptoms and bring about functional improvements. The specificity of cell loss in HD makes it a good target for cell transplantation as a viable therapeutic option (Rosser and Dunnett 2003). Transplants using primary human foetal striatal tissue have

demonstrated 'proof of principle', have shown to be safe and not accelerate disease progression (Rosser *et al.* 2002), and importantly demonstrate partial functional recovery in at least some patients (Bachoud-Levi *et al.* 2006; Bachoud-Levi *et al.* 2000; Kelly *et al.* 2009).

However, there are ethical issues associated with the use of human foetal tissue that is obtained from elective termination of pregnancies, as well as logistical issues arising from the amount of foetal tissue required per patient (on average 1-2 foetal donors per side per HD patient). To date, all clinical transplants in HD have used tissue obtained from surgical terminations. Some subsequent trials will now also utilise tissue from medical terminations of pregnancy (MTOPs) (Kelly *et al.* 2011). Although the MTOPs have increased throughput of tissue, there is still a problem of tissue availability, as well as a problem of ensuring a high degree of standardisation with cell transplantation protocols. Hence the need for alternative, renewable cells sources such as ESCs and induced pluripotent stem cells (iPSC), recently reviewed for their use in cell transplantation (Perrier and Peschanski 2012; Precious and Rosser 2012).

ESCs are generated from the inner cell mass (ICM) of the developing embryo, are pluripotent and have the potential to become any cell of the three germ layers, ectoderm, endoderm or mesoderm (Evans and Kaufman 1981; Martin 1981; Thomson *et al.* 1998).iPSCs were discovered in 2006 by Yamanaka and colleagues. These are somatic cells that are capable of being re-programmed, initially by the addition of four factors, to a pluripotent stage, whereby they share the same properties as ESCs (Takahashi and Yamanaka 2006). iPSC research is currently a "hot topic" and there is an imperative to limit the number of re-programming factors used, and to understand the extent to which these cells are comparable to ESCs. Having a bank of renewable, properly specified cells would facilitate a stable source for use in transplantation (Perrier and Peschanski 2012). Despite their ability to generate large numbers of cells, hESCs must be further differentiated into specific neural phenotypes. In the case of HD, the target cells are MSNs. This remains the major obstacle to their clinical application (Dunnett and Rosser 2013; Rosser *et al.* 2011). The development and differentiation of striatal MSNs is a complex process that requires tight genetic regulation. Fully understanding the spatial and temporal expression of all the genes involved and subsequent interactions will be crucial for optimising protocols to direct

the fate of renewable cell sources to a fully functional MSN phenotype. DARPP-32 is not expressed until later in MSN development, which is a major problem for the regenerative medicine field, where there is a need to identify MSNs at immature stages for transplantation strategies. Identifying specific genes to detect MSN precursors, such as *Foxp1*, rather than relying on markers of terminally differentiated MSNs, would accelerate the process of generating donor MSNs. Moreover, earlier markers of putative MSNs could be used to track progressive neuronal differentiation in grafts over time.

The potential for ESCs to be directed to MSNs has been demonstrated in animal models and there are published protocols for the generation of DARPP-32 positive neurons from human ESCs (hESCs) (Aubry *et al.* 2008; Carri *et al.* 2013; Ma *et al.* 2012; Nicoleau *et al.* 2013; Song *et al.* 2007) and are summarised in Table 1.3. Briefly, hESC generated from the different protocols were all successfully grafted into quinolinic acid (QA) lesioned (mimics HD by depleting MSNs in the striatum, sparing the interneurons (Beal et al., 1987) rat or mouse brains. The differentiated cells in all the reports were grafted at various time points during the differentiation protocol, but consistently once there was down regulation of proliferation markers and up-regulation of early neuronal makers such as nestin. Differences in the number of DARPP-32 positive neurons occurred as a direct result of the stage of the differentiation protocol at which the cells were transplanted at. This highlights the need for proper *in vitro* characterisation of renewable cells to determine the crucial stage between proliferation and differentiation, at which the cells need to be transplanted.

The main issues with all these published methods are the reproducibility within groups and the length and complexity of protocols which increases the room for error and makes GMP translation difficult, therefore emphasising the need for a standardised, simplified protocol. Additionally, the functionality of these cells also needs to be fully characterised to ensure a correct and mature phenotype is achieved. It is also likely that more specific MSN factors are required within the culture system to increase the number of MSNs for use in cell transplantation. More thorough behavioural characterisation post transplantation, using larger cohorts and extended behavioural assessments, is also needed if one is to definitively associate motor and cognitive recovery with cell transplantation therapy.

Protocol	Cell Type	Host	Transplant	Brief Summary of Results
(Song *et al.* 2007)	hESC1 (Miz)	QA lesion rat striatum	20,000 cells Survival 3 weeks	No tumours. Improved apomorphine rotations at 1, 2 and 3 weeks compared to shame group.
(Aubry *et al.* 2008)	hESCs (H9)	QA lesion striatum into nude rats	50,000-200,000 cells transplanted Survival 4-6 weeks	Grafts from "early" stage cells (day 21-30 of the protocol) showed no DARPP-32 expressing cells and developed "teratoma-like regions" whilst cells grafted from the "later" stage (day 46-59) of the protocol showed clusters of DARPP-32 positive cells (21% of NEUN population) and contained P-zones, but also showed overgrowth 13-15 weeks after the graft.
(Ma *et al.* 2012)	hESCS	QA lesion striatum into SCID mice	100,000 cells transplanted Survival 4 months (16 weeks)	Shorter protocol than previous attempts to generate LGE neural precursors that predominately differentiated into DARPP-32-expressing neurons. Cells grafted after 40 days *in vitro*, no overgrowth reported and 58.6% of the grafted neurons were GABA and DARPP-32 positive. Behavioural recovery seen on the rotarod and an increase in stride length due to the host cortical and nigral inputs to the grafts. Projections afforded to the SN from the grafts.
(Carri *et al.* 2013)	hESCs (H9 and HS401)	QA lesion striatum of rats Daily cyclosporine	500,00 cells transplanted Survival at 3, 6 and 9 weeks	Used the same concentration of SHH as *Ma et al* to induce a ventral telencephalic identity and characterised extensively to ensure LGE precursors. Cells grafted at Day 38 of the protocol, DARPP-32, FOXP1 and found in the grafts but not quantified. Amphetamine-induced rotations were compared before and after grafting and although results hinted at there being functional recovery, animal numbers were too low to suggest a significant behavioural effect.
(Nicoleau et al., 2013)	hESCs (H9)	QA lesion striatum into nude rats	150,000 cells transplanted Survival at 5 months.	Optimised concentration of SHH and WNT signalling to produce human ventral-telencephalic precursors that were characterized extensively before grating. Day 25 differentiated hESC grafted, DARPP-32 and FOXP1 found in grafts, no behaviour carried out yet.

Table 1.3 Summary of key protocols to date that direct hESCs towards functional DARPP-32 positive MSNs

1.6.1 **Foxp1 and HD**

Interestingly a direct link between *Foxp1* and HD has also been reported. An Affymetrix screen using tissue from the striate of the TG R6/1 HD mice showed that FOXP1 was significantly down regulated when compared to control samples. Similarly, this same result was identified in the post mortems of HD patients (Desplats *et al.* 2006). Last year, a genome-wide association study (GWAS) was undertaken using samples from a TG Q111 HD cell line in which *Foxp1* was over expressed. The genes that were significantly up regulated were grouped and were shown to be associated with signalling pathways connected with HD or with immune signalling (Tang *et al.* 2012). As a way to validate the *in vitro* GWAS study, transcriptional analysis was also studied *in vivo* in a different TG HD mouse line (YAC128) in which *Foxp1* expression has not shown to be differentially expressed when compared with age-matched WT control mice. To look at the *in vivo* effects of FOXP1 on HD, a virus either over expressing FOXP1 or expressing GFP (control) was injected bilaterally into the striatum of YAC128 HD TG mice at 3 months of age. Subsequent microarray analysis showed that the genes that were significantly up regulated were also associated with the immune signalling (Tang *et al.* 2012).

When the results were compared with previous microarrays from other TG HD mouse lines or from human brain post mortems (where *Foxp1* is down regulated) (Desplats *et al.* 2006), there was a negative correlation between the genes that were down regulated in the disease samples compared to the samples in which *Foxp1* was over expressed i.e. genes involved in inflammation and gliosis were up regulated in diseased brains but down regulated in the samples over expressing *Foxp1* (Tang *et al.* 2012). Similarly histological analysis from YAC128 mouse sections in which *Foxp1* was over expressed, showed a decrease in GFAP staining and microglia markers. This suggests that loss of optimal FOXP1 expression leads to less repression of immune related genes, resulting in an increase in the damaging cytokines observed in the HD brain. As FOXP1 staining has been shown within HTT inclusions commonly found throughout the brains of R6/1 mice (Tang *et al.* 2012), immunopercipitation (IP) of FOXP1 and HTT was undertaken and showed that FOXP1 and HTT are capable of binding with each other. It was therefore suggested that the reduced FOXP1 levels in HD brains is caused by HTT-mediated sequestration of FOXP1 and subsequent loss of FOXP1 self-

regulation. Overall these results suggest that FOXP1 is a repressor of gliosis and that in WT conditions FOXP1 has a neuroprotective role whereby it counteracts the stimuli that are associated with glia response to pathogens (Tang *et al.* 2012).

1.7 **Autism Spectrum Disorder (ASD) and associated disorders**

As well as being associated with HD, *de novo* and micro-deletions in the human FOXP1 gene have been identified and associated with ASDs (Palumbo *et al.* 2013), (Hamdan *et al.* 2010; Horn *et al.* 2010). ADHD is a clinically heterogeneous neurodevelopmental disorder and the DSM-IV diagnostic criteria for ADHD include inattention, hyperactivity and/or impulsivity (Biederman and Faraone 2005). ADHD shares a high degree of comorbidity, and as suggested by twin studies, shares inherited factors with ASD (Lichtenstein *et al.* 2010; Ronald *et al.* 2011; Thapar *et al.* 2013). For example some ASD patients have been shown to be associated with poor attentional switching, resembling the inattention seen in ADHD patients (Polderman *et al.* 2013). ADHD is the most prevalent psychiatric disorder diagnosed in youths with a global prevalence of 3-7% in children and adolescents (Nair *et al.* 2006) but since no formal objective tests for its diagnosis exist, this may be an underestimation (Polanczyk et al., 2007).

ADHD is highly heritable and may result from several different gene mutations, together with environmental factors (reviewed in (Thapar *et al.* 2013)). From concordant twin studies, it has been estimated that the heritability of ADHD is 76% (Faraone *et al.* 2005). Following candidate gene studies based on case-control and family-based studies odds ratios (ORs) for the association between gene mutation and ADHD phenotype were analysed (Faraone et al., 2005). From these studies a number of genes, many of which relate to catecholamine function were found to be associated with the aetiology of ADHD; the dopamine D4 receptor gene (*DRD4*), the dopamine D5 receptor gene (*DRD5*), the dopamine active transporter gene (*DAT*), the dopamine beta hydroxylase gene (*DBH*), the serotonin transporter gene (*5-HTT*), the serotonin receptor *HTR1B* gene and the synaptosomal associated protein-25 gene (*SNAP-25*) (Faraone *et al.* 2005). The ORs for the association between gene mutation and ADHD phenotype were small stressing that ADHD is likely caused by many genes of little effect. Thus it is highly likely additional genes may be found through future candidate gene studies

with larger population sizes that will enhance understanding of the complexity of the genetics involved in ADHD.

The precise aetiology of ADHD is unknown but it is widely thought that at the physiological level, ADHD is caused by dysregualtion of the catecholaminergic system leading to imbalances in the dopamine (DA) and noradrenaline (NA) neurotransmitter systems (Arnsten 2009; Biederman and Faraone 2005). Indeed, current treatment focuses on agents that interfere with these systems, such as catecholaminergic re-uptake inhibitors that increase extracellular concentration of DA and/or NA. Specifically the CNS stimulants methylphenidate (Ritalin) (DA and NA re-uptake inhibitor) and atomoxetine (NA re-uptake inhibitor) can be prescribed for the treatment of children with severe and persistent symptoms of ADHD. The later drug is not processed in the nucleus accumbens and thus does not have the addictive element associated with it that Ritalin does.

1.7.1 **Animal models of ADHD**

To gain a better understanding of the pathology of disease states and to develop therapeutic platforms for clinical trials, animal models with good construct (physiologically mimic the disease) and face validity (shown similar phenotype to the disease) are required that can provide the necessary predicative validity (respond to the drugs associated with the disease) for the study of neuropathology and associated therapeutic efficacy in clinical trials. Current animal models of ADHD include those induced chemically (such as postnatal exposure to alcohol) and environmentally (rat pups reared in isolation), and importantly for this highly heritable condition, a variety of genetic models.

The most widely used genetic model is the spontaneously hypertensive rat (SHR) (Sagvolden *et al.* 1993), which displays an ADHD-like behavioural phenotype and has predictive validity, although the high blood pressure also associated with this model is problematic as it has not been associated with ADHD. Attempts to breed out the hypertension resulted in animals with reduced hyperactivity that no longer responded to Ritalin. Additionally, the control line used in behavioural testing is questionable, as they are a typically lethargic species (Drolet *et al.* 2002). The DA transporter KO (DAT-KO)

mouse lacks the DA transporter gene (Giros *et al.* 1996) and shows increased DA levels and hyperactivity that can be reduced by psycostimulants (Gainetdinov *et al.* 1998)ʼ(Jones *et al.* 1998). However, Ritalin and Amphetamine both target DAT, thus the mechanistic processing of these drugs in this model are unknown. Secondly, there is no evidence for hyper-dopaminergic tone in ADHD patients (Arime *et al.* 2011; Cheon *et al.* 2004). Another model, the thyroid hormone receptor (TR)-beat (1) TG mouse that carries a mutant human TRβ1 gene meets face, predicative and construct validity for a model of ADHD, but the role of the thyroid system in ADHD is still unknown (Arime *et al.* 2011). A number of other models exist, such as the coloboma mouse (Searle 1966) (mutation in the SNAP-25 gene), the alpha synuclein lacking mouse, the acallosal mouse strain, and the Naples high excitability strain (bred for excitability), which provide face validity and construct validity to variable degrees, but in which predictive validity is lacking or low (reviewed in (Sontag *et al.* 2010)). Recently, astrocyte-specific disruption of SynCAM1, thought to lead to deficits in astrocyte adhesion, has produced a mouse that is hyperactive and impulsive and shows a reduction in hyperactivity when amphetamine is administrated in the open field task (Sandau *et al.* 2012). However, to date, attention deficits and impulsivity have not been properly characterised in this model and it is currently unclear which brain regions were affected by this genetic disruption. To summarise, many animal models of ADHD already exist but owing to the heterogeneity of the disease, and the likelihood it is caused by many genes of little effect, offer the opportunity for novel models to be generated.

1.8 **Genetic Knockouts (KOs)**

In order to study transcriptional regulation in discrete populations of developing cells, gene-targeting strategies can be employed. To study the function of a gene, it can be knocked out during development and changes in the immature or adult phenotype can be assessed. Genetic KO studies are routinely undertaken in mice but are frequently used in other model organisms such as *Caenorhabditis elegans* and recently *Dictyostelium discoideum*. For the purposes of my PhD, I will discuss the use of genetic KOs in mice. Mice are commonly used to study the function of genes in neuronal development as they show many similarities in their nervous system to humans as well as convenience as a lab animal. A conventional genetic KO arises from mating two mice together that are heterozygous for the gene of interest (GOI). This will, according to

Mendelian inheritance, produce a quarter of first generation (F1) offspring that are homozygous KOs for the GOI, a quarter of offspring that are WT and half that are heterozygotes. However, this breeding strategy knocks out the gene everywhere it is expressed, therefore if the gene is crucial for development it is possible the embryo will die without its expression, these KOs are termed embryonically lethal. To bypass such lethality's a CKO can be made which is commonly mediated through the Cre-Lox method. Specifically this method utilises the Cre tyrosine recombinase enzyme (Cre) that was originally isolated from the bacteriophage P1. This enzyme has the ability to catalyse recombination between two 34 base pair (bp) *LoxP* sites also located in the DNA of the bacteriophage (Gaveriaux-Ruff and Kieffer 2007). When the Cre enzyme and LoxP sites meet, there is an irreversible excision of the DNA located between the two *LoxP* sites. This system was first trialled in mammalian cells in 1988 (Sauer and Henderson, 1988) and has successfully been manipulated for use in mouse genetic KO technology, as there are no endogenous *LoxP* sites present in the mouse genome. Briefly to create a "floxed" allele the isolated genomic clone is engineered so that two LoxP sites flank a critical exon(s). Upon successful ESC selection and subsequent breeding, "floxed" mice have two functional alleles as if WT, as the presence of the LoxP sites alone do not affect the phenotype. The "Cre" mouse is created via pronuclear injection, whereby a Cre enzyme is attached to a specific promoter, i.e. a promoter that drives gene expression in an area in which you want to study. When a "Cre" and a "floxed" mouse are subsequently bred together a quarter of the offspring should have the GOI conditionally knocked out.

If one has decided that a CKO is needed, the next question is if the gene needs to be continuously turned off from a specific developmental time, i.e. "Cre-mediated recombination" which is directly dependant on the choice of promoter used to drive the Cre expression. Or, alternatively, if the gene of interest needs to be induced, which requires the Cre to be on at specific developmental time points only. Characterising the functional roles of *Foxp1* in MSN development would require the earlier approach i.e. developing a "Cre-mediated" CKO mouse line as *Foxp1* is embryonically lethal at E14.5 (Wang *et al.* 2004a). Therefore choosing the correct Cre line to drive recombination is important to ensuring that recombination occurs in the correct location and at the right time.

As previously mentioned, *Foxg1* is a TF that shows widespread expression throughout the telencephalon by E10.5 (Martynoga *et al.* 2005; Xuan *et al.* 1995). The *Foxg1*-Cre has shown to be expressed from E9.5 in the neuroepithelial cells of the telencephalon, and would be an obvious choice for striatal deletion of *Foxp1* (Hebert and McConnell 2000). This Cre has been used successfully to conditionally KO *Fgf8* in the developing telencephalon to study Notch signalling (Mason *et al.* 2005), and, recently, to KO *Arl13bin* (Higginbotham et al. 2013). However, there are several caveats to using *Foxg1*-Cre mice to produce conditional mutations. Firstly, the *Foxg1*-Cre allele is predicted to be a null allele for FOXG1 function, due to replacement of the *Foxg1* coding sequences with the Cre gene (Herbert and McConnell, 2000). Therefore, it is a possibility that any phenotype seen is from the heterozygosity of *Foxg1*. Of note, work carried out by Eagelson (2007) and colleagues showed that the presence of the Cre-recombinase downstream of the *Foxg1* promoter in C57BL/6J mice resulted in a reduction in the volume of the neocortex, striatum and hippocampus (Eagleson *et al.* 2007). Secondly, when crossed with either a ROSA26 (R26R) line (Soriano 1999) or a Z/AP line (Lobe *et al.* 1999) considerable differences were seen in reporter expression pattern. The R26R line showed expression comparable to *Foxg1* normal expression. However, the expression pattern from the Z/AP mouse line was inconsistent, and when backcrossed onto six different mouse strains, showed various expression patterns in tissues not known to express *Foxg1*, which in some instances encompassed the whole body (Hebert and McConnell 2000). Therefore, even though this Cre is preferentially expressed consistent with MSN development, its expression pattern inconsistencies would be problematic for conditionally knocking out *Foxp1*, which is widely expressed in many developing tissues including the lung and heart (Shu *et al.* 2007; Wang *et al.* 2004a). At the commencement of the project, in the absence of any commercially available, embryonic striatal specific Cre lines the Nestin-Cre and hGFAP-Cre lines, known to be expressed in neuronal precursor cells in the telencephalon, and have previously been reported to knock out genes during cortical development (Barbosa *et al.* 2008; Li *et al.* 2008), were chosen to KO *Foxp1* in the developing telencephalon.

The *Nestin*-Cre mouse line is expressed from E9 in all neuroepitehlial cells and subsequently all neurons (Tronche *et al.* 1999), and the hGFAP-Cre line is expressed in RG and is active from E13.5 (Malatesta *et al.* 2003; Zhuo *et al.* 2001). The opinion that a Cre attached to a promoter synonymous with glia should only KO the GOI in cells

fated to become astrocytes, and not neurons, should not be assumed. As discussed earlier, since 2000, considerable work, largely by Magdelana Gotz and colleagues, has shown that at least 80% of neurons are born from RG and thus this Cre should knock out *Foxp1* from E13.5. However, as eluded to earlier, even though striatal neurons are born largely from RG, they pass through this stage before the onset of hGFAP expression, thus it is likely that a CKO using this Cre would KO Foxp1 from all of the cortex, allowing the link between Foxp1 and ASDs to be explored, but only from a small population of cells in the striatum. However, it was anticipated that the Nestin Cre would KO Foxp1 from both the striatum and cortex.

1.9 <u>**Aims of thesis**</u>

It is evident from the research outlined in this introduction that the transcriptional repressor *Foxp1* is implicated in many areas of development of which telencephalon development is likely included. Results from the affymetirx screen carried out in the host lab together with the current literature and public databases have shown that *Foxp1* is highly up regulated during peak striatal development and that co-localisation is restricted to striatal projection neurons. It is also known that *Foxp1* is expressed in the developing and adult cortex, where like in the striatum, expression is restricted to cortical projection neurons, thus suggesting a general function of this TF in neuronal development.

Firstly I aim to understand the function of *Foxp1* in striatal development with the expectation that expanded knowledge of MSN differentiation will be important in identifying earlier markers of MSN precursors for use in cell protocols for cell replacement therapies in HD. Secondly, as it has already been shown that addition of *Foxp1* to hESC enhances the number of TH positive neurons, and that it is also expressed during cortical development, understanding the function of *Foxp1* may also provide a more over-arching functional role of this gene during development. For example, in other developmental areas such as myocyte development it is an important factor in mediating the switch from proliferation to differentiation thus a further understanding of function could be translatable to a variety of for cell replacement therapy protocols and also interesting for drug discovery research. The final aim will be to study the effects of the loss of *Foxp1* from the mouse cortex by creating a *Foxp1*

CKO model and linking any behavioural and or histological differences seen to diseases associated with *Foxp1*, such as ASD and associated disorders. Providing a new mouse model, caused by the loss of a single gene will also serve as an excellent platform for testing existing drugs associated with the phenotypic otucomes as well as allowing novel drugs to be tested.

<u>Main Objectives</u>

- To further characterise the expression pattern of FOXP1 throughout embryonic and postnatal development and how this relates to current MSN markers.

- To investigate *in vitro* differences in MSN development in the absence of *Foxp1* compared to controls, specifically looking at any differences in differentiation, proliferation and the electrophysiology of the cells.

- As *Foxp1*$^{-/-}$ embryos die at E14 *in vitro* experiments were restricted to this age. Therefore it was decided to look at how striatal cells from E14 WT, *Foxp1*$^{+/-}$ and *Foxp1*$^{-/-}$ embryos survive and mature once transplanted into the adult QA lesioned mouse striatum and to see if there are any genotypic differences between the grafts. Although in principal this experiment can only show how the cells survive and mature in a graft scenario, it will still facilitate one to look at how striatal neurons develop in the absence of *Foxp1* for a longer period than is possible *in vitro,* however it is understood that development will not be completely akin to as if the cells were left to mature in the mouse. It will also allow differences in DARPP-32 to be more readily identifiably as the grafted cells will have the chance to mature and to make some of their normal connections with host neurons.

- To generate and maintain a *Foxp1* CKO mouse colony that selectively depletes *Foxp1* in the adult cortex. Once the colony is developed a series of behavioural tests will be carried out that investigate specific phenotypic differences in the mice that would strengthen the link between *Foxp1* and ASDs. Suitable drugs will also be tested on the animals if specific behavioural phenotypes are found. Histological differences will also be looked for.

2 *Materials and Methods*

2.1 **Mouse Lines**

2.1.1 **Mouse Lines and Breeding**

All animal experiments were performed in agreement with local ethical guidelines and accepted animal care according to the UK Animals (Scientific Procedures) Act 1986 and its subsequent amendments.

When required to maintain colony numbers female C57BL/6 mice were bought from Charles River. When *Fox* het time mates were required breeding pairs were set up over night (O/N). The next morning females were removed and checked for the presence of a vaginal plug (before 9:30am); a plug suggested that mating had been successful. The hGFAP-Cre mouse line (FVB-Tg (GFAP-Cre) 25Mes/J) (stock #4600) and the Nestin-Cre line (B6.Cg-Tg (Nes-Cre)1Kln/J(stock#3771) were purchased from JAX laboratories. The *Foxp1* KO mouse and the *Foxp1* "floxed" mouse (*Foxp1$^{fl/fl}$*) were gifts from Professor Tucker at the University of Texas. For work outlined in Chapters 3 and 4 time mating's were set up between two *Foxp1* heterozygote mice (*Foxp1$^{+/-}$*), maintained on a C57BL/6 background. Females were checked daily for a vaginal plug, the day of plug discovery was recorded as E0. Pregnant dams were sacrificed at the required embryonic age and pups were dissected from the uterine horn as outlined in Chapter 2.1. Embryos were either snap frozen, or individual striate were dissected and individually cultured or grafted. Animals were genotyped using the tail biopsies taken during dissections.

For the *Foxp1* CKO line (discussed in Chapter 5) mice heterozygous for the *Foxp1* floxed gene (*Foxp1$^{fl/+}$*) and hGFAP-Cre were bred to mice of the same genotype, as shown in Figure 2.1. The floxed mouse has been previously engineered to have a *Lox*p sites either side of exons 11 and 12 on the *Foxp1* gene (Feng *et al.* 2010). These mice were on a Swiss 129 background strain. The possible offspring from this breeding strategy are shown in Table 2.1.
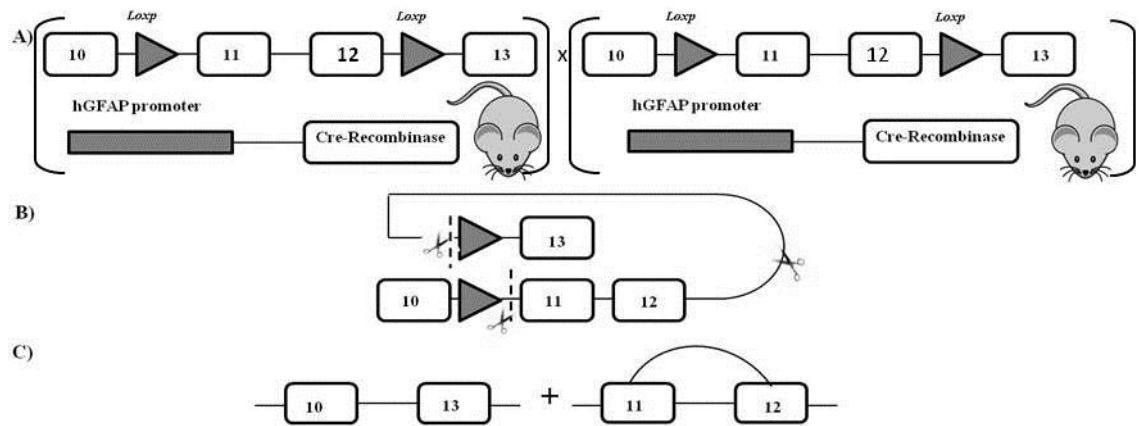
Figure 2.1 Schematic of the conditional knock out breeding strategy (A) Mice heterozygous for the *Foxp1* floxed target gene (*Foxp1*+/fl) and the h*GFAP*-Cre gene were bred to mice of the same genotype. **(B)** In the cells of the offspring where the hGFAP-Cre is expressed, and where it contacts the *loxP* sites, recombination occurs and exons 11 and 12 are excised. **(C)** Offspring that are homozygous for the *Foxp1*^{fl/fl} allele and carry the hGFAP-cre have *Foxp1* knocked out. *Boxes with numbers in represent exons.*

Floxed	Cre	Phenotype
Homozygous Floxed	Cre positive	(*Foxp1* $^{fl/fl}$/*hGFAP*$^{+/-}$) **Experimental (*Foxp1* CKOs)**
Heterozygous Floxed	Cre positive	(*Foxp1* $^{fl/+}$/*hGFAP*$^{+/-}$) **Breeder**
WT	Cre positive	**Control** (*Foxp1*$^{+/+}$/*hGFAP*$^{+/-}$)
Homozygous Floxed	Cre negative	**Control** (*Foxp1* $^{fl/fl}$/*hGFAP*$^{-/-}$)
WT	Cre negative	**WT/WT- Not used**

Table 2.1 Possible genotypes from a hGFAP/*Foxp1*$^{fl/fl}$ cross.

The *Mef2c* KO mouse and the *Mef2c* "floxed" mice (*Mef2c*$^{fl/fl}$) were gifts from Eric Olson's lab that is based at the South Western medical centre also at the University of Texas. For the *Mef2c* CKO line mice heterozygous for the KO allele (*Mef2c* $^{+/-}$) and Nestin allele (*Mef2c*$^{+/-}$/Nestin) were bred to mice heterozygous for the *Mef2c* floxed allele (*Mef2c*$^{fl/+}$), discussed in Appendix 8.

2.2 *In vitro* methods- Embryonic Analysis

2.2.1 Cell Culture – Plate Preparation and Dissection of Primary Mouse Tissue

Cells are cultured as a single-cell suspension on 13 mm glass cover slips placed in 24 or 4 well plates. To prepare a plate(s) tweezers are aseptically prepared and used to place an autoclaved glass cover slip per well. 500 µl of poly-l-lysine (PLL) (1 mg/ml) (*Sigma*) was added per well to coat the cover slips. Plates are stored at 4°C. Following incubation the PLL is removed and the cover slips are washed 3 times with sterile water. The plate(s) are then put under UV for 45 minutes before beginning culture work.

Pregnant CD1 or C57Bl/6 mice were sacrificed by cervical dislocation (Schedule 1) and their embryos were collected in Hanks Balanced Salt Solution (HBSS) (*Gibco*) at different embryonic ages. On removal of the head region (Figure 2.2A), either the brain was snap frozen, fixed in 4% PFA (see Appendix 9.1) or the striatal eminences (WGE) were dissected according to (Dunnett 1996) (Figure 2.2) and used for either RNA extraction, immunohistochemistry, cell culture, calcium imaging or for transplantation.
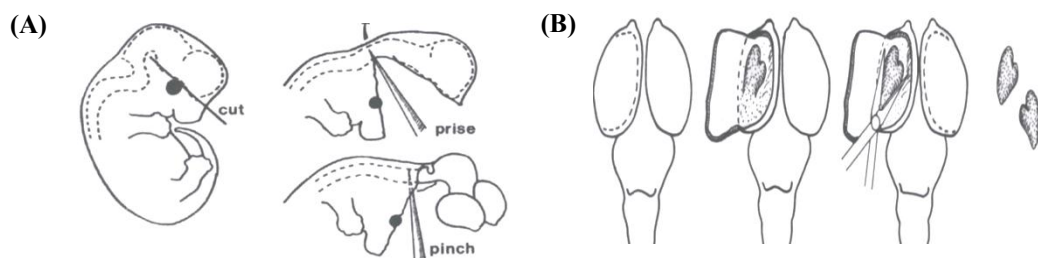
Figure 2.2 Dissection Techniques (A) A single vertical cut is made just above the eye at the base of the brain back into the ventral mesencephalic flexure. Fine forceps are used to remove the overlying skin and meninges leaving the brain free to be pulled away. **(B)** Striatum (WGE) removal. The brain is positioned on its ventral surface with the dorsal cortex facing upwards. A longitudinal cut is made through the medial cortex which once folded over exposes the striatum on the floor of the lateral ventricle. Iridectomy scissors are used to remove the striatum from both hemispheres (Adapted from Dunnett, 1996).

2.2.2 **WGE primary mouse cultures**

HBSS media was removed from the tissue and replaced with 0.1 % Trypsin (*Worthington Biochemical Corporation*) (*Sigma*) (see Appendix 9.1) and 0.1 % DNAse for an incubation period of 20 minutes at 37°C. Trypsin inhibitor (*Sigma*) was then added to the tissue for a further 5-minute incubation period. The tissue was then washed with Dulbecco's modified Eagle's medium (DMEM-F12) (*Life technologies*) supplemented with 1% PS (penicillin, streptomycin) (*Life technologies*), and collected by centrifugation at 1000 rpm for 3 minutes. The supernatant was discarded and the remaining pellet (cells) was re-suspended in 200 µl of DMEM/F-12 and triturated ~ 15 times with a 200 µl Gilson pipette to produce a quasi-single cell suspension. Cells were counted using a trypan blue (0.4% trypan blue solution) (*Sigma*) exclusion assay in order to assess cell viability. Specifically, 10 µl of cell suspension was diluted through 3 x 40 µl drops of DMEM/F-12 (1:5, 1:25, 1:125 dilutions) and 1 x 10 µl drop of trypan blue (final dilution of 1:250) and transferred to a haemocytometer with a glass cover slip and viewed under the microscope. Cells in the centre square and the 4 corner squares were counted and the number of cells per µl was calculated, as well as total cell number, taking the dilution factor into consideration. The following formula was used:

Cells/Number of squares x 10 x Dilution Factor = cells/µl

Cells were re-suspended in neuronal differentiation media and seeded onto PLL coated-cover slips at a 100,000 cells/cm^2 in a total volume of 30 µl. After the cells had adhered to the coverslips (~ three hours) the wells were flooded with 500 µl of differentiation media (Appendix 9.1) and were incubated at 37°C in humidified 5% CO_2 and 95% atmospheric air. Differentiation media was replaced after 3 days of incubation.

2.2.3 **Immunocytochemistry- Cell culture**

Following differentiation for the required time period (24hrs or 7 days *in vitro* (DIV)) cells were fixed. Firstly, the differentiation medium was removed and cells were washed in 1 X PBS (Appendix 9.1) for 5 minutes. On removal of PBS the cells were fixed for 20 minutes using fresh 4% paraformaldehyde (PFA) (Appendix 9.1) followed by 3 x 5 minute washes in 1 X PBS. For different antibody stains, the cells underwent one of two protocols. For protocol A, cells were permeabilised with 100% ethanol for 2 minutes or,

for protocol B, with 0.05M lysine (freshly made) for 15 minutes, both followed by 3 x 5 minute washes in 1 X PBS. To prevent non-specific binding of the antibody the cells were blocked for 1 hour (3% normal horse/goat serum (NHS/NGS), 3% bovine serum albumin (BSA) (Sigma) in 1 X PBS-T (0.5% Triton) (*Sigma*). After blocking the primary antibody(s) was added (if double labelling was required, both primary antibodies were added at the same time provided they were raised in different species) in block solution, and left to incubate at 4°C O/N. A full list of antibodies used and details of relevant concentrations and protocols are outlined in Appendix 9.1. Removal of the primary antibody (retained and re-used up to 3 times) was followed by 3 x 5 minute washes in 1 X PBS. Secondary antibodies (all 1:200) made in block solution (Appendix 9.1) were then added to the cells for 2 hours in the dark. The secondary antibody was removed and kept and cells were washed for 3 x 5 minutes in 1 X PBS before the nuclear stain Hoechst (10µg/ml) (1:10:000) (*Sigma*) was added for 10 minutes. Cells underwent final washes in 1 X PBS (3 x 5 minutes) and then the cover-slips were mounted onto glass slides using Fluroment (*Sigma*), and stored in the dark at 4°C until cell counts were carried out.

2.2.4 __Immunocytochemistry – BrdU__

BrdU (2 µg/ml) was added to the cells 24 hours before fixation. Cells were either fixed at 48 hours or 7 DIV as described previously. Cells were initially treated for 30 minutes in K-PBS with 0.4% Triton to aid permeability. Cells were then washed in 1 X PBS for 5 minutes before being treated with 2M hydrochloric acid (HCL) for 10 minutes at 37ºC and then with 0.1M sodium borate for 10 minutes. Cells were subsequently washed for 3 x 5 minutes in 1 X PBS before being blocked for 1 hour in PBS-T (0.1% Triton) plus 1% NGS. Following blocking, primary antibodies were added (Anti-rat BrdU with either anti-mouse TUJ1 or anti-rabbit GFAP), in block solution and left to incubate O/N at 4°C.

The next day the primary antibody was removed and kept and coverslips were washed for 3 x 5 minutes in 1 X PBS. The secondary antibody was made in block and put on the coverslips for a 2-hour incubation period in the dark. Following incubation the cells were washed for 3 x 5 minutes in 1 X PBS before the nuclear stain Hoechst was added to the cells for 10 minutes. A further 3 washes (5 minutes each) in 1 X PBS took place before cover slips were mounted and analysed as described previously.

2.2.5 **Calcium Imaging**

Striatal cultures from a *Foxp1 Het* (*Foxp1$^{+/-}$*) x *Foxp1$^{+/-}$* cross were cultured for 24 hours and analysed to look for any differences in their responses to common neurotransmitters. The ratiometric Ca^{2+} sensitive dye Fura-2-AM (*Molecular Probes, Eugene, OR, USA,* dissolved at 1 mg/ml in DMSO (*Sigma*) and covered to avoid exposure to light) was used to measure intracellular free Ca^{2+}. 1 µl of Fura-2-AM was added to 250 µl of differentiation media, applied to the cells 30 minutes prior to testing and incubated at 37°C in a humidified incubator. This incubation allowed for Fura-2-AM to be taken up by the cells, cleaved and turned into the active dye Fura-2. Fura-2-loaded cells were placed in a specialised perfusion chamber, designed to allow direct access of the microscope oil-immersion lens with the bottom of the coverslip, mounted upon an Olympus IX71 equipped with a Cairn monochromator-based fluorescence system (Cairn Instruments, Faversham, UK). Extracellular solution (ECS) (Appendix 9.2) was applied to the coverslip to stop the cells drying out. Fura-2 was alternately excited using fluorescence light emitted from the monochromator at 340 and 380 nm. Images at 510 nm were acquired at 0.33 or 0.2Hz by a slow-scan CCD camera (*Kinetic Imaging Ltd, Nottingham, UK*). Solutions, agonists and antagonists were applied to the cells using the gravity-driven rapid solution changer (20 ms solution change time). The solutions used were high K^{+} (50 mM KCl in an equimolar replacement of NaCl from standard ECS), GABA (50 µM), GABA (50 µM in a low chloride ECS (equimolar replacement of all NaCl with sodium isethionate in standard ECS)), NMDA (50 µM), AMPA (50 µM) and Kanite (50 µM), all in standard ECS unless stated otherwise (further information can be found in Appendix 9.2). Raw data in the form of emission intensities at 510 nm alternate excitation at 340 or 380 nm were recorded and stored using the Andor 1Q 1.3 software package (*Andor Technology, Belfast*). Following background subtraction, emission ratios (340/380 nm) were calculated off-line using Microsoft Office Excel.

2.2.6 **Brain Slices-Preparation for Immunohistochemistry**

To assess FOXP1 during development in WT mice, time mates were ordered from Harlen and pregnant dams were sacrificed when embryos were at the required embryonic age. Whole embryos (E10, E12, and E14) or just heads (from E16 onwards) were snap frozen and sectioned at 15 μm on the cryostat. Brains were removed as described in 2.2.1 from a range of embryonic ages (E10-PO) and were snap frozen using iso-pentane (*Sigma*) on dry ice and stored at -80°C. The brains were cut on a cryostat (14 μm) onto superfrost plus slides (*Fisher*) and left to air dry at 37°C before being stored at -80°C.

Day 1

Slides were brought out of the freezer and put into ice cold, 100% acetone (*Fisher Scientific*) for 2 minutes and then left to dry at 37°C for 20 minutes. For Di-aminobenzidine (DAB) reactions slides were quenched with 1% H_2O_2 (*VWR*) in 100% methanol (*Fisher Scientific*) for 30 minutes to make the reaction slower and were subjected to 3 x 5 minute washes in 1 X PBS. Antigen retrieval then took place whereby the slides were placed in citrate buffer (Appendix 9.3) for 20 minutes at 95°C and left to cool down at room temperature (RT) before being washed in 1 X PBS for 5 minutes. Slides were blocked (3% NHS)/NGS) in 1X PBS-T (0.1% Triton) for 1 hour. Slides were then incubated with various antibodies; see Appendix 9.3, made up with 1% NHS/NGS in 1X –PBS-T (Appendix 9.3), covered with parafilm strips and incubated at 4°C O/N.

For fluorescent staining, slides were put in Acetone for 10 minutes and then left to dry for 30 minutes. Slides were washed in ice cold 1 X PBS (3 x 5 minutes) before being blocked for 1 hour in 1 X PBS-T (0.3% Triton) and1 % BSA. Primary antibodies were made up in the block solution (see Appendix 9.3).

Day 2

Parafilm strips were removed and slides were washed in 1 X PBS for 5 minutes. For diaminobenzidine (DAB) stains slides were incubated with a biotinylated secondary antibody (see Appendix 9.3) made with 1% NHS/NGS in 1 X T-PBS (0.1% Triton) for 2 hours at RT. For fluorescent staining the secondary antibodies were made in 1 X T-

PBS (0.3% Triton) with 1% BSA and also left on for 2 hours. All slides were then washed in 1 X PBS for 3 x 2 minutes. For DAB staining, an avidinbiotin-complex solution (AB-C complex) was added (1:200) with 1% NHS/1%NGS in 1 X T-PBS for 2 hours, this step was not needed in the fluorescent protocol and slides were washed in 1 X PBS following the removal of the secondary antibody and the nuclear stain Hoechst was added for 10 minutes. The slides then underwent a final 3 washes in 1 X PBS and were cover slipped using PBS: DABCO. Following the ABC step in the DAB protocol, slides were washed in 1 X PBS for 3 x 5 minutes and were equilibrated in 1 X Tris Non Saline (TNS) (Appendix 9.6) for 5 minutes and then for at least 20 minutes. The antibody stain was visualised using DAB. A 1:5 dilution of DAB was used to have more control over development. Slides were left in DAB until a clear reaction could be seen. To stop the DAB reaction, slides were placed in 1 X PBS. Finally dehydration of slides took place through decreasing concentrations of ethanol (75%, 95% and 100%), 5 minutes per concentration. Slides were then placed in xylene (*Lab3*) and cover slipped using DPX (*Fisher*) mounting medium.

2.2.7 **Quantification of Immunohistochemistry/ immunocytochemistry**

Fluorescent and non-fluorescent staining was visualised using a Leica DRMBE microscope. The wavelengths used to visualise each fluorescent stain were 594 nm (red), 488 nm (green) and 356 nm (blue). For immunocytochemistry, cell counts were taken at 40 X magnification using a counting grid. In order to prevent bias, 5 random fields were chosen to take counts from. On all occasions there were at least 3 replicate coverslips for each condition. Colour images were visualised under a Leica DRMBE fluorescent microscope and images were captured using a Leica DFC420 camera and Leica Application Suite image analysis software. Images were processed using Adobe Photoshop. Immunohistochemistry analysis was qualitative to look at where and when expression took place. For non-fluorescent microscopy, images were visualised at the required magnification on the Leica DRMBE microscope. For work carried out at the University of Barcelona, a confocal microscope was used and the nuclear stain DAPI was used instead of Hoechst. Image J was used to process the pictures from the confocal microscope.

2.2.8 **Statistical Analysis- Cell counts and Grafting**

PAWS Statistics (SPSS) V.18 was used to carry out statistical analysis of all cell counting and grafting data. For all experiments, where applicable, a one-way analysis of variance (ANOVA) was used in analysis with Tukey-krammer *post-hoc* analysis when applicable. In addition, this test was used in analysis of the ACCC's between genotypes.

2.3   **Molecular Methods**

2.3.1   **RNA extraction for RT- PCR and qPCR**

WGE were dissected as described in 2.2.1 and snap frozen on dry ice and stored in RNA later (*Sigma*) for RT-PCR and qPCR. At the start of the protocol, the sample tissue was weighed and RNA was extracted using the Qiagen RNAeasy Mini Kit, RNAse-free DNAse set and QiaShredder (all *Qiagen, West Sussex,UK*) according to manufacturer's instructions. Following extraction, the RNA yield and quality was tested using a Nanodrop Spectrophotometer (2μl) and used for subsequent cDNA synthesis. For pure RNA, $_{260/280}$ is ~2.

2.3.2   **Primer Sequences**

All qPCR primers were previously designed and calculated to melt at 60˚C, be 18-22 bp and generate a transcript of 80-120 bp. qPCR primer sets are found in Appendix 9.5. Briefly, primer pairs were generated using the Mouse Genome Informatics and Ensembl websites for sequence information and primer 3 Input for design.

2.3.3   **cDNA Synthesis**

For first strand synthesis, RNA samples were standardised and a maximum of 1 μg of DNase-treated RNA was incubated with random primers (100ng) (*Invitrogen*) and 10mM dNTP mix (*Bioline)* for 5 minutes at 65˚C. Following a brief chill on ice, 5X first strand buffer, 0.1M DTT and RNase OUT (40 u/μl) (*all Invitrogen*) were added and incubated for 2 minutes at 25˚C. Finally, Superscript II (200 u) (*Invitrogen*) was added and incubated at 25˚C for 10 minutes, 42˚C for 50 minutes and finally 70˚C for 15 minutes. cDNA was used for subsequent PCR reactions. RT-ve controls were also carried out by substituting superscript with water.

2.3.4   **RT-PCR- Reverse Transcription -Polymerase Chain Reaction**

For PCR amplifications, cDNA from first strand synthesis was used and a PCR mix was used that consisted of 10X Bioline NH$_4$ Reaction Buffer (*Bioline, London UK*), 50mM MgCl$_2$ (*Bioline, London UK*), 10mM dNTP, BioTaq DNA polymerase (1u/μl) (*Bioline*), oligo pair at 0.5 pmol each (MWG Eurofins) and RNAse-free water (*Sigma*), to make a

25µl reaction. A GADPH PCR (Appendix 9.5) was carried out on all samples to test quality and to optimise cDNA reaction volumes. PCR products were analysed by electrophoresis on a 1.5 % agarose gel and visualised with Ethidium Bromide (*Sigma*). A 100 bp ladder (*Promega*) was used as a reference for band size.

2.3.5 **DNA Extraction for Genotyping**

Mice were genotyped using PCR to determine whether the gene (*Foxp1*) was present and to determine the presence of the Cre (hGFAP or Nestin). Specific primer combinations used for the different stages of breeding are outlined in Appendix 9.5. DNA was extracted from tail biopsies for use in genotyping. 500 µl of lysis buffer (Appendix 9.4) was added to each tail and samples were vortexed and left O/N at 55˚C in an incubated shaker. The next day, 500 µl of Phenol/Choloroform/Isoamylalcohol (24:24:1) (*Sigma*) was added to the samples before being added to Eppendorf Phase Lock tubes (*Lab3*) and spun for 5 minutes at full speed (210000g). The upper phase was added to fresh eppendorf tubes and 500 µl of Propan-2-ol (isopropanol) (*Sigma*) was added. Samples were mixed well and centrifuged on maximum speed for 10 minutes. The upper phase was discarded and the pellet was washed with 70% molecular grade Ethanol (*Sigma*) and spun for a further 10 minutes at full speed. Following washing, the supernatant was discarded and the pellet was left to dry at 37˚C for 15 minutes and then re-suspended in 1 ml of distilled water. The samples were left at 55˚C for 30 minutes and stored at -20˚C.

2.3.6 **Genotyping-PCR**

DNA was extracted from the tail biopsies obtained on dissections and the relevant PCRs were carried out. For PCR amplifications the DNA extracted from the embryos, 10 X NH$_4$ Reaction Buffer (*Bioline*), 50mM MgCl$_2$ (*Bioline*), 10mM dNTPs, an oligo pair (0.5 pmol), BioTaq DNA polymerase (1u/µl) (*Bioline*) and water were added to make a 25 µl reaction. Briefly, to identify the correct genotype of the *Foxp1* embryos two primer sets were used, one that showed the presence of the TG allele (~280 base pairs (bp) that is not evident in WT embryos, whereas the second set identified a larger band (~ 430bp) which is present in both heterozygous and WT embryos. An example gel is shown in Figure 2.4. Two separate PCRs were carried out per tail to determine the

genotype of Foxp1 CKO or WT mice, one to detect the presence of the Cre (hGFAP ~190bp) and one to determine the presence of the floxed allele (~ 734bp). The full list of primer sets and PCR conditions used for genotyping can be found in Appendix 9.5.
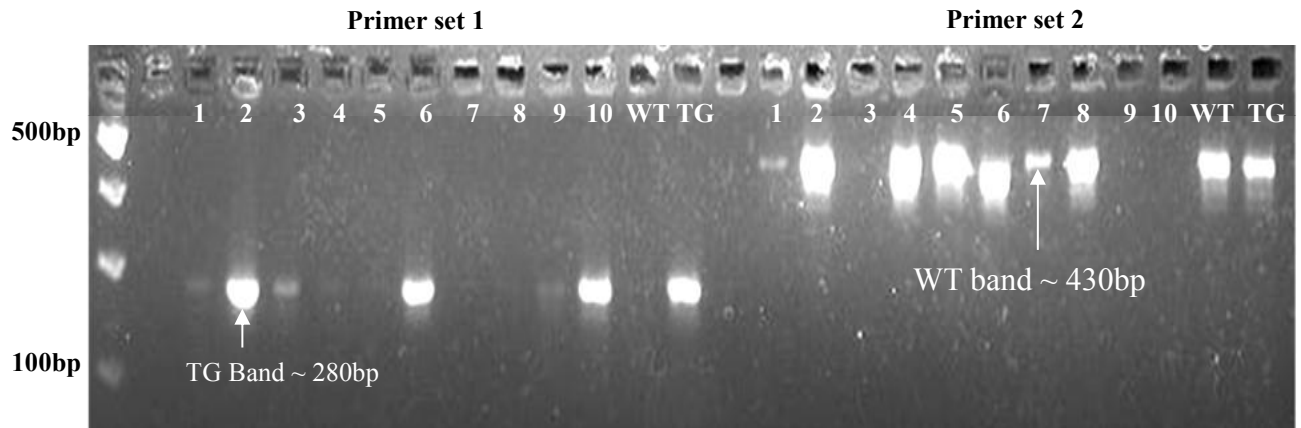

Figure 2.3 Example genotyping results of embryos used in the E14 transplantation experiment- A 3% agarose gel showing genotyping results of the pups transplanted. Two sets of primers were used. Primer set 1 shows the presence of the TG allele (~280 bp) and is not evident in WT emrbyos. Primer set 2 shows the presence of the WT allele (~480bp) and is absent from the *Foxp1*^-/- pups. The heterozygote embryos have both bands. In this example pups 4, 5 7 and 8 are WT, 1, 2, and 6 are *Foxp1*^+/- and 3, 9 and 10 are *Foxp1*^-/-.

2.3.7 <u>Agarose Gel Electrophoresis</u>

To run PCR samples a 1, 1.5% or 3% agarose gel (1%W/V) made in 1% Tris-acetate-EDTA (TAE) running buffer was used (Appendix 9.5 outlines which PCR products required which gel). 3 µl/50ml of Ethidium Bromide (*Sigma*) was added to visualise the gel. A 100 bp ladder (*Promega*) was used to determine the size of the bands. The gel was run at ~100V and viewed under UV in a transilluminator. The genotype of the animals could then be determined.

2.4 *In vivo* **Methods**

2.4.1 **Animal care and Anaesthesia**

All animal experiments were performed in agreement with local ethical guidelines and accepted animal care according to the UK Animals (Scientific Procedures) Act 1986 and its subsequent amendments. For surgery, adult C57BL/6 female mice (*Charles River, UK*) weighing 20-30g at the start of the experiment were used, and were housed in cages of up to 5 in a natural light (06:00-18:00)-dark cycle (18:00-06:00) with access to food and water ad libitum.

All surgery was performed under gaseous isoflurane anaesthesia. Anaesthesia was induced in an induction chamber with isoflurane (5%) and oxygen (0.8%) and maintained by passive inhalation of isoflurance (1-2%) and a mixture of oxygen (0.8%) and nitrous oxide (0.4%). Animals were recovered in a warmed recovery cage following surgery.

2.4.2 **Quinolinic Acid (QA) Lesion**

Quinolinic acid (QA) (stored at -20°C) was dissolved in 0.1M phosphate-buffer saline making a final concentration of 90 mM solution. The skull was exposed, a small burr hole drilled (drill bit size ½) and QA was injected into the right striatum through a cannula attached to a 10 µl Hamilton syringe driven by a mechanical pump

For QA lesions in mice, 0.75 µl of 90 mM QA was infused at one site for 6 minutes at a pump rate of 15. The stereotaxic coordinates for injection sites were 0.0 tooth bar (TB), +0.8 mm rostral to Bregma (AP), -2.0 mm lateral to midline (L) and -3.0 ventral from dura (DV). The needle was left at the lesion site for a further 3 minutes to prevent reflux of the toxin up the needle tract. The incision was sutured (Vicryl Rapide (*Ehticon*)) and animals were administered a subcutaneous injection of 0.5 ml saline glucose into the scruff of the neck and an intramuscular (IM) injection of 30 µl Diazepam and 50µl of Meloxicam (*Metacam*).

2.4.3 __Unilateral Striatal Grafts__

10 or 6 days (largely dependent on timed matings) following lesions grafting took place. WGE from E14 or E12 *Foxp1*$^{-/-}$, heterozygotes or WTs was grafted into the lesioned adult mouse brains. 2 µl of cell suspension (250,000cells/µl) (for E14 grafts) or 2 WGE (quasi suspension) (for E12 grafts) per mouse were delivered at a rate of 1 µl/min at two different heights below the dura, (-3.2 and -2.8mm) (2 minutes in total) using a 10 µl Hamilton syringe. Grafts were placed ipsilateral to the side of the lesion using the stereotaxic co-ordinates outlined in 2.4.2. Following grafting, the needle was left at the graft site for a further 3 minutes before being withdrawn. For the E12 grafts a further refinement was also made so that between grafts the Hamilton syringe was flushed through with boiling water to ensure less cross contamination from the other suspensions The incision was sutured and the animals were administered with a subcutaneous injection of 0.5 ml saline glucose and 50 µl of meloxicam.

2.4.4 __Perfusions and Sectioning__

Mice were terminally anaesthetised by intraperitoneal (i.p) administration of 0.2 mg/ml sodium pentobarbital (Euthatal) and transcardially perfused with a prewash solution (PBS, pH 7.3) (Appendix 9.6) for 3 minutes followed by 1.5% PFA solution, pH7.3 for 3 minutes (Appendix 9.6). The flow rate used would suggest animals received ~90 ml of prewash and PFA per animal. The brains were removed, post-fixed in 1.5% PFA O/N and transferred to 25% sucrose (*Sigma*) in prewash solution until they sank and remained in this solution until they were sectioned.

Brains were cut in the required orientation on a corkboard using a single sided razor blade (4 cm) to remove the cerebellum. The brains were then frozen using distilled water onto a freezing platform of a calibrated sledge microtome and were sectioned coronally at a thickness of 40 µm and sections were stored in 0.2% sodium azide in Tris-buffered saline (TBS) or anti-freeze (Appendix 9.6), in 96/24 or 36 well plates at -20°C until needed for immunohistochemistry.

2.4.5 <u>**Cresyl Violet Staining**</u>

Brain sections (1 in 12 series) were mounted onto glass microscope slides, previously double-subbed with 1% gelatin and allowed to dry. Cresyl violet (CV) (Appendix 9.6) staining was automated on a Shandon tissue processing machine that firstly dehydrated the sections through increasing levels of alcohol from 70% to 95% to 100% and then agitation for 20 minutes in chloroform/alcohol. Sections were then subjected to decreasing concentrations of alcohol (95%, 70%), before being placed in distilled water for 5 minutes and then in the CV stain (*Sigma*) for another 10 seconds. Following this, slides were put back into distilled water for a minimum of 30 minutes before being dehydrated in the alcohols once again (70%, 95%). If the sections were considered "too dark", a 1-2 minute step in acid alcohol (Appendix 9.6) was introduced at this stage. Sections then went into 100% ethanol, followed by xylene, and were mounted using DPX.

2.4.6 <u>**Immunohistochemistry on Free-Floating Tissue Sections**</u>

<u>**Day 1**</u>

A 1 in 12 or 1 in 6 series of brain sections were washed in TBS and then quenched with 10% hydrogen peroxide (*VWR*) and 10% methanol (*Fisher*) in distilled water for 5 minutes followed by three 5 minute washes in TBS, pH 7.4. Blocking solution of 3% NHS/NGS serum in 0.2% Triton X-100 in TBS (TXTBS) (Appendix 9.6) was added for 1 hour, and then, without washing, block was discarded and primary antibody was added at the appropriate concentration (Appendix 9.6) in 1% serum in TXTBS and incubated overnight at RT on a shaker. If being left for the weekend, sections were left on a shaker at 4ºC.If primary antibodies were newly bought in then antibody validation was carried out. This involved the protocol being carried out as normal but the sections being left in1% serum in TXTBS with 1% NHS/NGS O/N without the addition of the primary antibody. The second day protocol was carried out as normal (described below).

<u>**Day 2**</u>

Sections were washed 3 times in TBS before biotinylated secondary antibodies were added for 3 hours at a concentration of 1:200 in 1% serum in TBS. The secondary antibody solution was washed off with 3 washes in TBS and streptavidin ABC (A and B

both at 1:200 dilution with 1% NGS/NHS serum in TBS; prepared 30 minutes before addition) was added for a further 2 hours. The sections were washed 3 times in TBS followed by twice more in 0.05M Tris non-saline (TNS) pH 7.4 (Appendix 9.6). Positive staining was visualised using either DAB at 0.5 mg/ml in TNS with 12 µl of H_2O_2, which reveals the cells as brown colour, or using the vector SG kit (*Dako, Glostrup, Denmark*), which, as with DAB, is made up in TNS and has a greyish-blue stain. Following the appropriate colour change, sections were washed twice in TNS before being mounted on gelatinised glass microscope slides, allowed to dry and dehydrated in increasing levels of alcohol, followed by xylene and cover slipped using DPX.

Quantification-Striatal Volume

To determine the striatal volume of heterozygote and WT brains, the striatal area, of both hemispheres was drawn around at 1.6X magnification using the Leica Application Core V3.6 software microscope. Striatal volume was then calculated using the formula:

$$V = (\Sigma a * M)/f$$

Where: **V** = Volume, **a** = area (mm^2), **M** = section thickness (40µM) and **f** = frequency of sampled sections (1:12 or 1:6).

2.4.7 **Stereology**

Cells expressing markers of interest were counted using a Leitz light microscope and Olympus CASTgrid v1.60 stereology software. Stereological analysis was carried out blind to genotype. At 4 X magnification the striatal and cortical areas were defined and equated; this is shown in Figure 2.4. At 40 X magnification the number of cells within the sampling frame (622µm^2) throughout a sampling grid was quantified. Slides were imaged using the Leica DFC420 Camera and images taken using the Leica Application Core V3.6 software microscope and analysed in Adobe Photoshop. Cell densities (cells per mm^3) were carried out for the striatum and cortex using the formula:
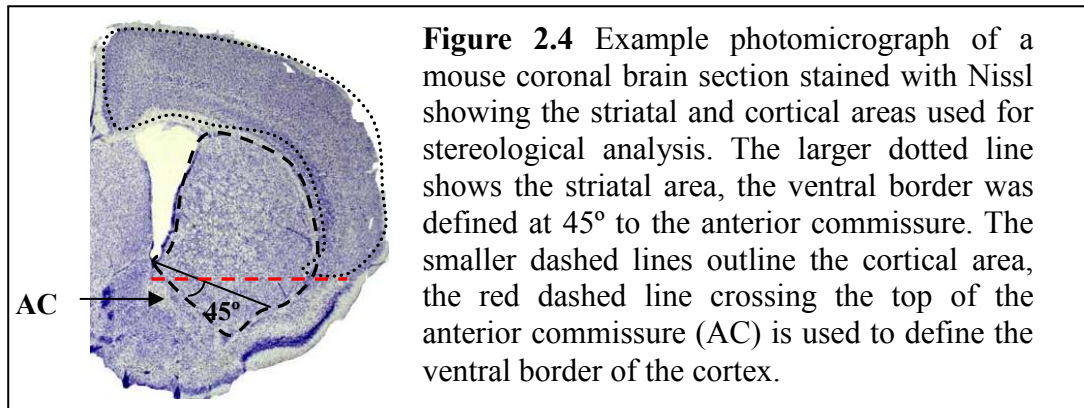
$$C = \Sigma(c * A/n * a. * v) * 10E9$$

$$\text{Where } v = \Sigma (A * M)$$

C= number of cells per mm^3 A= area of striatum/cortex (µm^2), n= number of sampling frames used, a = area of sampling frame (622µm^2), v= volume of striatum/cortex, M = section thickness (40µm), D= cell diameter

Abercrombie corrected cell counts (ACCC) per mm^3 were calculated using the
Abercrombie Formula (Abercrombie 1946) shown below:

ACCC= 1/f*A*(M/(D+M))

f= frequency of sections **A** = cell counts per animal, **M** = section thickness (40 μm) **D**= mean cell diameter

Figure 2.4 Example photomicrograph of a mouse coronal brain section stained with Nissl showing the striatal and cortical areas used for stereological analysis. The larger dotted line shows the striatal area, the ventral border was defined at 45º to the anterior commissure. The smaller dashed lines outline the cortical area, the red dashed line crossing the top of the anterior commissure (AC) is used to define the ventral border of the cortex.

2.5 **Behaviour**

2.5.1 **Automated Activity Boxes**

Animal activity was assessed using automated Med Associate hardware (Med Associates, St Albans VT, USA) and MED-PC (IV) software over a period a 32 hours. 16 animals were housed in individual plastic cages (L42 cm, W26 cm and D 19cm) with 3 infrared beams crossing the base of each box. Animals were allowed to acclimatise in the cages before the start of the experiment and were given access to food and water. Beam breaks were recorded from each animal crossing and were totalled and averaged per animal for 32 hours and ultimately grouped according to genotype.

2.5.2 **Rotarod**

The rotarod apparatus (*Ugo Basile, Varese, Italy*) was used to provide an overall assessment of motor coordination and balance. Mice received 5 days of training with 3 trials a day at varying speeds. For the first day, training was set at 4 rev per minute (rpm) to allow the mice to acclimatise to the exercise and on the remaining training days the speed gradually accelerated from 4 rpm to 22 rpm. On the test day the speed was set to accelerating (speed: 4 to 44 rpm over 300s). The time when the mouse fell was recorded as the outcome measure and the average of the two best trials calculated. The apparatus is shown in Figure 2.5.

Figure 2.5 Mouse Rotarod apparatus. 5 mice were tested on the apparatus simultaneously. When the animal's fall onto the panels at the bottom, the automated counter stops and re-sets to 0.

2.5.3 **Inverted Cage Grip Test**

The inverted grip test is a measure of the grip strength of the fore and hind limbs of the mouse. To start the trial animals were placed onto the centre of a metal cage lid where a square (20 cm x 20 cm) was taped off. The grid was then slowly inverted and placed 30 cm above the workbench with towels placed underneath to soften falls. The time the mouse spent grasping the grid without falling was recorded, a maximum cut off of 1 minute was used and analysed.

2.5.4 **The Elevated Plus Maze (EPM)**

The elevated plus-maze is used for the assessment of anxiety in rodents. The maze consisted of four cross-shaped arms, two open arms measuring 50 cm x 8 cm, and two enclosed arms measuring 50 cm x 8 cm x 10 cm (Figure 2.6). The platform was elevated 90 cm from the floor. There was a central area that the mouse started the task from. Prior to each trial the EPM was cleaned with 70% ethanol in distilled water. The experimenter remained in the room for the duration of the task (5 minutes) given the mouse may fall and need to be placed back onto the maze. Entries into and time spent on enclosed and open arms were measured. An entry occurred whenever the mice crossed from one arm to another with all four paws. The number of entries into, and time spent on the open arms were evaluated as a percentage of total arm entries and the total time spent on all four arms respectively.
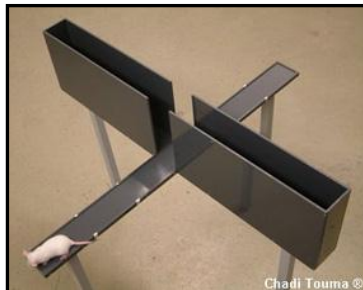

Figure 2.6 Picture of the Elevated Plus Maze (EPM) for mice. There are 4 arms, 2 open "safe arms" and 2 enclosed arms. There is a central platform where the task starts. Photo accessed by www.mpipsykl.mpg.de on 25th July 2013.

2.5.5 <u>**Open Field Activity**</u>

Animals were tested in an arena (80 cm x 80 cm), which was white with a video camera positioned overhead, linked to a computer to record the activity. The programme works by calculating the contrast differences between the white background of the arena and the coat colour of the animals (black and brown). Animals were habituated for 2 consecutive days in the arena and then tested on the third day. The programme used to analyse the animal's behaviour was EthoVision (Noldus).

2.5.6 <u>**Marble Burying Task**</u>

For the assessment of anxiety related behaviour 20 glass marbles were evenly spaced out in 5 rows of 4 (5 cm apart) in the centre of a novel cage with enough sawdust to allow burying; a mouse's normal response is to bury marbles (Archer *et al.* 1987; Broekkamp *et al.* 1986). The test was conducted in a plastic box measuring 30 cm by 50 cm by 15 cm which was filled with 5 cm of non-allergenic bedding sawdust. 10 test stations were set up, allowing 10 mice to be tested simultaneously. Animals were left for 30 minutes in the cage, with a plastic lid over the top so that they could not escape or climb on it. The experimenter was not in the room whilst testing occurred. Following the 30 minutes, individual cages were photographed and the number of marbles buried and counted analysed.

2.5.7 <u>**Operant Testing - Operant Boxes**</u>

Testing was conducted using sixteen mouse 9-hole operant chambers under the control of a computer operating the Cambridge Cognition Control System *(BNC Control,Campden Instruments, Loughborough);* an example box is shown in Figure 2.7A. The dimensions of each chamber were 14 cm x 13.5 cm x 12.5 cm in which the curved rear wall was fitted with a horizontal array of nine response holes (11 mm diameter, separated by 2 mm) positioned 15 mm above the stainless steel floor. Each hole had a photocell detector at the front to detect entries into holes (i.e. nose pokes) and an LED stimulus light (24V). In the present experiment, the 5 choice serial reaction time task (5-CSRTT), 5 of the 9 response holes were used (holes 1, 3, 5, and 7 and 9), and the remaining un-used holes were blocked. On the opposite wall, a reward magazine was fitted into which 2.5 µl of strawberry milk (*Yazoo, Campina, UK*) could

be delivered as a reward via a peristaltic pump, shown in Figure 2.7. A horizontal infrared beam across the entrance of the magazine detected entries by the mice when a reward was collected. The chamber was also fitted with two additional "house" lights on the sidewalls, which illuminated to signal the end of a trial and time-out periods. Each chamber was housed in a sound-attenuating box with continuous airflow.
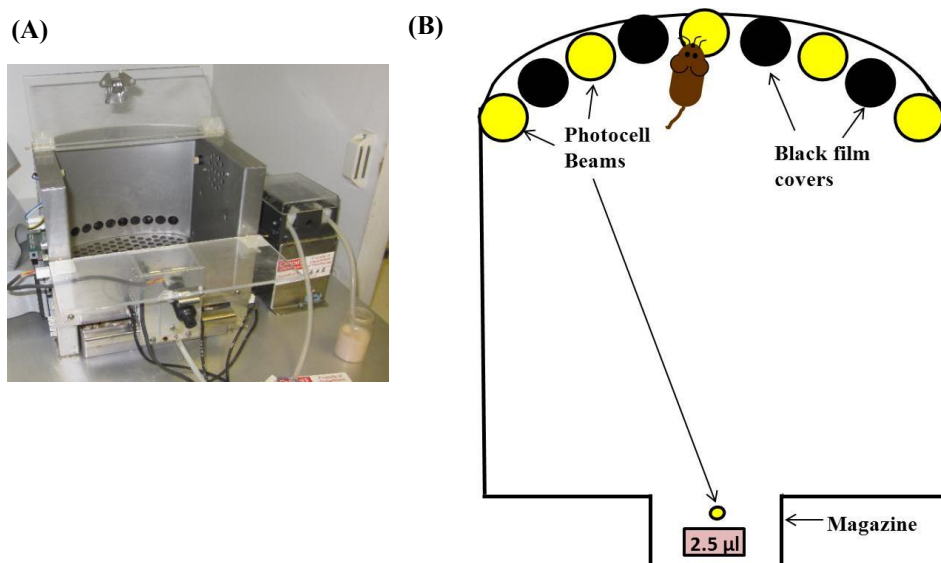
Figure 2.7 (Previous page) An example nine-hole operant box chamber for behavioural testing in mice. **(A)** An example photograph of one of the operant boxes used showing the 9 holes on the rear of the apparatus. Strawberry milk (shown in the small bottle) is delivered through the plastic tubing via a peristaltic pump into the magazine on completion of a correct response by the animal.**(B)** Schematic diagram of the nine-hole box set up for the 5-CSRTT with holes 2, 4, 7 and 9 covered up. 24V bulbs are at the rear of each hole and act as a visual stimulus for poking. Infra red photocell beams at the front of each hole, and magazine record entries made by the mouse.

2.5.8 **Operant Training**

Behavioural testing was started 3 days after the introduction of the food restriction regime (mice were food restricted to no more than ~ 85% of their initial body weight to ensure motivation on the operant task). Training for the operant task was split up into different elements. Firstly, the mouse was introduced to the test chamber and the magazine light was left on continuously for the duration of the programme (20 minutes) and a 25 µL reward was delivered into the magazine, i.e. no poking was required at this stage. This initial shaping session served to habituate the animal to the environment and reward. The next days of training were to enhance magazine reward. The house light was turned off with the magazine light illuminated to show there was a 5 µL reward, on retrieval of the reward the magazine light was extinguished, and there was delay of 10 seconds before the magazine light was illuminated once more, this pattern was repeated for the duration of the session (30 minutes). The next stage of the training involved the mice learning to poke a specific hole and associate poking with a reward. A small amount of strawberry milk was painted around the perimeter of hole 5 during this task to encourage the mice to nose-poke. At the start of the trial, the house light was turned off, followed by illumination of hole 5. A correct nose poke into this hole caused the light to be extinguished and the delivery of strawberry milk into the magazine. On retrieval of the reward, the magazine light was extinguished and the house light was turned off for 10 seconds before hole 5 was illuminated once more, this sequence was repeated for the duration of the trial (20 minutes). This session was carried out once a day until the mice retained a high level of accuracy (~80%), i.e. had learnt to associate poking with a reward.

2.5.9 **5-choice serial reaction time task (5-CSRTT)**

Once all animals learned to respond to the stimuli, they were tested on the 5 choice serial reaction time task (5-CSRTT), which is outlined in Figure 2.8. The 5-CSRTT provides an effective test of vigilance and attention (Robbins 2002). Following training, all animals began the 5-CSRTT. This required the mice to respond to the illumination of different holes. As mentioned, holes 1, 3, 5, 7 and 9 were uncovered, and each test began with the illumination of the house light, followed by it being extinguished and one of the 5 holes being illuminated at random, initially

for 10 seconds. A correct nose poke into the illuminated hole saw the extinction of the light with simultaneous illumination of the magazine and delivery of 5 µl of strawberry milk. On collection of reward the magazine light was extinguished followed by a fixed inter trial interval (ITI) of 2 seconds before the next trial began. Incorrect nose-pokes into a non-illuminated hole, poking before the onset of illumination (impulsivity) or not poking at all (omission) were all were recorded and were punishable by a 5 second time-out period in which the house light was illuminated and no reward was delivered. The duration that the stimulus light was illuminated for was altered as the task progressed. Initially, the illumination period was 10 seconds (5 days) before being reduced to 1 second (5 days), and finally half a second (10 days). The number of correct responses/total responses determined accuracy and reaction time and total number of omissions (no response) was also recorded and analysed.
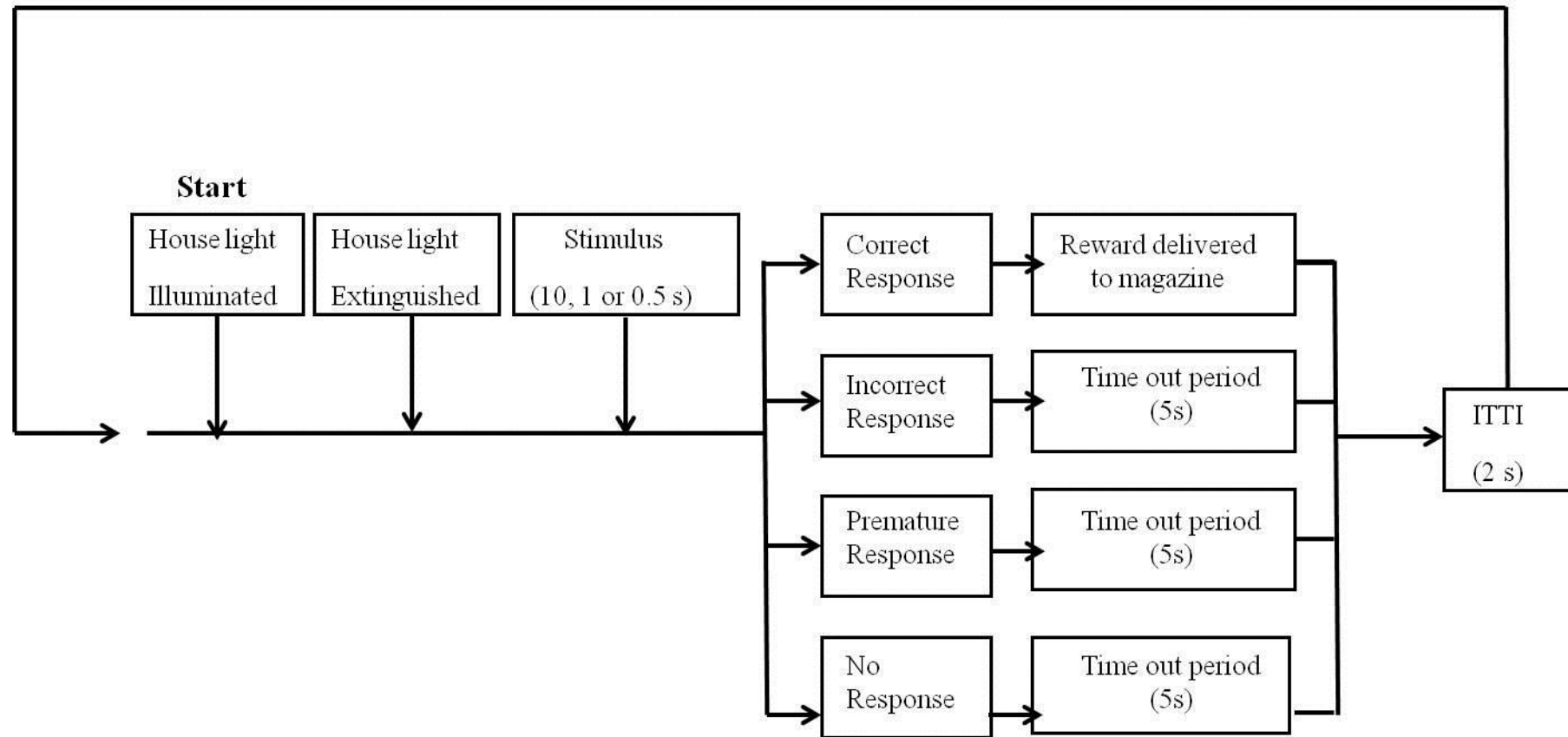
Figure 2.8 Schematic representation of the 5-CSRTT. At the start of each trial the house light was illuminated to signal the initiation of a new trial, followed by illumination of one of the 5 stimulus lights with all other lights being switched off. During initial training the stimulus duration was set to 10 s. Once the performance of all mice reached asymptote (>80% correct) the stimulus duration was set to either 1 or 0.5 s. Correct nose pokes were rewarded with 5 μL of strawberry milk being delivered into the magazine, with simultaneous illumination of the magazine light and extinction of the hole light. Upon reward collection the magazine light was extinguished and there was a fixed inter trial interval (ITI) of 2 s before the next trial began. Incorrect nose pokes (i.e. poking into the wrong hole) were recorded as incorrect responses, poking before the light came on and no pokes at all (omissions) were punishable with a 5 s time out period in which the house light was illuminated and no reward was delivered.

2.5.10 **Pharmacological Intervention**

Methylphenidate (Ritalin) (*Tocris*) (5, 10 or 30 mg/kg) (doses established from a preliminary Latin square dose-response trial) and atomoxetine (*Tocris*) (1, 2 or 4 mg/kg) (Bymaster *et al.* 2002) were, on separate occasions, administered to mice via an i.p injection. Both drugs were dissolved in a 0.9% isotonic saline solution (0.9% NaCl). Ritalin was made up to be in a final volume of 10 ml/kg (i.e. 30g mouse- 30μl of the dose) whereas problems with atomoxetine dissolving required it to be made at a final volume of 20 ml/kg. Directly following the injection, mice were tested in the locomotor activity boxes as outlined in 2.5.1, but on a 2 hour programme which started at 18:00- start of the dark phase of the animal's cycle. All animals in the task received all doses of drugs over a period of 4 days. Animals were also given Ritalin (5 mg/kg) and tested on the 5-CSRTT.

2.5.11 **Behavioural Data Statistical Analysis**

PAWS Statistics (SPSS) V.18 was used to carry out statistical analysis of all data. To look at differences in behavioural tasks either a one way analysis of variance was used (rotarod, grip strength, open field, EPM, MBT) or a 2-way ANOVA (activity box data and operant data) with genotype always the between subject factor. For the marble burying task a Man-Whitney non-parametric analysis was also carried out. A 2-way ANOVA needed to be used in the later behavioural tasks to account for the additional levels of hole number, stimulus delay and/or drug as well as genotype for the 5-CSRTT and similarly for locomotor activity to account for drug and period of time as well as genotype. The alpha level for significant F-ratios was set at 0.05 for all analyses.

3 *The Characterisation of Foxp1 in the Developing Mouse Brain*

3.1 **Summary**

Foxp1 is a TF identified as having a fundamental role in many aspects of development and has shown to be expressed in both the developing and adult brain. Foxp1 was the most highly up-regulated gene in an Affymetrix screen carried out by the host lab, which used mouse WGE to look for significant differences in gene expression over peak striatal development (E12-E16). The purpose of this Chapter was to further characterise Foxp1 levels during embryonic and early post-natal development using immunohistochemistry, before attempting to understand the functional role of this TF in MSN development using Foxp1 KO mice. However, Foxp1 homozygous KO mice are embryonic lethal at E15 due to cardiac defects. The possibility of using adult Foxp1$^{+/-}$ was considered, however, when compared to WT mice the Foxp1$^{+/-}$ mice had no obvious phenotype, therefore experiments in this Chapter were limited to analysis at E14.

In vitro experiments showed that in the absence of Foxp1 there was a significant decrease in the number of CTIP2 and DARPP-32 positive cells after 7 DIV, but that there was no effect on proliferation or neuronal homogeneity as shown through calcium imaging studies. Fluorescent immunohistochemistry also suggested that FOXP1 is reduced in Gsh2 KO mice, and in the SVZ of Ascl1 KO mice, suggesting that Foxp1 could possibly function downstream of these important striatal TFs.
.

3.2 __Introduction__

MSNs develop from the telencephalon, identifiable at E8.5 by *Foxg1* expression (Hebert and McConnell 2000; Shimamura and Rubenstein 1997). The developing telencephalon is subsequently divided and regions discernible by differential gene expression. The dorsal telencephalon gives rise to the developing cortex; whereas the ventral telencephalon is concerned with striatal development and further divides into the LGE, MGE and CGE. MSNs principally originate from the LGE as a population of *Ascl1$^+$*, *Gsh2$^+$* and *Dlx1/2/5/6$^+$* precursors that reside, and proliferate in the VZ and SVZ (Campbell 2003). These striatal precursors migrate out of the VZ and differentiate in the MZ of the developing striatum between E11 and E15, in two different waves, and are identifiable by TFs such as *Ctip2* (Arlotta *et al.* 2008), *Helios* (Martin-Ibanez *et al.* 2012)*Ikaros* (Martın-Ibanez *et al.* 2010) and Foxp1 (Tamura *et al.,* 2004) and will eventually mature to become GABAergic, DARPP-32 positive MSNs. An affymetrix screen which used mouse WGE to look for significant differences in gene expression over peak striatal development (E12-E16) identified many genes as being differentially expressed, of which the above mentioned genes were included (Precious e*t al*, submitted 2013). As mentioned, *Foxp1* as the most highly up-regulated gene suggesting a role in MSN differentiation.

Foxp1 is a TF that has been implicated in several developmental processes including heart and lung development (Shu *et al.* 2001; Wang *et al.* 2004a), in which its role in heart development was identified through utilisation of *Foxp1* KO mice (Wang *et al.* 2004a). *Foxp1* has also shown to be important in aspects of CNS development; specifically, it has shown to be an accessory factor in Hox transcriptional output which regulates motor neuron diversity and connectivity to target muscles (Dasen *et al.* 2008; Rousso *et al.* 2008). *In vitro* work using mESCs has also shown that *Foxp1* has a functional role in DA neuron development. It was shown that the addition of *Foxp1* to mESCs activated the expression of PITX3; a protein exclusively expressed in midbrain dopaminergic neuron that is vital for their correct differentiation and survival during development *in vitro* and *in vivo* (Konstantoulas *et al.* 2010). Recently, mutations in the human FOXP1 gene have suggested it is also required for the speech and language development (Hamdan *et al.* 2010; Horn *et al.* 2010).

Of importance to the work outlined in this thesis, and in support of the Affymetrix results obtained by our lab group, is that *Foxp1* has shown to be expressed in both the developing and adult striatum and co-localises with DARPP-32 (Ferland *et al.* 2003; Tamura *et al.* 2004). Specifically in mice, *Foxp1* mRNA has shown to be expressed in the developing striatum from E12.5 in the SVZ and MZ of the LGE (Ferland *et al.* 2003), a region synonymous with differentiating, post-mitotic neurons (Campbell 2003; Stenman *et al.* 2003). Consistently, *Foxp1* is also expressed in the developing human striatum over an equivalent gestational window and with a similar anatomical distribution to that seen in the mouse (Precious et al., submitted 2013). FOXP1 immunohistochemistry also showed co-localisation with CTIP2, another routinely used MSN marker also expressed in developing and adult MSNs (Arlotta *et al.* 2008).

However, although *Foxp1* is expressed during MSN development, its function, and its relationship to the genetic pathways already known in striatal development are largely unknown but are likely to be important for the optimisation of *in vitro* protocols that aim to direct renewable cells sources, such as ESCs, to functional MSNs for use in cell replacement therapies (Kelly *et al.* 2009). Information from mouse models in which key genes involved in striatal development have been knocked out have hinted at what TFs may be functioning downstream of *Foxp1* but no functional analysis has been undertaken. Rubenstein's group used an Affymetrix screen to look at differences in the expression profiles of over 100 genes in the LGE of *Dlx1/2* KO mice and notably showed a severe reduction in FOXP1in the SVZ and MZ (Long *et al.* 2009). Similarly, when the TF *Ctip2* was knocked out there was a decrease in both DARPP-32 and FOXP1 at P0 (Arlotta et al., 2008).

The *Foxp1* KO mouse has been valuable in understanding the function of this gene in several systems. However, homozygous *Foxp1* KO mice (*Foxp1^{-/-}*) are embryonically lethal by E15 due to heart defects, and *Foxp1* heterozygote embryos did not show any obvious differences from the WTs (although adult mice were not studied) (Wang *et al.* 2004a). Therefore, studying the function and looking at downstream or upstream targets of *Foxp1* after E14 is challenging and it ideally requires a conditional KO (CKO) mouse line to be developed. A striatal specific CKO is being developed by myself, but unfortunately was not available during the time course of this Thesis. Nevertheless, one

can attempt to explore the function of *Foxp1,* by studying differences up to the point of lethality.

First this Chapter looked at the expression profile of *Foxp1* in the developing WT striatum and this was characterised from early in development (E10) through to adulthood. A phenotypic comparison between WT and *Foxp1*$^{+/-}$ adult mice showed no obvious phenotypic differences, and therefore, analysis was undertaken using the *Foxp1*$^{-/-}$ mice. Analysis focused on the characterisation of the *Foxp1* KO line with an emphasis on characterising differences in MSNs at E14, as this age was coincident with peak MSN neurogenesis (Mason *et al.* 2005). To determine differences in MSNs between the genotypes, the striatal markers CTIP2, and where possible, DARPP-32 were used. Following 7 DIV, E14 striatal cultures generated from *Foxp1*$^{-/-}$ striate were shown to have significantly fewer DARPP-32 and CTIP2 positive cells than cultures generated from WT or *Foxp1*$^{+/-}$ striate. Differences in proliferation were also explored and as a means of assessing neuronal homogeneity calcium imaging was also carried out on E14 striatal cultures. In addition on a visit to the Canal's group at the University of Barcelona I carried out immunohistochemistry using an anti-FOXP1 antibody on brain slices of known striatal KO mice to gain a further understand what genes *Foxp1* may be functioning up or downstream of.

## 3.3 <u>**Experimental Design and Procedures**</u>

Experiment 1-Aim: To establish the full expression pattern of FOXP1 in WT mice from E10 through to P7 using fluorescent immunohistochemsitry. FOXP1 was compared to the two striatal markers CTIP2 and DARPP32.

Experiment 2-Aim: To circumvent the embryonic lethality of the *Foxp1*$^{-/-}$ mice at E14, adult *Foxp1*$^{+/-}$ mice were analysed and compared to WT mice to determine if there was a striatal phenotype evident, therefore providing a possible alternative model to the *Foxp1*$^{-/-}$ mice to study differences in striatal development after E14 without the need to create a CKO line.

Experiment 3-Aim: Gross anatomical comparison of WT, *Foxp1*$^{+/-}$ and *Foxp1*$^{-/-}$ embryos. Differences in brain size, striatal morphology and overall striatal cell number were compared.

Brain

Striatum
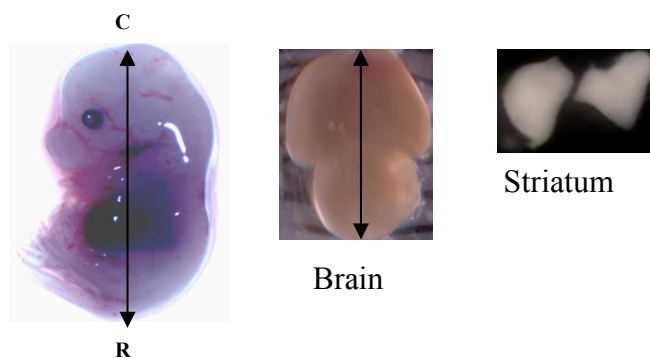
Experiment 4-Aim: Assesses differences in neuronal number, proliferation and responsiveness to GABAergic agonists in WT, *Foxp1*$^{+/-}$ and *Foxp1*$^{+/-}$cultures generated from E14 embryos.

WGE dissection

**Striatal Cultures
24hrs or 7 DIV**

Immunocytochemistry

Calcium Imaging
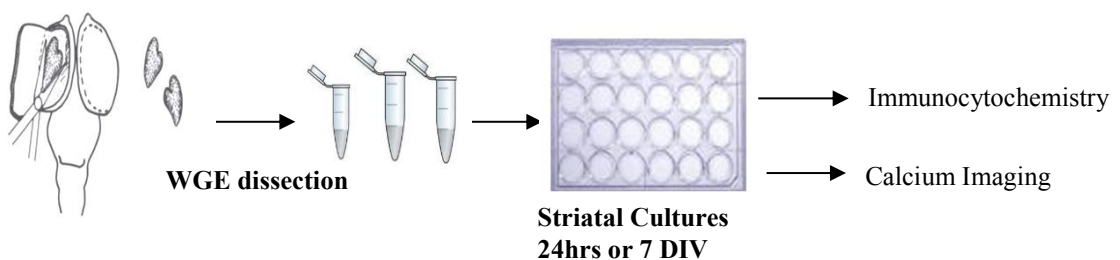
Experiment 5 -Aim: Look at FOXP1 differences in established genetic KO mouse lines using immunohistochemistry.

3.4 **<u>Results</u>**

The expression pattern of FOXP1 in the embryonic and postnatal striatum compared to the MSN markers CTIP2 and DARPP-32.

To look at the protein levels of FOXP1 in the developing and postnatal mouse brain fluorescent immunohistochemistry using anti-FOXP1, anti-CTIP2 and anti-DARPP-32 was carried out on WT brain sections from E10 (when the ganglionic eminences are emerging), through to P7. At E10 there were patches of FOXP1 positive staining in the area likely to be the SVZ (Figure 3.1A, B). There were no identifiable CTIP2 positive cells at this age. At E12, FOXP1 staining was once again evident in the SVZ with few positive cells also being identified out of this proliferative region. CTIP2 staining was absent from the proliferative regions but positive staining was seen in the perspective MZ, the area where post-mitotic neurons migrate to and differentiate, however there was no co-localisation seen with FOXP1 (Figure 3.1C, D). By E14, CTIP2 and FOXP1 clearly show co-localisation within the MZ of the striatum (Figure 3.1E, G), although complete co-localisation is not apparent with FOXP1 positive/CTIP2 negative patches evident in the MZ and the SVZ (Figure 3.1.E. F).
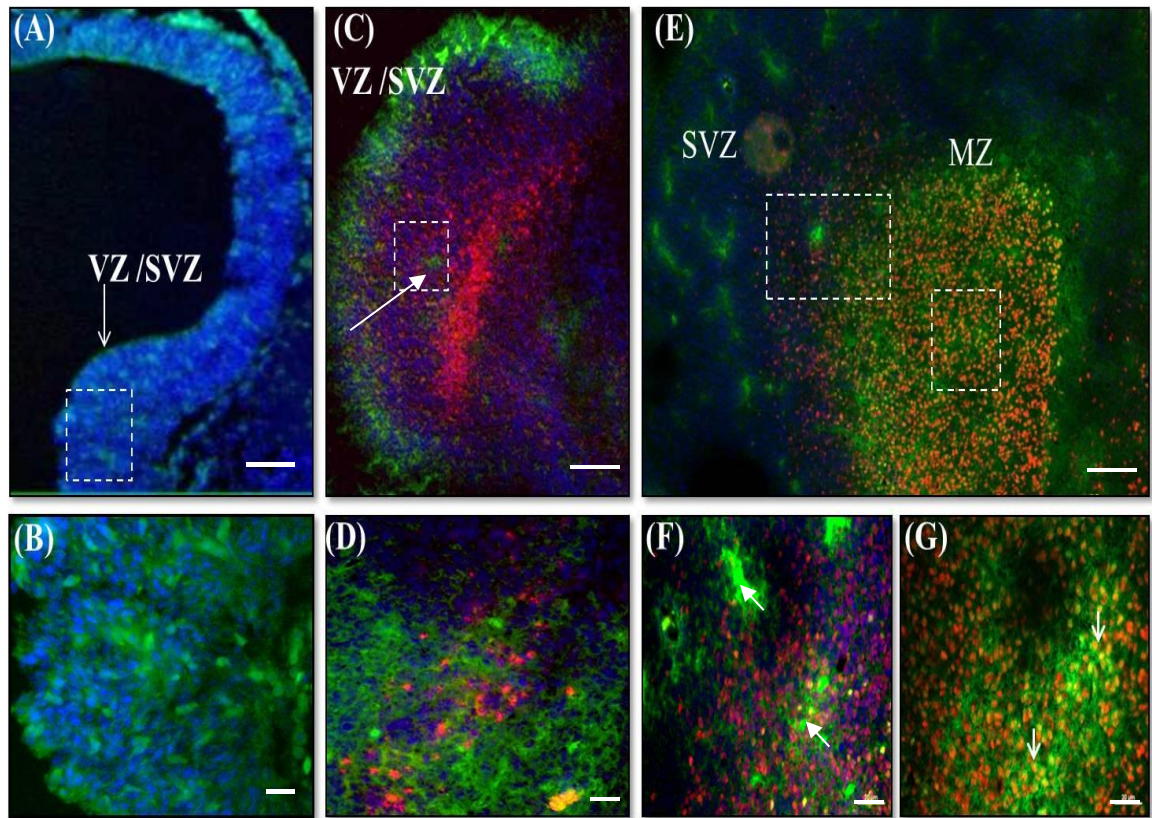
Figure 3.1 WT characterisation of FOXP1 and CTIP2 co-localisation in the mouse striatum between E10-E14. Double staining of FOXP1 (Green) and CTIP2 (Red) and the nuclear stain Hoechst (Blue). Pictures represent merged images of the three stains. **(A)** At E10 there are patches of FOXP1 staining seen in the proliferative SVZ. **(B)** Higher magnification of staining at E10. **(C)** At E12 FOXP1 positive staining is still most prominent in the SVZ but small patches can be seen out of this proliferative region (shown by an arrow). CTIP2 positive cells can be identified in the MZ. **(D)** Higher magnification of staining at E12. **(E)** At E14 FOXP1 positive patches are still evident in the SVZ but staining is most prominent in the MZ where it co-localises with CTIP2. Boxes indicate regions that are displayed at a higher magnification in F and G. **(F)** Staining in the SVZ at a higher magnification; arrows show patches of FOXP1 positive/CTIP2 negative staining. **(G)** Staining in the MZ at a higher magnification. Examples of nuclear co-localisation of CTIP2 and FOXP1 are shown by arrows. *Abbreviations; SVZ= sub ventricular zone, VZ=ventricular zone, MZ=Mantle Zone, Scale bars= low mag 50µm and high mag 20µm.*

From E16 through to P7, FOXP1 and CTIP2 had overlapping patterns of expression in the MZ of the striatum, with staining preferentially being nuclear (Figure 3.2A-P). Within these regions, numerous patches of intense FOXP1 staining can also be seen which are indicated with arrows in the representative photomicrographs in Figure 3.2; these patchy regions are not evident in CTIP2 staining.

As DARPP-32 is currently the "gold standard" marker of MSNs, co-localisation of FOXP1 and DARPP-32 was assessed using fluorescent immunohistochemistry from E10 to P7. DARPP-32 staining was not evident in our sections until E18 (Figure 3.3B-D), which correlates with previous reports that show that DARPP-32 is not evident in the developing mouse striatum until E18. At E18 and P0, FOXP1 staining, as described above, was seen throughout the striatum preferentially in the nucleus of cells, with marked patches of darker staining (Figure 3.3A, E), whereas DARPP-32 staining was seen in defined patches within the striatum and unlike FOXP1 staining, was not nuclear and appeared to be cytoplasmic or membranous (Figure 3.3B, F). At P7 the staining pattern of FOXP1 remained the same (Figure 3.3I) but the DARPP-32 patchy staining had become more homogenous and was evident throughout the striatum (Figure 3.3J). At all ages, DARPP-32 and FOXP1 did co-localise within the striatum (Figure 3.3D, H, L), and although there were subsets of FOXP1 positive/DARPP-32 negative cells identified, all DARPP-32 positive cells always appeared to co-localise with FOXP1 positive cells (Figure 3.3C-D, G-H, K-L).
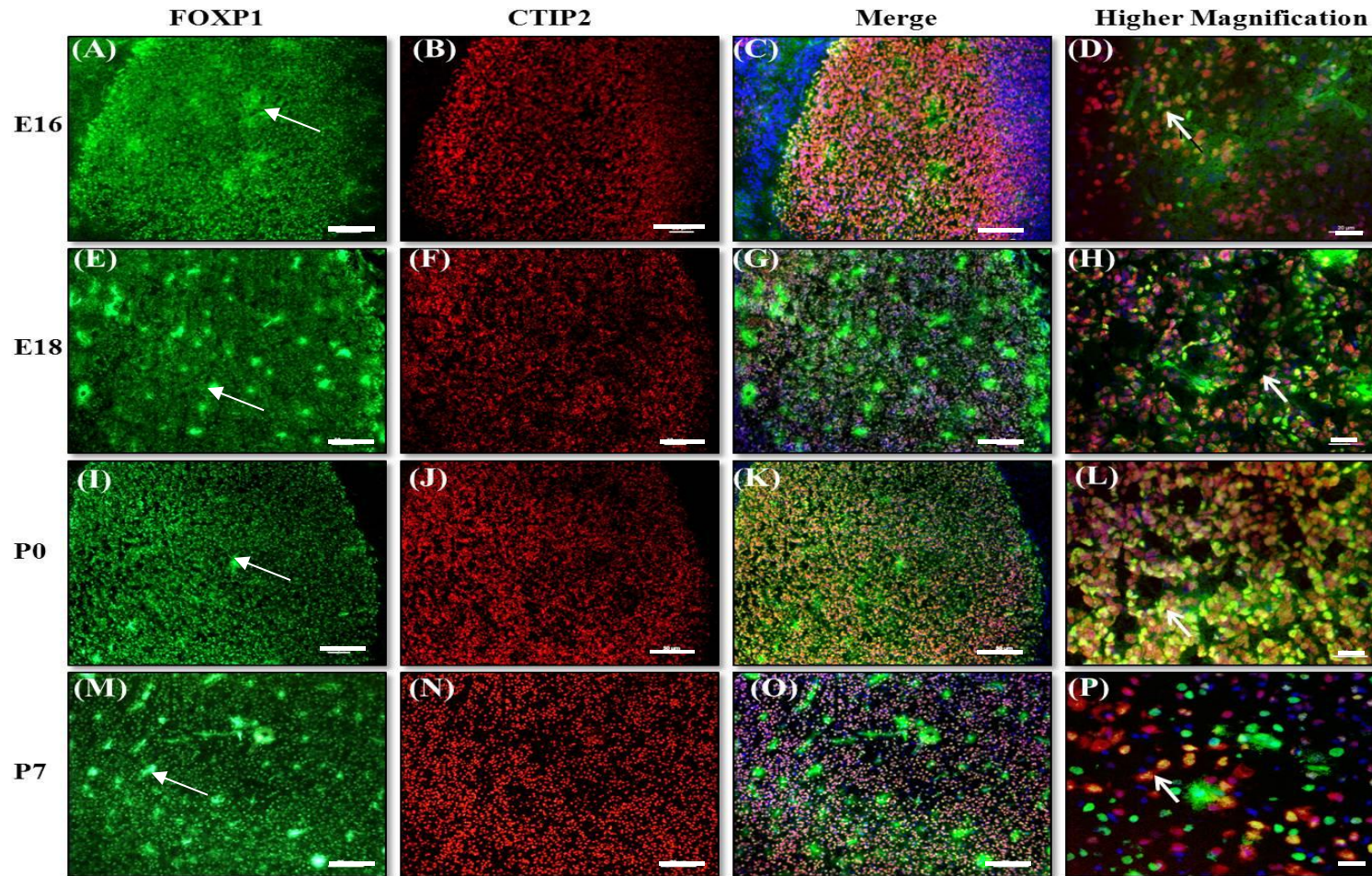
Figure 3.2 WT characterisation of FOXP1 and CTIP2 staining in the mouse striatum between E16-P7. Double staining of FOXP1 (Green) and CTIP2 (Red) and the nuclear stain Hoechst (Blue). The third column represents merged images of the three stains and the final column is the merged image at a higher magnification. **(A-D)** At E16, nuclear co-localisation of FOXP1and CTIP2 is seen within the striatum. **(E-P)** At E18, P0 and P7 nuclear co-localisation of FOXP1 and CTIP2 is still seen throughout the striatum, examples of co-localised cells are shown with arrows in H, L and P. Within the striatum there are darker patches of FOXP1 staining indicated with arrows in A, E, I and M which are not evident in the CTIP2 stained sections. *Scale bars= low mag 50μm and high mag 20μm*
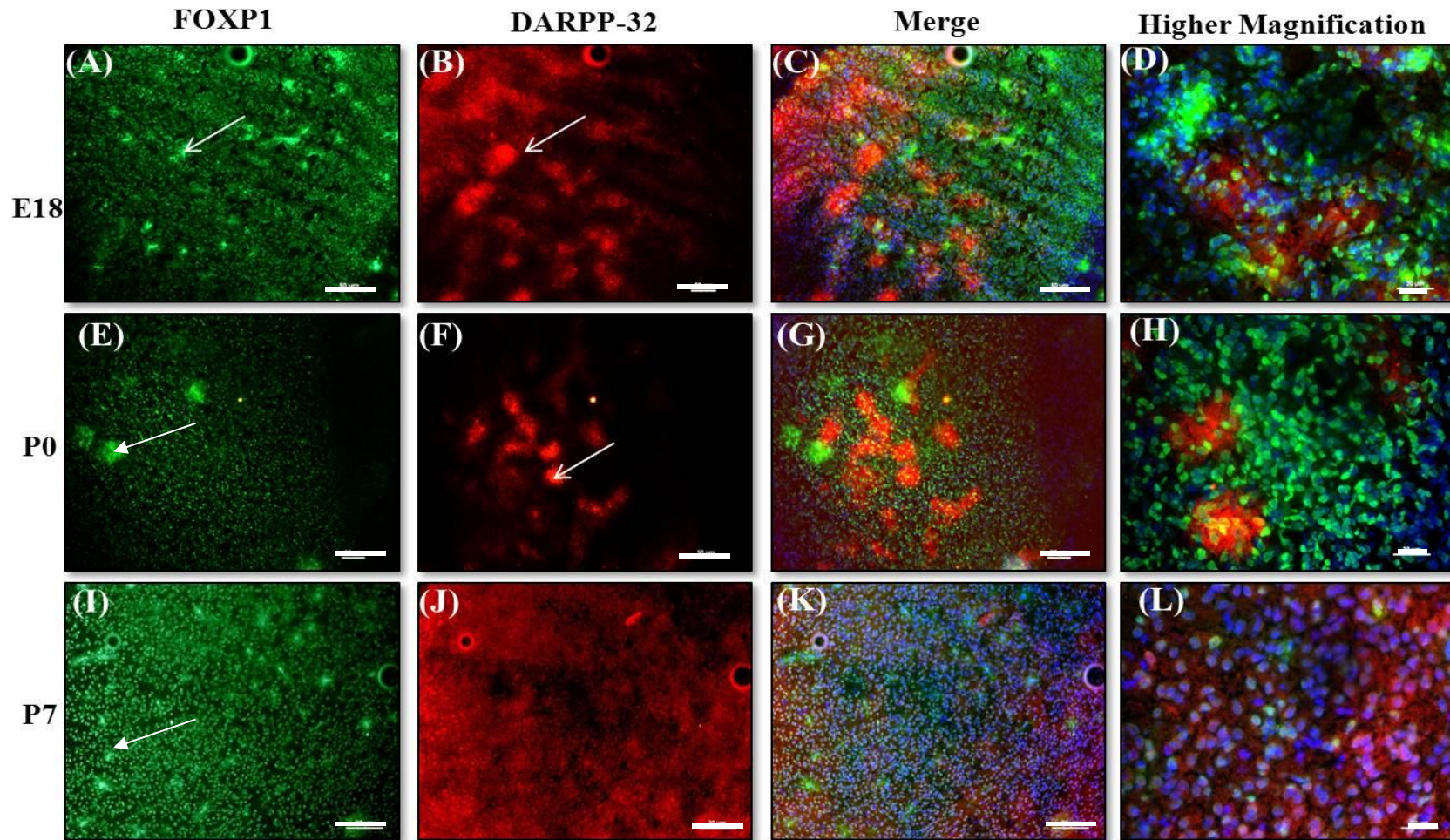
Figure 3.3 WT characterisation of FOXP1 and DARPP-32 staining in the mouse striatum between E18 and P7. Double staining of FOXP1 (Green) and DARPP-32 (Red) and the nuclear stain Hoechst (Blue). The third column represents merged images of the three stains and the final column is the merged image at a higher magnification. **(A, E and I).** FOXP1 staining is seen throughout the striatum at E18, P0 and P7. Within the striatum there are darker patches of FOXP1 staining indicated with arrows. **(B, F)** At E18 and P0 DARPP-32 staining is cytoplasmic/membranous and evident in defined patches throughout the striatum, indicated with arrows. **(J)** At P7 DARPP-32 staining showed more uniform staining throughout the striatum. At all ages DARPP-32 positive cells co-localised with FOXP1 cells however, there were subsets of FOXP1 positive/DARPP-32 negative cells. *Scale bars= low mag 50μm and high mag 20μm.*

Weight analysis of adult WTs and Heterozygote (*Foxp1⁺ᐟ⁻*) mice

To determine if there were any differences between adult WT and heterozygote mice weights of male and female mice were recorded at 7, 9, 12 and 16 weeks (female mice were needed for breeding and they were unable to be weighed at 16 weeks). Males and females have been evaluated separately as male mice are generally heavier than female mice. Overall, WT female mice show a trend to be slightly heavier than *Foxp1⁺ᐟ⁻* mice but there was no significant interaction between the weights over time and group (Group, Time $_{(2,\,62)}$ F = 1.99, p =n.s.); this is shown in Figure 3.4A. As with the female mice, male, WT mice showed a trend to be heavier than *Foxp1⁺ᐟ⁻* mice but there was no significant interaction between the weights over time and group (Group, Time $_{(3,\,117)}$ F = 0.56, p =n. s); this is shown in Figure 3.4B.

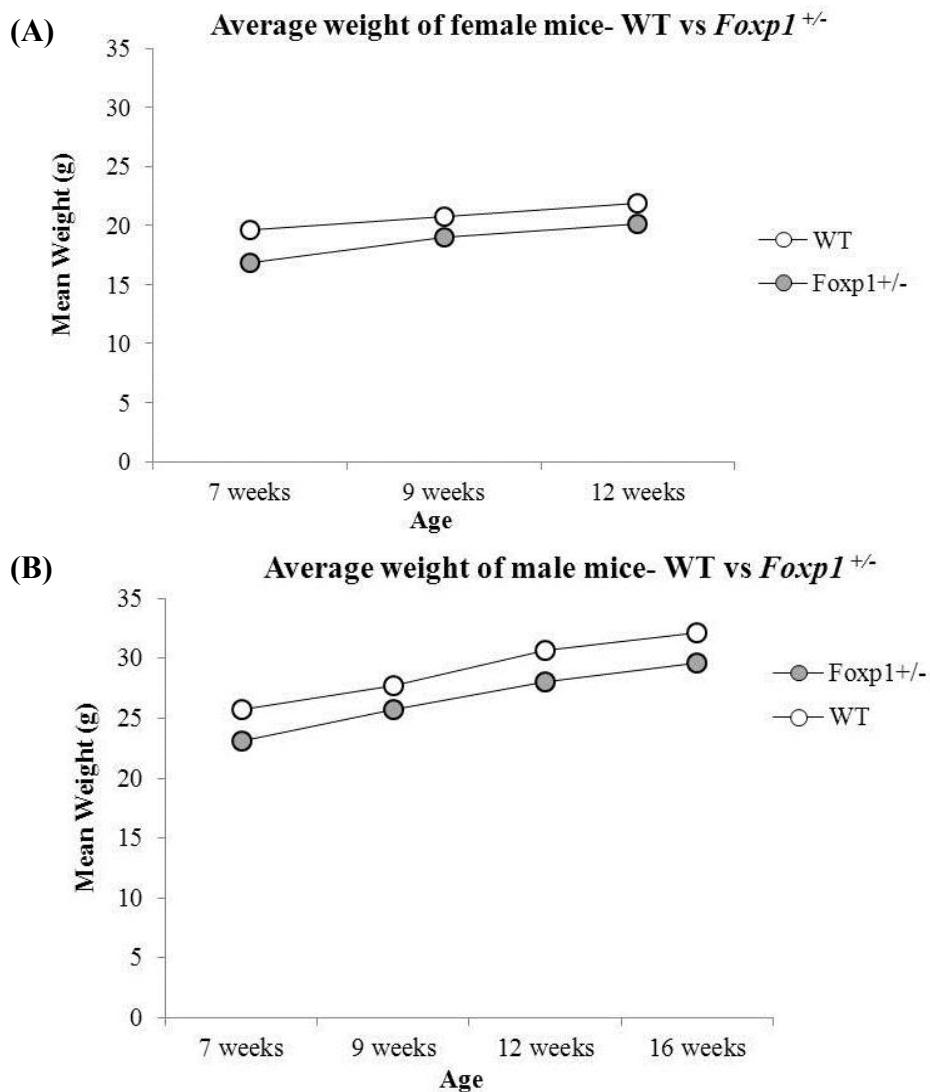**Figure 3.4 Average weights (g) of WT and *Foxp1⁺ᐟ⁻* adult mice. (A)** Female WT and *Foxp1⁺ᐟ⁻* adult mice weighs from 7 weeks to 12 weeks. **(B)** Male WT and *Foxp1⁺ᐟ⁻* adult mice weights from 7 weeks to 16 weeks. *Error bars are SEM.*

Phenotypic comparison of adult *Foxp1$^{+/-}$* with WTs

In order to assess any differences in the brains of WT and ***Foxp1$^{+/-}$*** mice animals were sacrificed at 20 weeks and striatal volumes were calculated. Ideally, female and male mice would have been used in comparison studies, however, female mice were valuable as routinely required for breeding and therefore male *Foxp1$^{+/-}$* mice were chosen. Observations of the brains upon dissection showed that there were no obvious differences between the genotypes (Figure 3.5A) and cresyl violet (CV) staining confirmed that there were no morphological differences between the brains of each genotype, (Figure 3.6A, C). Graft volume was estimated using graft area as determined by Nissl staining and showed that there was no significant difference in striatal volume between the genotypes ($F_{1, 9}$ =0.00, p=n.s.) (Figure 3.5B). Immunohistochemistry using anti- FOXP1 suggested that there were no differences in the amount of FOXP1 in the striatum and cortex of both genotypes, shown in Figure 3.6B and D.
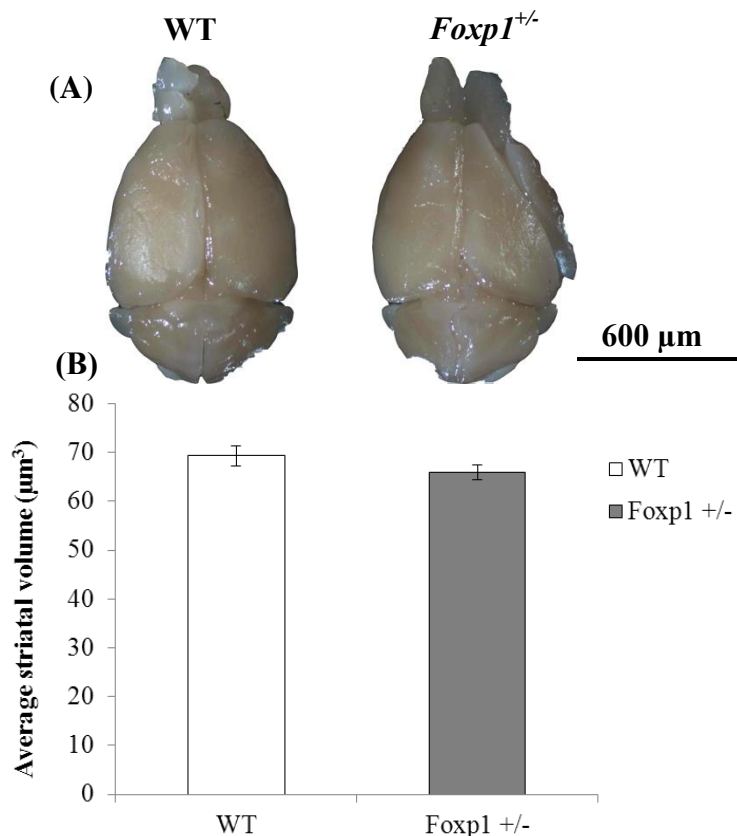

Figure 3.5 (A) Representative brains from a WT and a *Foxp1$^{+/-}$* mouse **(B)**.The bars represent the mean striatal volume from 5 WT and 5 *Foxp1$^{+/-}$* mice. *Error bars are SEM.*
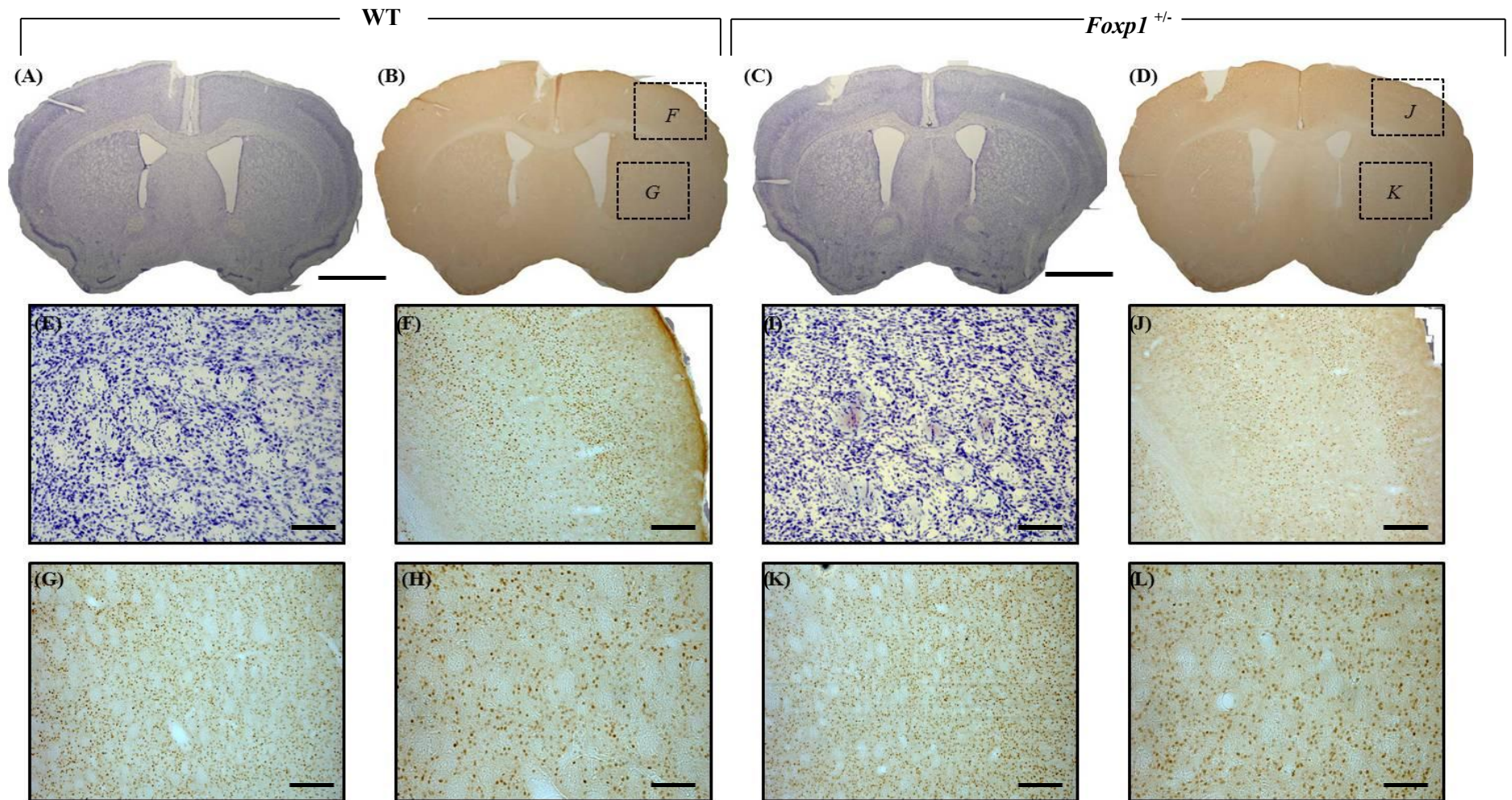
Figure 3.6 CV staining and immunohistochemistry using FOXP1 in WT and *Foxp1*$^{+/-}$ mice at 20 weeks of age. (A and C) CV staining showing there are no differences in morphology between the WT and *Foxp1*$^{+/-}$ animals. **(E-I)** CV staining at a higher magnification. **(B, D)** FOXP1 is seen throughout the brains of WT and *Foxp1*$^{+/-}$ mice. **(F, G-H)** Higher power of FOXP1 staining in the cortex and striatum, respectively in WT brains. **(J, K-L)** Higher power of FOXP1 staining in the cortex and striatum, respectively in *Foxp1*$^{+/-}$ brains. *Scale bars: low power images= 500μm, high power images= 50 μm.*

81

Phenotypic characterisation of *Foxp1*^{-/-} mice at E14

As there were no obvious differences between the WT and *Foxp1*^{+/-} adult mice i.e. the loss of one *Foxp1* allele did not make any noticeable phenotypic differences, homozygous *Foxp1* KO (*Foxp1*^{-/-}) was analysed. Due to the embryonic lethality, analysis of *Foxp1*^{-/-} animals was limited to E14. Crown rump (CR) lengths and brain diameter (as shown in 3.3) were taken upon dissections of all the pups born from a *Foxp1* heterozygous cross at E14, and were recorded for the duration of work presented in this thesis. Upon dissection, it was apparent that *Foxp1*^{-/-} embryos had a "bloodier" appearance when compared to WT and heterozygotes (*Foxp1*^{+/-}) embryos, with the later two genotypes being indistinguishable. A representative WT and a *Foxp1*^{-/-} embryo from E14 is shown in Figure 3.7A. When analysed, there was no significant genotypic difference in the CR length of the embryos ($F_{2, 122} = 2.77$, p=n.s.) (Figure 3.7B) or any observable differences in the brains, with no significant difference in brain diameter between the groups at E14 ($F_{2, 79} = 0.39$, p=n.s.) (Figure 3.7C and D). If striate were dissected from the brains, it was noted that the majority of striate from the *Foxp1*^{-/-} embryos had distinct blood spots, reminiscent of haemorrhaging (82%), which were rarely observable in littermates (8%), with the WT and *Foxp1*^{+/-} striate being indistinguishable. Representative photomicrographs of a WT and *Foxp1*^{-/-} striate are shown in Figure 3.7E. The cortex of *Foxp1*^{-/-} pups also had blood spots on it. To confirm that there was embryonic lethality associated with the *Foxp1*^{-/-} embryos after E14, a litter was taken at E16. Figure 3.7G shows a representative photomicrograph of a WT and two *Foxp1*^{-/-} embryos. The *Foxp1*^{-/-} embryos were considerably bloodier, smaller, showed no retraction on poking, and were under developed when compared to WT embryos.

When striate were taken through the cell culture protocol, individual cell counts per pair of striate were carried out using the trypan blue exclusion assay. There was a significant difference in total number of striatal cells between groups ($F_{2, 75} = 4.43$, p<0.01). *Post-hoc* comparisons showed that there were significantly fewer total striatal cells per pair of striate from *Foxp1*^{-/-} embryos (14,092±1023) compared to from WT embryos (20,480±2392) (p<0.01).
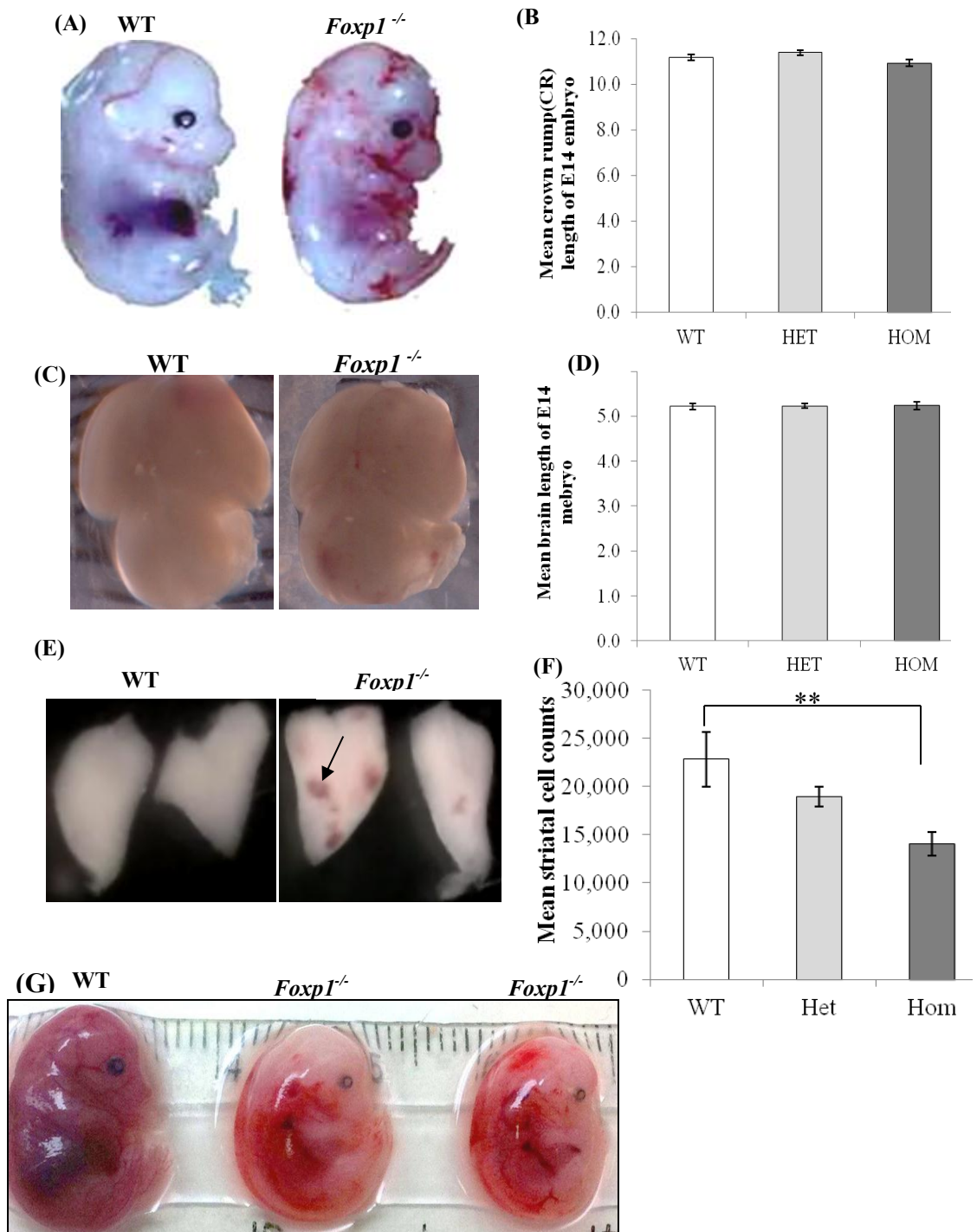
Figure 3.7 Dissection observations at E14. (A) Representative photomicrographs of a WT and a *Foxp1*$^{-/-}$ embryo at E14, the *Foxp1*$^{-/-}$ clearly shows a more bloody appearance than the WT embryo. **(B)** The mean CR lengths of WT embryos (n= 43)was 11.2 mm, for *Foxp1*$^{+/-}$ embryos (n= 52) was 11.4 mm and for *Foxp1*$^{-/-}$ embryos (n= 28) was 10.9 mm. **(C)** Representative photomicrographs of a WT and a *Foxp1*$^{-/-}$ brain. **(D)**There was no difference in brain length, the average diameter for all genotypes was 5 mm. **(E)** Representative photomicrographs of a pair of striate from a WT and a *Foxp1*$^{-/-}$ embryo, the *Foxp1*$^{-/-}$ striatae have a distinct spotty appearance that is absent from WT and *Foxp1*$^{-/-}$ striate. **(F)** Mean striatal cell counts from a pair of striate from each genotype determined through trypan blue exclusion assays. **(G)** Representative photomicrographs of E16 pups. The two *Foxp1*$^{-/-}$ embryos are smaller and underdeveloped when compared to the WT embryo. Significant *post-hoc* differences are indicated with brackets (** p<0.01).

Confirmation of KO

Following initial characterisation of the *Foxp1$^{-/-}$* pups at dissection, it needed to be established that FOXP1 was not being produced in the *Foxp1$^{-/-}$* pups. To confirm this, immunohistochemistry was carried using anti-FOXP1 out on E14 sections. Results showed that there was no FOXP1 positive staining present in striatum or cortex of the *Foxp1$^{-/-}$* compared to WT embryos; shown in Figure 3.8A. To further confirm the loss of *Foxp1*, RNA was extracted from striate from the embryos of all genotypes and subsequently reverse transcribed into cDNA for RT-PCR analysis. The cDNA was normalised to the housekeeping gene GAPDH. Following normalisation *Foxp1* specific primers were used. Figure 3.8B shows a representative agarose gel showing that samples generated from WT and *Foxp1$^{+/-}$* embryos produced a positive band (~500bp) indicating *Foxp1* was present whereas there was no band evident from *Foxp1$^{-/-}$* samples, confirming *Foxp1* was not being actively transcribed.
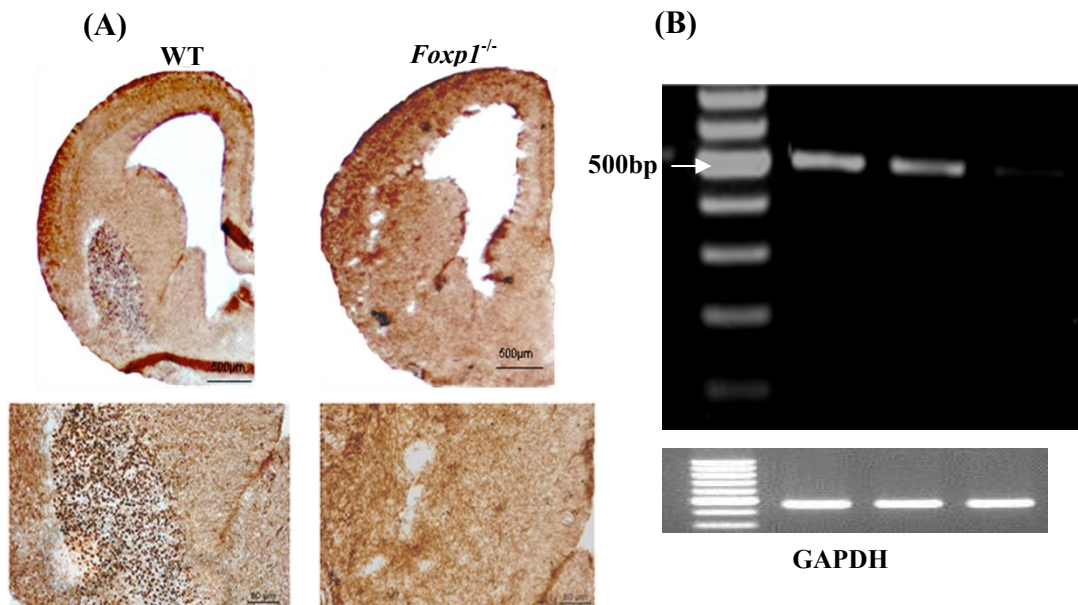
Figure 3.8 Confirmation of loss of Foxp1 in *Foxp1$^{-/-}$* line (A) Representative photomicrographs showing FOXP1 immunohistochemistry confirming that there were no FOXP1 positive cells in the *Foxp1$^{-/-}$* striatum or cortex in contrast to WT striatum. **(B)** RT-PCR normalised to GAPDH, confirming FOXP1 is not present in the *Foxp1$^{-/-}$* striatum, and is reduced in the *Foxp1$^{+/-}$* striatum, compared to the WT striatum.

In vitro analysis of striatal differentiation cultures in the absence of *Foxp1* after 24 hours

To look for differences in the developing mouse striatum pairs of striate (WGE) from individual pups of each genotype were separately cultured in differentiation medium (1% FCS, 2% BSA) and fixed after 24 hours or 7 DIV. Following fixation several stains were carried out to establish any differences in neuronal number and more specifically MSN development.

As expected, there were no FOXP1 positive cells in cultures derived from *Foxp1*$^{-/-}$ striatae at 24 hours ($F_{2, 14}$ = 96.66, p<0.001). *Post-hoc* comparisons confirmed that this significance was from cultures generated from the *Foxp1*$^{-/-}$ striate (0±0.27) compared to cultures generated from WT (16±1.72) and *Foxp1*$^{+/-}$ striate (7±0.70) (p<0.000). There were also significantly fewer FOXP1 positive cells in the *Foxp1*$^{+/-}$ cultures compared to WT cultures (p<0.01) (Figure 3.9A). Consistently, there was a significant genotypic difference in the number of FOXP1 positive cells when calculated as a percentage of total β-Tubulin 111(TUJ1) positive cells after 24 hours ($F_{2, 13}$ = 48.316, P<0.000). *Post-hoc* comparisons showed this significance was evident between the WT and *Foxp1*$^{+/-}$ cultures when compared to *Foxp1*$^{-/-}$ cultures (p<0.000), there was no significant difference between the other two genotypes (p=n.s.) (Figure 3.9A) There was no significant difference between the overall numbers of TUJ1 positive cells as a percentage of Hoechst positive nuclei ($F_{2, 13}$ = 1.245, p=n.s.) (Figure 3.9A). Representative photomicrographs of the cultures are shown in Figure 3.10. There were no obvious differences in nuclear or neuronal morphology, as determined by Hoechst and TUJ1 staining respectively, in the absence of *Foxp1*.

To look at specific differences in the number of MSNs, once again the markers CTIP2 and DARPP-32were used. As the cells were fixed after only 24 hours *in vitro* there was very little DARPP-32 staining, as a percentage of total Hoechst positive cells, seen across all of the cultures, irrespective of genotype (WT=2±2.2, *Foxp1*$^{+/-}$=1±0.38, *Foxp1*$^{-/-}$=1±0.24 ($F_{2,14}$ = 0.864,p=n.s.). Equally, there were no differences in the number of DARPP-32 positive cells as a percentage of total CTIP2 positive cells ($F_{2, 14}$ = 1.41, p=n.s.) (Figure 3.9B). There was a trend for the number of CTIP2 positive cells, as a percentage of total Hoechst positive cells to increase in cultures generated from *Foxp1*$^{-/-}$ striate (75±6.13) compared to cultures from WT (67±4.73) and *Foxp1*$^{+/-}$striate

(51±9.29), although this difference was not significant ($F_{2,14}$ = 0.15, p=n.s.) (Figure 3.9B). Representative photomicrographs of the cultures are shown in Figure 3.11.
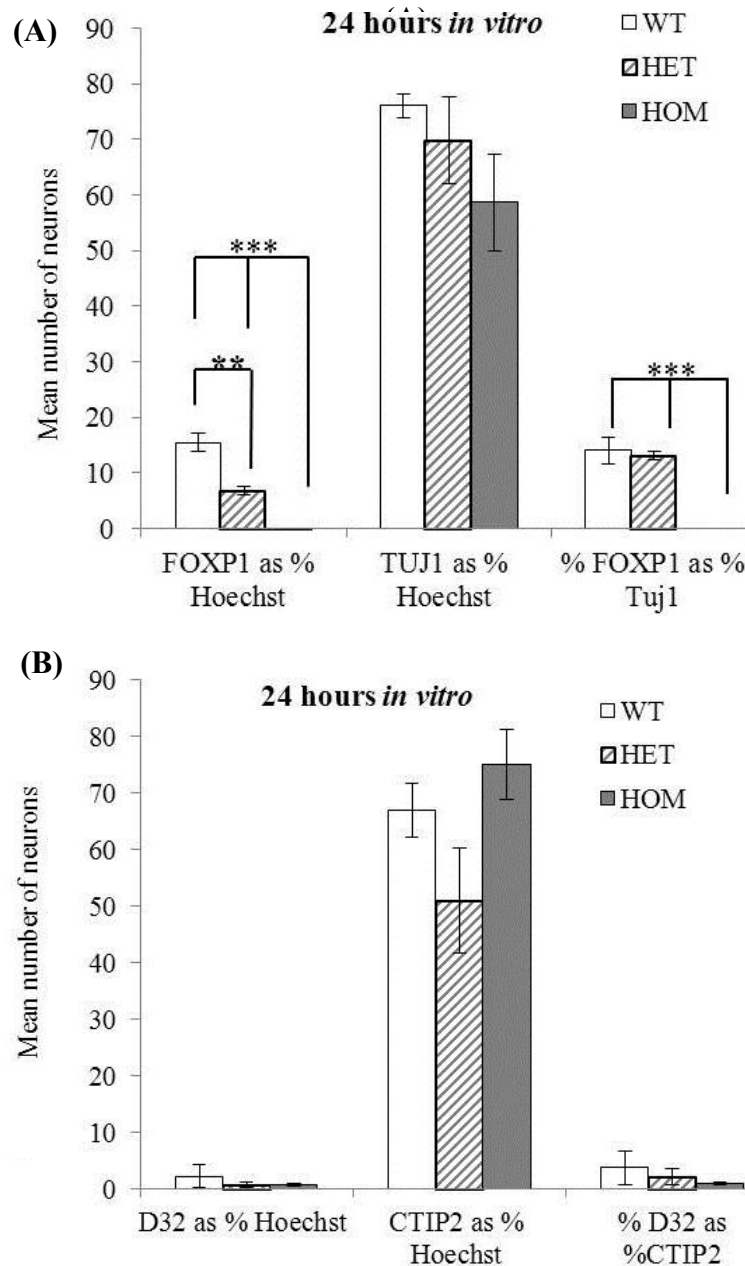
Figure 3.9 *In vitro* **cell counts at 24 hours. Cultures were generated and cultured individually from WT,** *Foxp1*$^{+/-}$ **and Foxp1**$^{-/-}$ **striate and fixed after 24 hours** *in vitro*.**(A)** FOXP1 and TUJ1 cells were counted and are represented as a percentage of total Hoechst positive nuclei. FOXP1 counts are also represented as percentage of total TUJ1 positive cells. **(B)** CTIP2 and DARPP-32 cells were counted and are represented as a percentage of total Hoechst positive nuclei. DARPP-32 counts are also represented as percentage of total CTIP2 positive cells. Each bar on the graph represents a mean of at least 3 different cultures and error bars are SEM. Significant *post-hoc* differences are indicated with brackets (***p<0.001,** p<0.01).

Figure 3.10 *In vitro* analysis at 24 hours. E14 mouse WGE cultures from each of the three genotypes were plated down and left to differentiate for 24 hours *in vitro*. Following fixation cells were double labelled for FOXP1 (Red) and TUJ1 (Green) and the nuclear stain Hoechst (Blue). The fourth column is a merged image of the first three photomicrographs. Arrows represent examples of co-localised cells. *Scale bars = 50μm*.

88

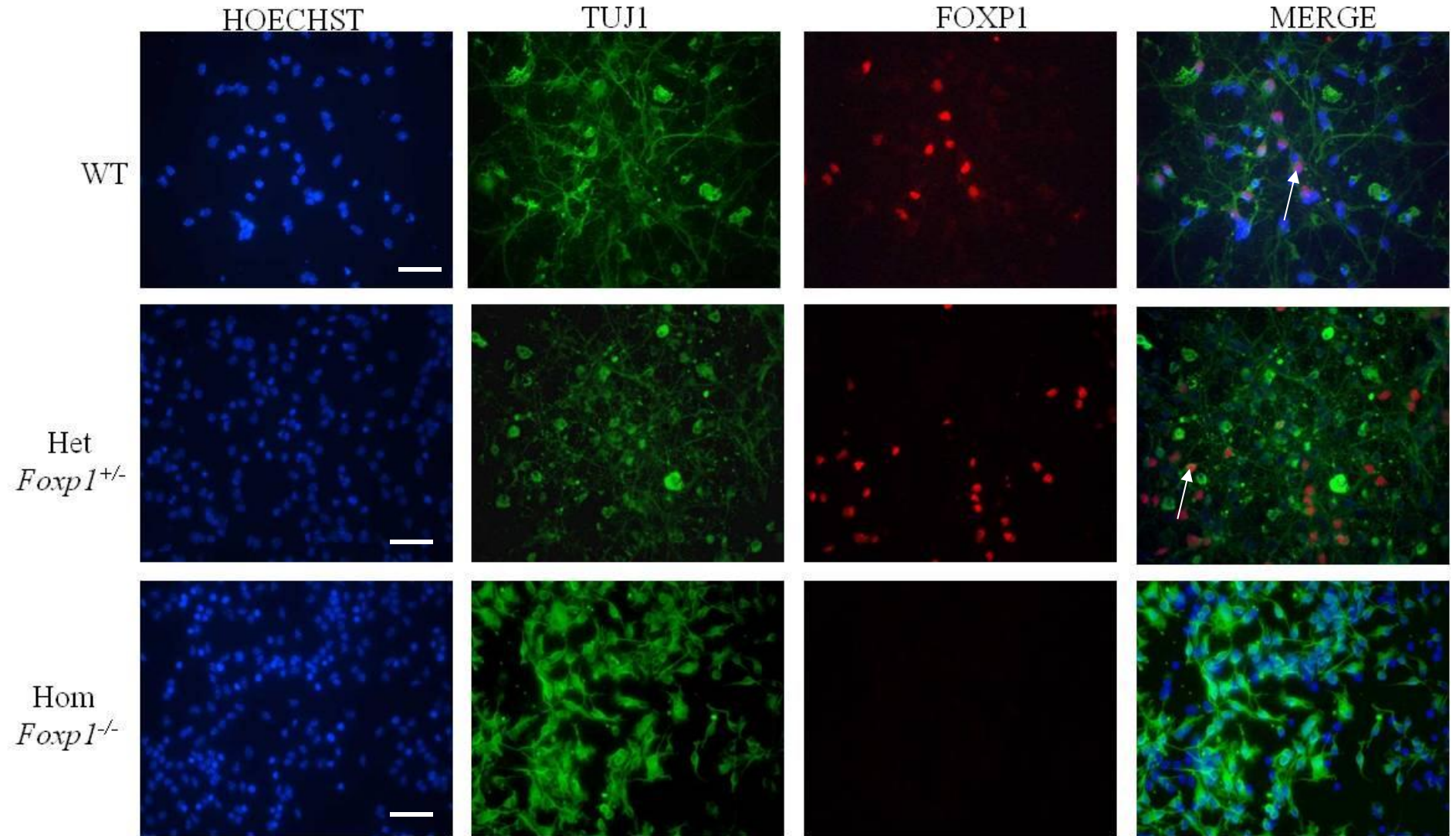**Figure 3.11 *In vitro* analysis at 24 hours.** E14 mouse WGE cultures from each of the three genotypes were plated down and left to differentiate for 24 hours *in vitro*. Following fixation, cells were double labelled for CTIP2 (Red) and DARP32 (Green) and the nuclear stain Hoechst (Blue). The fourth column is a merged image of the first three photomicrographs. Arrows represent examples of co-localised cells. *Scale bars = 50μm.*
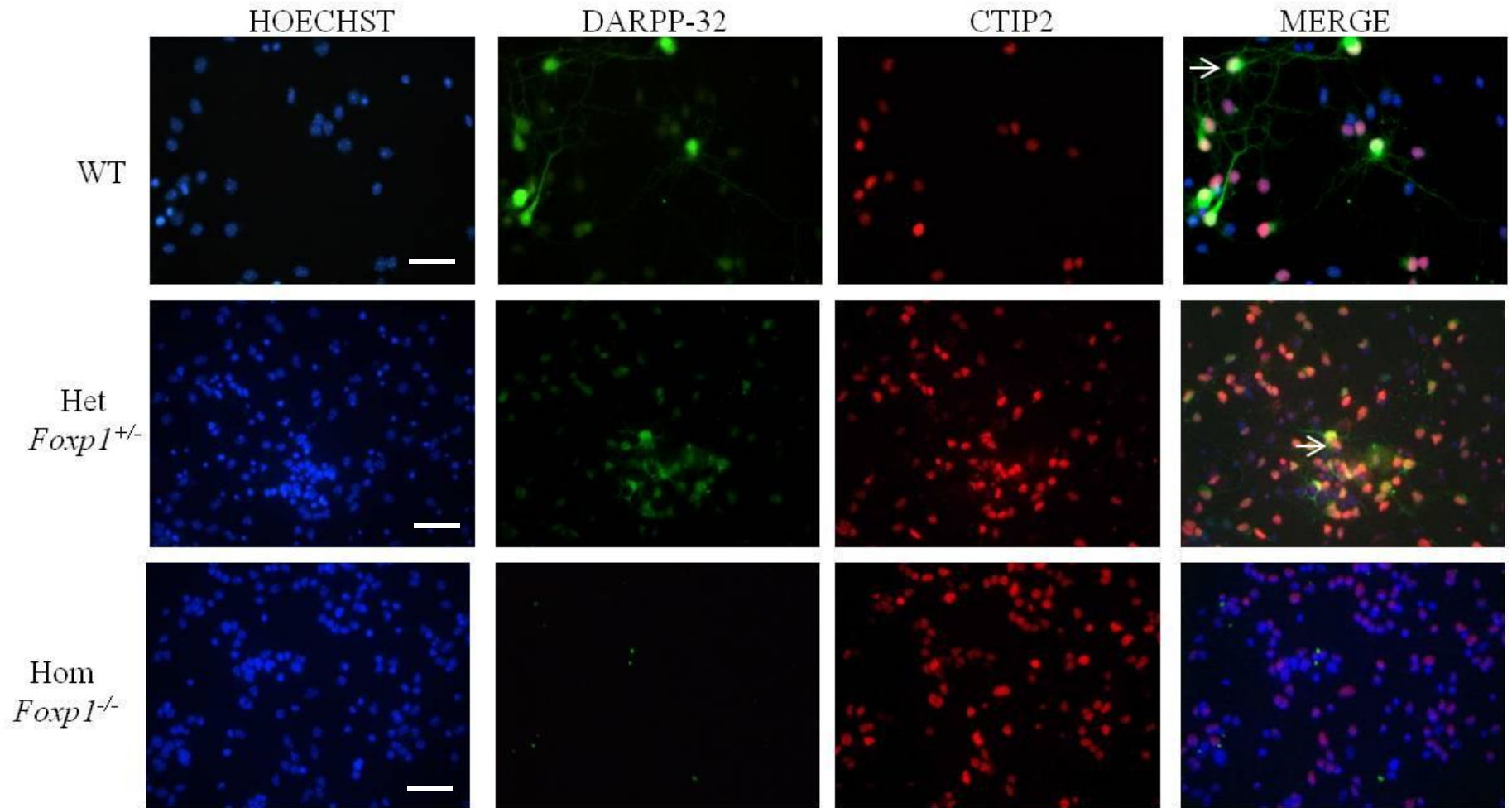
In vitro analysis of striatal differentiation cultures in the absence of *Foxp1* after 7 DIV

Following fixation after 7 DIV once again there were no FOXP1 positive cells in cultures derived from *Foxp1$^{-/-}$* striate ($F_{2, 16}$ = 108.077, p<0.001). *Post-hoc* comparisons showed that there were significantly fewer FOXP1 positive cells in the cultures generated from the *Foxp1$^{-/-}$* striate (0±0) compared to cultures generated from WT (35±1.02) and *Foxp1$^{+/-}$* (26±3.5) striate (p<0.001). Moreover, there were significantly fewer FOXP1 positive cells in the *Foxp1$^{+/-}$* cultures compared to WT cultures (p<0.05) (Figure 3.12A). There was also a significant genotypic difference in the number of FOXP1 positive cells when calculated as a percentage of total TUJ1 positive cells ($F_{2, 16}$ = 199.02, p<0.001). *Post-hoc* comparisons revealed this significance was concerning differences between both WT and *Foxp1$^{+/-}$* cultures compared to *Foxp1$^{-/-}$* cultures (p<0.000); there was no significant difference between WT and *Foxp1$^{+/-}$* cultures (p= n.s.) (Figure 3.12A). There was no significant difference between the overall numbers of TUJ1 positive cells as a percentage of total Hoechst positive nuclei ($F_{2, 16}$ = 2.841, p= n.s.) (Figure 3.12A). Representative photomicrographs of the cultures are shown in Figure 3.13. Once again there were no obvious differences in nuclear or neuronal morphology, as determined by TUJ1 and Hoechst staining, in the absence of *Foxp1*.

Leaving the cultures to differentiate for 7 DIV allowed more time for the cells, specifically the MSNs, to mature and consequently express DARPP-32. There was a significant difference in the number of positively stained DARPP-32 cells as a percentage of total Hoechst positive cells across the different groups ($F_{2, 17}$ =3.72, p=0.05). *Post-hoc* comparisons showed that there were significantly fewer DARPP-32 positive cells in the cultures generated from the *Foxp1$^{-/-}$* striate (1±0.40) compared to cultures generated from WT striate (5±1.41). There was no significant difference in the number of DARPP-32 positive cells between *Foxp1$^{-/-}$* and *Foxp1$^{+/-}$* cultures (2±0.54) (p=n.s.) or between WT and *Foxp1$^{+/-}$* cultures (Figure 3.12B). There was a significant difference in the number of DARPP-32 positive cells as a percentage of CTIP2 positive cells ($F_{2, 14}$ =1.41.p=n.s.). *Post-hoc* comparisons showed this significance was only apparent between WT and *Foxp1$^{-/-}$* cultures (p<0.05) (Figure 3.12B). In contrast to the results at 24 hours, there was a significant difference in the overall number of CTIP2 positive cells as a percentage of total Hoechst positive nuclei between the groups ($F_{2, 17}$ = 4.96, p=<0.05). *Post-hoc* analyses indicated that there were significantly fewer CTIP2

positive cells in the cultures generated from the *Foxp1*$^{-/-}$ striate (57±3.96) compared to cultures generated from WT striate (72±2.11). There were no significant differences between WT and *Foxp1*$^{+/-}$ cultures (Figure 3.12B). Representative photomicrographs of the cultures are shown in Figure 3.14.

In addition to the markers described, the astrocyte marker GFAP was also used; astrocytes are not present after 24 hours *in vitro* and thus the reason why it was not used to stain cultures at this time (data not shown). GFAP and TUJ1 staining was carried out simultaneously, and for both stains, there were no significant differences across the groups ($F_{2, 16} = 0.29$, p=n.s., $F_{2, 16} = 1.76$, p= n.s. respectively) (Figure 3.12C). There was also no co-localisation between TUJ1 and GFAP. Representative photomicrographs are shown in Figure 3.15.

(B)

(C)
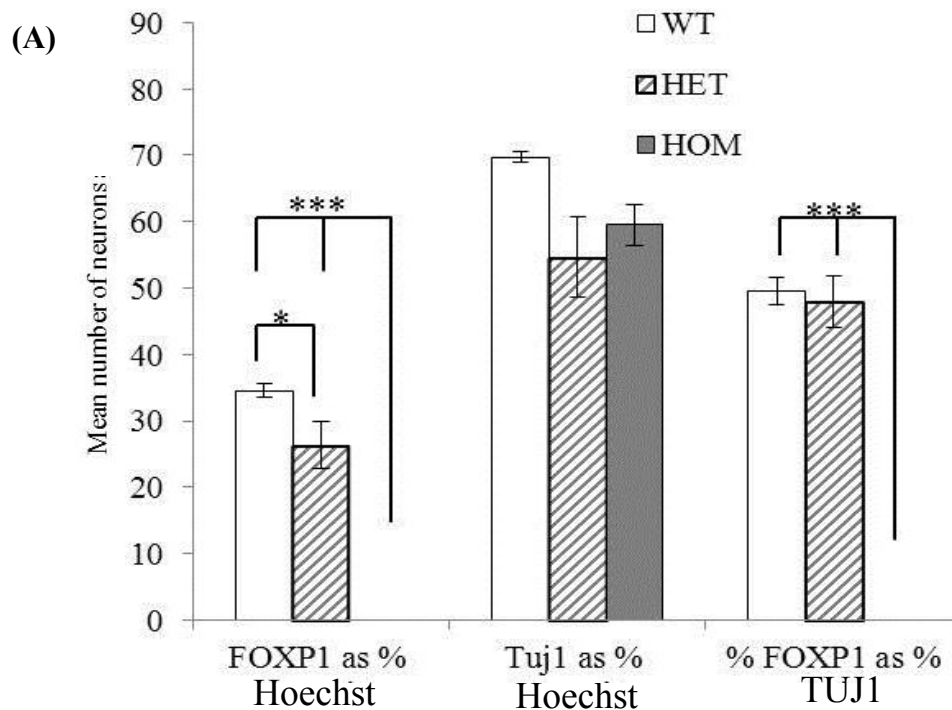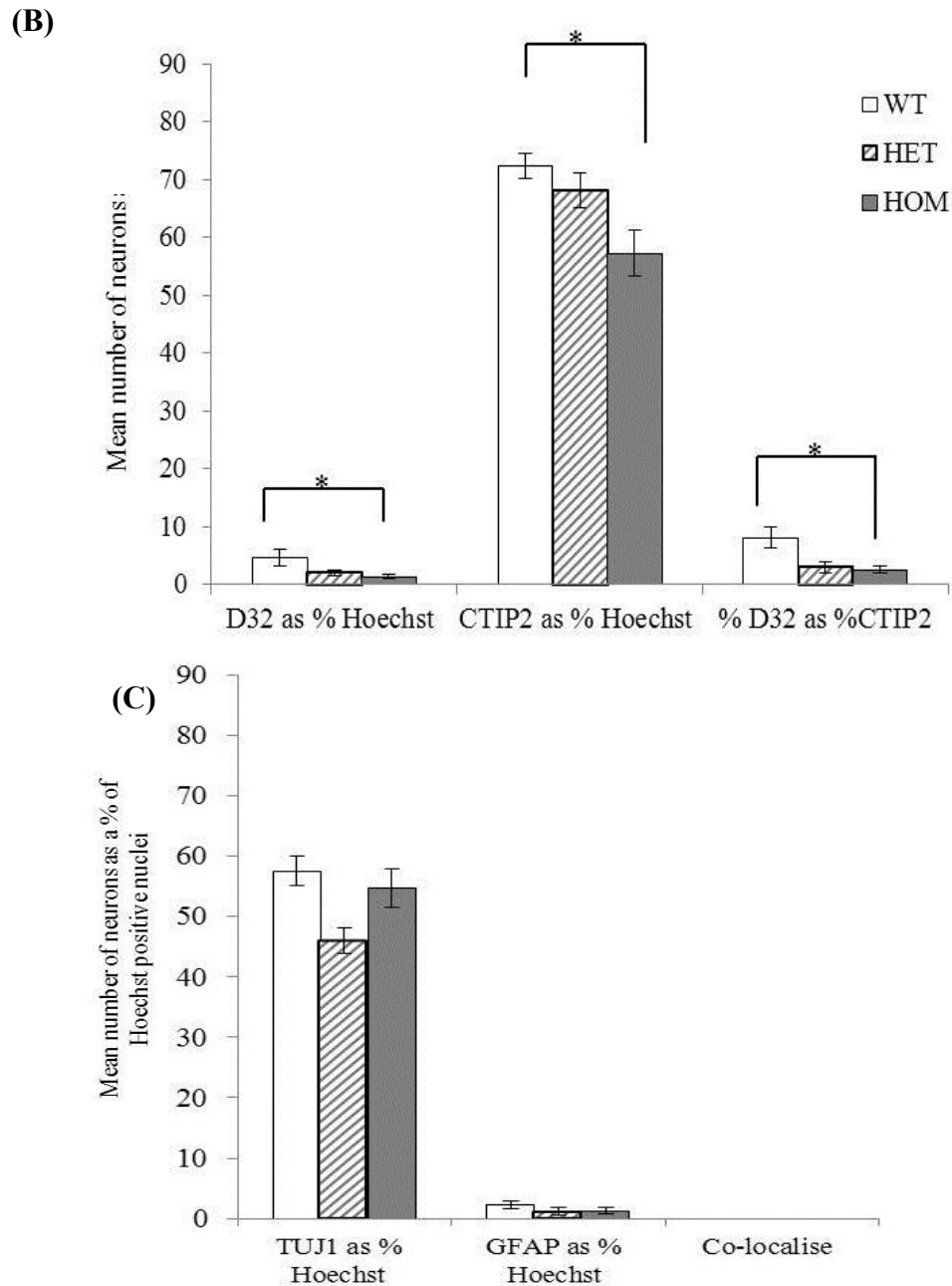
Figure 3.12 *In vitro* cell counts after 7 DIV. Cultures were generated and cultured individually from WT, *Foxp1*$^{+/-}$ and *Foxp1*$^{-/-}$ striate and fixed after 7 DIV. **(A)** FOXP1 and TUJ1 cells were counted and are represented as a percentage of total Hoechst positive nuclei. FOXP1 counts are also represented as percentage of total TUJ1 positive cells. **(B)** CTIP2 and DARPP-32 cells were counted and are represented as a percentage of total Hoechst positive nuclei. DARPP-32 counts are also represented as percentage of total CTIP2 positive cells. **(C)** TUJ1 and GFAP were counted and are represented as a percentage of total Hoechst positive nuclei. Each bar on the graph represents a mean of at least 3 different cultures and error bars are SEM. Significant *post-hoc* differences are indicated with brackets (***p<0.001,* p<0.05).

Figure 3.13 ***In vitro*** **analysis at 7 DIV.** E14 mouse WGE cultures from each of the three genotypes were plated down and left to differentiate for 7 DIV. Following fixation, cells were double labelled for FOXP1 (Red) and TUJ1 (Green) and the nuclear stain Hoechst (Blue). The fourth column is a merged image of the first three photomicrographs. Arrows represent examples of co-localised cells. *Scale bars = 50μm.*

Figure 3.14.*In vitro* **analysis at 7 DIV** E14 mouse WGE cultures from each of the three genotypes were plated down and left to differentiate for 7 DIV. Following fixation cells were double labelled for CTIP2 (Red) and DARPP-32 (Green) and the nuclear stain Hoechst (Blue). The fourth column is a merged image of the first three photomicrographs. Arrows represent examples of co-localised cells. *Scale bars = 50μm.*
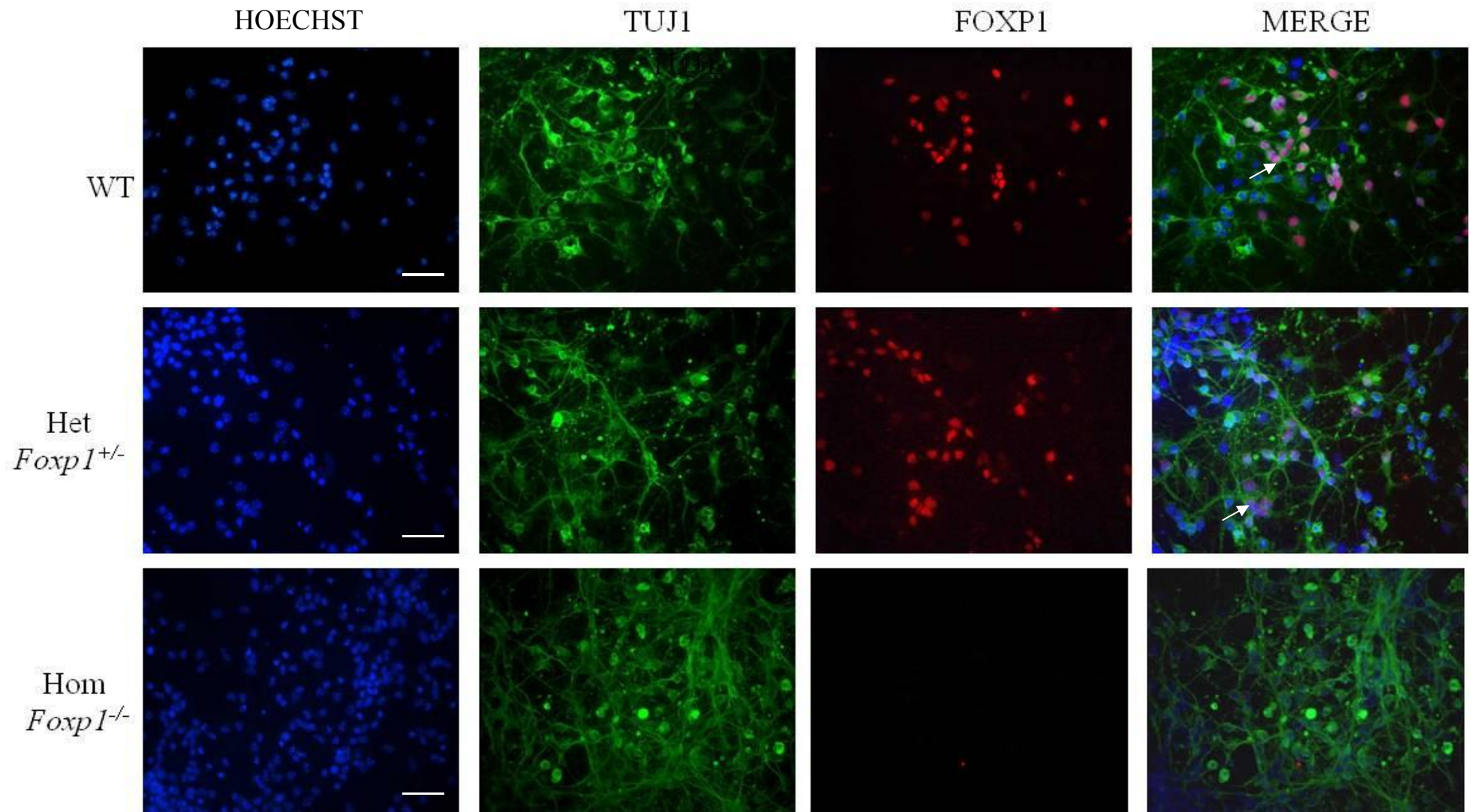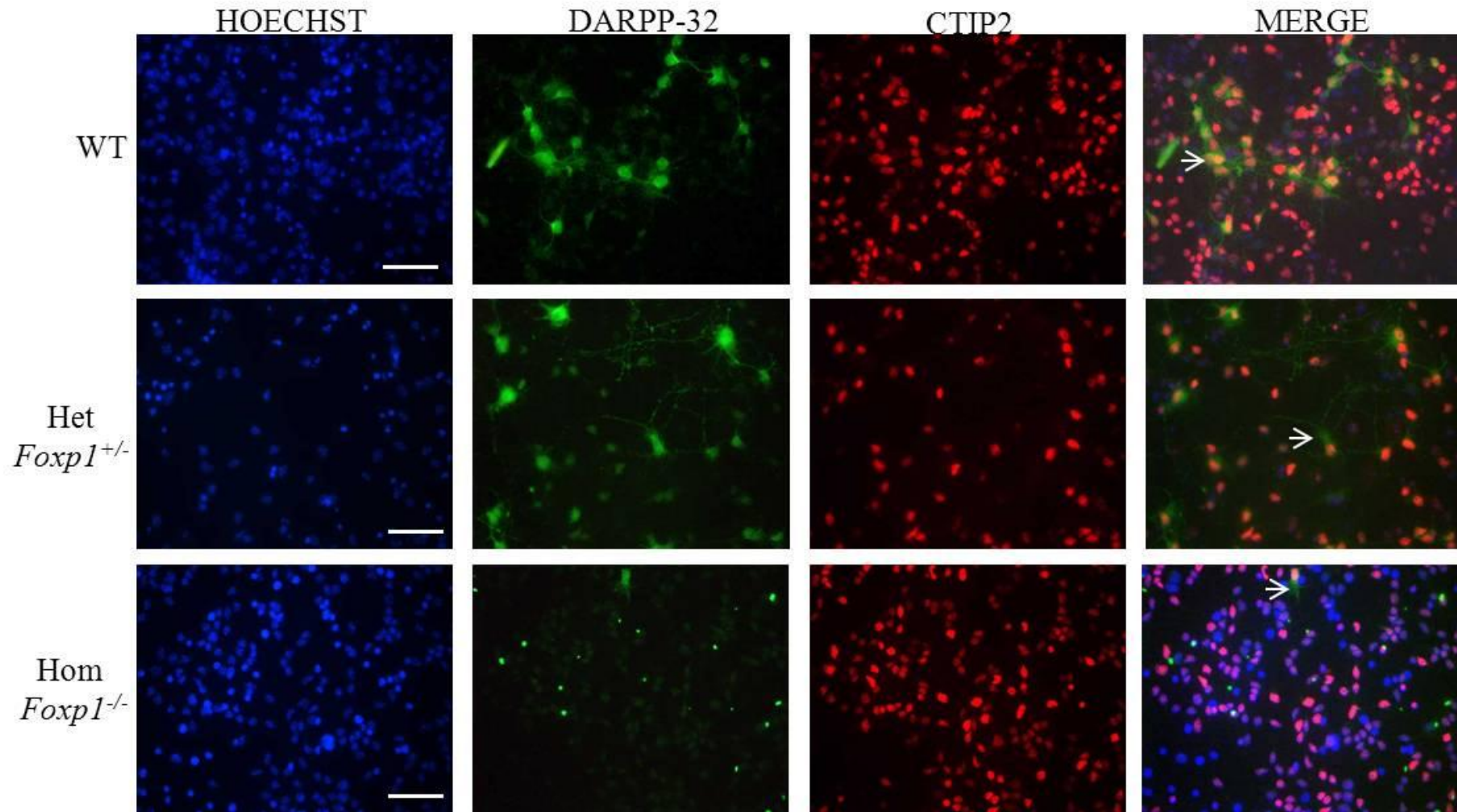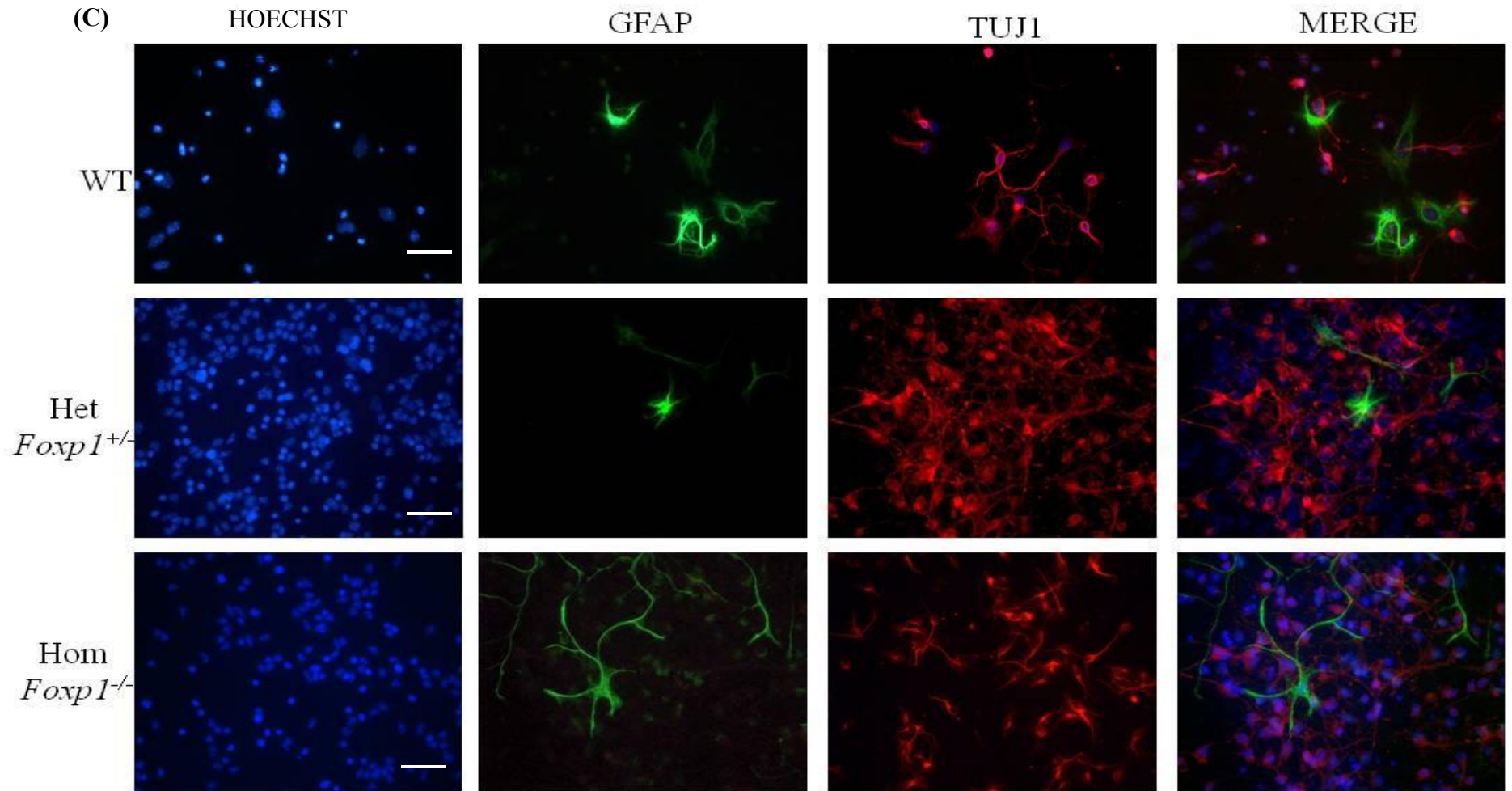
(C)

Figure 3.15 *In vitro* **analysis at 7 DIV.** E14 mouse WGE cultures from each of the three genotypes were plated down and left to differentiate for 7 DIV. Following fixation cells were double labelled for TUJ1 (Red) and GFAP (Green) and the nuclear stain Hoechst (Blue). The fourth column is a merged image of the first three photomicrographs. *Scale bars = 50μm.*

The absence of *Foxp1* does not affect proliferation in the developing striatum

To look at any differences in proliferation in the absence of *Foxp1* BrdU, a thymidine analogue that is incorporated at the S phase of mitosis (i.e. DNA replication) was added to the differentiation media 24 hours before fixation. After 24 hours, there was no difference in the number of TUJ1 positive cells ($F_{2, 11} = 0.27$, p=n.s.) or the number of BRDU positive cells as a percentage of Hoechst positive nuclei between the groups ($F_{2, 14} = 0.15$, p= n.s.) (Figure 3.16). When analysed at 7 DIV there was a significant difference between the number of TUJ1 cells as a percentage of Hoechst positive nuclei ($F_{2, 19} = 3.59$, p<0.05), and *post-hoc* analysis revealed this to be between WT and *Foxp1*$^{+/-}$ cultures (p<0.05). There was no difference between the numbers of BRDU positive cells as a percentage of Hoechst throughout the groups ($F_{2, 19} =1.07$, p= n.s.) (Figure 3.17A). Representative photomicrographs are shown in Figure 3.17B. BRDU positive cells were not seen to co-localize with TUJ1 positive cells at 24 hours or 7 DIV and only limited co-localisation was seen with GFAP (data not shown) and thus further experiments are needed to determine what these proliferating cells are.
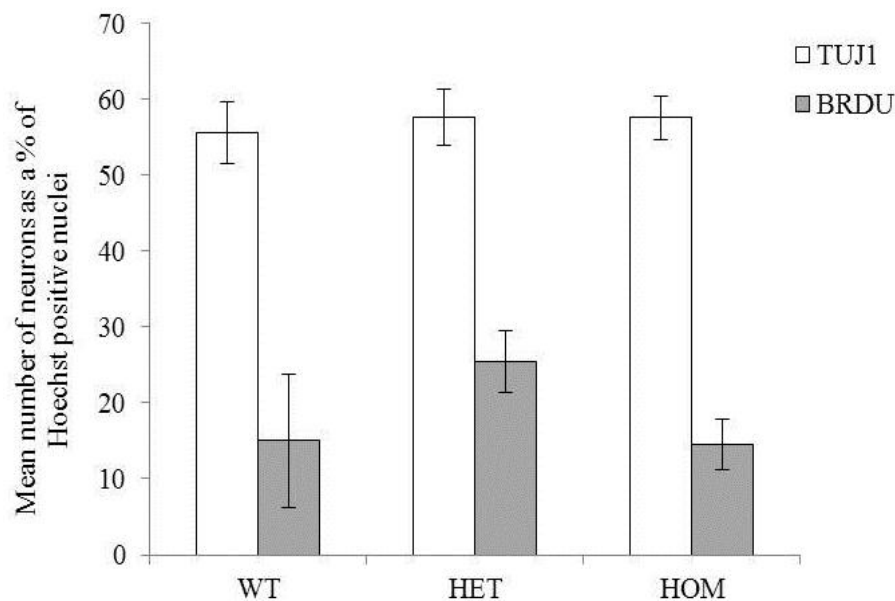
Figure 3.16 BRDU and TUJ1 cell counts after 24 hours *in vitro*. Cultures were generated and cultured individually from WT, *Foxp1*$^{+/-}$ and *Foxp1*$^{-/-}$ striate. BrdU was added to the differentiation media upon flooding. TUJ1 and BRDU positive cells were counted and are represented as a percentage of total Hoechst positive nuclei. Each bar on the graph represents a mean of at least 3 different cultures and error bars are SEM. Significant *post-hoc* differences are indicated with brackets (p* <0.05).

(A)

(B)
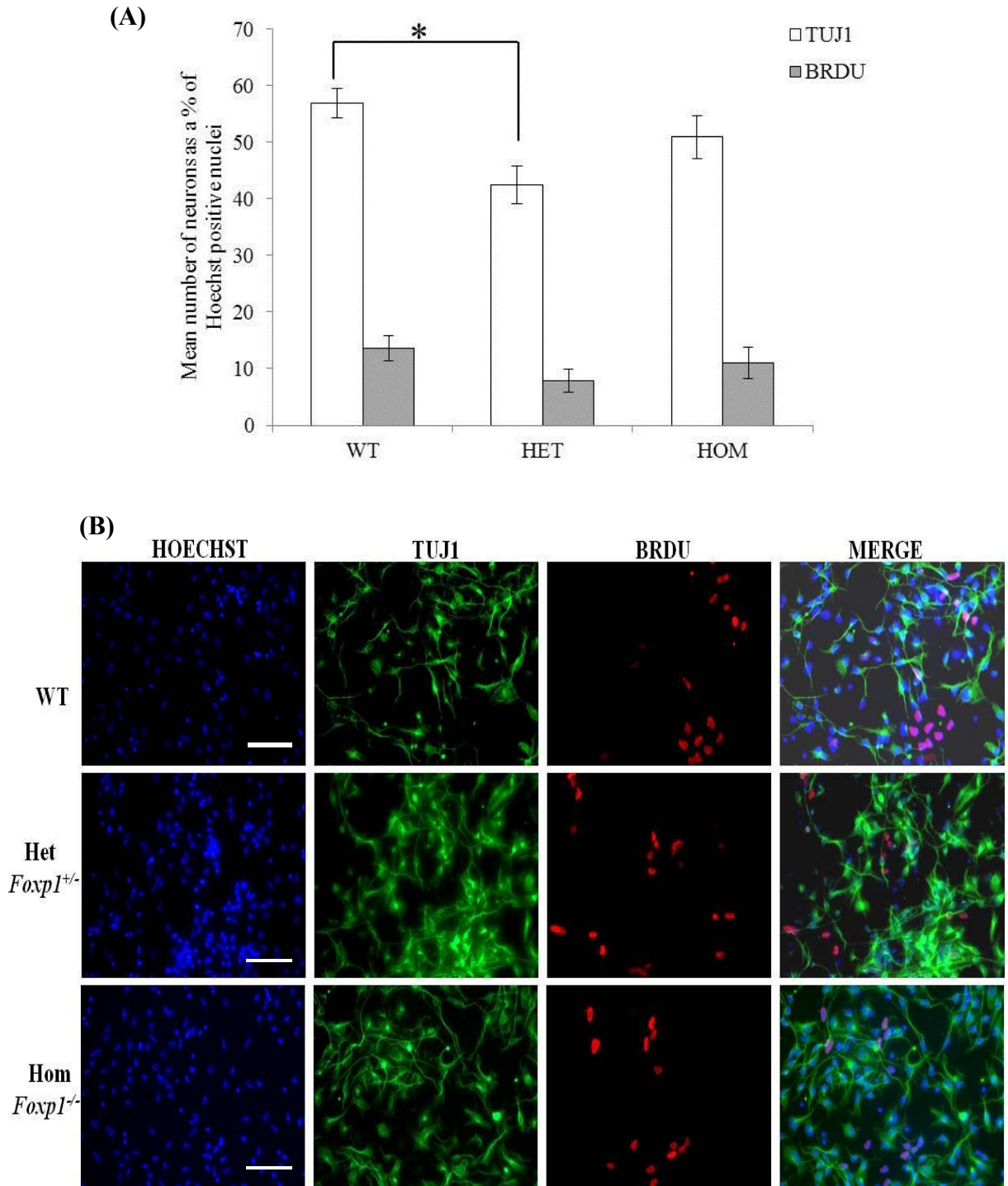
Figure 3.17 Cultures were generated and cultured individually from WT, *Foxp1*^{+/-} **and** *Foxp1*^{-/-} **striate. BrdU was added to the differentiation media after 6 DIV**. **(A)** BRDU and TUJ1 cell counts after 7 DIV *in vitro*. TUJ1 and BRDU positive cells were counted and are represented as a percentage of total Hoechst positive nuclei. Each bar on the graph represents a mean of at least 3 different cultures and error bars are SEM. Significant *post-hoc* differences are indicated with brackets (p* <0.05). **(B)** Following fixation, cells were double labelled for BRDU (Red) and TUJ1 (Green) and the nuclear stain Hoechst (Blue). The fourth column is a merged image of the first three photomicrographs. *Scale bars = 50µm.*

Calcium Imaging

Subsequent to looking at differences in MSN maturation and proliferation functional analysis of E14 derived striatal cultures following 24 hours *in vitro* was carried out to determine whether there were measurable differences in key physiological readouts of the cells, and thus test for differences in neuronal homogeneity. Ca^{2+} imaging was used to assess the effect of intracellular Ca^{2+} upon the application of a depolarising 50 mM K^+ solution and of several known neuronal agonists, namely GABA normal chloride (NC), GABA low chloride (LC), NMDA, AMPA, kainate and AchE.

The mean response to the different agonists by cells of each genotype is shown in Figure 3.18A. For the context of this work, analysis was concentrated on differences in GABA excitation peaks. Example traces (i.e. fluorescence ratio increases as a percentage of baseline), and corresponding Fura-2 filled cells (fluorescent dye) are shown in Figure 3.18B. Results showed that cells from all genotypes respond to high K, GABA NC and GABA LC. The percentage excitatory response was worked out for each of the genotypes by calculating the differences in the excitation peaks generated as a response to GABA NC compared to GABA LC. There was a significant difference between the response of the *Foxp1$^{-/-}$* cells to GABA LC ($F_{2, 11} = 8.5$, $p<0.05$), with *post-hoc* tests displaying a significant increase compared to cells cultured from WT and *Foxp1$^{+/-}$* cultures ($p<0.05$). There was no significant difference in the percentage excitation between the genotypes ($F_{2, 11} = 3.03$, $p=$ n.s.) (Figure 3.18C).

Figure 3.18 (overleaf) Ca^{2+} imaging studies on E14 striatal cultures at 24 hours *in vitro*. **(A)** Mean rises in Ca^{2+} in response to high K^+ and each agonist plotted as a percentage increase in fluorescence above baseline for each genotype. **(B)** Rises in intracellular Ca^{2+} in exemplar individual cells derived from each genotype in response to brief application of solutions. Example photomicrographs of the cells filled with the fluorescent dye Fura2. **(B)(iii)** The cells of the *Foxp1$^{-/-}$* cultures had a higher overall response to GABA LC than **(i)** WTs or **(ii)** *Foxp1$^{+/-}$* cultures. **(C)** The response of the cells to GABA LC and the percentage excitation. Bars represent the mean of all the cells. Error bars are SEM. Significant *post-hoc* differences are indicated with brackets (* $p<0.05$).

(A)

(B) (i) (ii) (iii)

WT   Het (*Foxp1$^{+/-}$*)   Hom (*Foxp1$^{-/-}$*)

(C) GABA LC   % Excitatory
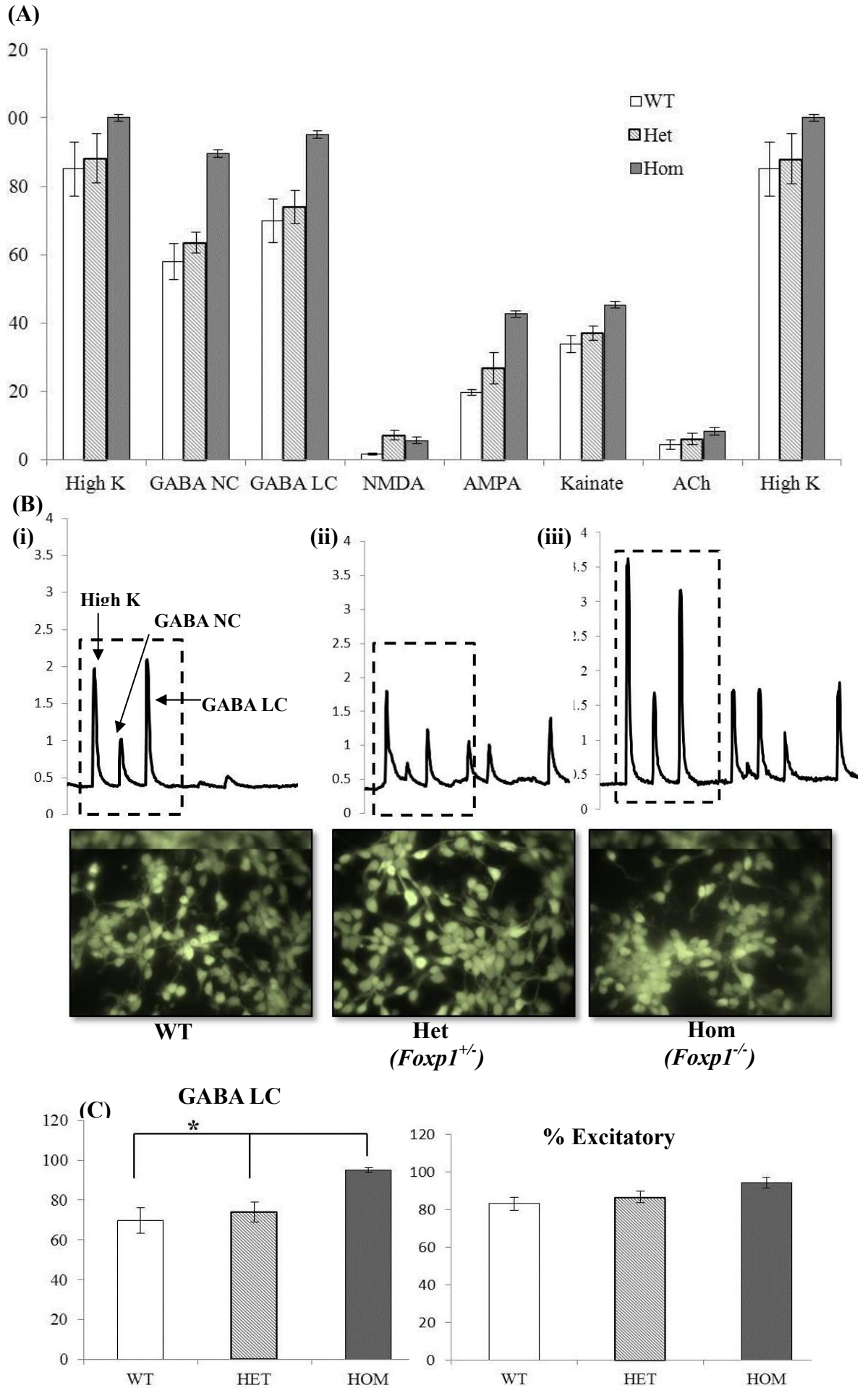
Characterisation of FOXP1 in mouse models that have key genes associated with striatal development knocked out

As mentioned in Chapter 1 there are many genes implicated in striatal development and subsequently mouse models that have some of these genes knocked out have been created. Josep Canals' lab in Barcelona have access to sections from some of these models and on a visit to his lab I carried out fluorescent immunohistochemistry on embryonic brain sections from *Ascl1*$^{-/-}$ and *Gsh2*$^{-/-}$ mice at E14, and on *Ikaros*$^{-/-}$ and *Helios* $^{-/-}$ mice at E18 in an attempt to learn more about the downstream targets of *Foxp1*. In the *Gsh2*$^{-/-}$ sections there appears to be reduced FOXP1 staining in the MZ of the striatum compared to the WT sections (Figure 3.19A). In the *Ascl1*$^{-/-}$ sections, FOXP1 expression in the SVZ appeared to be reduced when compared to WT sections but expression was retained in the MZ (Figure 3.19B).

There were no differences in FOXP1 staining in the *Ikaros*$^{-/-}$ or *Helios*$^{-/-}$ sections compared to WT sections (Figure 3.20A). When CTIP2 positivity was looked at in the E14 *Foxp1*$^{-/-}$ sections, there was no obvious difference in expression (Figure 3.20B). However of this occasion these stains could not be quantified and therefore the qualitative analysis presented here should be interpreted with this in mind.
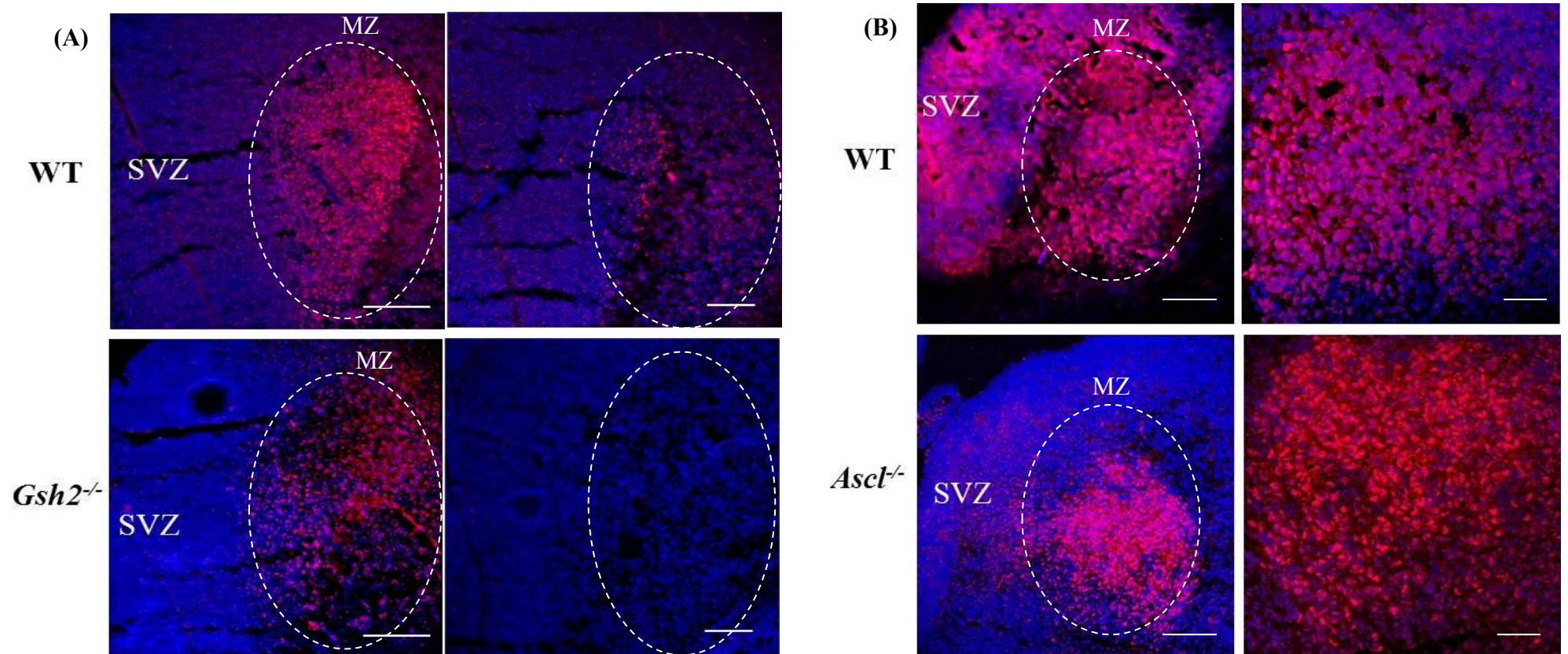
Figure 3.19 Photomicrographs showing fluorescent immunohistochemical analysis of FOXP1 (Red) co-stained with the nuclear marker DAPI (A) WT and *Gsh2*^{-/-} E14 brain sections and (**B)** WT and *Ascl1*^{-/-} E14 brain sections. In A and B the second column shows the images at a higher magnification. The dotted circles indicate the region of FOXP1 staining. Abbreviations: SVZ- sub-ventricular zone, MZ Mantle zone. *Scale bars = 50μm and 20 μm at the higher magnification*.
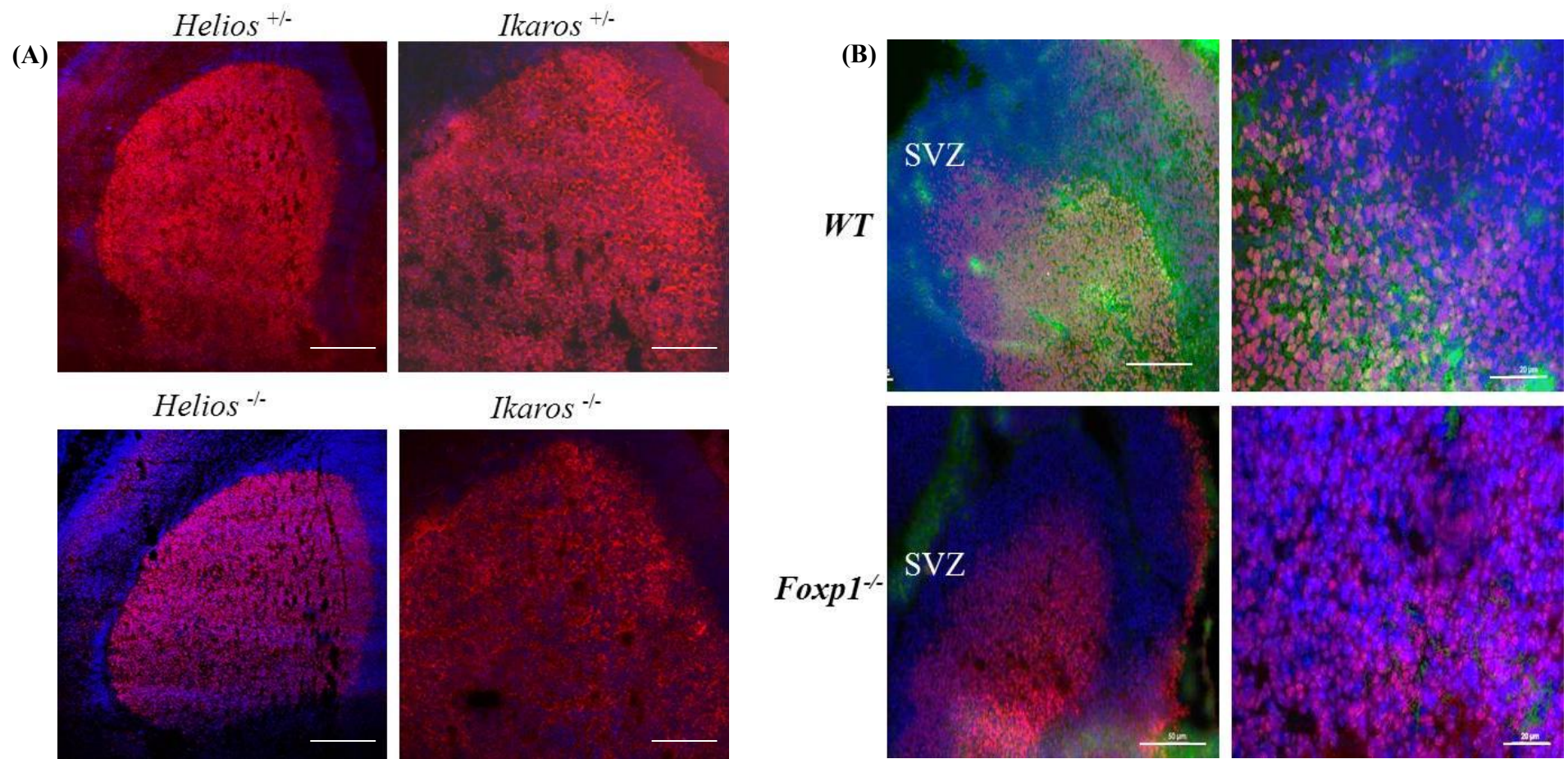
Figure 3.20(A) Photomicrographs showing fluorescent immunohistochemical analysis of FOXP1 (Red) co-stained with the nuclear marker DAPI in WT*, Helios*^{-/-} and *Ikaros*^{-/-} E18 brain sections. **(B)** CTIP2 (Red) FOXP1 (Green) and Hoechst (Blue) staining in *Foxp1*^{-/-} E14 sections. The second column displays the images at a higher magnification. Abbreviations; SVZ- sub-ventricular zone, MZ –Mantle Zone *Scale bars = 50µm and 20 µm at the higher magnification.*

3.5 **Discussion**

WT expression of FOXP1 from E10-P7

The WT profile of FOXP1 from E10 through to P7 was carried out using fluorescent immunohistochemistry. Two commonly used striatal markers, CTIP2 and DARPP-32 were used for comparison with FOXP1 stains as expression of DARPP-32, the current "gold-standard" marker of MSNs is not expressed until E18 in mice (Anderson and Reiner 1991; Ehrlich *et al.* 1990), whereas CTIP2 has been reported to stain both MSN precursors and mature MSNs from E12.5 (Arlotta *et al.* 2008).

Thus far the focus of FOXP1 research in the developing brain has been carried out to determine in which CNS areas FOXP1 is expressed. Although *Foxp1* mRNA expression has been reported in the spinal cord from E9.5 (Tamura *et al.* 2003), mRNA expression has not been reported in the developing telencephalon until E12.5 (Tamura *et al.* 2003) and by another group not until E14.5, in which it was also reported to be seen at a protein level (Ferland *et al.* 2003). Contrary to this data, results presented here show that FOXP1 is seen from E10. Specifically, FOXP1 staining is evident on the medial edges of the developing GEs, an area coincident with the developing proliferative zones. As it is known that protein lags behind mRNA production it is possible that FOXP1 may be being expressed before E10 at a time coincident with the emergence of the telencephalon (Jain *et al.* 2001) but further experiments are needed to ascertain this. This early expression of FOXP1 suggests that *Foxp1* is present in neuronal precursor cells, hinting that FOXP1 is needed in striatal development.

By E12 FOXP1 staining is more defined in the SVZ, a proliferative zone that is unique to the telencephalon (Campbell 2003). CTIP2 staining is also apparent at E12 but is restricted to the MZ, an area in which post-mitotic neurons reside and differentiate. This staining profile for FOXP1 and CTIP2 is in line with what was observed by Rubenstein and colleagues (Long *et al.* 2009). At E14 FOXP1 and CTIP2 co-localise in the MZ of the developing striatum and co-localisation in this region was seen through all the ages studied in this work. However, as alluded to, the expression of these two genes does not overall throughout the developing striatum as FOXP1, unlike CTIP2 is expressed in the SVZ. Specifically, distinct patches of FOXP1 staining are evident within the SVZ and, from E16; these patches are also easily recognisable within the MZ. It is known that

striatal projection neurons across mammals display a mosaic like organisation defined into striosomes ("patches") and matrices (Gerfen *et al.* 1985) and it has been established that the "patches" are born first (Gerfen *et al.* 1985) and that in mice this is evident between E11 and E13 (Mason *et al.* 2005). Therefore the distinct areas of FOXP1 shown could suggest FOXP1 to be the earliest known patch marker to date, as currently the first unique marker for distinguishing striatal patches is DARPP-32 at E18 (Foster *et al.* 1987). Failing that, one may suggest that the patches seen are in fact an artefact of the antibody. This possibility was ruled out, as several different concentrations were trialled to eliminate the chance that the staining was background and an additional control was carried out in which no primary antibody was applied. When the FOXP1 antibody was used on sections from *Foxp1*$^{-/-}$ embryos there was no staining present, therefore serving as an extra control. As reported DARPP-32 is not detected until E18 (Foster *et al.* 1987), and this was also true of the results presented in this thesis, where DARPP-32 staining was apparent in distinct patches from E18 and by P7 staining was homogeneous throughout the striatum. FOXP1 co-localised with all DARPP-32 positive cells at all stages, although there were regions of FOXP1 positive/DARPP-32 negative cells that has been suggested to represent a proportion of striatal projection neurons that are independent of DARPP-32 staining (Precious et al., submitted 2013; Arlotta et al., 2008).

This lineage study of FOXP1 not only confirms that FOXP1 does co-localise with established MSN markers, but promotes FOXP1 as an earlier, more specific MSN marker than CTIP2, and suggests a specific function for FOXP1 in MSN development. This interpretation is strengthened twofold; firstly by the fact that CTIP2 is preferentially expressed in the cortex during striatal development and secondly, expression of CTIP2 was not changed when *Dlx1/2* and *Ascl2* were simultaneously knocked out at E15 (Long *et al.* 2009). Thus it is likely CTIP2 has a more general role than FOXP1 in striatal development.

There are no differences in the adult *Foxp1*$^{+/-}$ mice compared to WT mice

There were no differences in the weights of *Foxp1*$^{+/-}$ mice when compared to WT littermates and although no behavioural testing was undertaken on these animals observational analysis of the animals in their home cage, and upon handling, showed that *Foxp1*$^{+/-}$ animals were indistinguishable from WT littermates. As the female mice

were needed for breeding and as a direct result sacrificed regularly to obtain E14 embryos only male mice were able to be sacrificed for phenotypic examination at 20 weeks. Gross dissection analysis showed that the brains from male *Foxp1*$^{+/-}$ were not obviously different to WT brains. Nissl staining using CV also confirmed that there were no phenotypic differences in striatal morphology or striatal volume and there were no noticeable differences in striatal, or cortical FOXP1 immunohistochemistry between the groups. From these analyses it was concluded that no phenotype was evident in the *Foxp1*$^{+/-}$ mice and that any differences in the striatum beyond E14, caused by the loss of *Foxp1,* would ideally require a *Foxp1* CKO model to be used.

Gross dissection analysis of E14 pups

As with reported cases (Wang *et al.* 2004a) I showed that *Foxp1*$^{-/-}$ pups at E16 were pale, had no retraction when poked and were confirmed as dead. Thus, analysis as expected was focused on E14 pups. Analysis was largely restricted to E14 as this time is coincident with peak MSN neurogenesis (Mason *et al.* 2005), successful striatal cultures are routinely and easily cultured from this age ((Martın-Ibanez *et al.* 2010) and the developing striatum is easily identifiable upon dissection. However it is also planned to look at differences earlier in development.

When E14 *Foxp1* KO mice have been looked at previously, example photomicrographs showed that there was a difference in embryo size and that embryos appeared bloodier than littermates, coincident with cardiac defects (Wang *et al.* 2004a). For the duration of this work CR lengths of E14 embryos were recorded upon dissection and showed no differences between genotypes. However, as no measurements were available to support the representative *Foxp1*$^{-/-}$ photomicrograph presented by Wang and colleagues it is possible this photo may not have been reflective of the groups. There were no phenotypic differences in the brains at E14, however striate from the *Foxp1*$^{-/-}$ embryos, had a spotty appearance. It is unlikely that this spotty appearance is of relevance to the questions addressed in this thesis (i.e. MSN development) and is more likely caused by haemorrhaging due to the defects in the cardiac system associated with the loss of *Foxp1*. Nevertheless this striatal phenotype is novel, and as was evident in over 80% of *Foxp1*$^{-/-}$ pups examined, served as an excellent indicator upon dissection that *Foxp1*$^{-/-}$ pups were included in the litter being studied and thus in subsequent analyses.

A significant decrease in total cell number per pair of striate from *Foxp1*$^{-/-}$ embryos was also reported, suggesting that even though there was no difference in brain diameter across the genotypes there was a difference in overall cell number that may influence the overall number of DARPP-32 positive MSNs.

In vitro analysis

The cell culture system provides an excellent analytical tool to study gene function *in vitro* as cells can be monitored and easily fixed at different developmental time points. It also allows individual cells to be analysed in detail as well as comparisons to be made on a population basis. Using this system I was able to plate down E14 WGE from the different genotypes to look at differences in overall neuronal number using the marker TUJ1, an isoform of β-Tubulin that is associated with post-mitotic neurons (Lee *et al.* 1990), and any differences in MSNs using DARPP-32 and CTIP2.

In vitro cell culture analysis following 24 hours and 7 DIV confirmed that there were no FOXP1 positive cells in cultures from *Foxp1*$^{-/-}$ embryos. TUJ1 analysis at both time points showed no difference in neuronal number or neuronal morphology between the genotypes. There were no obvious differences in Hoechst positive nuclei observed, and specifically no differences in the incidence of fragmented nuclei, which are indicative of cell death. This latter difference was not unexpected given that *Foxp1* has not been associated with apoptosis. After 24 hours *in vitro* there was very limited DARPP-32 expressed in all of the cultures, irrespective of genotype, which was expected as expression is not routinely evident until E18 (Anderson and Reiner 1991; Ehrlich *et al.* 1990). After 7 DIV, which some people have suggested is equivalent to P0 (Olsson *et al.* 1995), there were more DARPP-32 positive cells present within the cultures. Interestingly there were significantly fewer DARPP-32 positive cells in cultures generated from *Foxp1*$^{-/-}$ striate compared to cultures generated from WT and *Foxp1*$^{+/-}$ striate. Coincident with this, there were also fewer CTIP2 positive neurons in cultures generated from *Foxp1*$^{-/-}$ striate compared to cultures generated from WT and *Foxp1*$^{+/-}$ striate after 7 DIV.

There were no differences in proliferation after 24 hours or 7 DIV suggesting that early stages of MSN development are not affected by the loss of *Foxp1*. This result is opposite to what was observed when *Foxp1* was knocked out in developing

cardiomyoctes in which proliferation was increased (Wang et al., 2004). Although in subsequent experiments, loss of *Foxp1* caused a decrease in proliferation in the heart endocardium (Zhang *et al.* 2010) therefore emphasising the effect the local environment can have on gene expression. At 7 DIV there were fewer TUJ1 cells identified in *Foxp1*$^{+/-}$cultures compared to WT cultures but this result is likely caused by counting errors as it has been shown from the above mentioned *in vitro* studies that there were no differences in TUJ1 number between the groups at 7 DIV.

Several conclusions can be drawn from these results. Firstly the overall increase in the number of DARPP-32, FOXP1 and CTIP2 positive cells in the WT cultures between 24 hours and 7 DIV suggest that the cells are differentiating normally in our culture system. Secondly, that in the absence of *Foxp1* there is a decrease in the number of DARPP-32 and CTIP2 positive MSNs after 7 DIV suggesting *Foxp1* has a direct or indirect role in MSN development. There are no known FOXP1 binding sites on the *Darpp-32* gene, but there is a known *Foxp1* binding site upstream of the *Ctip2* promoter (Tang *et al.* 2012), suggesting FOXP1 and CTIP2 could function in synergy in aspects of MSN differentiation. Thirdly, that as no differences in overall neuronal number were seen this could suggest that in WGE cultures, MSNs do not constitute the majority of the neuronal populations. It is possible that if the cultures were derived solely from the LGE, the main source of striatal projection neurons (Marin *et al.* 2000; Stenman *et al.* 2003; Wichterle *et al.* 2001), as oppose to WGE, the neuronal population would be more biased towards MSNs thus likely to cause an overall loss in neuronal number, due to the increased loss of MSNs apparent in *Foxp1*$^{-/-}$cultures. However, a more likely reason is that the striatal neurons are still being born, are proliferating correctly but are less mature and thus would still stain positively for TUJ1 in the *Foxp1*$^{-/-}$ cultures. Due to time restraints this hypothesis could not be explored thoroughly but further experiments using specific markers of the cell cycle, and both immature and mature neuronal markers (NESTIN and MAP2 respectively) will be carried out.

Calcium imaging was also carried out on the striatal cultures following 24 hours *in vitro*. This technique allowed us to monitor any genotypic differences in the neuronal homogeneity of the cells. Upon cellular uptake, and subsequent activation of the membrane-soluble fluorescent dye Fura-2, GABA-evoked, depolarisation-mediated activation of voltage-gated Ca^{2+} channels was measured indirectly and was used to

ascertain differences in action and resting membrane potentials of the cells of the different genotypes. It is assumed that MSNs during embryonic development are largely excitatory and become inhibitory upon maturation (Owens *et al.* 1996). Results showed that the cells from all three genotypes had functional Ca^{2+} channels as they produced excitatory peaks in response to high K. Likewise all neurons produced action potentials (APs) in response to NC and LC showing that GABA at this stage, as expected, is still being utilised as an excitatory neurotransmitter, thus showing, in the absence of *Foxp1,* there are no significant differences in the normal physiology of MSNs. However, the *Foxp1^{-/-}* neurons did have a significantly larger overall response to GABA LC than cells from *Foxp1^{+/-}* and WT cells, possibly suggesting an increase in the number of GABA channels. And secondly *Foxp1^{-/-}* cells showed a trend to have an increased excitatory GABAergic response, suggesting possible immaturity of the *Foxp1^{-/-}* cells. However, further tests must be carried out to confirm or refute this.

Analysis of FOXP1 in KO's of genes associated with striatal development.

It is known that when *Dlx1/2* were knocked out in the developing striatum there was a "severe reduction" of *Foxp1* in the SVZ and MZ, suggesting that *Foxp1* may function downstream of this signalling pathway (Long *et al.* 2009). However, as there wasn't a complete loss of MSNs in the absence of *Dlx1/2*, and disruption was only evident in the dLGE, sparing neurons of the vLGE, other TFs that function independent and simultaneous to *Dlx1/2* are also needed for MSN development. Two such factors are *Ascl1* and *Gsh2* that are primarily expressed in the vLGE and showed increased expression when *Dlx1/2* were KO (Long *et al.* 2009). Further analysis showed that *Dlx1/2* and *Ascl1* work synergistically in MSN differentiation and to maintain the dLGE/vLGE divide. Therefore, fluorescent immunohistochemistry was carried out to look at the differences in FOXP1 in the *Ascl^{-/-}* and the *Gsh2^{-/-}*.

In the *Ascl1^{-/-}* sections, FOXP1 staining appeared reduced in the SVZ when compared to WT sections. Unfortunately in the *Ascl1, Dlx1/2* triple KO microarray differences in *Foxp1* were not reported in the publication (Long *et al.* 2009) but would have been useful to corroborate this finding in the absence of quantification at this time point. Nethertheless this apparent reduction of FOXP1 in the SVZ could suggest it functions downstream of *Ascl1* in MSN precursors. Additionally there was reduced FOXP1 in the *Gsh2^{-/-}* brain section, exploring the idea that *Foxp1* may be functioning downstream of

this TF*,* in addition to downstream of *Dlx1/2* and *Ascl1*. Therefore as WT lineage results presented in this Chapter clearly showed that FOXP1 is expressed throughout the MZ with no dorsal/ventral bias it is possible that *Foxp1* is a downstream target of all these TFs, and thus would be implicated in various, and possibly independent genetic pathways controlling different MSN lineages.

Relatively new markers of MSNs are *Helios* and *Ikaros* (Martin-Ibanez *et al.* 2012; Martın-Ibanez *et al.* 2010). *Ikaros* has shown to be expressed in the MZ of the striatum and results showed that this TF was a modulator of cell cycle exit for neuronal progenitors born in the second wave of neurogenesis, and that it is expressed downstream of *Dlx1/2/5/6* (Martın-Ibanez *et al.* 2010). Helios is also a member of the Ikaros family, and has shown to be associated with a subset of striatal projection neurons that co-localise with *Foxp1* and *Ctip2* at E18.5 (Martin-Ibanez *et al.* 2012). The authors suggest *Helios* is implicated in MSN neuronal lineage derived from the LGE that ultimately populates the matrix region and suggest that *Foxp1* and *Ctip2* are associated with the same lineage (Martin-Ibanez *et al.* 2012). However, when FOXP1 was analysed in either *Helios*$^{-/-}$ or *Ikaros*$^{-/-}$ sections there were no difference when compared to WT sections. Finally, differences in CTIP2 were looked for in the FOXP1 KO at E14. There was no apparent difference in CTIP2 expression when compared to staining in the WT. However, all these immunohistochemical results can only go as far as suggesting differences/no differences as quantification was not undertaken on this occasion. Nevertheless, results from an on-going microarray assessing independent differences in the LGE and MGE, from *Foxp1*$^{-/-}$ striate compared to WT striate will optimistically yield more definitive answers, and narrow the genes that can function up/downstream of *Foxp1*.

3.6 **Conclusion**

This Chapter characterised the expression profile of FOXP1 through co-localisation of two routinely used MSN markers, CTIP2 and DARPP-32 and showed that FOXP1 co-localised with both genes from the onset of their expression. Owing to the embryonic lethality associated with the homozygous *Foxp1* KO embryos and no reported phenotypic differences between WT and *Foxp1*$^{+/-}$ embryos, phenotypic differences in

Foxp1^{+/-} adult mice were looked for. Results showed no obvious differences when compared to WT mice therefore limiting experimental analysis to E14.

Striatal cultures from E14 *Foxp1*^{-/-} embryos that had been left to differentiate for 7 DIV had fewer CTIP2 and DARPP-32 positive cells than cultures from *Foxp1*^{+/-} or WT embryos, with no differences identified in proliferation or neuronal homogeneity. Finally immunohistochemical staining suggested that there was less FOXP1 in *Ascl1*^{-/-} and *Gsh2*^{-/} E14 brain sections, suggesting that FOXP1 may be acting downstream of these genes. Taken together these results propose that, at least until E14, MSN development is aberrant in the absence of *Foxp1,* and that *Foxp1* has an important role, likely downstream of *Ascl1* and *Gsh2,* in later aspects of MSN development.

4 *In vivo Characterisation of Primary Striatal Tissue Transplanted into a Quinolinic acid (QA) Mouse Model of HD*

4.1 **Summary**

The in vitro experiments described in Chapter 3 strongly implicate Foxp1 in MSN development and differentiation. However, these results relied to a large extent on analysis of markers such as CTIP2, as detection of DARPP-32 is notoriously difficult in cell culture. The reasons for this are likely to be because DARPP-32 is expressed in mature MSNs and full expression may depend upon the MSNs making normal afferent connections. One way to study this would be to generate striatal specific FOXP1 CKOs and indeed this is underway but involves a complex and time consuming breeding strategy which was unable to be completed in the time of this PhD. Therefore a complementary approach was taken which was to transplant E14 striatal cells (before they die) into the adult lesioned mouse striatum. This allows striatal neurons from Foxp1$^{-/-}$ mice to survive for much longer periods than is possible in vitro and to allow them the opportunity to make some of their normal connections. Moreover it allows one to see how striatal cells without Foxp1 develop in vivo once grafted.

Primary striatal tissue generated from E14 embryos from a Foxp1 heterozygote cross was grafted into adult mice that had received a quinolinic acid (QA) lesion and the tissue was left to mature in vivo for 12 weeks. Surviving grafts showed that there was a decrease in DARPP-32 in the grafted tissue from the Foxp1$^{-/-}$ embryos when compared to grafts from WT and Foxp1$^{-/+}$ embryos. However, although E14 is the generally accepted gestational age at which to transplant primary striatal cells from rodents, the E14 grafts were small, making confident analysis of graft cell content difficult. Therefore further grafts were undertaken using donor tissue from E12 embryos on the basis that the accepted age of E14 tissue is based largely on rat transplant data and the

mouse gestational period is slightly shorter. As hypothesised, the E12 grafts were bigger than those seen at E14, and showed comparable results to grafts using E14 donor cells that in that the absence of Foxp1 there is a decrease in DARPP-32 staining.

4.2 **Introduction**

Cell transplantation is a useful tool for studying donor cell differentiation, maturation, and integration over prolonged periods of time, which *in vitro* methods, including cell culture are unable to offer. Differentiation cultures using primary mouse striatal tissue, allow differences in MSN precursors to be assessed, but are restricted to a maximum of two weeks *in vitro* before considerable cell death is seen.

Chapter 3 of this Thesis addressed differences in striatal development in the mouse in the absence of *Foxp1* up to E14, the point of embryonic lethality in *Foxp1* KO mice. However, to adequately assess differences in expression of striatal DARPP-32, the current "gold standard" marker of MSNs, it is necessary to look beyond E14, as DARPP-32 expression is not evident until later in development (~E18) (Anderson and Reiner 1991; Ehrlich *et al.* 1990), and isn't optimally expressed until postnatal (P) weeks 2-3 (Gustafson *et al.* 1992). Due to the embryonic lethality of *Foxp1*$^{-/-}$ at E14 one way of addressing differences in DARPP-32 was attempting through the use of CKO mice, this approach will be discussed in Chapter 5. Here, cell transplantation is employed in a novel to look at expanded development of striatal cells from embryos of a *Foxp1* heterozygous cross when grafted into a lesioned environment. This method allows one to look at differences in developing tissue beyond that of their known lethality, and beyond that available in the cell culture system permitting differences in mature MSNs within the graft to be analysed using DARPP-32.

One of the best-used models for striatal transplantation is the HD quinolinic acid (QA) striatal lesion model. When injected directly into the striatum of rodents, QA, a selective NMDA receptor agonist, has shown to cause striatal atrophy and loss of MSNs, sparing striatal interneurons and aspiny neurons (Beal *et al.* 1986; Schwarcz and Kohler 1983; Schwarcz *et al.* 1983). It has also been shown by our lab group that the QA model causes loss of DARPP-32 and FOXP1 expressing MSNs (Precious et al., submitted 2013) making it the ideal model to look at differences in MSN development *in vivo*.

Grafting considerations in mice are largely based upon what was trialled and shown to be successful in the rat. For rat allograft experiments it was shown that E14 primary striatal tissue produced bigger and more reliable grafts than those derived from E12

tissue and thus E14 is the generally accepted donor age used for primary WGE grafting experiments (Watts *et al.* 2000a). It has been shown that the addition of trypsin to the donor cells prior to trituration supports functional grafts and integration within the host (Watts *et al.* 2000b), but whether cell suspensions (cells undergo multiple triturations) yield better survival than tissue "pieces" (triturated minimally ~ twice) following the initial trypsin step is debated in rodent protocols. Differences in trypsinised cell suspensions and trypsinised tissue pieces were tested in rat allograft experiments. Both groups produced comparable volumes of the striatal component within the grafts (Watts *et al.* 2000b), however, the proportion of the graft that showed functionally relevant AchE positive P-zones, and the largest number of DARPP-32 cells was greater from the grafts derived from cell suspensions as oppose to tissue pieces, even though the latter group produced bigger grafts (Watts *et al.* 2000b). However, after 3 months modest recovery was seen on the paw-reaching task in rats that received grafts from tissue pieces rather than cell suspensions(Watts *et al.* 2000b).

Commonly, striatal cell transplantations in rats are performed using E14 cell suspensions and the same conditions are subsequently used in mouse allograft experiments. However, there is a developing problem in the mouse grafting field in which small grafts are emerging as a general problem in the field (Cisbani *et al.* 2013; Johann *et al.* 2007; Kelly *et al.* 2007; Tate *et al.* 2002), and a way of producing large , consistent grafts is needed. One method for producing larger striatal grafts in mice is to use younger donor tissue from embryos. On the basis that gestational age in the mouse is shorter than in the rat, the optimal age of E14 in the rat may not be applicable to the mouse. E12 in the mouse is a direct comparison to E14 in the rat and it is possible that this is the optimal age for grafting mouse tissue.

The work outlined in this Chapter compares the differences in the differentiation of donor cells born from the embryos of a *Foxp1*$^{+/-}$ cross, i.e. WTs, *Foxp1*$^{+/-}$ and *Foxp1*$^{-/-}$ at 12 weeks post transplantation using the QA mouse model. Using a battery of striatal markers (CTIP2, DARPP-32 and FOXP1) it was anticipated that I would be able to assess clearly how the striatal cells from the three different genotypes developed *in vivo* within the graft over a time frame and environment unattainable *in vitro*. Although this method can only directly assess how the cells mature within in a graft, it is likely the cells, as are in the midst of peak neurogenesis and exiting the cell cycle (Mason *et al.*

2005), will maintain some of their genetic cues and develop as if left in their natural milieu, although it is known that results obtained cannot be directed attributable to the normal developmental process.

Initially, the standard mouse allografting protocol was used in experiments, i.e. E14 striatal cell suspensions; but these grafts were small making confident assessment of the cell content difficult. Consequently, a further round of transplantations was undertaken using E12 donor tissue, which produced larger grafts. It was shown that cells grafted in the absence of *Foxp1* (*Foxp1*$^{-/-}$ striate), using both E14 and E12 donor tissue, showed a decrease in the number of DARPP-32 positive cells when compared to grafts derived from WT and *Foxp1*$^{+/-}$ donor cells.

4.3 **Experimental Procedures**

Experimental Outline

(A)

	WT	FOXP1 KO
WT	WTWT	WT/FOXP1KO
FOXP1 KO	WT/FOXP1KO	FOXP1 KO/KO

(B) Unilateral QA lesions into female C57B6/J mice → Dissect individual E14/E12 striatum and make cell/quasi cell suspensions from WT, *Foxp1*$^{+/-}$ or *Foxp1*$^{-/-}$ pups. → Graft tissue into lesioned
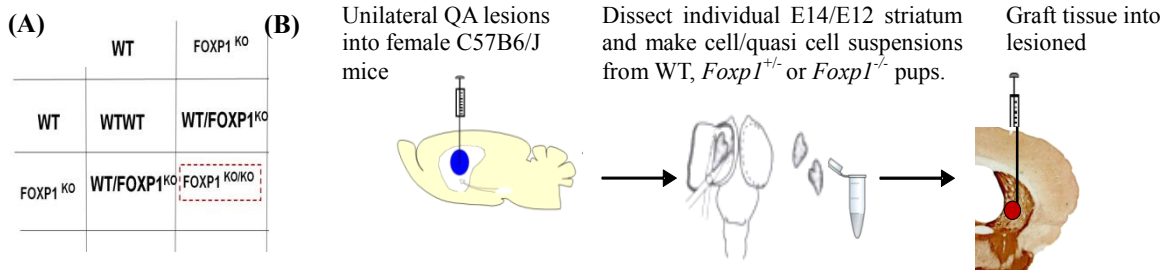
Figure 4.1 Breeding strategy (A) *Foxp1* heterozygote mice were paired overnight. The possible genotypes of the F1 offspring from a *Foxp1*$^{+/-}$ x *Foxp1*$^{+/-}$ are shown in the punnet square. **(B)** Experimental outline of the QA lesion and grafting procedure.

Pregnant dams were sacrificed at either E12 or E14 and striate were dissected from each embryo. Animals were genotyped following grafting. It was assumed that the genotypes of the pups would reflect the expected Mendelian ratio from a heterozygote cross (2:1:1) as shown in Figure 4.1.

E12 graft analysis

For the E12 grafts a grading system was used to distinguish the amount of staining identified in the grafted cells within the lesioned area as shown in Figure 4.2. This method was used as unexpectedly small, unbalanced groups (i.e. genotypes) ended up being used in the experiment (WT=3, *Foxp1*$^{+/-}$ =11 and *Foxp1*$^{-/-}$=1) and therefore seemed more appropriate than stereology in light of a comparison in the *Foxp1*$^{-/-}$ group.

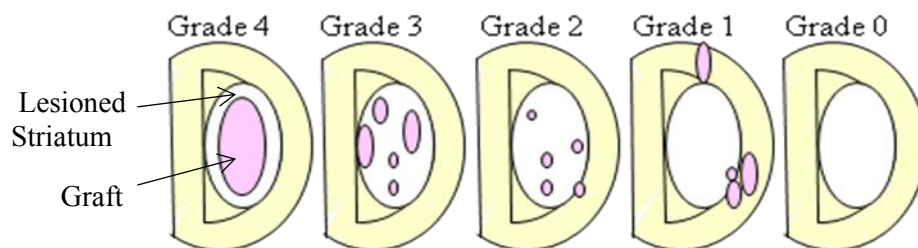| Grade Number	Description
4	Dense staining of the antibody, recognisable grafted cells throughout the lesioned area
3	Dense staining of the antibody restricted to certain patches throughout the lesioned area
2	Minimal staining of the antibody in the grafted region
1	Graft outside striatal area
0	No graft

Figure 4.2 Table and schematic showing the criteria in which E12 grafts were graded. The grading system aimed to distinguish the amount of staining identified in the grafted cells within the lesioned area.

4.4 **Results**

Graft analysis after 4 weeks *in vivo*

In order to assess if the QA lesion in the striatum and grafting protocol had been successful five mice from each grafting group (WT, *Foxp1*$^{+/-}$ and *Foxp1*$^{-/-}$) were perfused at four weeks post transplantation and histological analysis was undertaken. Nissl staining using CV was carried out to identify the presence of the grafts in the brain and to determine the size of the lesion, as shown in the right hemisphere of the brains in Figure 4.3A-D. The Nissl stain also shows enlargement of the right ventricle due to cell death attributable to the QA toxin (Figure 4.3C). Grafted tissue can be recognised by the increased density of the Nissl stain in the right hemisphere.

There were surviving grafts present in 81% of the animals sacrificed. Unsuccessful grafts did not have a genotype bias. FOXP1 immunohistochemistry was carried out to show the amount of FOXP1 in the grafts. Results showed there was FOXP1 staining in the grafts that received donor tissue from WT (Figure 4.3E) and *Foxp1*$^{+/-}$ embryos (data not shown), but that there was a considerable reduced amount of FOXP1 staining in the grafts that received donor tissue from *Foxp1*$^{-/-}$ striate (Figure 4.3G). When the number of cells in the grafts were quantified it was shown that there were was a significant difference in the number of FOXP1 cells between the groups ($F_{2,14}$ = 12.55, p=<0.001), with *post-hoc* comparisons showing a significant decrease in the number of FOXP1 positive cells in the grafts which had donor cells from *Foxp1*$^{-/-}$ embryos (105±54.2) compared to grafts that received WT (p<0.01) (796±144.2) or *Foxp1*$^{+/}$ donor tissue (p<0.001) (1093±180.4), this is shown in Figure 4.4.
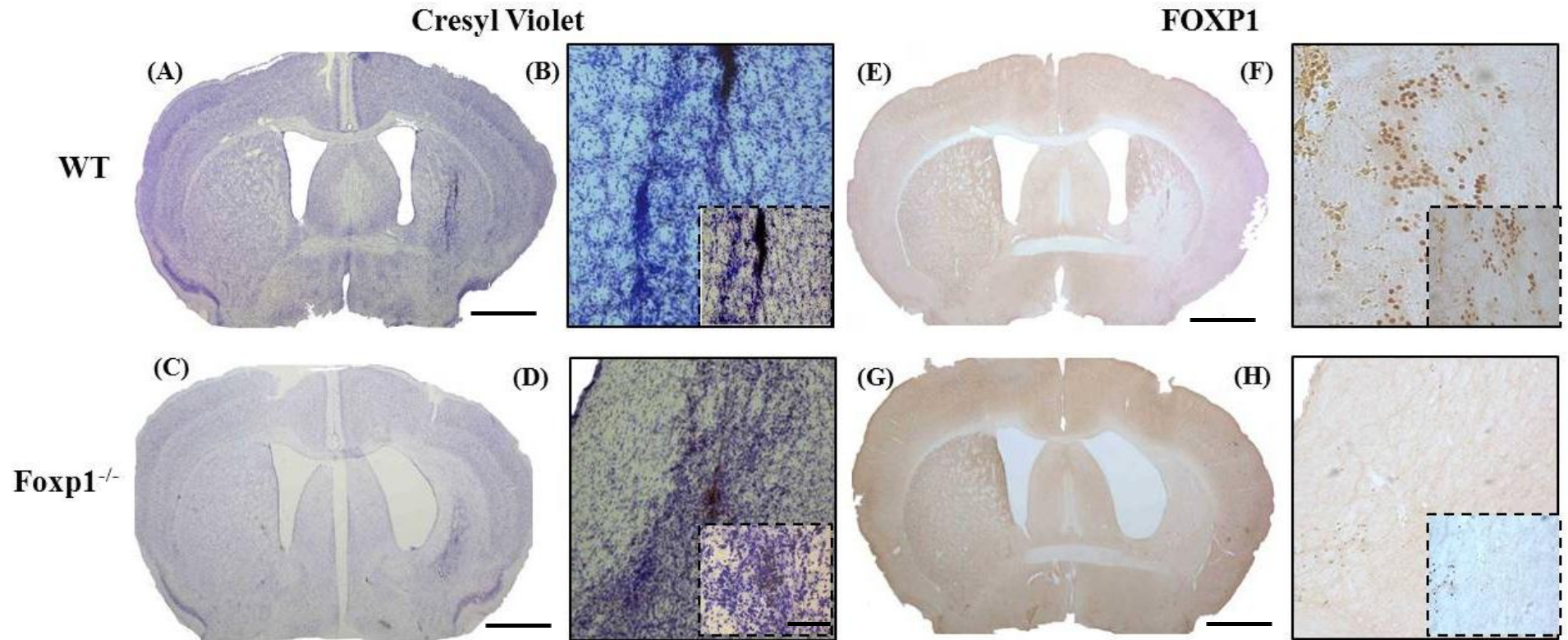
Figure 4.3 Representative photomicrographs validating the lesion and grafting technique after 4 weeks *in vivo*. (A-D) Coronal sections of Nissl staining with cresyl violet showing the presence of a graft in the right hemisphere of animals grafted with WT or *Foxp1*^{-/-} tissue, the left hemisphere is not lesioned. **(B)** and **(D)** show the grafted regions at a higher magnification, the dotted boxes indicate higher magnification. **(E and G)** FOXP1 immunohistochemistry identifies the lesioned area. **(E)** FOXP1 positively stains the grafted cells from the WT donor. **(F)** The grafted cells stained for FOXP1 at a higher magnification. **(G)** In the *Foxp1*^{-/-} grafts there are very few FOXP1 positively labelled cells **(H)** Shows the grafted cells stained for FOXP1 at a higher magnification The dotted boxes indicate the areas that are magnified. *Scale bars: low power images= 500μm, high power images= 50 μm.*
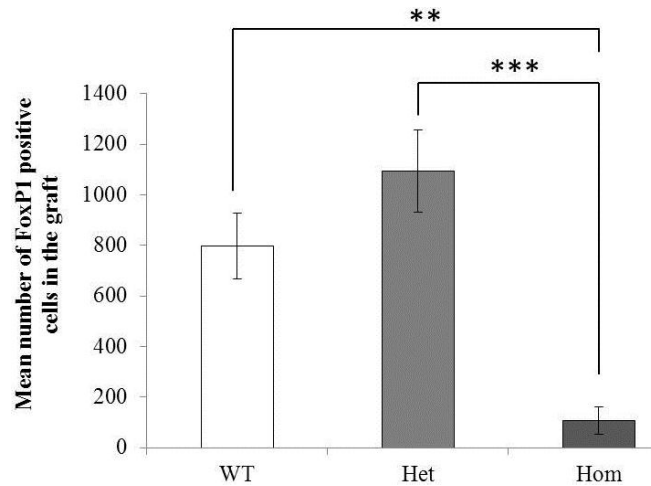
Figure 4.4 Quantification of FOXP1 positive cells in grafts after 4 weeks *in vivo*. FOXP1 positive cells in each graft were counted. Bars represent the mean counts from 5 animals. Errors bars represent the (SEM), Abbreviations, *WT= Wild Type, Het= Heterozygote, Hom=Homozygote.* Significant *post-hoc* differences are indicated with brackets *(**p<0.01, ***p<0.001).*

Graft survival and morphology of E14 grafts after 12 weeks *in vivo*

Following the evidence of graft survival seen at 4 weeks the remaining grafts were left for 12 weeks thereby allowing more time for the cells to fully mature. At 12 weeks post-transplantation there were successful grafts in 78% of animals sacrificed with no genotype bias. Nissl staining showed the presence of small, pencil-like grafts in all genotypes at 12 weeks; representative examples are shown in Figure 4.5. Graft volume was estimated using graft area as determined by Nissl staining. There was no significant difference between graft volume and genotype (F= $_{2, 25}$ = 1.18, p=n.s.), shown in Figure 4.6.

Anterior ←———————————————————————→ Posterior
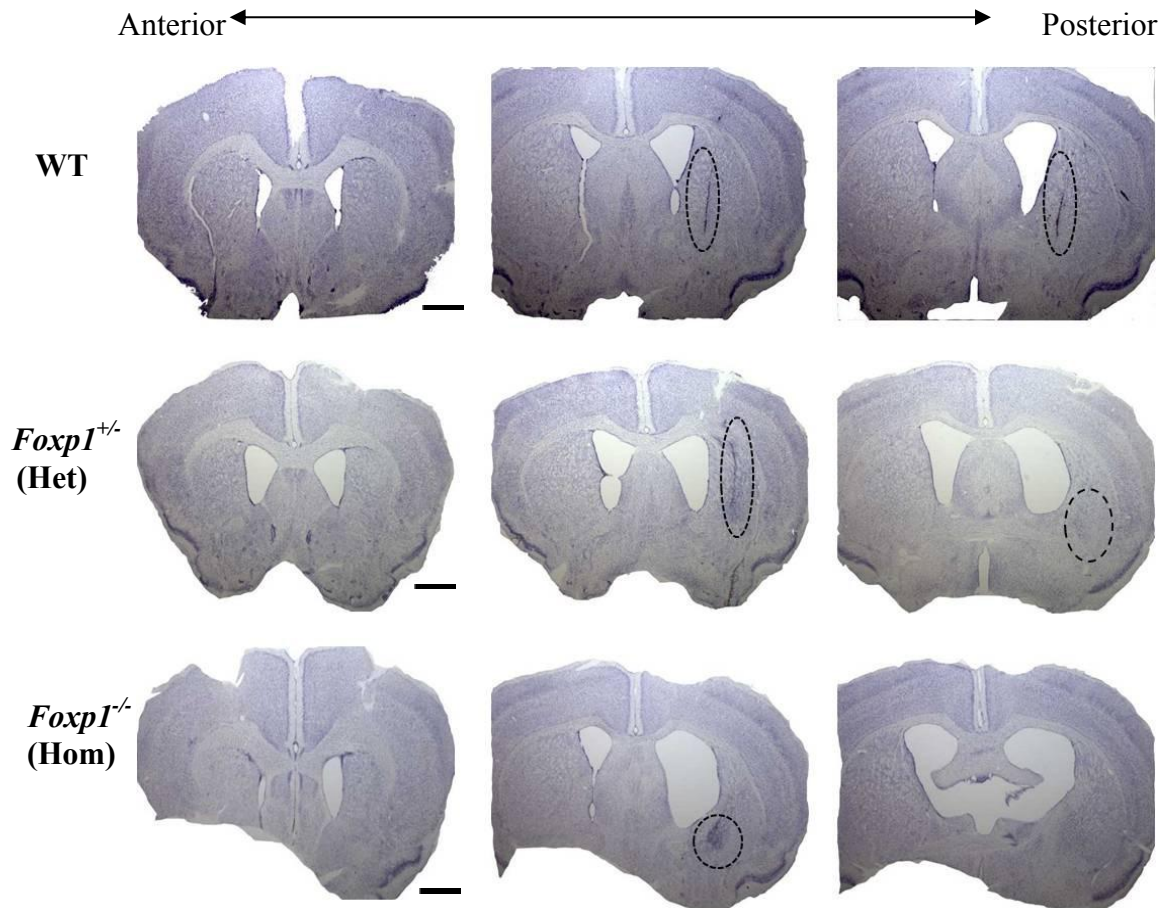
Figure 4.5 Representative photomicrographs of coronal sections showing Nissl staining using cresyl violet at 12 weeks post transplantation. Example brains show grafts from each of the genotypes at E14, WT, *Foxp1*$^{+/-}$ and *Foxp1*$^{-/-}$. Black dotted lines outline the grafted region as indicated by darker staining of the cresyl violet in the right hemisphere. *Abbreviations WT= Wild Type, Het= heterozygote, Hom=Homozygote Scale bars = 500µm.*
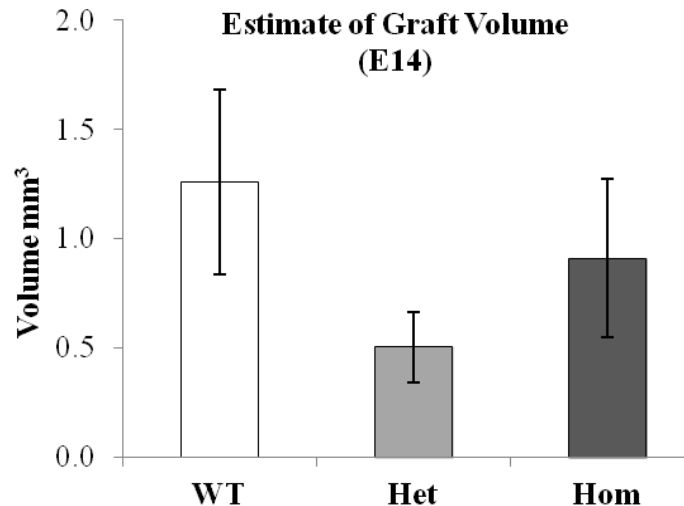
Figure 4.6 Graft volumes of surviving E14 grafts. Bars represent the mean graft volume per genotype (WT=10, Het= 9, Hom=9). *Error bars represent SEM. Abbreviations, WT= Wild Type, Het= Heterozygote, Hom=Homozygote.*

Graft Analysis of MSNs at 12 weeks from E14 tissue

Once graft presence was confirmed with the Nissl stain, to look at differences in the mature MSN phenotype immunohistochemistry using anti-DARPP-32 and anti-FOXP1 was used. Results were matched to corresponding CV stains and showed that there was FOXP1 and DARPP-32 staining in the grafts from the WT and Foxp1$^{+/-}$ animals (Figure 4.7A-J), but that this staining was minimal in the grafts from *Foxp1$^{-/-}$* animals (Figure 4.7K-O). As the grafts were consistently small throughout the groups all cells within the graft could be counted for each stain. As expected there was a significant difference in the number of FOXP1 positive cells between groups ($F_{2, 27}$ = 4.31, P<0.05). *Post-hoc* comparisons showed that there was a significant loss of FOXP1 positive cells in the grafts from animals grafted with *Foxp1$^{-/-}$* striate (452±127) compared to those grafted with WT striate (1308±28) (P<0.05). Significant differences were also evident in the amount of DARPP-32 positive cells ($F_{2, 27}$ = 3.81, P<0.05), and as with the FOXP1 cell counts, *post- hoc* comparisons showed that there were significantly fewer DARPP-32 positive cells in grafts that received donor cells from *Foxp1$^{-/-}$* animals (390±68) compared to those that received grafts from WT tissue (802±142) (p<0.05). Quantification of FOXP1 and DARPP-32 positive staining within the grafts is displayed in Figure 4.8.

.
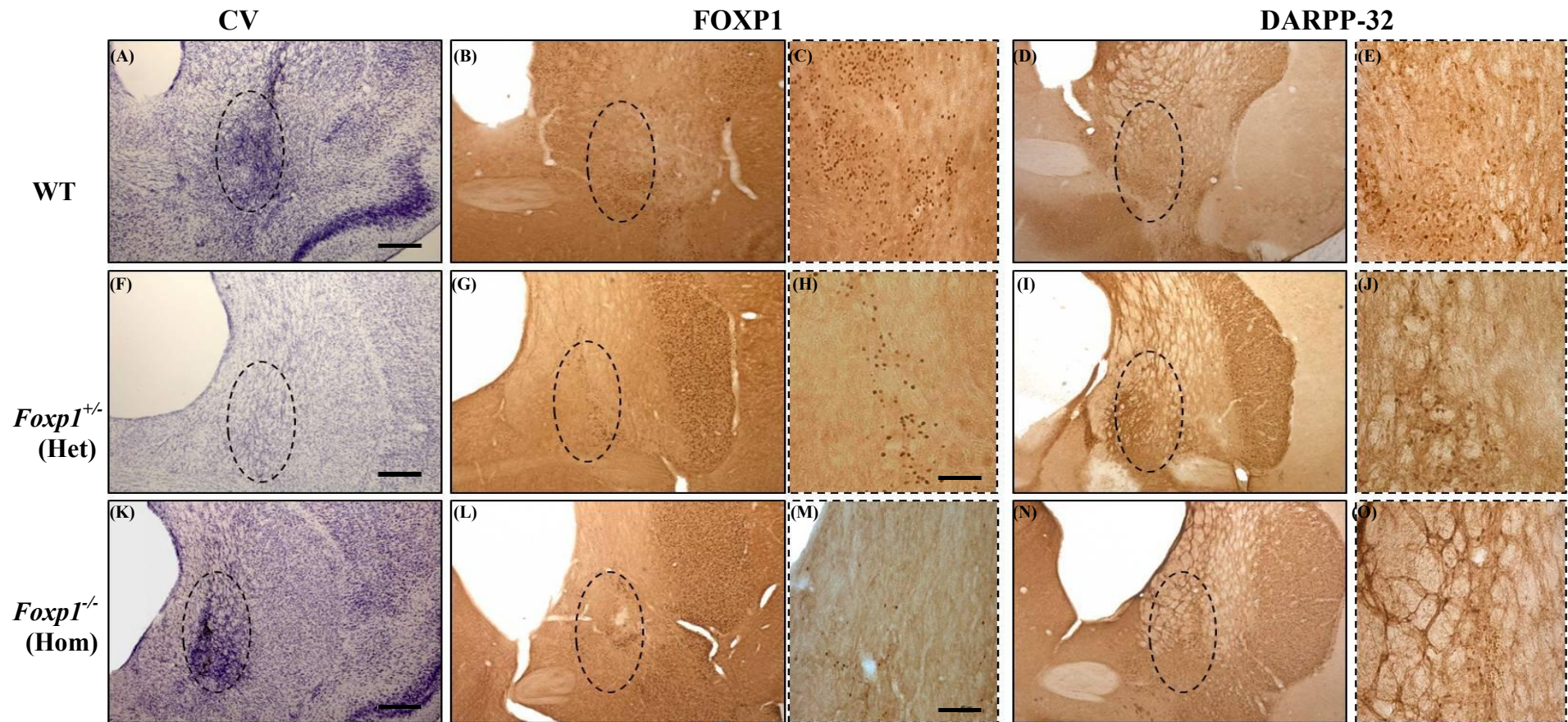
Figure 4.7 Example photomicrographs of coronal sections showing (A, F and K) Nissl (B-C, G-H and L-M), FOXP1 and (D-E, I-J and N-O) DARPP-32 staining in E14 grafts at 12 weeks post transplantation. Dotted ovals indicate the grafted region and dotted boxes in rows 3 and 6 are a higher magnification of this region. **(B –E; G-J)** There are FOXP1 and DARPP-32 positive cells identifiable in the grafted region of the animals that received donor tissue from WT and *Foxp1* [+/-] embryos. **(L-O)** There is little or no FOXP1 present in the animals that received grafts from *Foxp1*^{-/-} embryos. *Abbreviations, CV= Cresyl Violet, WT = Wild Type, Het = Heterozygote, Hom = Homozygote. Scale bars: low power images = 200µm, high power images =50 µm*

Figure 4.8 Quantification of FOXP1 and DARPP-23 positive cells in grafts after 12 weeks *in vivo* Bars represent the mean total cell counts per genotype (WT=10, Het= 9, Hom=9). *Error bars represent SEM. Abbreviations, WT = Wild Type, Het = Heterozygote, Hom = Homozygote. Significant post-hoc differences are indicated with brackets (*p<0.05).*

In addition to DARPP-32 and FOXP1, the MSN marker, CTIP2 was also used to look at differences in the grafted cells. However, results from this antibody were not conclusive as the DAB staining was inconsistent throughout sections. Example photomicrographs are displayed in Figure 4.9A. Nevertheless quantification was attempted and showed no significant difference in the amount of positive CTIP2 staining between the groups ($F_{2, 27} = 1.49$, p=n.s.) (Figure 4.9B). However due to the discrepancies with this stain this result should be interpreted with caution.

As an alternative to using the DAB stain, immunofluorescence was attempted whereby sections were double labelled with FOXP1 and CTIP2 together with the nuclear marker Hoechst (Figure 4.10). Once again this staining was not definitive due to small numbers of cells within the grafts but appeared to confirm DAB staining. Quantification was not undertaken.

CTIP2

(B)
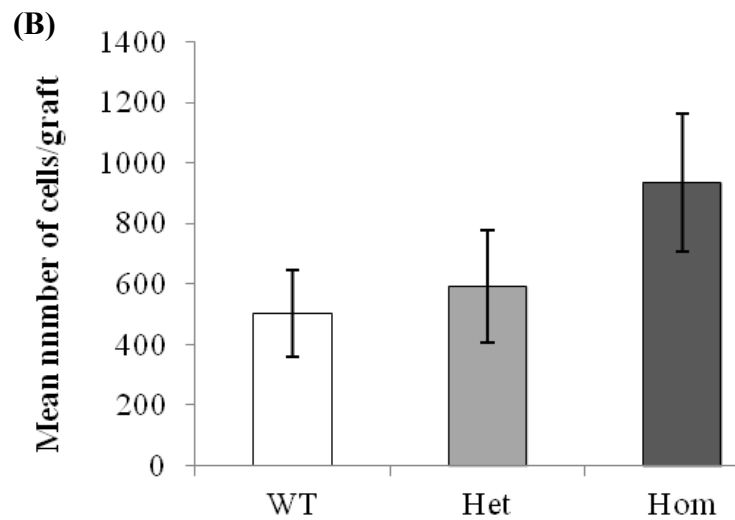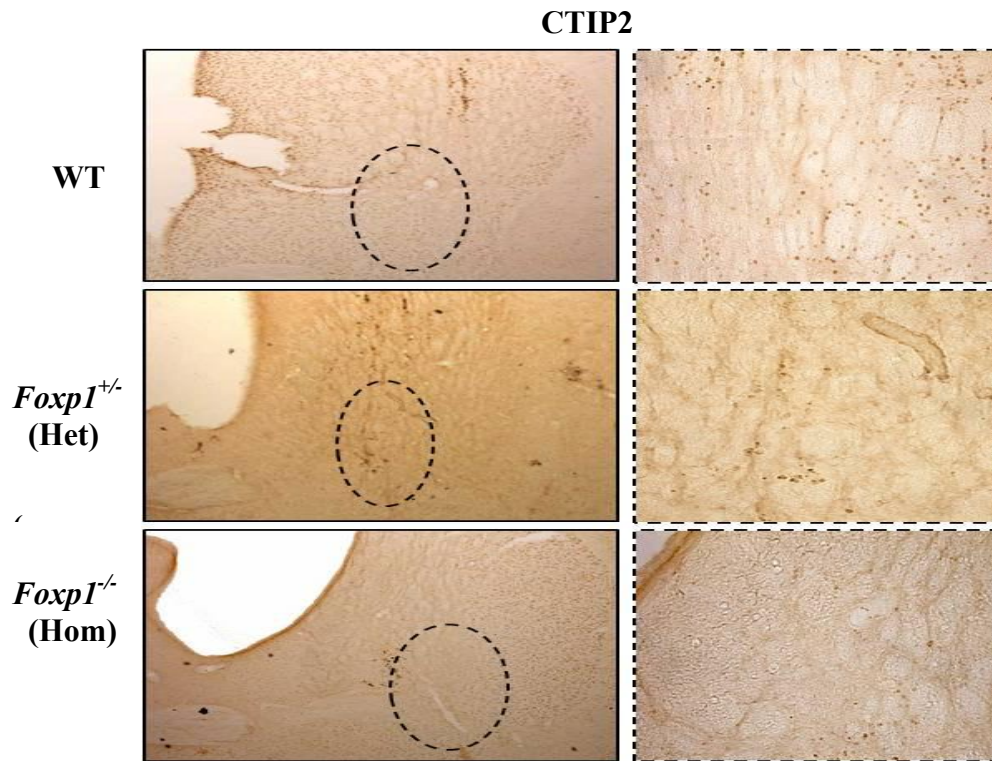
Figure 4.9 (A) Example photomicrographs of coronal sections showing CTIP2 in grafts from the three genotypes WT, *Foxp1*^{+/-} and *Foxp1*^{-/-} at 12 weeks post transplantation. Dotted ovals indicate the grafted region and dotted boxes are a higher magnification of this region. **(B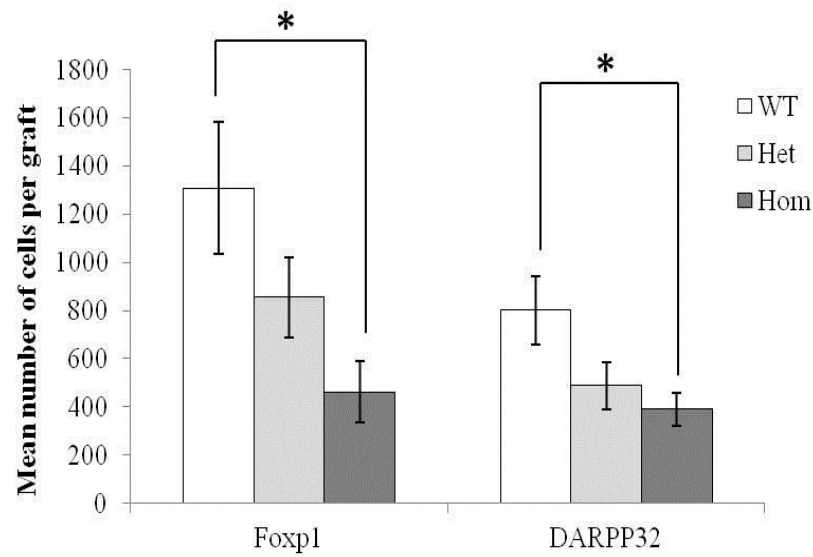) Quantification of CTIP2 positive cells in grafts after 12 weeks *in vivo*** Bars represent the mean total cell counts per genotype (WT=10, Het= 9, Hom=9). Error bars represent SEM. *Abbreviations WT= Wild Type, Het= Heterozygote, Hom=Homozygote. Scale bars low power images= 200μm, high power images=50 μm.*
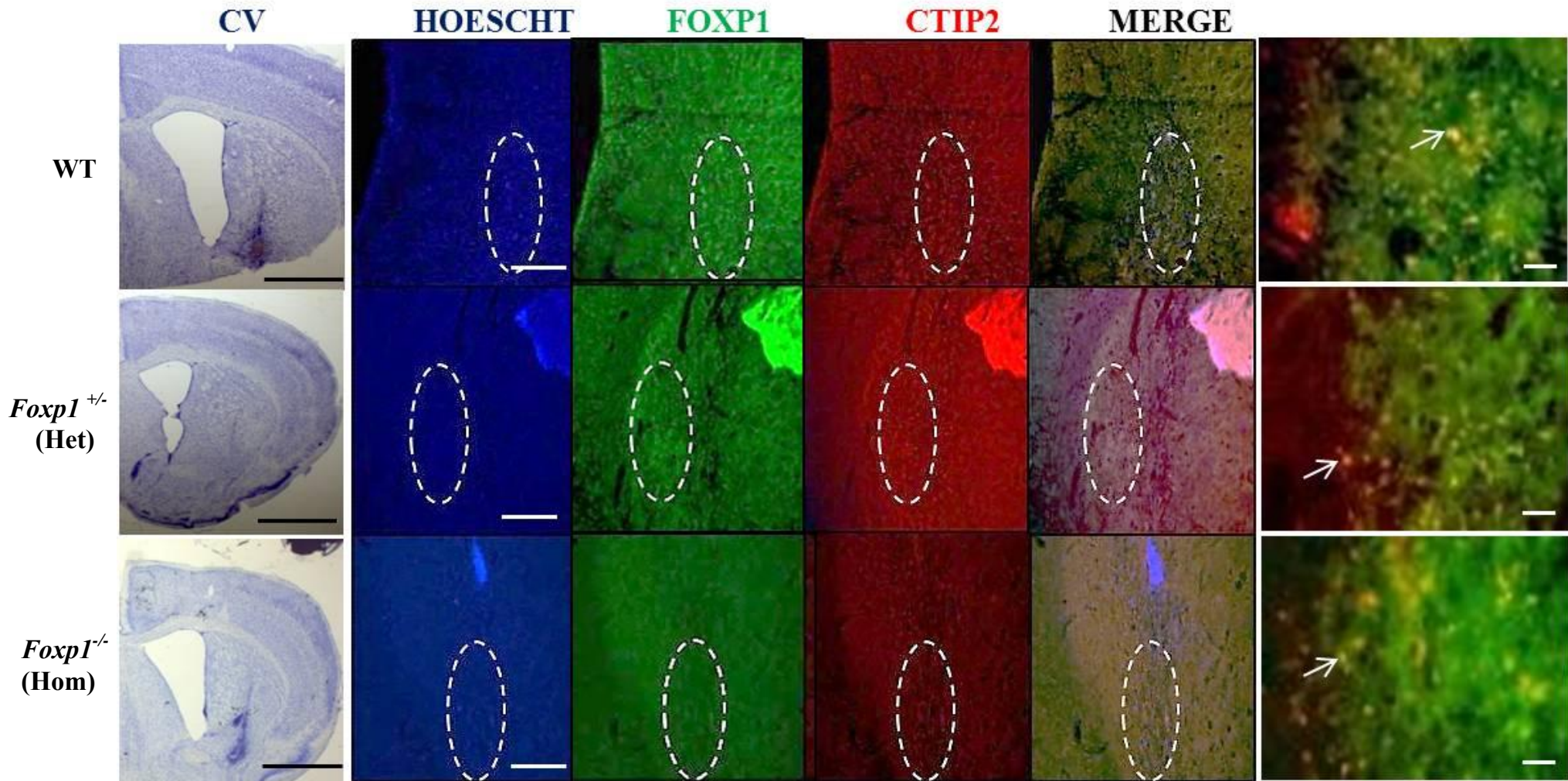
Figure 4.10 Examples of immunofluorescence staining of coronal sections stained for FOXP1 (Green) and CTIP2 (Red) and the nuclear stain Hoechst (Blue) at 12 weeks post transplantation. The fourth column is a merged image of the three stains. Nissl staining indicates the grafted area**.** Dotted ovals indicate the grafted region. Double stained cells appear yellow and are shown with arrows. *Abbreviations CV- Cresyl Violet, WT- Wild Type, Het= Heterozygote, Hom=Homozygotes. CV scale = 500µm, low power images= 200µm, high power images=50 µm.*

Survival and morphology of E12 grafts following 12 weeks *in vivo*

As the volume and cell numbers within the grafts from E14 donors s were typically low across all the genotypes it was not possible to interpret the results with complete confidence. As the mouse protocol is largely based on rat experiments, for which E14 tissue is used for grafting, for the final experiment, in a hope of achieving bigger striatal grafts, used E12 striatal tissue, as this age more closely correlates with E14 in rat. As before, grafts were left to mature *in vivo* for 12 weeks. Nissl staining suggested successful grafts were present in 86% of animals and also showed the presence of larger grafts than at E14, representative examples are shown in Figure 4.11. Graft volume was once again estimated by Nissl staining and these are shown in Figure 4.12. Genotyping showed that only one pup was a *Foxp1*$^{-/-}$ and therefore only 1 animal received a graft from this genotype making an accurate comparison of graft volume between the three genotypes not possible. However, it can be shown that there was no significant difference in volume between WT and *Foxp1*$^{+/-}$ grafts ($F_{1, 14} = .40$, p= n.s.). When all graft volumes were averaged across groups for each age, E12 graft volumes were significantly larger than those at E14 ($F_{1, 41} = 12.16$, P<0.01), this is shown in Figure 4.13.

Anterior ⟵⟶ Posterior
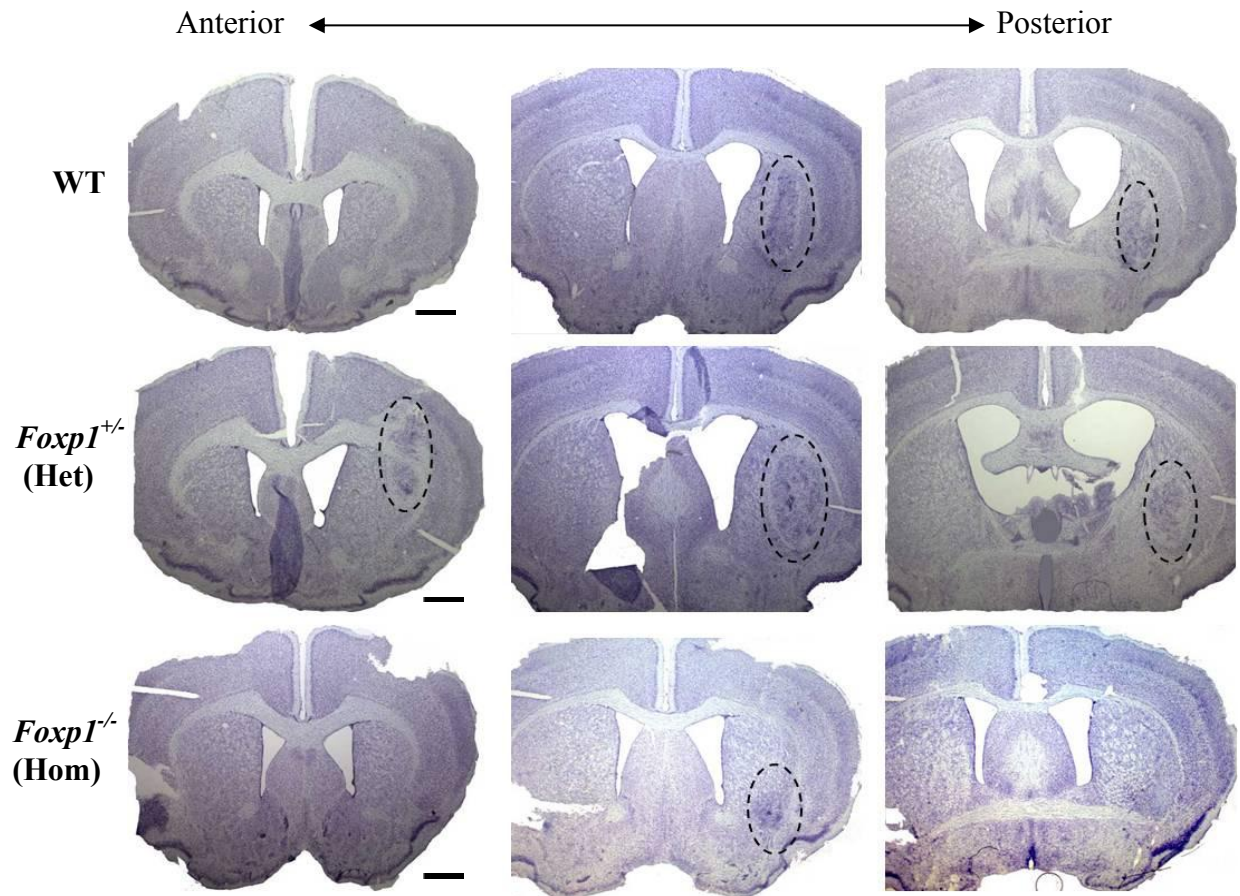
Figure 4.11 Representative photomicrographs of coronal sections showing Nissl staining using cresyl violet at 12 weeks post transplantation. Example brains show grafts from each of the genotypes at E12, WT, *Foxp1*$^{+/-}$ and *Foxp1*$^{-/-}$. Black dotted lines outline the grafted region as indicated by darker staining of the cresyl violet in the right hemisphere. *Abbreviations, WT = Wild Type, Het = heterozygote, Hom = Homozygote Scale bars= 500μm*
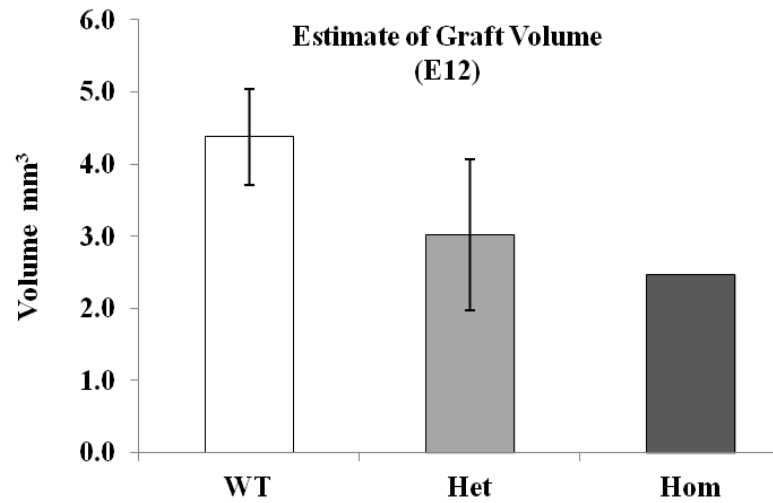
Figure 4.12 Graft volumes of surviving E12 grafts. Bars represent the mean graft volume per genotype (WT=3 Het= 12, Hom=1). *Error bars represent SEM. Abbreviations, WT = Wild Type, Het = Heterozygote, Hom =Homozygote.*
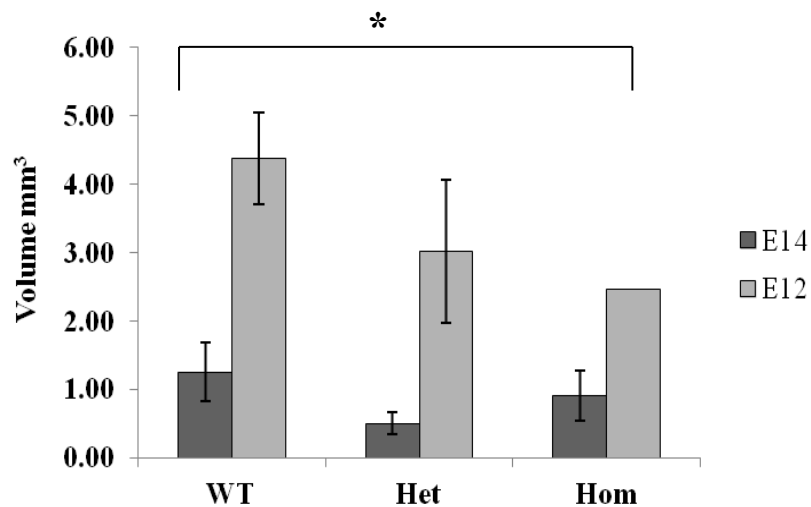
Figure 4.13 E12 and E14 graft volume comparisons Bars represent the mean graft volume per genotype (E14, WT=10, Het= 9, Hom=9). (E12; WT=3 Het= 12, Hom=1). Error bars represent SEM. *Abbreviations, WT = Wild Type, Het = Heterozygote, Hom = Homozygote.* Significance is indicated with brackets *(*=p<0.05).*

Graft Analysis of MSNs at 12 weeks from E12 tissue

A with the E14 grafts, MSN differentiation was assessed in the E12 grafts using Anti-DARPP-32, Anti-FOXP1 and Anti-CTIP2 immunohistochemistry. Additionally Anti-NEUN immunohistochemistry was also carried out to complement CV stains and to verify that the grafts did contain neuronal cells. Figure 4.14 shows Nissl staining identifying the graft region and corresponding sections stained with NEUN. In all groups there was NEUN staining throughout the grafted region. FOXP1 positive cells were identified in grafts from WT and *Foxp1*$^{+/-}$ donors but very little positivity was evident in the graft that received the *Foxp1*$^{-/-}$ donor tissue. The pattern of DARPP-32 positive staining matched that of the FOXP1 staining and for both stains positive cells were clustered into "patchy" zones, with more patches evident in the FOXP1 stained sections. This is shown clearly in Figure 4.15. CTIP2 staining, as with the E14 grafts, was inconsistent and positive cells were difficult to identify as shown in Figure 4.16. Due to the low numbers of animals in each transplant group (WT=3, *Foxp*$^{+/-}$=12, *Foxp1*$^{-/-}$ = 1) cell counts were not carried out on any of the stains. As an alternative, a grading system was implicated whereby each graft was given a number dependant on what description it best fit as shown in Figure 4.17.
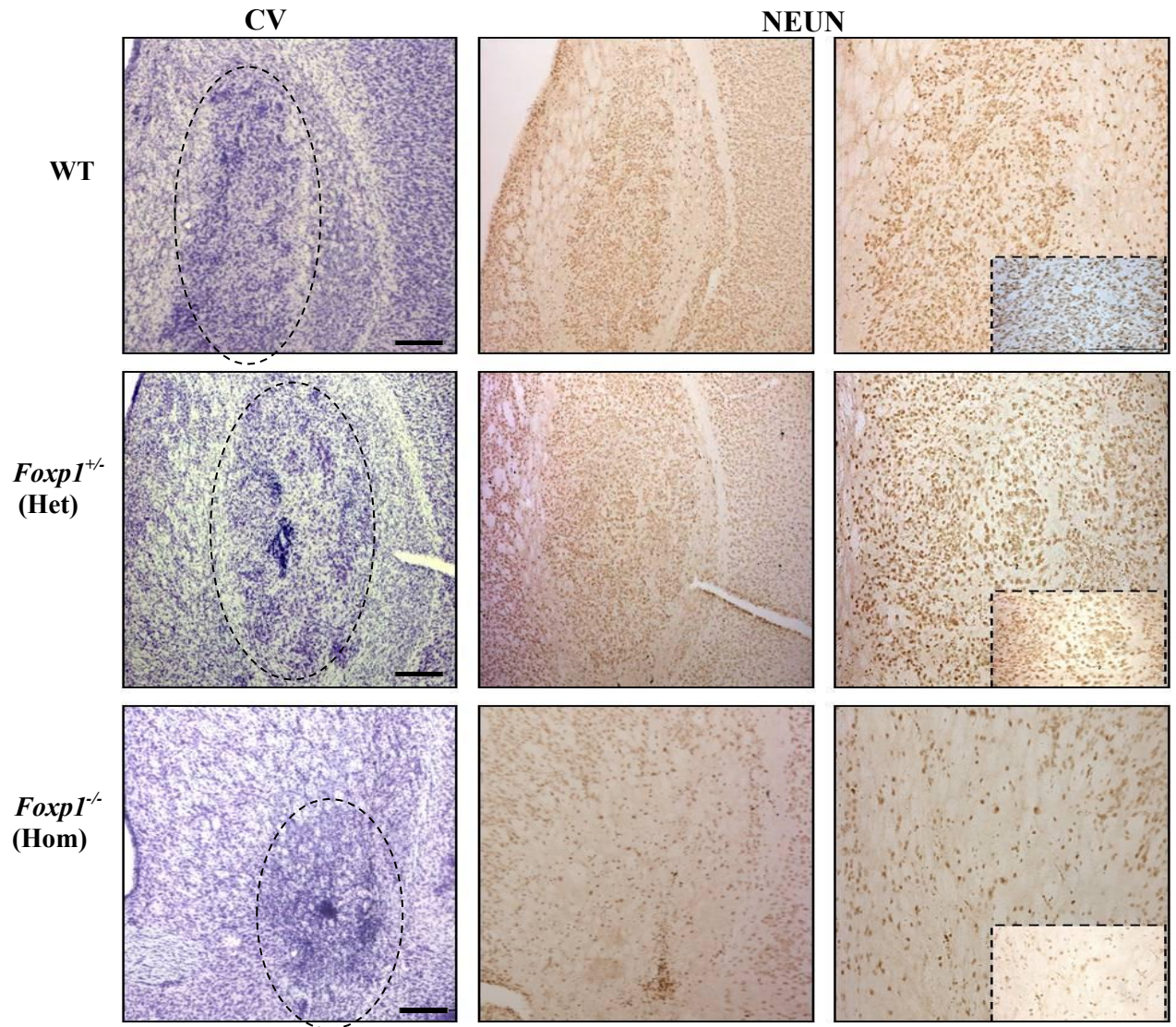
Figure 4.14 (A) Example photomicrographs of coronal sections showing CV and NEUN at 12 weeks post transplantation from E12 tissue. CV identifies the grafted region. Dotted ovals indicate the grafted region and dotted boxes are a higher magnification of this region. Photomicrographs show that there is NEUN present throughout the grafted area in all three genotypes. *Abbreviations, CV = Cresyl Violet, WT = Wild Type, Het = heterozygote, Hom = Homozygote, Scale bars: Low power= 200 μm, high power = 50 μm.*
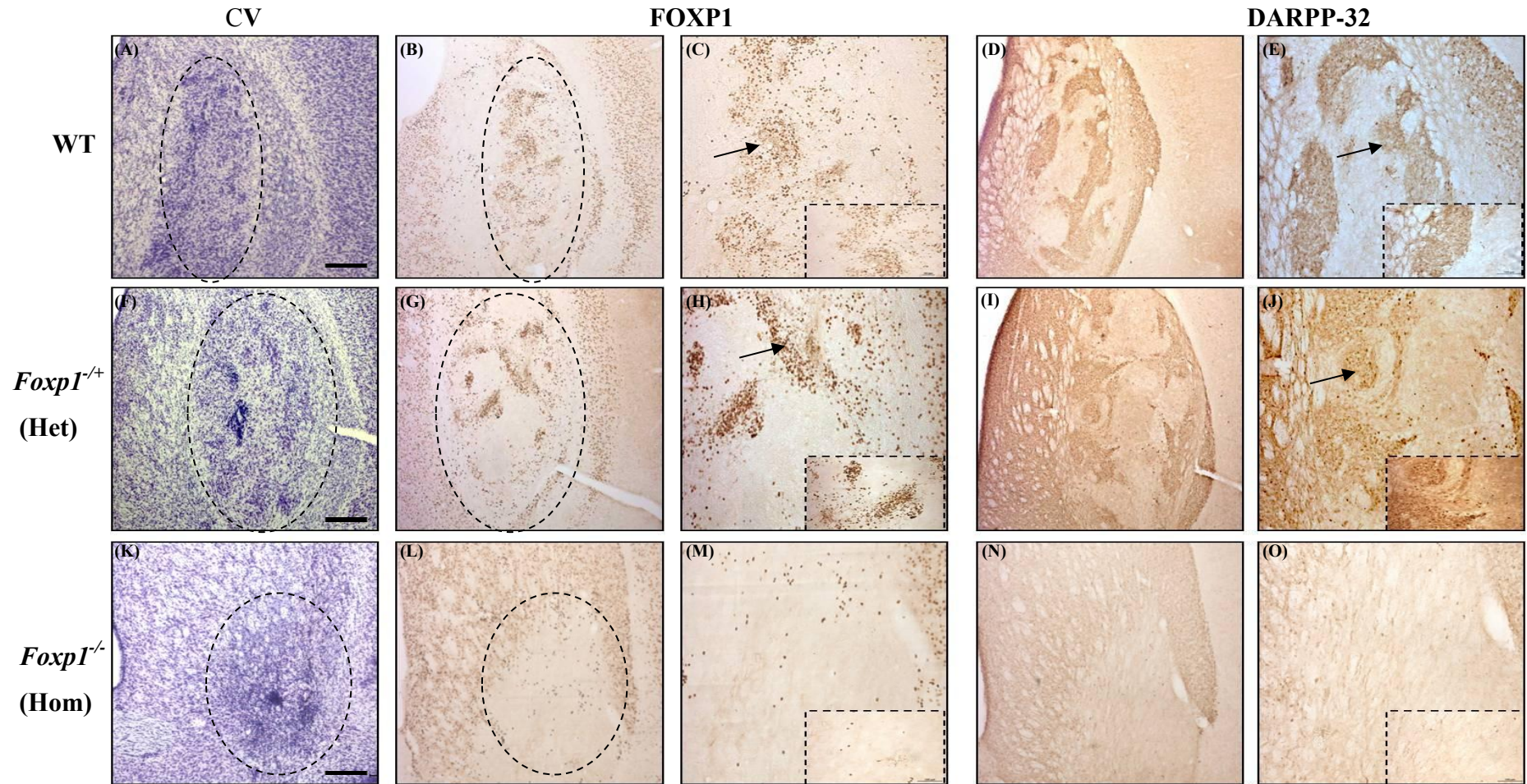
Figure 4.15 Example photomicrographs of coronal sections showing (A, F and K) Nissl, (B-C, G-H and L-M) FOXP1, and (D-E, I-J and N-O) DARPP-32 staining of E12 grafts 12 weeks post transplantation. Dotted ovals indicate the grafted region and dotted boxes are a higher magnification of this region. **(B-E, G-J)** FOXP1 and DARPP-32 staining shows patchy distributions within the grafted area, indicative of "P-Zones", examples are indicated with arrows. **(L-O)** There is little or no FOXP1 or DARPP-32 present in the grafts from the *Foxp1⁻/⁻* tissue when compared to grafts receiving tissue from WT and *FoxP1⁺/⁻* embryos. *Abbreviations, CV = Cresyl Violet, WT = Wild Type, Het= heterozygote, Hom=Homozygote Scale bars: Low power= 200 μm, high power = 50 μm.*
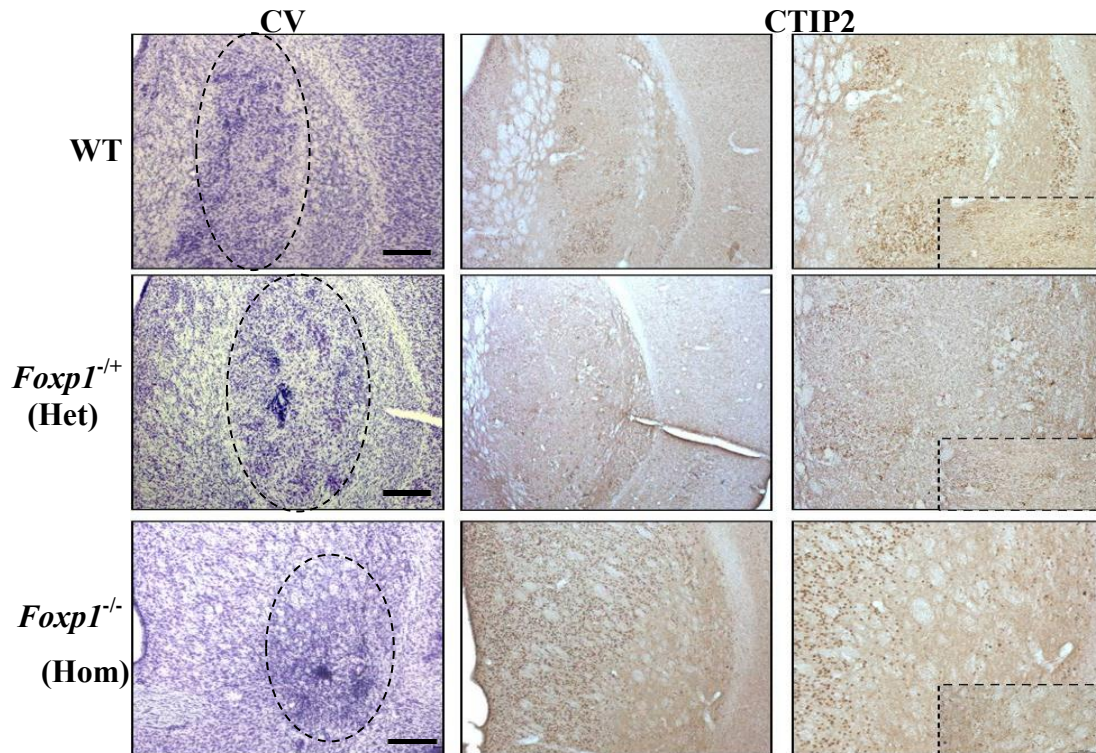
Figure 4.16 (A) Example photomicrographs of coronal sections showing CTIP2 at 12 weeks post transplantation. Dotted ovals indicate the grafted region and dotted boxes are a higher magnification of this region. *Abbreviations WT- Wild Type, Het= heterozygote, Hom=Homozygote Scale bars: Low power= 200 μm, high power = 50μm*

(A)

Grade Number	Description
4	Dense staining of the antibody, recognisable grafted cells throughout the lesioned area
3	Dense staining of the antibody restricted to certain patches throughout the lesioned area
2	Minimal staining of the antibody in the grafted region
1	Graft outside striatal area
0	No graft

(B)

Stain	WT	Foxp1$^{+/-}$ (Het)	Foxp1$^{-/-}$ (Hom)
NEUN	4,1,4	3,0,0,4,2,2,2,2,4,4,4	3
FOXP1	3,1,3,	3,0,0,3,1,2,2,1,3,3,3	2
DARPP-32	3,1,3,	2,0,0,3,1,1,1,2,3,3,3	2
CTIP2	2,1,3	2,0,0,2,1,2,2,2,3,4,	2

Figure 4.17 Quantification of E12 grafts (A) The grading system designed as a way to quantify grafts due to the low numbers of animals within the groups **(B)** Quantification of the grafts suggested that there was les DARPP-32 in the grafts from the *Foxp1*$^{-/-}$ grafts compared to WT and *Foxp1*$^{+/-}$ grafts.

4.5 **Discussion**

Cell transplantation: a novel approach to a commonly used method

The aim of the experiments outlined in this Chapter were to circumvent the embryonic lethality associated with *Foxp1$^{-/-}$* KO mice at E15 in order to look at differences in mature MSNs, in a graft scenario, in the absence of *Foxp1*. Cell transplantation studies in rodents are typically used to assess graft survival and functional recovery as a means of validating cell replacement therapy for use in diseases such as HD and PD. Here it was used in a novel way to look at phenotypic differences in MSN development. By dissecting primary striatal tissue, before the onset of lethality, it was anticipated that the tissue, once grafted, would continue to develop and differentiate in an environment more akin to that of their natural milieu, as oppose to in the *in vitro* conditions outlined in Chapter 3.

However, it is understood that grafting into a lesioned striatum is not identical to the "natural" striatal environment as there are, for example, molecules such as inflammatory cytokines circulating the lesioned area which could influence graft survival and subsequent differentiation (Dunnett *et al.* 1997). Still, the approach can be used to provide a good approximation of natural development, which is aided by the fact that the majority of neuronal precursors by E14 "fated" to become MSNs are undergoing their final mitotic cell divisions and have started differentiating into their predetermined phenotype i.e. MSNs (Anthony *et al.* 2004; Dunnett *et al.* 1997; Malatesta *et al.* 2003), thus one would predict that the cells would continue to develop as if left *in vivo*. Another potential caveat is the distress caused to the cells during the transplantation programme. Nevertheless, mouse allograft experiments have proven to be successful and survive the transplantation process (Dobrossy *et al.* 2011; Dunnett *et al.* 1998; Kelly *et al.* 2007). Consequently, using the cell transplantation method has allowed cells from all genotypes the opportunity to develop and mature over a prolonged period of time *in vivo* and answered questions unachievable from the previous *in vitro* experiments, although it is known that results obtained cannot be directed attributable to the natural process.

Graft Analysis- Differences in the MSNs in the absence of *Foxp1*

The donor age of the tissue commonly used in mouse allografting experiments (E14) is based on what was shown to be successful in the rat (Watts *et al.* 2000a, b) and thus was chosen for these experiments. Five animals from each genotype were sacrificed after 4 weeks *in vivo* to check for the presence of grafts as determined by Nissl staining using CV, and thus validated that the transplantation protocol had worked. Nissl staining showed that 78% of grafts survived across transplantation groups. Nissl staining also showed an increase in ventricular volume ipsilateral to the graft caused by cell loss and subsequent shrinkage of the striatum as a result of the QA (Dobrossy and Dunnett 2005). FOXP1 immunohistochemistry showed animals that had received donor cells from *Foxp1*$^{-/-}$ embryos had significantly fewer FOXP1 positive cells (105±54) than those grafted with cells from WT (796±144) or *Foxp1*$^{+/-}$ (1093± 180) embryos. It was unexpected that FOXP1 positive cells were identified in grafts from the *Foxp1*$^{-/-}$ embryos and reasons for this could be due to cross contamination from the other cell suspensions within the grafting syringe, or that host cells could have been mistakenly counted as grafted cells due to the absence of a donor specific label, an issue addressed later. From these preliminary results, it was decided the remaining animals would be left for an additional 8 weeks to allow further maturation of the grafted cells.

At 12 weeks post transplantation, average graft volumes (independent of genotype), were 0.89 mm ± 0.3mm^3. These are comparable with those reported in previous mouse grafting studies, 0.80 ± 0.09 mm^3 (Kelly *et al.* 2007), and similar graft volumes have also been demonstrated by other colleagues using the mouse-mouse system within the group (Roberton *et al.* 2013), and elsewhere (Cisbani *et al.* 2013; Johann *et al.* 2007; Tate *et al.* 2002). However, there are studies that appear to contradict these small mouse-mouse grafts. One study that grafted E13-14 LGE into the striatum of the TG R6/2 mouse model showed photomicrographs suggesting the presence of a large graft in both a WT and TG host 6 weeks post transplantation (Dunnett *et al.* 1998). Yet, no graft volumes were included in this study suggesting the example photomicrographs chosen for publication were perhaps not representative of the groups. Additionally, when striatal tissue from the M4-BAC-GFP mouse line was grafted into the QA lesioned striatum of mice a large graft was shown. Yet, graft volumes were once again not displayed and thus photomicrographs may not represent all the groups (Dobrossy *et al.* 2011). Equally, when this method was trialled in our lab using either C57BL/6J or CD1

embryos as donors, grafts were not reproducible to the extent of those published suggesting that donor strain, or the mouse brain as a suitable host for transplanted tissue (Roberton *et al.* 2013), may have a role to play in the success of grafting in mice, and this is actively being explored in the lab.

Nevertheless, the grafts from E14 donor tissue showed that there were significantly fewer FOXP1 positive stained cells in the grafts from the *Foxp1*^{-/-} (461±127) donors compared to those grafted with cells from WT (1308±275) or *Foxp1*^{+/-} (854±164) embryos. To address differences in mature MSNs within the grafts DARPP-32 was used. DARPP-32 expression in striatal neurons is not fully developed until the second or third postnatal week (Gustafson *et al.* 1992), and in agreement with this DARPP-32 expression has been shown 2 weeks following transplantation of E14 tissue, which the authors suggest is equivalent to P7 (Olsson *et al.* 1995). Striatal neurons 12 weeks post grafting would therefore be expected to express DARPP-32. There was DARPP-32 staining in grafts although considerably less than FOXP1 staining irrespective of genotype (Figure 4.8) and the reasons for differences in staining patterns are numerous. Firstly, although FOXP1 has shown to co-localise with DARPP-32 (Tamura *et al.* 2004), FOXP1 has shown to stain MSNs from an earlier time point when the neurons are more immature (Ferland *et al.* 2003). Secondly, it must also be considered that as these grafts are WGE derived, rather than LGE derived, FOXP1 immunohistochemistry could have labelled cells in the graft that were derived from the developing cortex, where FOXP1 is known to be expressed at E14 (Ferland *et al.* 2003; Tamura *et al.* 2004). Thirdly, that DARPP-32 does not stain the entire population of MSNs (Arlotta *et al.* 2008), an observation made by both Arlotta (2008) and Precious et al (2013, submitted). These groups report that DARPP-32 co-localises with all CTIP2 and FOXP1 positively labelled cells respectively, but that there were FOXP1/CTIP2 positive/DARPP-32 negative cells present. This subset of cells did not co-localise with any known interneuron marker suggesting a population of striatal projection neurons that do not express DARPP-32 (Arlotta *et al.* 2008). Fourthly, not all cells, fated to become MSNs were mature enough to express DARPP-32 and longer *in vivo* periods are needed for maturation, however as optimal expression is apparent by three weeks after birth this is unlikely. Finally, it may be that if the donor cells were transplanted at an early time point the number of DARPP-32 positive cells would be greater, as proposed by Fricker-Gates (Fricker-Gates *et al.* 2004).

Despite low cell numbers within the grafts there were significantly fewer DARPP-32 positive cells in the grafts from the *Foxp1*$^{-/-}$ embryos (390 ±68) compared to animals grafted with cells from WT embryos (802±68). These initial experiments using E14 donor tissue for transplantation were comparable to the *in vitro* findings of Chapter 3 that in the absence of *Foxp1* there is a decrease in the number of DARPP-32 positive cells. In addition to DARPP-32, CTIP2, another MSN marker that has shown to co-localise with FOXP1 in the striatum, was used. (Arlotta *et al.* 2008). Quantitative analysis showed that there was no significant difference in the number of CTIP2 positive cells. However, staining was inconsistent throughout the sections, and results should be interpreted with this in mind. CTIP2 was the last stain carried out and inconsistencies in staining can perhaps be attributed to degradation of the tissue from prolonged storage in the fridge. Fluorescent immunohistochemistry was attempted as a means of validating the DAB staining, and although not quantified, observations suggested the same pattern. However, the technical problems associated with the CTIP2 staining warrant caution and experiments need to be repeated to establish confidence in these findings.

Grafts-Limitations and Alternative Strategies

Another limitation with allografts is being able to confidently identify cells as host or donor within the lesioned area. In the absence of the donor cells being labelled in some way e.g. with a fluorescent tag, it is possible that allograft experiments may be under or over representative due to the difficulties in reliably identifying the cells. This problem is exaggerated in small lesions where neuronal loss is limited making the host/lesion boundary difficult to define. Labelling of the donor cells would therefore facilitate more reliable and reproducible results. A mouse allograft experiment using M4-GFP tagged donor cells, which express GFP in all MSNs implicated in the direct pathway, allowed grafted cells to be easily identifiable up to 24 weeks following grafting (Dobrossy *et al.* 2011). However, donor cells from the M4-GFP line would not be possible for the transplantation experiments described here as the importance of the work was to look at specific differences in the development and differentiation of the donor cells from the three different genotypes and therefore an alternative method would be needed to label the cells used in these experiments. One alternative would be to transfect plasmids carrying a label such as LacZ or GFP. However, successful transfection of plasmids into primary cells is difficult due to the delicate nature of the cells. Where success has been

seen it is at very low efficiencies (Urban *et al.* 2010). Throughout this PhD several different methods of transfection for experiments in primary E14 striatal cells were trialled. Methods included electroporation (*Neon Transfection system*), Lipofectamine, and a new delivery method, Nanofection, which uses magnetic resonance to drive the plasmids into the cells and is reliant on endocytosis. Unfortunately, following several attempts of optimization for each method the outcomes were either high transfection rates but at the expensive of increased cell death, or very low transfection efficiencies in favour of cell survival, none of which are ideal for differentiation or grafting studies. Appendix 9.7 shows a table summarising results from these transfections. Thus from this preliminary work it can be concluded that a virus, which doesn't need an artificial delivery method of entering the cells, would be one of the best options to label primary cells, such as a LacZ virus as was shown by Kelly et al (2007), and something that will be considered for future allograft experiments. Another possibility is grafting donor cells from the Fox heterozygote cross into a mouse that globally expresses fluorescent protein such as GFP or m-cherry. Therefore the cells from the donor would not stain positively for GFP/RFP allowing one to confidently ascertain which cells was definitely graft derived rather than host. This method would also one to confidently identify if there was integration between the host and graft tissue.

In some instances, when a specific Cre is not available to create a regional specific KO, or to look more closely at complex tissue-tissue interactions, chimeric mouse models can be used. In this instance instead of grafting cells from a heterozygote cross, and parallel to the creation of a CKO, *Foxp1* chimeras could be created similar to the aggregation chimeric model that looked at *Pax6* during development of the eye (Collinson *et al.* 2000; Quinn *et al.* 1996), as like *Foxp1,* knocking out this gene is also lethal to development. Creating chimeras would mean the mouse would contain a random mix of both WT and *Foxp1* mutant cells thereby allowing the functional role of *Foxp1* to be investigated in the developing brain past the point of embryonically lethality apparent in the homozygous nulls. Specifically one can compare the behavior of WT and mutant cells in chimeras and assess the capability of mutant cells to contribute to MSN development when in direct competition with WT cells. Of course, in order for such analyses a label e.g. GFP, RFP or LacZ would first need to be added to one or both of the lines to distinguish between the cells. The results could then be directly compared to a striatal specific CKO of *Foxp1*. However, this approach will take

a long time and thus grafting the cells, but changing some of the parameters to increase graft size was a better option in this instance given the time restraints of my PhD.

Increased graft volume and cell number within the graft using E12 donor tissue

Small graft size made interpretation of the results difficult and an attempt to achieve transplants with greater cell volumes was trialled to increase the reliability of the results. Two possible manipulations to the grafting protocol were considered; donor age and preparation of donor tissue (cell suspension or "pieces"). It has been reported that striatal grafts have an increased number of P-zones in grafts from younger donor tissue (Fricker-Gates *et al.* 2004). Recently this has been supported by Döbrössy and colleagues who showed that grafts from E13 rat embryos had more P-zones, showed the highest amount of DA afferents (re-establishment of the nigrostrital projection pathway) and the most consistent long term recovery on behavioural tests when compared to E14 or E15 grafts (Schackel *et al.* 2013). These results suggest that more immature striatal progenitors, that have not yet formed afferent or efferent connections (Hamasaki *et al.* 2003) are capable of continuing maturation and differentiation *in vivo* and provide a better donor source for striatal cell transplantation experiments (Fricker-Gates *et al.* 2004; Schackel *et al.* 2013). In support of this is what is understood about the equivalent gestational time points between rats and mice. Based on rat studies, E14 is the most commonly used donor age for mouse transplantation experiments. However, E14 in the rat is equivalent to E12.5 in the mouse and therefore if this age was used it is possible mouse allografts would be more comparable to rat allograft experiments.

It is also unknown whether tissue "pieces" or trypsinised cell suspensions should be used to produce the best grafts. It has been shown that trypsinised, triturated cell suspensions produced grafts with increased functional AchE positive zones and an increased number of DARPP-32 positive cells compared to grafts from tissue pieces (Watts *et al.* 2000b). However grafts from tissue pieces yielded larger graft volumes and showed modest functional recovery on the paw-reaching task (Watts *et al.* 2000b). Additionally, in human trials, patients that received transplants from tissue pieces, showed better recovery than those that received grafts from cell suspensions (Bachoud-Levi *et al.* 2006), although it is appreciated that the number of patients within this trial was very small.

Therefore, for the final experiment E12 donor cells were used, and as the WGE in mice at this age is very small, and not able to be pooled in the absence of a known genotype, each pair of striatum were trypsinised minimally and grafted as "pieces" (1 striate pair per lesioned animal) rather than as a trypsinised cell suspension as the E14 grafts. It is recognized that this experiment was not designed to systematically address the issue of optimal donor age and tissue preparation, but done in a way that would optimistically yield the biggest grafts to confirm the results interpreted from the E14 grafts. A thorough systematic assessment of the mouse-mouse grafting protocol is underway by the host lab to determine the optimal donor age, tissue type and how much time post lesion, are best for grafting. For the final experiments refinements were also made to the grafting protocol as a measure of reducing cross contamination of the cell suspensions. To achieve this multiple grafting syringes were used (it was not feasible to have a different syringe for each animal) and flushed through with boiling water in-between each graft.

E12 grafts

Due to small litter sizes (~5 pups/ mother) several different litters had to be used for this experiment and unfortunately, by chance, there was only 1 *Foxp1*$^{-/-}$ embryo, 3 WT and 11 *Foxp1*$^{+/-}$ embryos born. Due to the small number of animals receiving tissue from either the WT, or *Foxp1*$^{-/-}$ donors, grafts were analysed qualitatively with a grading system used in an attempt to quantify the grafts as oppose to stereology as this method did not seen appropriate in the absence of any comparable results. As expected, based on Nissl staining grafts were larger at E12 than at E14 and on average, across all genotypes, produced significantly larger graft volumes (3.29±0.85mm^3). Immunohistochemistry for the mature neuronal marker NEUN was used to confirm the neuronal content of the grafts and served as a way to confirm graft presence with the Nissl stains. Within the grafted area, NEUN showed positive staining throughout the grafts, although it was apparent that staining in the *Foxp1*$^{-/-}$ graft was less dense compared to grafts from the other genotypes. It is known from E14 striatal counts (Figure 3.7) that on average there were fewer cells in a pair of WGE from *Foxp1*$^{-/-}$ embryos when compared to WT or *Foxp1*$^{+/-}$ embryos. It is anticipated that this result would have been apparent at E12 and therefore in this experiment, as cell number wasn't controlled for, this maybe the reason for the apparent less dense NEUN staining in the graft of the animal that received *Foxp1*$^{-/-}$ cells.

As with E14 graft analysis, FOXP1 and DARPP-32 immunohistochemistry was carried out on the E12 grafts. Specifically, it is known that P-zones make up one third of WGE grafts and are identifiable as being AchE-rich, DARPP-32 positive patches of MSNs. The remaining regions called NP zones do not stain for striatal markers (Graybiel *et al.* 1989; Pakzaban *et al.* 1993). In contrast to the results from the E14 grafts, P-zones were readily identifiable within the grafts from animals that received WT and *Foxp1*$^{+/-}$ donor cells and positively stained for DARPP-32 and FOXP1. There was no FOXP1 or DARPP-32 staining in the NP zones. To date FOXP1 has not been routinely used to identify P-zones within a grafted region and these findings suggest it may be used in addition to DARPP-32 as a marker of these areas. As a comparison to the cell counts carried out on the E14 grafts, more FOXP1 positive P-zones could be seen than DARPP-32 positive P zones. No FOXP1 or DARPP-32 positive P-zones were identified in the grafts from the mouse that received cells from the *Foxp1*$^{-/-}$ embryo. CTIP2 was once again used, and, as with E14 grafts, staining was inconsistent throughout the grafts and further experiments will be needed to learn more about the relationship between FOXP1 and CTIP2.

Future Work

Work presented in this chapter highlights potential caveats to the mouse-mouse allograft protocol and suggests the need for systematic assessment of the mouse striatum as a viable host for transplantation and the age and type of donor cells used. For example by grafting LGE as oppose to WGE it would be anticipated that the number of P-Zones within the graft would increase (in LGE grafts P-zones can label 80-90% of the total graft (Pakzaban *et al.* 1993)) and thus, for work presented in this chapter, would enhance the genotypic differences concerning DARPP-32 staining.

Improvements to the mouse allograft field are needed to allow transplantation of mESCs and iPSCs, directed towards the phenotype of interest to be trialled in TG mouse models that offer a better physiological and behavioural comparison to neurological diseases than those from excitotic lesions such as QA. Therefore a thorough and systematic approach to the transplantation protocol will be needed to fully understand the best combination of donor age, tissue type and if the donor source is optimally delivered as a cell suspension or tissue pieces, in the aim of applying these results to the mouse allograft protocol facilitating routine and successful grafts in mice.

Additionally the possibility that the adult mouse striatum is a hostile host for neural transplant survival is also being explored as increased amounts of activated microglia and thus graft rejection are re-occurring problems in both mouse allo- and xenografts (Roberton *et al.* 2013).

4.6 <u>**Conclusion**</u>

In this Chapter cell transplantation was used to study differences in MSNs after E14, to circumvent embryonic lethality, simultaneous to the CKO colony being established. Individual cell suspensions consisting of E14 striatal tissue from one of three genotypes was grafted into the mouse QA lesioned striatum. 12 weeks following transplantation there was a significant decrease in the number of positively stained DARPP-32 cells in grafts from *Foxp1*$^{-/-}$embryos compared to grafts from WT donors. However these grafts were typically thin and contained few cells. Therefore it was decided as a means of supporting these results; the protocol needed improving to ensure larger graft volumes.

Subsequently, tissue was grafted from E12 embryos (the gestational age most akin to E14 in the rat) and the cells were in the form of a quasi-suspension ("pieces") as opposed to a fully triturated cell suspension. E12 grafts proved to have significantly larger graft volumes than E14 grafts and also appeared to have less DARPP32 in the absence of *Foxp1*. Grafts also displayed the typical P-Zones that indicate MSN rich regions. For the first time, FOXP1 was shown to stain P-zones, offering itself as a mature label of MSNs within grafts derived from WGE. However, owing to small grafts at E14, and lack of quantification at E12, these results will need to be corroborated by other experiments, such as results of the on-going microarray comparing WT and *Foxp1*$^{-/-}$ LGE and MGE at E14.

To conclude, we have shown that grafting at an earlier age (E12) with tissue pieces rather than cell suspensions, has at least for these experiments proved to be more successful than using the current mouse allo-grafting protocol that commonly uses E14 cell suspensions. Importantly the major conclusion from these results is that in the absence of *Foxp1* there is a decrease in DARPP-32 in cells grafted into the QA lesion environment, which also suggest that *Foxp1* is needed in MSN development.

5 <u>*Characterisation of a Mouse Model that lacks Foxp1 in the Adult Brain*</u>

5.1 <u>Summary</u>

CKO mice are considered a useful tool to study the loss of gene expression in a cellular or regional specific manner. In an attempt to study the effect of the loss of Foxp1 in the adult mouse striatum a conditional Foxp1 knock out mouse (Foxp1 CKO) was developed by crossing a mouse heterozygous for the Foxp1 LoxP allele with a mouse heterozygous for the hGFAP-Cre; hGFAP being expressed in radial glia, precursors for the majority of neurons in the CNS. However, histological analysis revealed that there was a complete loss of FOXP1 from all layers of the cortex in which Foxp1 is known to be expressed (III-V1a), but contrary to expectations FOXP1 in the striatum was retained. Although this pattern of loss was not what was aimed for the model appeared interesting in that it demonstrated a hyperactive phenotype. Systematic behavioural analysis demonstrated that the loss of cortical Foxp1 produced behavioural (hyperactivity) and cognitive (impaired attention) abnormalities compared to littermate controls. Further analysis showed that the behavioural phenotype associated with this Foxp1 CKO mouse model was responsive to atomoxetine, a drug prescribed to children with ADHD. Thus, taken together results suggest Foxp1 CKO mice to be a serendipitous model of ADHD.

5.2 **Introduction**

The development of MSNs, in the absence of *Foxp1* was discussed in detail in Chapter 3 but due to the embryonic lethality of the homozygous *Foxp1* KO mice no definitive conclusions could be drawn. Chapter 4 attempted to look beyond the point of lethality giving useful insights into differences in the mature MSNs in the absence of *Foxp1*; however, the method used was still limited in that the cells were not left to mature and develop normally and grafts were typically small. *Foxp1*$^{+/-}$ mice were also explored, but appeared to have no obvious behavioural or histological phenotype compared to WT mice. Thus, it was necessary to generate a *Foxp1* conditional knockout (CKO) mouse model.

CKO mice are a popular model used to bypass embryonic lethality in order to study genes of interest (GOI) and commonly utilise the Cre-Lox system in which the Cre recombinase enzyme, attached to a specific promoter, has the ability to catalyse recombination between two *LoxP* sites that flank the GOI (Gaveriaux-Ruff and Kieffer 2007). When the Cre enzyme and *LoxP* sites meet there is an irreversible excision of the DNA located between the two *LoxP* sites. Conditional mouse models can be developed to either have the GOI knocked out from when the promoter driving the Cre is initially expressed, or can be inducible and thus drive recombination and subsequent deletion in response to administration of a drug such as Tomixfen or Doxycycline. For the work outlined in this Chapter, recombination was from when the promoter was initially expressed.

CKO mice facilitate functional analysis by allowing behavioural characterisation of the animals through the use of specific behavioural tests to assess differences compared to littermate controls. Such tests can range from basic hand tests including the rotarod and locomotor activity to more complex tasks such as the five choice serial reaction time task (5-CSRTT) that looks at differences in the learning and attention of mice in operant boxes (Robbins 2002). *Foxp1* CKO mice have been created to look at spinal-motor neuron formation (Rousso *et al.* 2008) and sensory-motor connections in the spinal cord (Surmeli *et al.* 2011) but to date, no brain-specific CKO mouse models have been generated.

Developing CKO mice involves choosing the correct promoter to achieve successful recombination in the region of interest at the desired time. It is therefore paramount that the promoter driving the Cre expression is expressed in the same cells as the GOI or else recombination will be inefficient, not work at all, or lead to erroneous recombination at an undesirable region. For the work described in this Chapter we attempted to create a constitutive *Foxp1* CKO to investigate differences in striatal development in the absence of the *Foxp1* gene.

In the absence of an available, developmental striatal specific Cre line two of the most commonly used and commercially available neural-specific Cre-lines, the *Nestin*-Cre line, and the *hGFAP* Cre-line were chosen in an attempt to CKO *Foxp1* in the developing striatum. The *Nestin*-Cre line is expressed from E11 in all neuroepithelial cells, a stage which all neurons pass through, and therefore it would be expected that if *Foxp1* was knocked out at this early stage it would subsequently be absent during MSN development (Tronche *et al.* 1999). Secondly, the *hGFAP*-Cre line is expressed in radial glia (RG) and switches on at E13.5 (Malatesta *et al.* 2003; Zhuo *et al.* 2001). It is understood that the majority of neurons in the CNS pass through a RG stage in their development (Malatesta and Gotz 2013; Malatesta *et al.* 2000; Noctor *et al.* 2002) and thus it was supposed that this line would also knock out *Foxp1* in developing striatal neurons. Both Cre lines are expressed during MSN development and as the preferable time to KO *Foxp1* is largely unknown it was decided that both Cre-lines would be crossed to the *Foxp1*$^{fl/fl}$ mouse line. This would also allow phenotype differences, as a direct result of knocking out *Foxp1* at different developmental times to be compared. However, for reasons discussed later only the hGFAP/*Foxp1*$^{fl/fl}$ line was pursued.

Despite the reasoning above, the resulting *Foxp1*$^{-/-}$ CKO using the hGFAP promoter did not result in loss of *Foxp1* in the striatum, but rather resulted in loss of *Foxp1* in the neocortex, sparing expression in the striatum and the animals displayed a clear hyperactive phenotype. Combined with the recent reports of *de novo* and micro-deletions in the FOXP1 gene in humans in autism spectrum disorders (ASDs) (Palumbo *et al.* 2013), and in speech and language deficits (Hamdan *et al.* 2010; Horn *et al.* 2010), the possibility that the *Foxp1* KO mice represented an animal model of ADHD was raised. This was felt to be of sufficient interest in terms of a broader understanding of the actions of *Foxp1* to justify further analysis of the behavioural and histological

phenotype. Thus, this Chapter presents a detailed behavioural and histological analysis of the conditional *Foxp1 $^{fl/fl}$* KO using the hGFAP promoter (from here on in referred to as the *Foxp1* CKO).

5.3 **Results**

Animal Weights

As shown in Chapter 3 there were no phenotypic differences between the adult *Foxp1*$^{+/-}$ and WT mice, therefore conditional *Foxp1* KO mice needed to be developed to look at differences in the adult brain in the absence of *Foxp1*. Therefore a *Foxp1* CKO mouse line was developed under the control of the hGFAP promoter. At the time of testing there was no significant differences either between the body weights of *Foxp1* CKO male mice ($F_{1, 12}$ = 1.33, p=n.s.) or *Foxp1* CKO female mice ($F_{1, 19}$ = 1.37, p= n.s.) when compared to littermate controls (Figure 5.1).
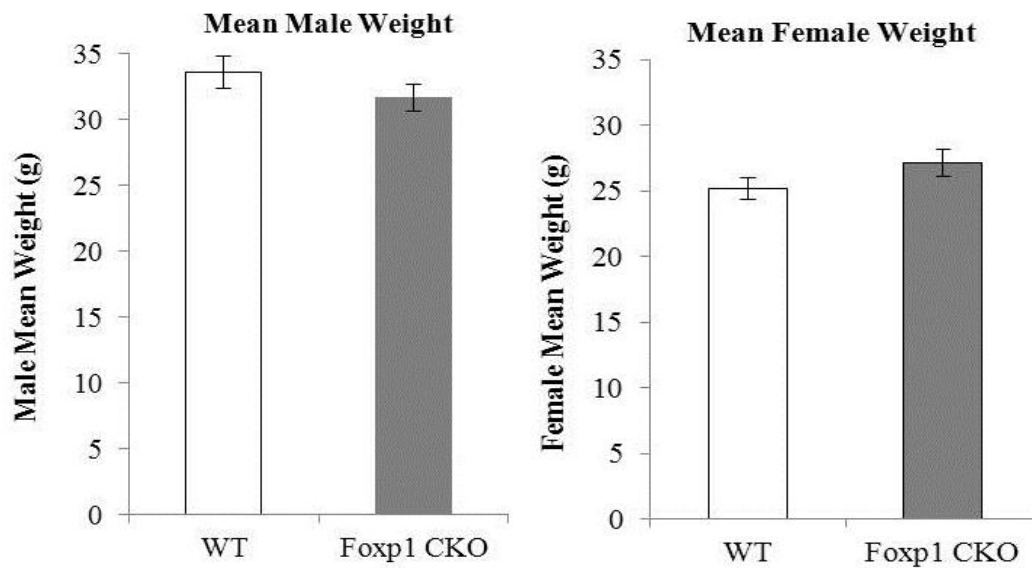
Figure 5.1 Average weights (g) of male and female, WT and *Foxp1* CKO adultmice *Error bars are SEM.*

Basic Behavioural Tests

Following genotyping, animals were grouped into either experimental or control groups and behavioural tests were carried out on the animals. Initially simple behavioural tasks were carried out to ascertain if there were any phenotypic differences apparent between the control and *Foxp1* CKO animals. Mice were tested on the rotarod apparatus (Ugo Basile, Varese, Italy) for the assessment of motor coordination, balance and general strength. It was shown that *Foxp1* CKO mice showed a trend to stay on the rotating rod for longer than littermate controls (WT 77.75±8.11 s, CKOs 74.92±25.4 s), although there was no significant difference between the groups ($F_{1, 14}$ = 0.07, p=n.s.) (Figure 5.2A).This test was only carried out on the initial litter due to the difficulties of handling the animals during training and testing. To test for differences in strength mice were also subjected to the cage lid grip strength task. In this task the *Foxp1* CKO mice retained their grip on the inverted cage lid for significantly less time (15±6.95 s) than controls (50±6.75 s) ($F_{1, 14}$ = 40.10, p =<0.001) this is shown in Figure 5.2B. As with the rotarod this test was only preformed on the initial litter due to the hyperactivity of the animals.
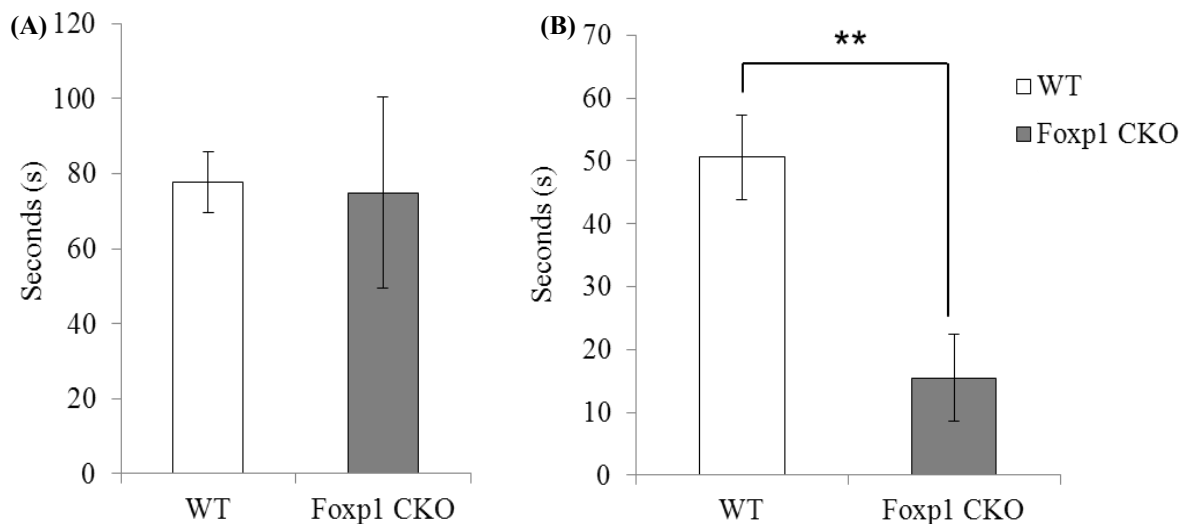
Figure 5.2 (A) Bars represent the mean time spent on the rotorod by WT and *Foxp1* CKO mice **(B)** Bars represent the mean time spent holding gripping on in the inverted cage lid task by WT and *Foxp1* CKO mice *Error bars are SEM (**= P<0.001).*

***Foxp1* CKO mice were significantly more active than littermate controls.**

As the *Foxp1* CKO mice had appeared to be more hyperactive and impulsive than their littermate controls further behaviour analysis took place to understand more about the behavioural phenotype. To assess overall activity and any differences in circadian rhythm between the genotypes, mice were placed in activity boxes at 12 weeks of age and the total number of non-perseverative beam breaks was assessed over 32 hours (only 24 hours of data was analsyed). *Foxp1* CKO mice displayed elevated levels of horizontal ambulatory activity (determined by total number of beam breaks) that significantly exceeded that of their control littermates ($F_{1, 39} = 14.68$, $p<0.00$). There was a significant interaction between time and genotype ($F_{24, 936} = 8.64$, $P>0.00$) with a significant difference in the activity of the *Foxp1* CKO mice during the "dark phase" of testing (18:00-06:00) when compared to littermate controls ($F_{1, 39} = $ minimum $F= 6.01$, $p<0.02$), shown in Figure 5.3.
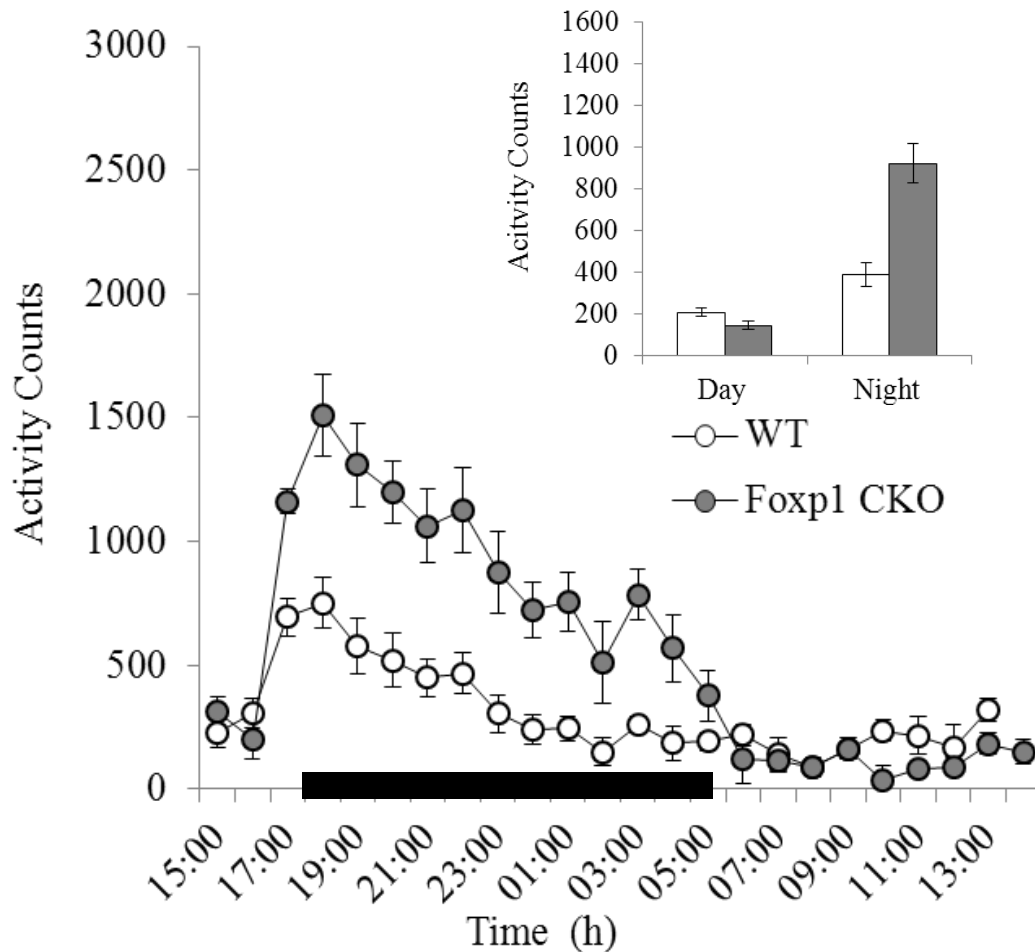
Figure 5.3 Open field locomotor activity-*Foxp1* CKO mice were significantly more hyperactive compared to littermate controls in the dark phase of the activity task (18:00-06:00), indicated with a thick black line. There was no difference in activity during the light phase. The bar chart shows total activity in both the light and dark phase of testing. *Error bars are SEM (*** P<0.001).*

Open field analysis also showed increased activity of the *Foxp1* CKOs compared to littermate controls.

To further probe the hyperactivity of the *Foxp1* CKO mice additional open field testing was carried out in a larger arena (80 cm x 80 cm) to look at open field activity within a 15 minute period using the video-tracking software EthoVision (*Noldus*). In addition to overall locomoter activity this software allowed velocity, distance travelled and rearing to be recorded. Results showed that *Foxp1* CKO mice covered a significantly greater distance in the testing arena ($F_{1, 15}$ = 6.24, $p<0.05$) and at a faster pace than WT mice ($F_{1, 15}$ = 6.24, $p<0.05$), shown in Figure 5.4A and B. *Foxp1* CKO mice also showed a significant increase in rearing compared to WT mice ($F_{1, 15}$ = 6.13, $p<0.05$) (Figure 5.4C). The Ethovision programme produces "traces" for each animal which display the area covered by the mice within the 15 minute testing period. Representative sample traces are shown in Figure 5.4D. The traces show that mice from both genotypes explored the entire arena, and did not just explore the perimeter.
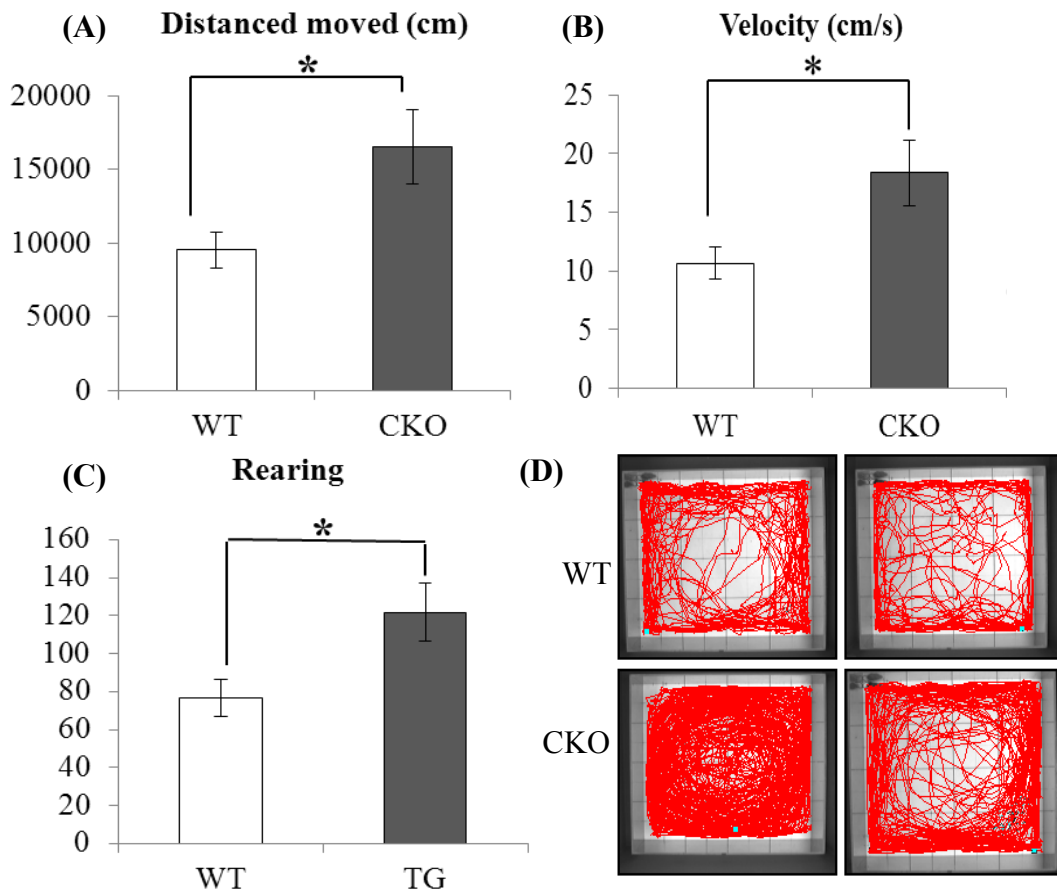
Figure 5.4 Open field activity during a 15 minute testing period using EthoVision (A) Bars represent the mean distance travelled by WT and *Foxp1* CKO mice within the arena **(B)** Bars represent the mean velocity of WT and *Foxp1* CKO mice within the arena **(C)** Bars represent the mean rearing of WT and *Foxp1* CKO mice within the arena **(D)** Sample traces from WT and *Foxp1* CKO mice displaying the exact movement pattern of the animals within the arena. *Error bars are SEM* (*=p<0.05).

***Foxp1* CKO mice did not display a phenotype associated with anxiety**

As the *Foxp1* CKO mice did not fear the centre of the open field arena this would suggest the animals were not over anxious. Therefore to look specifically for any differences in anxiety the marble burying task (MBT) and Elevated plus Maze Test (EPM) were carried out. These two tasks are designed to take advantage of a rodent's innate response of burying unknown objects and fear of heights combined with exposed, open arms, rather than safe enclosed arms. Example photomicrographs from the MBT are displayed in Figure 5.5A and the mean number of marbles buried is shown in Figure 5.5B. Although the control mice buried more marbles than *Foxp1* CKO mice (WT=5.57±2.01, CKO=0.80±0.49) this did not reach conventional levels of significance ($F_{1, 11} = 3.805$, p=0.08). Figure 5.5C shows the number of marbles buried per mouse and clearly identifies the one outlying result, which shows that one WT mouse buried 17 marbles. Non-parametric analysis showed that there was a significant difference between the numbers of marbles buried between the groups (U=2.00, p≤0.01). On the EPM there was no difference in the number of open arm entries between the genotypes ($F_{1, 12} = 3.81$, p=n.s.) (Figure 5.5D) but the *Foxp1* CKO mice spent significantly more time on the open arms ($F_{1, 12} = 6.84$, p=<0.05) than littermate controls (Figure 5.5E), determined as a percentage of total arm entries and total time spent on all four arms respectively. WT animals had a preference to stay in the enclosed "safe" arms.
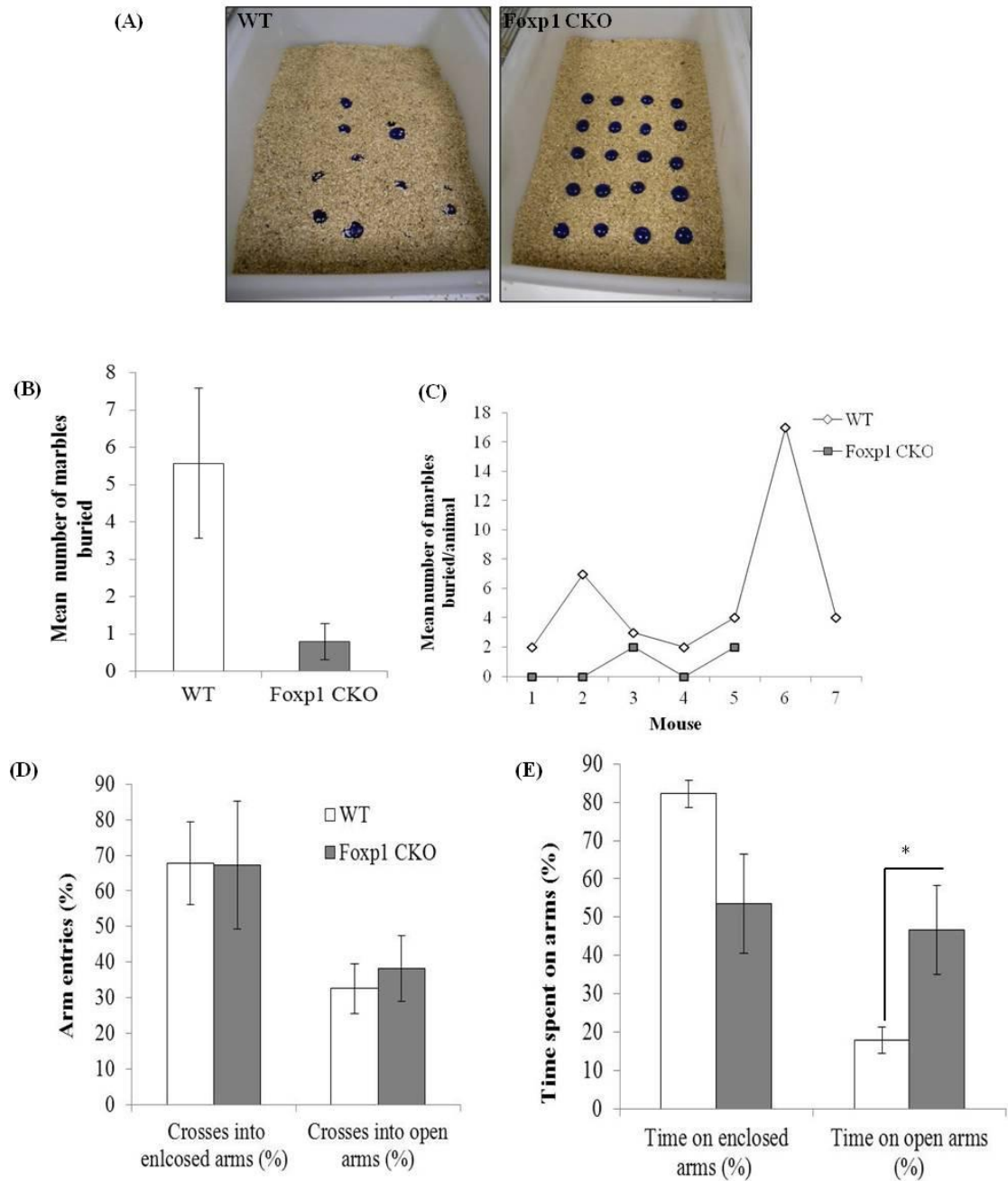
Figure 5.5 *Foxp1* CKO mice showed reduced anxiety in unconditioned environments (A) Representative photomicrographs of the MBT from a WT and *Foxp1* CKO mouse **(B)** Bars represent the mean number of marbles buried by the WT and *Foxp1* CKO mice **(C)** Line graph showing the number of marbles buried by each animal and shows the outlier result that 1 WT mouse buried 17 marbles. **(D)** Bars represent the mean number of crosses into enclosed or open arms (entry as a % of total crosses), by the WT and *Foxp1* CKO mice **(E)** Bars represent the mean time spent on either the open or closed arms (as a percentage of total time, on all four arms) by the WT and *Foxp1* CKO mice *Error bars are SEM. *P<0.05.*

Foxp1 CKO mice showed reduced attention compared to littermate controls.

It was clear from behavioural analysis that the *Foxp1* mice had a significant hyperactive phenotype compared to littermate controls, and from this the possibility of an ADHD phenotype was considered. As genetic links between *Foxp1* and ASD has been reported, and coupled with the fact that ADHD symptoms overlap with ASD, more specific behaviour analysis was carried to target other aspects of ADHD such as attention. The 5-CSRTT is carried out in operant boxes and requires the animals to respond to an illuminated hole for a reward. The period of time the light stays illuminated for can be manipulated and thus is a measure of attention.

Animals were initially trained, and then tested on the 5-CSRTT in 9 hole operant boxes in which two different stimulus delays were used (1 s and 0.5 s). There was a significant main effect between genotype and stimulus delay on accuracy ($F_{1, 9}$ = 1.911, p=$\leq$0.02; $F_{1, 9}$ =165.16, p<0.001 respectively). There was an overall effect on accuracy across holes ($F_{4, 36}$ = 3.64, p<0.02) but there was not a hole by genotype interaction ($F_{4, 36}$ = 0.82, p= n.s.). There was a significant interaction between stimulus delay and genotype ($F_{1, 9}$ = 8.26, p<.0.02) and further analysis showed there to be a significant difference in accuracy between the genotypes at both a 1 and a 0.5 second delay (p<0.05 and p<0.01 respectively) (Figure 5.6A). When reaction time (latency) was analysed there were no significant main effects between reaction time on stimulus delay or genotype ($F_{1, 9}$ = 0.57, 2.20 (respectively) p= n.s.). There was an overall effect on reaction time across holes ($F_{4, 36}$ = 9.95, p<0.00), but there was not a hole by genotype interaction ($F_{4, 36}$ = 3.21, p= n.s.), nor a stimulus delay by genotype interaction ($F_{1, 9}$ = 0.56, p=n.s.) (Figure 5.6B). Finally the number of omissions across all holes (no poking in the inter trial interval, (2 seconds)) was analysed. There were no significant main effects between the number of omissions on stimulus delay ($F_{1, 9}$ =0.572, p= n.s.). There was no overall effect on the number of omissions across holes ($F_{1, 9}$ = 9.95, p<0.00), but there was a significant main effect on the number of omissions and genotype ($F_{1, 9}$ = 12.13, p<0.02) and an overall effect on the number of omissions across holes ($F_{4, 36}$ = 3.71, p<0.05), but there was not a hole by genotype interaction ($F_{4, 36}$ = 2.27, p= n.s.), or a stimulus delay by genotype interaction ($F_{1, 9}$ = 0.03, p= n.s.) (Figure 5.6C).
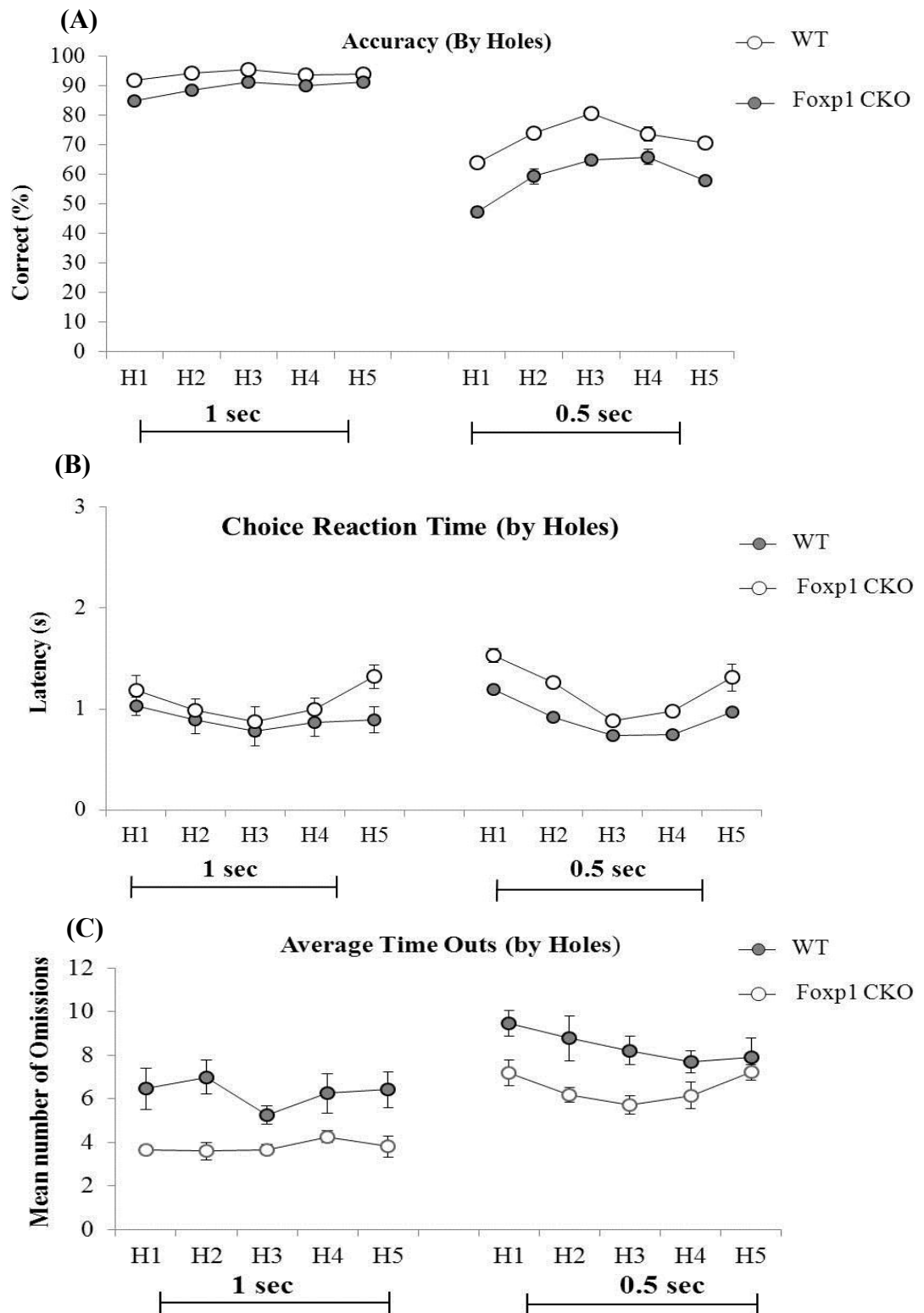
Figure 5.6 5-CSRTT performance by WT and *Foxp1* CKO mice (A) Accuracy: There was a significant interaction between stimulus delay and genotype, simple effects showing a decrease in total accuracy, across all holes, between the WT and *Foxp1* CKO mice (1 s p<0.05, 0.5 s p<0.01). **(B) Reaction time-** There was no interaction on reaction time between genotypes or stimulus delay **(C) Omissions**- There was no interaction between the number of omissions between genotypes or stimulus delay. *Error bars are SEM.*

156

Methylphenidate (Ritalin) improved accuracy in the 5-CSRTT but had no therapeutic effect on locomotor activity

As results significantly showed that the Foxp1 CKO mice were both hyperactive and inattentive pharmacological tests were carried out to look at predictive validity. Ritalin, a drug commonly prescribed to children which ADHD, is a DA and Noradrenalin (NA) reuptake inhibitor. All animals received all doses of Ritalin (saline, 5, 10 and 30 mg/kg) over the test period as a consequence of a drug trail on WT mice using a randomised Latin square design. Animals received an i.p. injection of the relevant dose and were tested in the locomotor activity boxes for 2 hours at the start of the dark phase (18:00). The total number of beam breaks per 10 minutes was recorded. Overall there were significant main effects of genotype on activity $(F_{1, 14}) = 123.18$ $p<0.001$) and drug dose on activity $(F_{3, 42}) = 18.00$ $p<0.001$) but there was no interaction between drug dose and genotype $(F_{3, 42} = 1.24$ $p=$ n.s.) (Figure 5.7).

The effect of Ritalin on accuracy in the 5-CSRTT was also tested and a dose of 5mg/kg was used. There were significant main effects of genotype $(F_{1, 9} = 10.37, p<0.01)$, drug dose $(F_{1, 9} = 12.70, p<0.01)$ and hole $(F_{1, 9} = 10.12, p<0.00)$ but although there was a trend for mice to improve in accuracy with Ritalin (notably the *Foxp1* CKO mice on hole 5) there was not a significant interaction between drug dose and genotype $(F_{1, 9} = 0.46, p=$ n.s.) or between drug dose and hole $(F_{4, 36} = 1.62, p=$ n.s.) (Figure 5.8).

157
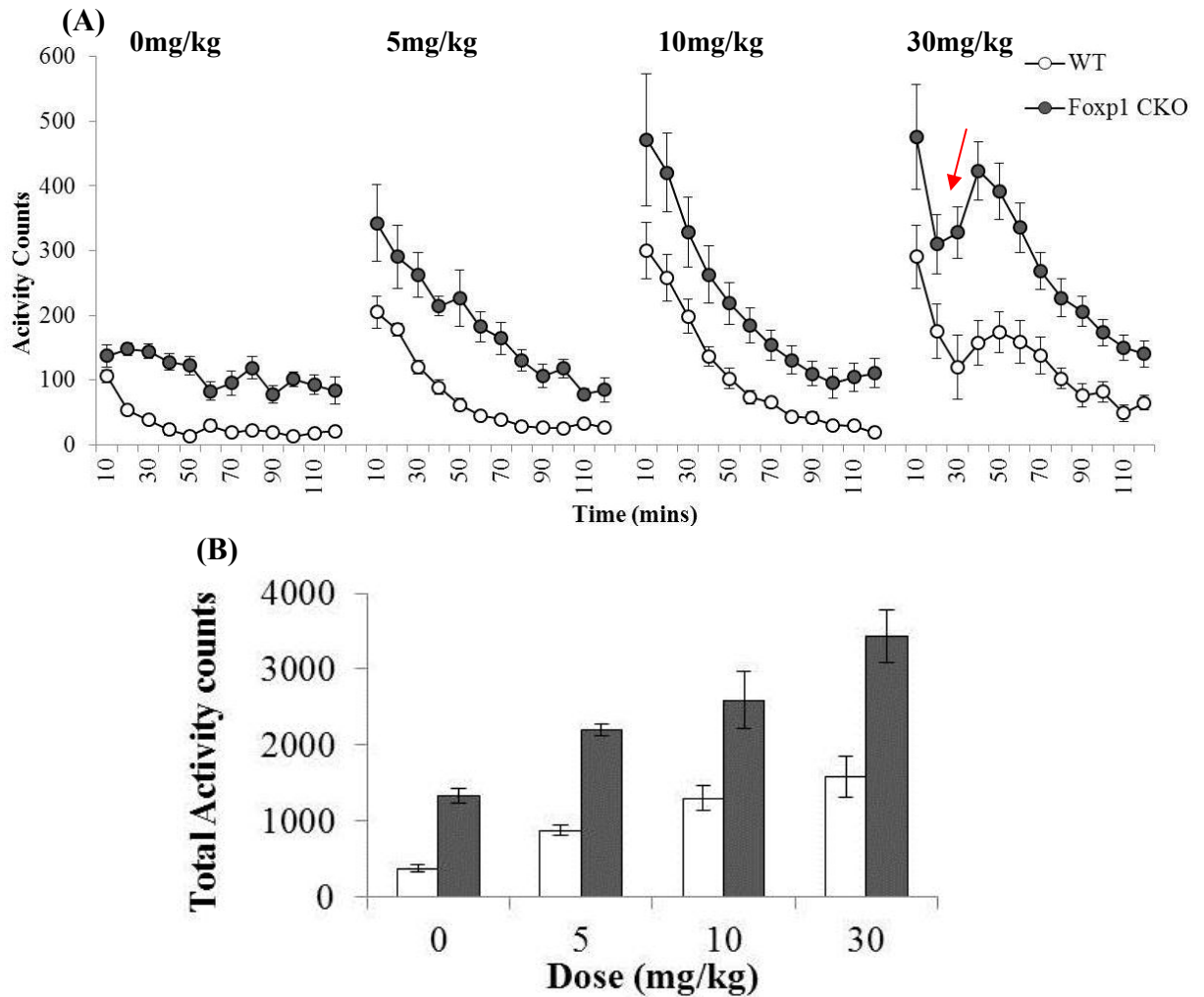
Figure 5.7 Ritalin increased locomotor activity-(A) Locomotor activity split into 10 minute bins over 2 hours. Activity increased in a dose dependant manner in both the WT and *Foxp1* CKO animals. At 30 mg/kg an overdose effect of the drug is seen and is shown with an arrow. **(B)** Bar chart displaying the total activity over the two hour period of testing. *Error bars are SEM.*
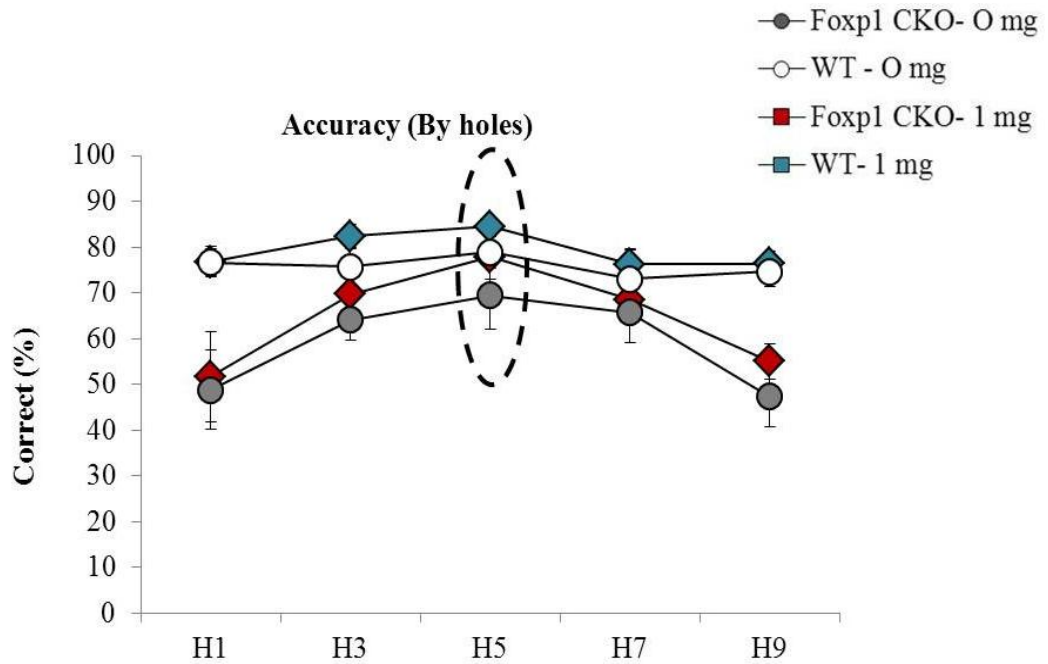
Figure 5.8 WT and *Foxp1* CKO mouse performance on the 5-CSRTT with Ritalin. Graph shows the percentage accuracy of WT and *Foxp1* CKO mice when tested on 5-CSRTT with a delay length of 0.5 seconds after being treated with Saline (Control) or Ritalin (5mg/kg). The dotted line indicates that the *Foxp1* CKO showed a trend to increase in accuracy on hole 5. *Error bars are SEM.*

Atomoxetine significantly reduced locomotor activity in the *Foxp1* CKO mice

As Ritalin did not show to ameliorate the hyperactivity or inattention of the animals another drug prescribed to ADHD patients, Atomoxetine was trialled on the mice. Atomoxetine is a selective NA reuptake inhibitor which has shown to aleivate ADHD like symptoms. As with the Ritalin, several doses of atomoxetine were tested on all animals based on published data over the test period (saline, 1, 2 and 4 mg/kg) (Bymaster *et al.* 2002). Overall there were significant main affects of genotype on activity ($F_{1, 26}$) =8.74 p<0.01) and drug dose on activity ($F_{3, 78}$) = 4.91, p<0.001). Although there was a trend for all doses to lower the activity of the *Foxp1* CKO, compared to saline treated controls there was no interaction between drug dose and genotype ($F_{3, 78}$ = 2.20, p= n.s.) (Figure 5.9A and B). A 1 mg/kg dose of atomoxetine reduced the total activity of the *Foxp1* CKO mice the most when compared to saline treated controls and subsequent analysis was carried out looking at the effect of this dose at 5 minute periods of activity. Figure 5.10A shows that after 15 minutes the activity levels of *Foxp1* CKO mice were reduced and that between 15 minutes and 55 minutes there was a significant interaction between genotype and drug dose ($F_{1, 26}$ = 4.30, p≤0.05) and simple effects showed there was a significant difference between the activity of the *Foxp1* CKO (p<0.01) compared to saline controls but there was no difference in WT activity (p= n.s.) when compared to saline treated controls (Figure 5.10).

(A)

(B)
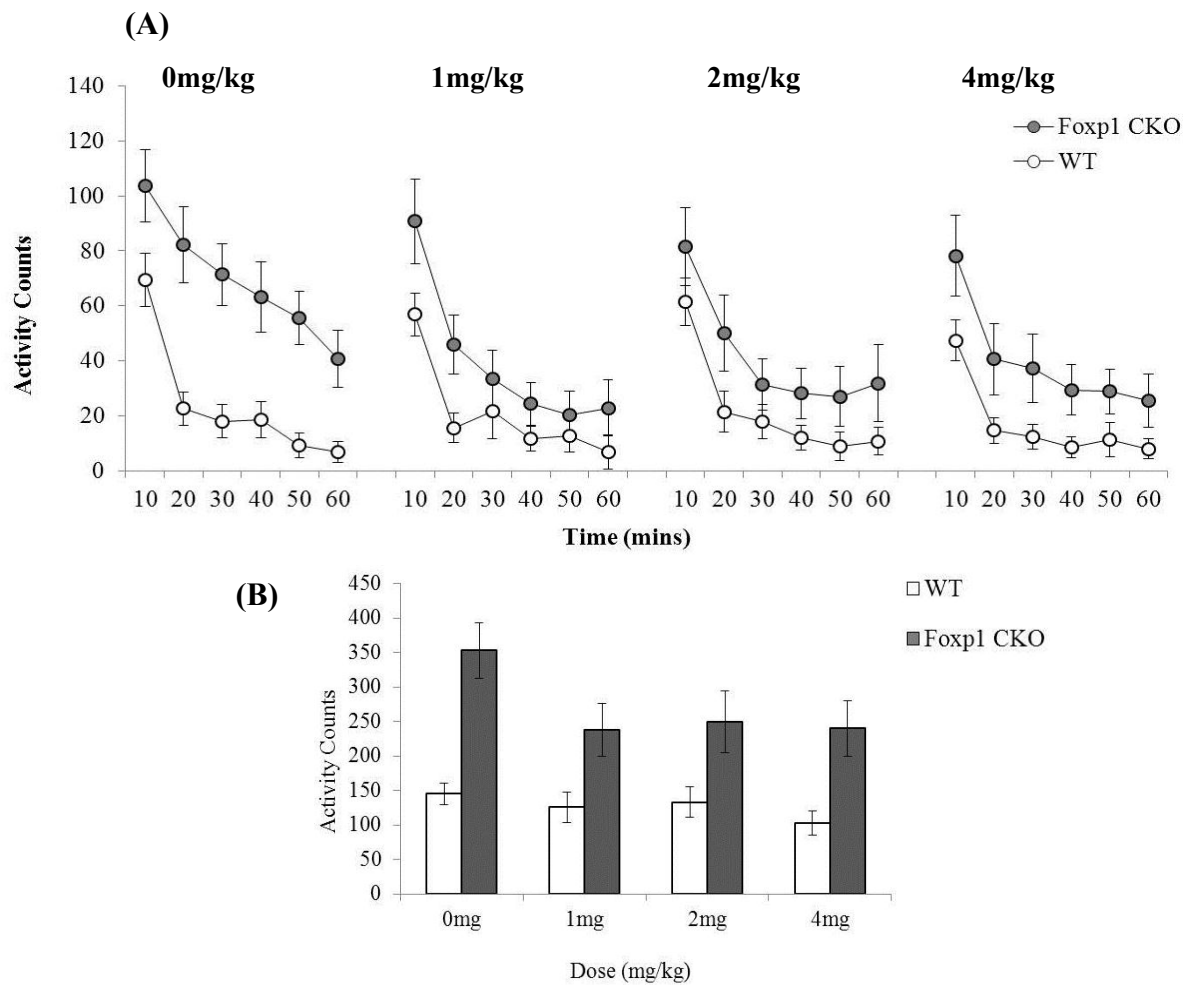
Figure 5.9 Effect of atomoxetine on locomoter activity in WT and *Foxp1* CKO mice (A) Locomotor activity was split into 10 minute bins over 1 hour. Activity in the *Foxp1* CKOs decreased at all doses. **(B)** Bar chart displaying the total activity over the testing period clearly showing the reduction in activity of the *Foxp1* CKO mice as a result of atomoxetine. *Error bars are SEM*.
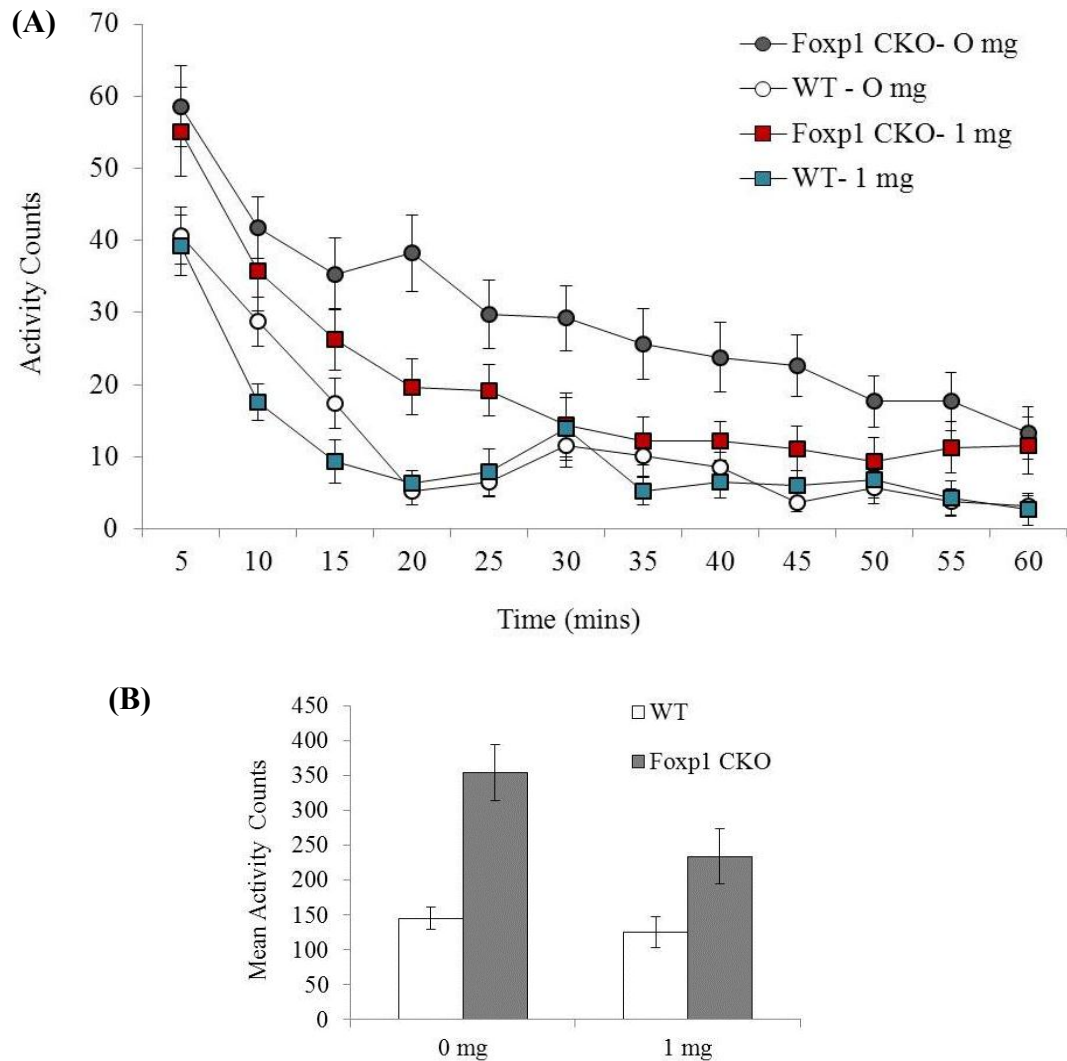
Figure 5.10 There was a significant effect of atomoxetine at 1 mg/kg on locomoter activity in the *Foxp1* CKO mice (A) Locomotor activity split into 5 minute bins over a 1 hour period. When atomoxitine at a dose of 1 mg/kg was administered, activity in the *Foxp1* CKO mice was reduced after 15 minutes compared to saline treated controls. There was no effect of atomoxetine on the activity of WT mice. **(B)** Bar chart displaying the total activity over the testing period clearly showing the reduction in activity the *Foxp1* CKO mice as a result of atomoxetine *Error bars show SEM.*

FOXP1 was absent from the cortex but not striatum.

Following behavioural testing a selection of animals from each genotype were sacrificed at approximately 3 months of age. Nissl staining using CV showed that there were no obvious morphological differences in the striatum between the groups (Figure 5.11). However on inspection of the cortex, cortical layers V and V1 of the *Foxp1* CKO mice appeared thinner than the corresponding layers of control mice, highlighted with arrows in Figure 5.11. Immunohistochemistry using an anti-FOXP1 antibody showed that FOXP1 was retained in the WT striatum and cortex (Figure 5.12A and B), but was completely absent from the cortex of *Foxp1* CKO mice (Figure 5.12C) and unexpectedly retained in the striatum of the *Foxp1 CKO* mice Figure 5.12D. An anti-NEUN antibody, which stains all neurons, showed that there were no gross histological differences in the striatum or cortex of WT and *Foxp1* CKO mice (Figure 5.12E-H). FOXP1 and NEUN positive cells were separately quantified using stereology and results are displayed and presented as mm^3 in Figure 5.13. There was a significant difference between the number of FOXP1 immunopositive cells in the cortex of the *Foxp1* CKO mice compared to WT mice ($F_{1, 16} = 43.501$, p= <0.00) but there was no difference in the number of *Foxp1* positive cells in the striatum ($F_{1, 16} = 1.325$, p= n.s.). There were no significant differences between the number of NEUN positive cells between genotypes in either the striatum ($F_{1, 15} = 2.07$, p =n.s.) or the cortex ($F_{1, 15} = 0.31$, p= n.s.).
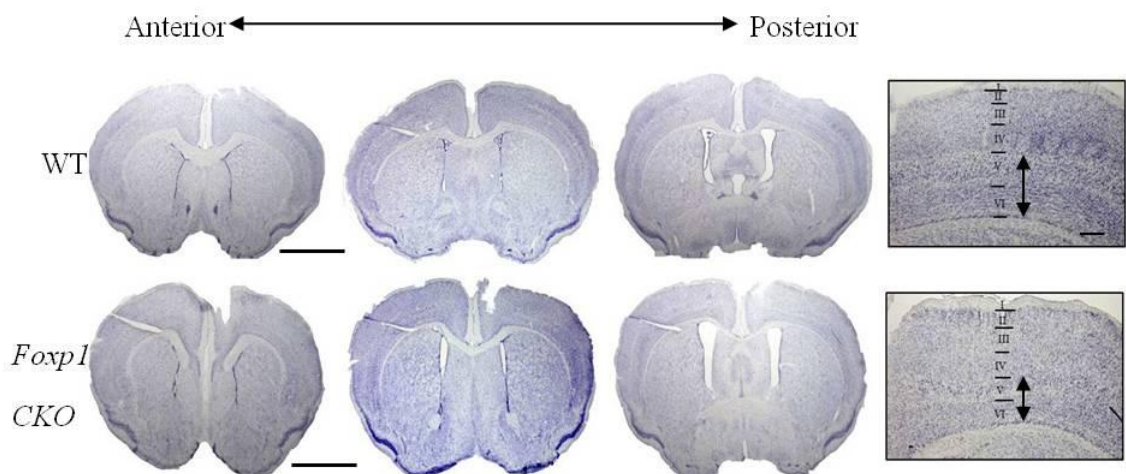
Figure 5.11 Representative examples of CV staining showing WT and *Foxp1* CKO mouse brains. There are no obvious differences in the striatum between the genotypes. Cortical layers V and VI appear thinner in the *Foxp1* CKO mice compared to in WT mice. *Scale bar = 500µm.*
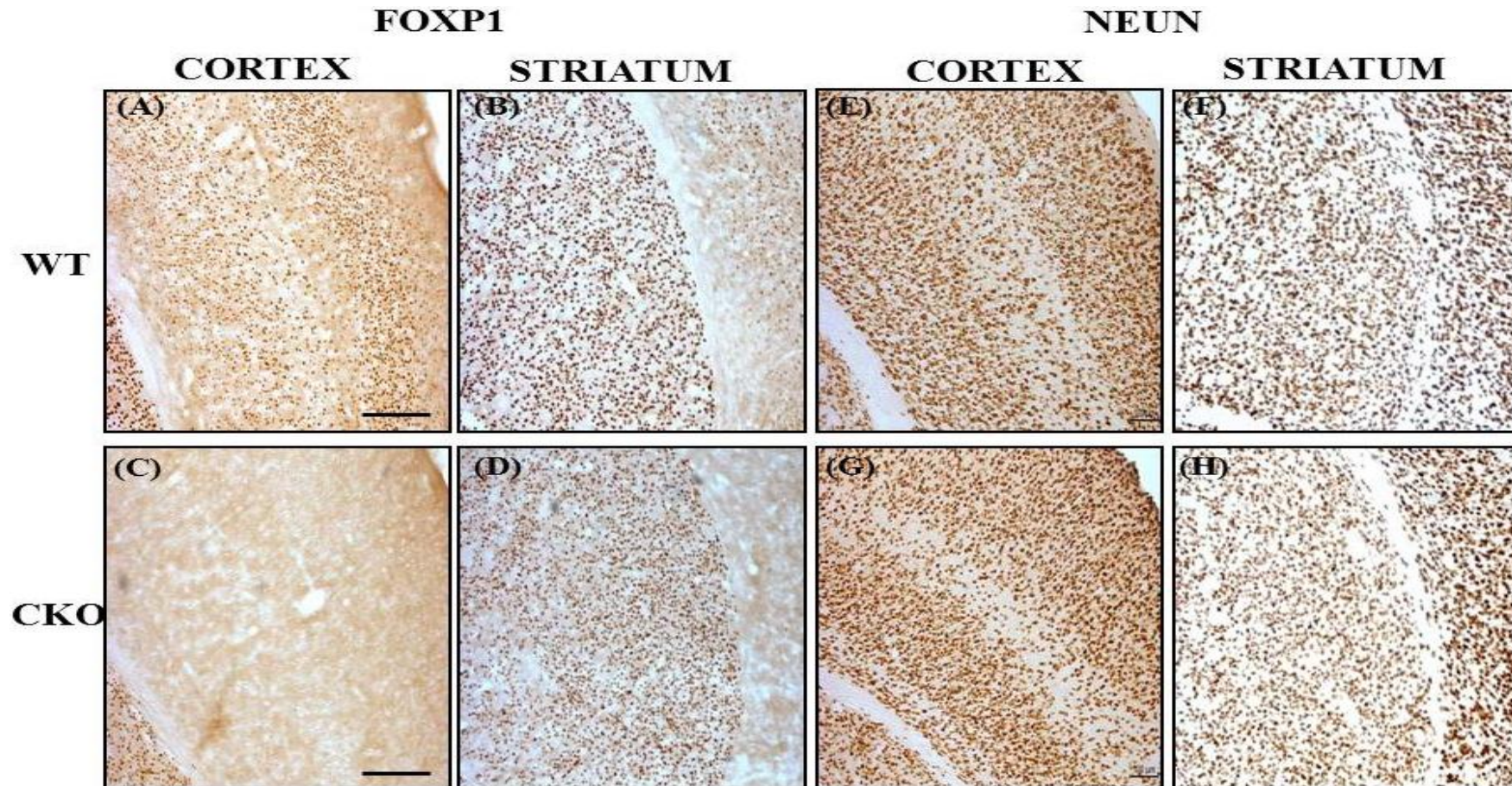
Figure 5.12 Representative photomicrographs showing immunohistochemistry of FOXP1 and NEUN staining in the WT and *Foxp1* CKO brain. (A and B) FOXP1 positive staining is apparent in the cortex and striatum of the WT mice. **(C)** There is no FOXP1 positive staining in the cortex of the *Foxp1* CKO mice. **(D)** FOXP1 positive staining in the striatum of the *Foxp1* CKO mice. **(E-H)** NEUN positive staining is seen throughout the cortex and striatum of WT and *Foxp1* CKO mice. *Scale bars= 200μm.*
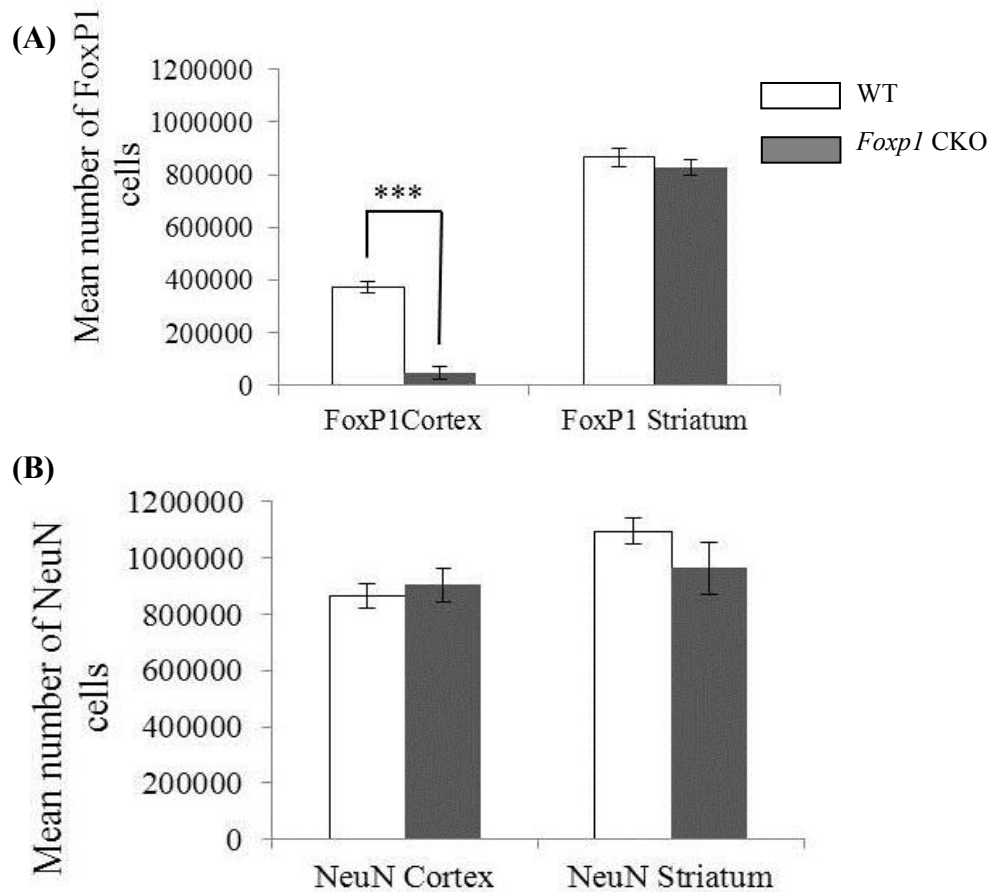
Figure 5.13 FOXP1 and NEUN cell counts per mm³.(A) Bars represent the mean total cell counts of FOXP1 positive staining in the cortex and striatum of WT and *Foxp1* CKO mice. **(B)** Bars represent the mean total cell counts of NEUN positive staining in the cortex and striatum of WT and *Foxp1* CKO mice. *Error bars are SEM. (∗∗∗ = P<0.001).*

Differences in cortical layer morphology

In an attempt to distinguish which specific cortical cells were affected by the loss of *Foxp1,* antibodies specific to the different cortical layers were tested and were assessed qualitatively. FOXP2 preferentially stains layer VI of the cortex, with some staining seen in layer V of the motor cortex, the region where FOXP1 and FOXP2 show the most overlap in staining. DARPP-32 was also used as a layer V1 marker and preferentially stains pyramidal neurons. CTIP2 preferentially stains layer V of the cortex but is also seen in layer V1. There was no difference in FOXP2 staining between genotypes as shown in Figure 5.14. Ectopic CTIP2 staining was evident in layers 3 and 4 of the cortex in the *Foxp1* CKO (Figure 5.15A and B). As anticipated from Chapter 3 there was little or no DARPP-32 staining evident in layer V1 of the cortex in the *Foxp1* CKOs when compared to WTs shown in Figure 5.15C and D.
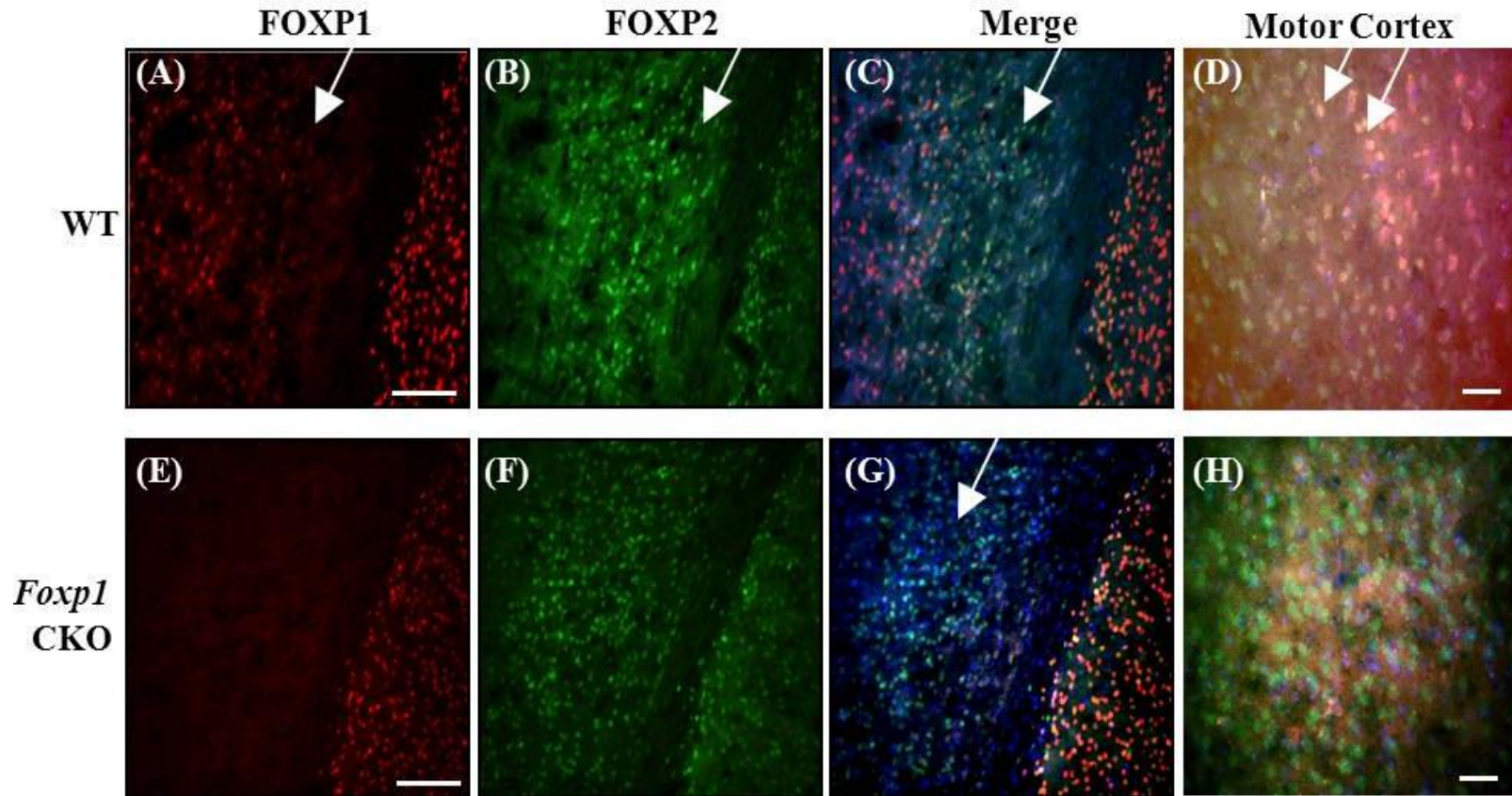
Figure 5.14 Immunohistochemistry of FOXP2 and FOXP1 in layer V1 of the cortex in WT and *Foxp1* CKO mice. Adult brain sections double labelled with FOXP1 (Red), FOXP2 (Green) and the nucelar stain Hoechst (Blue). The third column is a merged image of the first two photomicrographs. **(A)** FOXP1 staining staining is seen layers V1a and V of the cortex from WT mice **(B)** FOXP2 staining is shown in layer V1 of the cortex in WT mice **(C)** Merged image **(D)** FOXP1 and FOXP2 co-loclaise in the the motor cortex in WT mice**,** an example of co-loclisation is indicated with an arrow **(E)** FOXP1 staining is absent from the cortex in *Foxp1* CKO mice. **(F)** FOXP2 staining is shown in layer V1 of the cortex in *Foxp1* CKO mice **(G)** Merged image **(H)** FOXP2 positive staining is evident in in the motor cortex of *Foxp1* CKO mice, there is no *FOXP1* staining. *Scale bars = Low mag=200μm ,high mag= 50μm.*
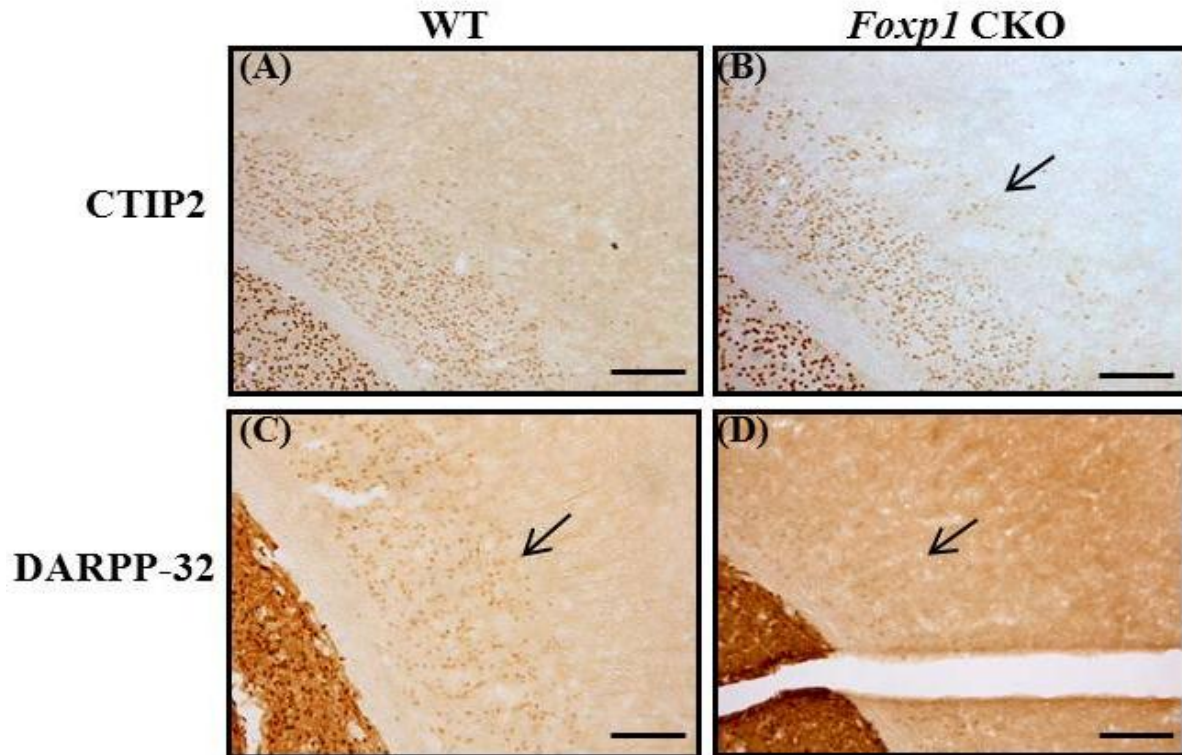
Figure 5.15 Immunohsitochemsitry for layers 5 and 6 of the cortex in WT and *Foxp1* CKO mice (A) CTIP2 postive staining is shown in layer V and V1 of the cortex in WT mice **(B)** CTIP2 staining can be seen in layers V and V1 of the cortex in *Foxp1* CKO but there is also ectopic CTIP2 staining in other cortical layers, labelled with an arrow. **(C)** DARPP-32 staining is shown in layer V1 of the cortex. **(D)** There is very litle DARPP-32 staining in cortex of the *Foxp1 CKO* animals. *Scale bar= 100µm*

5.4 **Discussion**

Choice of Cre line to conditionally KO *Foxp1* in the developing striatum

There are a number of TG Cre-lines that can KO genes selectively in the adult striatum, examples include the *Drd1a*-Cre, the *Drd2*-Cre, the Adensosine A2a receptor (*Adora2a*)-Cre (Gong *et al.* 2007) and the TG (*Camk2a*-cre)2Szi which has been used to conditionally KO DARPP-32 (Dragatsis and Zeitlin 2000). However, these Cre lines are expressed too late to achieve KO of *Foxp1* coincident with MSN neurogenesis. Therefore achieving a specific and conditional striatal KO initiating early in striatal development is difficult, as often the promoter driving the Cre is not exclusively expressed in the striatum (not problematic if GOI is striatal specific) or is expressed in the cells at the wrong time e.g too late. As discussed in detail in Chapter 1.7, the expression pattern of the *Foxg1*-Cre line would have been an ideal option for a striatal-specific deletions, however the inconsistencies reported with this line, such as a global expression pattern, made it unfavourable for this work. A recent striatal-specific line t is the *Gsh2*-Cre line (Kessaris *et al.* 2006). *Gsh2* is expressed from E9 in the LGE with limited expression in the MGE (Corbin *et al.* 2000; Toresson *et al.* 2000). Since being developed, the *Gsh2*-Cre line has been used, for example, to look at the heterogeneity of cells in the olfactory bulb (Young *et al.* 2007) and recently to look at the migration patterns of GABAergic neurons (Wu *et al.* 2011). However as this line is not yet commercially available it was difficult to source in the time restraints of this thesis.

The importance of selecting the correct promoter to drive specific recombination was well considered for these experiments and two well established Cre lines were initially chosen for this work; a *Nestin*-Cre (Li *et al.* 2008) and a *hGFAP* cre (Barbosa *et al.* 2008). It was anticipated that the *Nestin*-Cre line developed by Tronche et al (1999) would conditionally KO *Foxp1* in the striatum from E11. Specifically, this Cre-line has shown to cause recombination in proliferating neural stem cells (Tronche *et al.* 1999). However, for the present work, after several attempts of breeding (totalling over a year), there were no pups born that had the desired genotype (pups with the other genotypes were all born healthy), suggesting incompatibility between the *Nestin*-Cre and *Foxp1* floxed mouse (data not shown). As with the *Foxg1*-Cre the *Nestin*-Cre line expression pattern is inconsistent and has shown some expression in tissues other than the brain including the heart and kidney (Tronche *et al.* 1999). As *Foxp1* is also crucial in heart

development, it may be that recombination is also occurring in the heart and thus causing embryonic lethality that is associated with the *Foxp1*^{-/-} mice. Additionally it has recently been shown that the *Nestin*-Cre line, which of note, is the only commercial *Nestin*-line available, was poor in directing recombination in embryonic neural stem and progenitor cells at E12.5 and that expression was largely confined to post-mitotic neurons (Liang *et al.* 2012). In our hands, the *Nestin*-Cre was not able to conditionally KO *Foxp1* in the desired region and ultimately ended in embryonic lethality of the pups. In parallel to the *Nestin* breeding regime, *Foxp1* floxed mice were also crossed to *hGFAP*-Cre mice. Initially breeding of hGFAP/*Foxp1*^{+/-} mice was attempted to *Foxp1*^{fl/fl} mice to ensure a more thorough genetic KO, but as with the Nestin-Cre line no pups of the correct genotype were born using this method. Thus it was decided to cross hGFAP/Foxp1^{fl/+} to mice of the same genotype. This later breeding strategy was successful and all expected genotypes from the cross were born and thus this line was pursued.

Although there were no differences in the weights between the pups there were clear behavioural differences between genotypes when the mice were handled. The *Foxp1* CKO mice were noticeably hyperactive in their home cages, and very difficult to catch, compared to littermate controls. Often the animals cages needed to be placed in a deep sink to retrieve them from their cages to prevent them escaping. However histological analysis showed that FOXP1 staining was unexpectedly retained in the striatum but completely lost in all layers of the cortex in which it is expressed (III-VIa).

It is now clear that the loss of expression from only the cortex is a direct result of the pattern and timing of Cre-recombination. As stated previously, the *hGFAP*-Cre line is expressed in all RG and it is now apparent that striatal precursors do go through a RG stage in their development but before the *hGFAP*-Cre is expressed (i.e. before E14). Secondly by E15.5 when appreciable recombination of the *hGFAP*-Cre is shown (Anthony and Heintz 2008), RG in the developing striatum are largely gliogenic as shown by the astrocyte marker S100β being evident, whereas in the cortex neurogenesis from RG has only just begun (Anthony and Heintz 2008; Anthony *et al.* 2004) and gliogensis doesn't start in this region until P0 (Anthony *et al.* 2004). Although unexpected, specific cortical loss in the *Foxp1* CKO mice is interesting and unique and represents a way in which we can segregate the cortical and striatal function of FOXP1.

170

FOXP1 is lost from the cortex and not the striatum

Foxp1 is expressed in the developing cortex from E14.5, where expression is initially seen in layers III-V. After P6 more FOXP1 expressing cells are seen in layer V1a (Ferland *et al.* 2003). Results from histological analysis showed that there was a significant loss of FOXP1 from all layers (87% loss) of the cortex. The remaining FOXP1 positive staining (12%) could be from a population of neurons developing prior to Cre expression, or secondly, from differential Cre expression as a result of copy number differences or strain variation (Bai *et al.* 2013; Xu *et al.* 2012). It has recently been reported that mice which carry the *hGFAP*-cre on a C57B6/J background displayed weaker transgene expression than those on a FVB background (Bai *et al.* 2013). The *hGFAP*-Cre animals used in these experiments were maintained on an FVB background until the point of crossing to the *Foxp1* floxed animals which were on a C57B6/J background (Feng *et al.* 2010), thereby F1 offspring, and ultimately the breeders, would produce an F2 generation with a mixed background. However, for all experiments completed to date the loss of FOXP1 was consistent across all animals suggesting Cre activity to be reliable and consistent.

There was a small reduction of FOXP1 in the *Foxp1* CKO mouse striatum (4.5%) compared to WTs but this is unlikely to produce any phenotypic difference as supported by the *Foxp1*$^{+/-}$ mice. Additionally, any phenotype that would have been seen would be masked by the phenotype attributable to the significant cortical loss of FOXP1. Interestingly it has been reported that 4% of the total DARPP-32 positive cells found in the mature striatum derive from an *Emx1* positive lineage (Cocas *et al.* 2009). Of this lineage the majority of cells arise from *Emx1* positive cells that have migrated ventrally from the pallium (developing cortex) between E13.5 and E15.5, with a very small proportion arising later in development (after E13.5) from *Emx1* positive cells located in the LGE (Cocas *et al.* 2009). Therefore it is possible that the minimal striatal FOXP1 loss outlined in this chapter is due to the conditional loss of *Emx1* positive MSNs migrating from the developing cortex, where the hGFAP-Cre has shown to successfully recombine.

Although no significant differences in NEUN staining were found between the groups, this does not necessarily indicate that there was no neuronal loss caused by the absence of *Foxp1*. As *Foxp1* was lost from early in development it is possible that if *Foxp1*

positive neurons were not born at all, the developing cortical neurons and/or interneurons could have condensed to fill the space, thus the reason why there were no differences in NEUN counts between the groups. Therefore looking at differences in the cortex during development in the *Foxp1* CKO mice may be more informative and identify if and when compaction occurred due to the loss of *Foxp1*.

Loss of FOXP1 in the cortex has an effect on layers V and VI of the cortex

Nissl staining using CV suggested apparent cortical thinning in the *Foxp1* CKO mice compared to in WT mice, specifically layers V and V1. To look more specifically at the differences in layers V and V1 additional histological analyses were performed using specific markers for these layers, and these were analysed qualitatively. *Foxp2*, unlike *Foxp1*, preferentially stains layer VI of the mouse cortex and co-localisation of these family members is not seen in this region until P14 (Hisaoka *et al.* 2010). However before P14, *Foxp1* and *Foxp2* do show partial co-localisation in the motor cortex from P0 (Hisaoka *et al.* 2010). Double fluorescent immunohistochemistry showed that there was no difference in FOXP2 staining in the absence of *Foxp1* throughout layer V1 of the cortex. As FOXP2 and FOXP1 co-localisation is also evident in layer V of the motor cortex this region was also closely examined, and similarly no marked differences were found between genotypes. Therefore, even though these two TFs are known to function together (Shu *et al.* 2007), the loss of *Foxp1* has not caused aberrant expression of FOXP2.

Ctip2, as mentioned is a TF that like *Foxp1* is expressed in the cortex and striatum. Unlike in the striatum, *Foxp1* and *Ctip2* rarely co-localise in the cortex and label different populations of neurons in layer V. CTIP2 positive neurons project to the spinal cord (Arlotta *et al.* 2005) whereas it is thought FOXP1 is a marker of cortical callosal projection neurons (Hisaoka *et al.* 2010). Results from Chapter 3 which showed a decrease in CTIP2 in striatum would suggest there would be alterations in CTIP2expression in the cortex. Interestingly, CTIP2 was still present in layer V of the cortex in the *Foxp1* CKO mice but there were also ectopic CTIP2 positive cells evident in other layers of the cortex, notably layer 4, and Nissl staining showed that layer V was thinner in the cortex of *Foxp1* CKO compared to WT mice. Therefore *Foxp1* may be needed to ensure the correct organisation of layer V neurons.

In addition to labelling MSNs, DARPP-32 is known to stain dopamine-receptive, pyramidal neurons in layer VI of the cortex (Ouimet *et al.* 1984; Rajput *et al.* 2009; Wang *et al.* 2004b) and specifically in the motor cortex, it has been shown that approximately 56% of DARPP-32 positive neurons co-localise with FOXP1 staining (Hisaoka *et al.* 2010). Once again, as with CTIP2, results from Chapter 3 would suggest there would be less DARPP-32 in the cortex in the absence of Foxp1as was the case in the developing striatum. Results presented here showed that in the cortex of *Foxp1* CKO mice there was a noticeable loss of DARPP-32 in layer V1. As there was no obvious loss of FOXP2, another layer V1 marker, in the *Foxp1* CKO mice further experiments need to be carried out to determine what importance the loss of a subset of layer V1 neurons has on the phenotype observed in this model. It is anticipated that the results from on an on-going microarray experiment may serve to distinguish specific gene expression changes in the cortex of WT and *Foxp1* CKO mice that could assist in explaining the phenotype associated with this novel *Foxp1* CKO model.

Foxp1 CKO mice are hyperactive

Simple behavioural tasks highlighted that the *Foxp1* CKO mice were hyperactive compared to littermate controls. On average, WT mice stayed on the rotarod marginally longer than *Foxp1* CKO mice and the large standard error seen in the *Foxp1* CKO mice rotorod results is largely due to training difficulties associated with the phenotype. When the *Foxp1* CKO mice fell off during training, catching them was often difficult, hence the animal would need to be put back in its home cage rather than back on the rotarod due to the extent of hyperactivity, thus reducing the opportunity for these animals to train. The balance beam was also attempted but training also proved difficult and thus animals never progressed to the testing stage. In the cage grip strength test CKO mice held on for significantly less time than WT mice. Given our characterised phenotype, these results were unlikely due to a weakness in strength and are likely due to increased impulsivity of the mice. Therefore all basic behavioural data are confounded by the hyperactivity seen in these mice.

Foxp1 CKO mice were found to be have elevated total levels of horizontal ambulatory activity within the dark phase of testing (18:00-06:00) compared to WT mice. This task also highlighted that the animals have normal circadian rhythms, as there was no significant difference between the animals' total activity in the light cycle (06:00-

18:00). In addition, the results from the EthoVision programme showed that *Foxp1* CKO mice moved a greater distance in the testing arena and at a faster pace than WT mice, further emphasising the hyperactive phenotype of the *Foxp1* CKO mice.

Foxp1 CKO mice do not display an anxiety phenotype

Following motor behavioural characterisation, we also investigated whether CKO mice have higher functioning cognitive deficits. It is known that rodents will bury unconditioned objects such as food pellets and glass marbles and this is the rationale behind the MBT (Archer *et al.* 1987; Broekkamp *et al.* 1986). Early studies suggested that the MBT measures anxiety as the number of marbles buried by mice was reduced when anxiolytics were administered (Broekkamp *et al.* 1986; Nicolas *et al.* 2006; Njung'e and Handley 1991). However, it is debated if this "burying" action is a defensive mechanism to a novel object, or an innate pre-determined response (Thomas *et al.* 2009). In addition to anxiolytics, burying behaviour has shown to be reduced by antipsychotics suggesting that marble burying alone has limited predictive validity for anxiety (Broekkamp *et al.* 1986). Likewise, repeated exposure to marbles did not reduce the amount of marbles buried suggesting that the "novelty" factor was not the rationale behind burying the marbles (Broekkamp *et al.* 1986; Nicolas *et al.* 2006; Njung'e and Handley 1991; Thomas *et al.* 2009). Instead it has been suggested that the reasoning for burying the marbles is an innate, "digging" response, and that the MBT is a better indicator of obsessive/compulsive disorders (Gyertyan 1995; Li *et al.* 2008). Results in this Chapter show a trend for *Foxp1* CKO mice to bury fewer marbles than WT mice which could suggest the mice do not have an OCD phenotype (Gyertyan 1995), however this test would need to be repeated. Alternatively the mice may not be typically anxious, which is corroborated by both results seen in the open field activity traces and EPM.

The EPM is an "ethological" model of anxiety involving spontaneous exploration by rodents of an unconditioned environment with "natural" stimuli such as height, and is ultimately based on an animal's innate aversion to open spaces (Montgomery 1955; Pellow *et al.* 1985; Rodgers and Johnson 1995). The EPM predicts how an animal responds to an approach-avoidance situation involving "open" "potentially dangerous" arms versus enclosed "safe" arms (Lister 1987; Pellow *et al.* 1985; Rodgers and

Johnson 1995). Typically, anxiety-like behaviour is assessed by the percentage of entries, and time spent on the open arms, (Dawson and Tricklebank 1995; Rodgers and Johnson 1995), which has been shown to increase when anxiolytic drugs such as Diazepam were given to animals. As motor impairments are known to influence results the total number of closed arm entries is considered a measure of locomotor activity (Cruz *et al.* 1994). Normal mice classically spend less than 25% of their time exploring the open arms (Dawson and Tricklebank 1995). In agreement, the results outlined in this work showed that WT mice spent 18% of their time on the open arms whilst the *Foxp1* CKO animals spent 47% of their time on open arms. In addition the *Foxp1* CKO mice completed more open arm entries than littermates, suggesting an insensitivity to unconditioned fear and a lowered state of anxiety (Pellow *et al.* 1985). It has also been shown that a decrease in activity in the centre of the open field arena, coupled with a decrease in rearing indicates less anxiety (Li *et al.* 2008). The *Foxp1* CKO mice actively explored the centre of the arena and showed increased rearing in comparison to WT mice (CKOs 121.8±15.4, WT 76.8±9.7), supporting the results obtained in the MBT, and EPM that the *Foxp1* CKO mice are not over anxious.

Of interest is that in some instances the EPM has been used to look at differences in impulsivity. It has been hypothesised that increased entry into the open arms, as seen by the juvenile stroke prone spontaneously hyperactivity rat model (SHR) could be a direct result of intense impulsivity by the animals (Ueno *et al.* 2003). Patients who suffer with overanxious disorder (ANX) have shown comorbidity with ADHD and it has been demonstrated that ADHD patients also diagnosed with ANX are less impulsive than patients without ANX on tests such as the memory scanning test (Pliszka 1989). Therefore the 'reduced anxiety' shown by the *Foxp1* CKO mice could reflect increased impulsivity.

Foxp1 CKO mice are inattentive

The 5-CSRTT originated from the continuous performance task (CPT) task in humans (Robbins 2002) in which deficits have been shown to correlate highly with ADHD (Epstein *et al.* 2003). To test for any differences in visuo-spatial attentional deficits we used the 5-CSRTT in 9-hole operant chambers of which the key outcome measures are response accuracy to the randomly presented light stimuli and response times. The *Foxp1* CKO mice demonstrated a stimulus light-dependent decline in performance

accuracy relative to their WT littermates without a decline in response latencies indicating that the performance deficits were due to increased attentional load. Impulsivity can be measured in the 5-CSRTT by analysing the number of anticipatory hole pokes during the ITI period, however in this instance the ITI was only 2 seconds, and to properly measure impulsivity it has been suggested that the ITI has to be minimum of 5 seconds (Robbins 2002). Therefore future experiments will have this ITI parameter incorporated. The number of omissions, which is a measure of missed responses within the stimulus period, was increased in the *Foxp1* CKO mice compared to WT mice suggesting the *Foxp1* CKO mice are not pressing prematurely, or incorrectly, but are uninterested in poking at all. Overall an increase in errors of omission, coupled with the reduction in accuracy and increased reaction time, as a direct consequence of decreasing the stimulus length of the probes, indicates that the mice have a deficit in sustaining attention across the array (Robbins 2002; Trueman *et al.* 2012a).

A novel mouse model of Attention Deficit Hyperactivity Disorder (ADHD)

The results discussed thus far show that *Foxp1* CKO mice are hyperactive, inattentive and show some signs of impulsivity. ADHD is a clinically heterogeneous disorder observed globally and the DSM-IV criteria for diagnosis states that the core features of the disorder can include inattention, hyperactivity and/or impulsivity (Biederman 2005; Nair *et al.* 2006). Due to the heterogeneous nature of ADHD it has been suggested that its aetiology may result from a number of different gene mutations as well as environmental factors (reviewed in (Thapar *et al.* 2013)). ADHD related gene mutations have been identified in genome wide association studies (GWAS) and these mostly relate to catecholamine function including the dopamine transporter (DAT), dopamine receptors 4 (D_4) and 5 (D_5) (Faraone *et al.* 2005; Li *et al.* 2008) and noradrenalin transporter (NET) (Hahn *et al.* 2009), but to date short nucleotide polymorphisms (SNP) in FOXP1 have not been associated. However, the clear overlap of symptoms in ASDs (in which *FOXP1* has been linked) and ADHD has very recently been appreciated, and as of May 2013, the new DSM scale (DMS-V) allows for patients to be diagnosed as having both disorders simultaneously. Therefore results throughout this Chapter support the notion that cortical loss of *Foxp1* appears to match the face validity criteria needed for a novel animal model of ADHD, and considering the association of ASDs and

ADHD it is not unreasonable to hypothesise the role of *Foxp1* in the aetiology of ADHD.

At the physiological level, ADHD is thought to be caused by the dysregulation of the catecholaminergic system leading to imbalances in the DA and Noradrenaline (NA) neurotransmitter systems particularly in the prefrontal cortical regions (Arnsten 2009). ADHD treatment has been dominated by the use of monoaminergic pyschostimulants such as Ritalin and amphetamine and, of late, the catecholaminergic non-stimulant drug atomoxetine. Atomoxetine does not increase dopamine in the nucleus accumbens, the region associated with rewarding behaviours, and is therefore not associated with the drug abuse danger found with pyschostimulants, making it a favourable choice for ADHD sufferers (Bymaster *et al.* 2002). In all instances the dose of the drug prescribed is the key to ensuring that the abnormal behaviours are selectively targeted. It must be highlighted that such treatments can be therapeutic while not targeting the biological origins of the disorders, as in the case of ADHD, of which the aetiology it is not fully known.

The principal mode of action of the drugs prescribed to ADHD patients is to increase the availability of monoamines in the synapse by reducing uptake rates (i.e. block the transporters). Specifically, Ritalin, works as both a DA and NA reuptake inhibitor with the aim of increasing the extracellular concentration of DA and NA, although the precise mechanism by which Ritalin exerts its therapeutic affects is not known (reviewed in (Tripp and Wickens 2009)). A detailed molecular basis underlying the therapeutic effects of atomoxetine is still largely unknown. In rats it has been shown that i.p administration of atomoxetine increases extracellular NA and DA in the prefrontal cortex, occipital cortex, lateral hypothalamus, dorsal hippocampus, and cerebellum (Bymaster *et al.* 2002; Koda *et al.* 2010; Swanson *et al.* 2006). It has been suggested that atomoxetine selectively binds to the pre-synaptic noradrenalin transporter (NAT) (Swanson *et al.* 2006) and consequently increases the extracellular concentration of NA and DA (NAT non-selectively transports DA uptake in the cortex) in the prefrontal cortex enabling noradrenergic modulation of the limbic cortico-striatal circuitry (Chamberlain and Sahakian 2007). Recent microarray analysis has also been undertaken in WT rats to understand what affect genetic changes are brought about in response to atomoxetine (Lempp *et al.* 2013).

When WT and *Foxp1* CKO mice were administered with Ritalin, both groups showed increased activity in a dose dependent manor. These results are consistent with those observed by Koda et al (2010), which showed that higher doses of Ritalin (10 mg/kg) induced hyper-locomotion in the animals (Koda *et al.* 2010). I believe the fact that Ritalin did not ameliorate hyperactivity in *Foxp1* CKO mice is not a reason to invalidate its potential as a new ADHD mouse model. It is known that there are many subtypes of ADHD, which respond differently to stimulant drugs (Solanto 1998), and both responders and non-responders to Ritalin have been documented clinically (Heal *et al.* 2009). However, as Ritalin did not show any effect on reducing activity in the *Foxp1* CKO mice results could also suggest that loss of *Foxp1* has no effect on the dopaminergic system.

Interestingly, when animals were tested on the 5-CSRTT with Ritalin (5 mg/kg) there was a marked, although not a significant, improvement, in accuracy in both WT and *Foxp1* CKO mice, compared to saline treated controls. In particular *Foxp1* CKO mice displayed equivalent levels of percentage accuracy on hole 5 (central hole) as saline treated WT mice (WT=79%, CKO = 78%). Across all holes, when Ritlain was administered, the *Foxp1* CKO mice showed a 9% increase in total accuracy whereas the WT mice only improved by 4%. In line with this, it is known that lower doses of Ritalin (0.25-1mg/kg i.p.) improve cognitive function with no effect on heightened activity in open field analysis (Berridge *et al.* 2006). These experiments will need to be repeated with a bigger cohort of animals to further ascertain if Ritalin will significantly improve percentage accuracy in the 5-CSRTT. Furthermore testing animals with 1 mg/kg of Ritalin, rather than 5 mg/kg, on the 5-CSRTT may provide a more significant improvement on percentage accuracy, and is something to consider for future testing.

Atomoxetine was also administered to the animals, and unlike Ritalin, caused a significant decrease in locomotor activity in the *Foxp1* CKO mice 15 minutes following administration of the drug, with no effects on the locomotor activity of WT mice, in agreement with Koda et al (2010). As testing was initiated simultaneously with the mouse receiving an injection of atomoxetine it is likely that within the first 10 minutes of activity the drug had not become fully active and for subsequent experiments a 15 minute habituation period will be initiated before testing. In rats it has been shown that

after 1 hour the atomoxetine solution within the plasma has plateaued (Lempp *et al.* 2013). This plateau would likely be evident earlier in mice due to their increased metabolism and could possibly explain why the effect of atomoxetine on locomotor activity was lessened by 55 minutes following the injections.

Nevertheless, the decrease in activity seen in the *Foxp1* CKO mice complement those in a recent report that showed acute administration of atomoxetine (1, 3 mg/kg) reduced activity in the, SHR rat model, a known model of ADHD (Umehara *et al.* 2013). The fact that atomoxetine, and not Ritalin had an impact on reducing locomotor activity suggests that the absence of *Foxp1* maybe having at least some of its locomotor effects via the Noradrenergic system rather than the DA system. On-going experiments are in place to determine through which NA receptor atomoxetine is having its effect. While this work does not show what affect atomoxetine has on the 5-CSRTT, it is a planned experiment for the near future. From recent literature, one would expect atomoxetine to improve both the accuracy and reduce the number of premature nose pokes on the 5-CSRTT (Navarra *et al.* 2008).

Although a striatal specific *Foxp1* KO was not created on this occasion, it is still planned for future experiments. Apart from the *Foxg1*-Cre, in which its caveats have already been addressed, there are no commercially available embryonic striatal Cre lines. However, plans are underway to use the above mentioned *Gsh2*-Cre line from the Kassaris' lab to create a striatal KO phenotype which can be used in comparison to our established cortical KO model.

5.5 **Conclusion**

The aim of this Chapter was to create a striatal specific *Foxp1* conditional KO mouse. However, the timing of the Cre-specific recombination caused the loss of FOXP1 in all layers of the cortex, sparing the striatum. Behavioural analysis showed that homozygous *Foxp1* CKO mice were significantly hyperactive and inattentive when compared to littermate controls in a series of behavioural tests, notably open field activity and the 5-CSRTT. The MBT and EMP showed that *Foxp1* CKO mice were not overtly anxious and also hinted that these mice had increased impulsivity. Hyperactivity was

ameliorated on administration of atomoxetine, a drug commonly used in the treatment of ADHD.

For a model to be valid representation of a disease it must recapitulate cardinal symptoms of a disorder (face validity) and respond to the affect of biochemical therapeutics (i.e. the same drugs that are used to treat patients can be studied (predictive validity)). Construct validity is also a desired criterion however this is a difficulty accepted in the characterisation of animal models, such as those recapitulating ADHD in the absence of a known pathophysiological aetiology. Therefore, work presented here shows a serendipitous mouse model of ADHD that fulfils both predictive and face validity. Future work will aim to explore disease mechanisms so that construct validity can be achieved. Furthermore results from a microarray carried out at the time of thesis submission should highlight gene expression differences apparent due to the conditional loss of *Foxp1* in the cortex.

6 *<u>General Discussion</u>*

Foxp1 is an important TF that amongst other developmental roles, has been identified in the literature, and confirmed by the host lab to be up regulated during peak MSN development (E12-16). It is also expressed in both the developing and adult cortex. Further understanding of the functional role of Foxp1 in neuronal development will be useful for applying to directive cell protocols for use in cell transplantation therapies as well as a more general role for drug trials targeting neurodegeneration. Furthermore understanding the role of Foxp1 in the adult brain will also be useful for learning more about psychiatric disorders, such as ASDs, in which mutations in Foxp1 have been identified in patients.

HD is caused by the loss of MSNs in the striatum and as there is known cure one therapeutic approach is cell replacement therapy, which aims to replace MSNs in the hope the circuitry will reconnect with the relevant brain areas. The use of human foetal striatal tissue, i.e the 'natural' cells, has shown 'proof of principle' in clinical trials. However, this approach is associated with practical and ethical difficulties and renewable cell sources are needed such as stem cells. One challenge of using renewable stem cells is their differentiation to fully functional neurons. Hence, for the treatment of HD an understanding of the specific genes important for the differentiation of MSNs is crucial and thus in this Thesis I primarily looked at the expression profile and function of Foxp1 during striatal development in an attempt to understand its role in MSN differentiation.

Foxp1 was also conditionally knocked out in the adult brain, specifically in the cortex where the link between Foxp1 and ASDs was explored. This CKO left mice with a distinct phenotype reminiscent of ADHD which is genetically linked to ASDs. Thus this model was systematically explored using several behavioural tasks, drug trials and histology to explore its potential importance as a new model of neurological disease, in particular as a new mouse mode of ADHD or for elements of ASDs.

6.1 *Foxp1* **is a marker of immature and mature MSNs**

One therapeutic option that has shown proof of principle for the treatment of HD is cell replacement therapy, and specific protocols aiming to direct the differentiation of renewable cells towards DARPP-32 positive MSNs *in vitro* are actively being explored (Aubry *et al.* 2008; Carri *et al.* 2013; Ma *et al.* 2012; Nicoleau *et al.* 2013; Song *et al.* 2007). It is becoming increasingly apparent that DARPP-32 can no longer be used in isolation as a marker of MSNs as expression is not apparent until E18 and is not optimally expressed until 2-3 weeks post-natally in mice (Ehrlich *et al.* 1990). This prompted the need for a panel of genes expressed before and simultaneous to DARPP-32 to be used to identify MSNs at early and later stages of development. Therefore, for current and future *in vitro* protocols, a full detailed characterisation of hESCs at a genetic (specific markers) and functional level (electrophysiology) will be needed as identifying cells at the correct developmental stage will be crucial to the success of these cells for use in transplantation protocols.

Recently, *Foxp1* has started to be used as part of a battery of markers recognising MSNs in *in vitro* protocols (Carri *et al.* 2013), and subsequently, to label such cells following transplantation into the lesioned striatum (Carri *et al.* 2013). Likewise, *Foxp1* has also been successfully used by our group to identify MSNs following primary WGE grafts into the QA lesioned striatum (which has also shown to be devoid of FOXP1) (Precious et al., submitted 2013) and following directed differentiation of hESCs (Vinh et al., unpublished observations). In a number of publications, *Foxp1* has been associated with labelling only later born matrix neurons (Arlotta *et al.* 2008; Martin-Ibanez *et al.* 2012; Tamura *et al.* 2004) and reasons for this are two-fold. Firstly, *Foxp1* expression has not been shown to be visible until E12.5 in the developing telencephalon (Tamura *et al.* 2003), and secondly, co-expression of *Foxp1* mRNA was only detectable in 70% of DARPP-32 neurons following immunohistochemistry (Tamura *et al.* 2004).

In contrast to this, results presented in Chapter 3 showed that *Foxp1* expression was apparent in the developing striatum from E10 in the VZ/SVZ, before the onset of CTIP2 expression. Of note, is that this expression is coincident with the first wave of striatal neurogenesis that gives rise to patch neurons (Mason *et al.* 2005). Additionally, from E12 FOXP1 staining was shown in defined patches in the SVZ (Fig 3.1), in addition to

the staining throughout the MZ from E14, suggesting the possibility that *Fo*xp1 is a novel marker of proliferating patch neurons (as well as matrix neurons) from E12, which, until now, were not selectively identifiable until E18 in the MZ using DARPP-32 (Foster *et al.* 1987; Mason *et al.* 2005). Furthermore, in Chapter 4 FOXP1 was used to identify striatal cells that were transplanted in the mouse QA lesioned striatum. I have shown for the first time that FOXP1 together with DARPP-32 can be used to identify P-zones within the grafts (Fig 4.16), therefore offering itself as a mature label of MSNs following transplantation of WGE into the lesioned mouse brain. As *Foxp1* is also expressed in the human striatum it is likely that it will also serve as marker of P-zones in human primary WGE grafts. These results strongly suggest that *Foxp1* is a reliable marker of both patch and matrix neurons from early in development, and consistent with the literature and public databases,[i] that co-localisation is apparent with the two routinely used MSN markers, DARPP-32 and CTIP2, from the onset of their expression. Moreover, FOXP1 is expressed throughout in the adult striatum, and in WGE grafts, showing that it marks mature MSNs.

6.2   *Foxp1* **is required for correct development and maturation of at least one population of DARPP-32 expressing MSNs**

Foxp1 is an important TF implicated in many developmental processes and has been studied in lung, blood and B-cell development (Hu *et al.* 2006; Shu *et al.* 2007; Shu *et al.* 2001), and extensively in the heart where it has a specific role in the proliferation and maturation of cardiac myocytes (Wang *et al.* 2004a). In addition, *in vitro* studies using mESCs showed that *Foxp1* has a functional role in DA neuron development. Specifically, the addition of *Foxp1* to mESCs activated the expression of PITX3, a protein exclusively expressed in midbrain dopaminergic neurons that is vital for their correct differentiation and survival during development *in vitro* and *in vivo* (Konstantoulas *et al.* 2010). These key roles, together with its significant up-regulation during peak MSN differentiation (Precious *et al.,* submitted 2013) strongly suggested that *Foxp1* would have a similar functional role in MSN differentiation.

Chapters 3 explored phenotypic differences in MSNs in the absence of *Foxp1* through the use of the most readily used and accepted marker of MSNs, DARPP-32. In *Foxp1*^{-/-} cultures differentiated for 7 DIV there was a decrease in the number of DARPP-32

positive cells compared to in WT cultures, but no differences in overall neuronal number as determined by TUJ1 (Fig 3.12). No differences in the number of TUJ1 neurons together with no signs of increased cell death in the cultures (no fragmented nuclei), or any differences in proliferation (BrdU analysis) (Fig 3.16 and 3.17), suggests that the loss of *Foxp1* has not affected the early stages of MSN differentiation. Calcium imaging on cells from WT, *Foxp1*$^{+/-}$ and *Foxp1*$^{-/-}$ cultures showed that all neurons responded to GABA and showed the expected excitatory response to this neurotransmitter indicative of immature neurons (Owens *et al.* 1996). *Foxp1*$^{-/-}$ cells, although not significantly different, showed a trend for an increased excitatory response (response in normal chloride/ response in low Cl), which, if confirmed could be taken as an indicator of a greater degree of immaturity. More work is needed to confirm or refute this.

The results from Chapter 3 suggest that *Foxp1* is needed to ensure the correct differentiation of at least one population of DARPP-32 positive neurons and that this involvement is at a stage when the neurons have finished proliferation and have exited the cell cycle. In support of this is the fact that *Foxp1* has been reported to have a role in coordinating transitions between cell proliferation and differentiation in several other biological contexts including myocytes (Wang *et al.* 2004a; Zhang *et al.* 2010), neurons (Ferland *et al.* 2003; Konstantoulas *et al.* 2010; Rousso *et al.* 2008), monocytes and macrophages (Shi *et al.* 2008) and stem cells (Gabut *et al.* 2011). Furthermore at a protein level *Foxp1* has been shown to contain motifs capable of binding cyclin CDK2 (Banham *et al.* 2001), a gene implicated in cell cycle regulation. Additionally *Foxp1* is able to bind to the Foxp1 binding sites on the p21 promoter (Jepsen *et al.* 2008). Increases in p21 expression are correlated with withdrawal of cells from the cell cycle and with the differentiation of cardiomyocytes (Jepsen *et al.* 2008), therefore taken together it is plausible that *Foxp1* may also play a role in the transitional stages of proliferation to differentiation of MSN development. Future work focusing on differences in cell cycle markers such as p21 will perhaps give more answers to this hypothesis as would looking more specifically at early (NESTIN) and mature (MAP2) neuronal markers. Interestingly it has been shown that the miR-9 fine-tunes *Foxp1* expression in motor neurons (Otaegi et al., 2011). miR-9 has also recently been associated with aspects of neuronal development such as modulating neurite outgrowth and neural lineage determination (Coolen *et al.* 2013; Liu *et al.* 2012) thus it may be

possible that this micro-RNA may also fine tune *Foxp1* expression in aspects of neuronal specification, as with motor neurons.

Understanding what genes and subsequent genetic pathways *Foxp1* is involved with also needs to be answered, and results from this Thesis have hinted at some answers. *Dlx1* and *Dlx2* are expressed by subsets of progenitor cells in the VZ by E10.5 and by the majority of cells in the SVZ with expression switching off as cells start to migrate and differentiate in the MZ (Nery *et al.* 2003; Porteus *et al.* 1994; Yun *et al.* 2002). In *Dlx1/2$^{-/-}$* mice it was shown that *Foxp1* expression was severely reduced in the SVZ and MZ suggesting *Foxp1* is downstream of these TFs (Long *et al.* 2009). Similarly Chapter 3 showed that in the *Ascl1$^{-/-}$* and *Gsh2$^{-/-}$* brain sections, FOXP1 staining was reduced, prompting the idea that *Foxp1* may also function downstream of these TFs in the VZ, as shown in Figure 6.1. Although on this occasion the apparent loss of FOXP1 in the *Gsh1$^{-/-}$* and *Ascl1$^{-/-}$* brain sections was not quantified, results from an on-going microarray assessing independent differences in the LGE and MGE, from *Foxp1$^{-/-}$* striate compared to WT striate, will yield more definitive answers, comparable to results from the microarray analysis conducted by Long and colleagues in the *Dlx1/2* KO. It is known that there are biding sites for FOXP1 on *Foxp1* (Tang *et al.* 2012), thus it is possible that once *Foxp1* is expressed it can regulate its own expression in the MZ. Interestingly, it has been shown that during B-cell development the loss of *Foxp1* causes loss of expression of the TF *Ebf1* (Hu et al., 2006), a gene implicated in the development of matrix born striatal neurons, thus it is possible that these two TFs are also interacting similarly during MSN development. In future work it would be interesting to see if the expression of *Ebf1* is affected by the loss of *Foxp1* in the developing striatum. More molecular analysis, such as immunopreciptitation will also be useful in studying specific *Foxp1* interactions with genes known to be expressed at similar times in development as well as novel ones identified from the microarray.

There were some limitations to the *in vitro* work in Chapter 3. Firstly, as experiments were restricted to E14 due to the embryonic lethality of the *Foxp1$^{-/-}$* mice, DARPP-32 could not be looked for in coronal brain sections and thus differences relied on the immature MSN maker CTIP2, in which no obvious differences were observed at E14 (Fig 3.20B). However further quantification is needed to confirm or refute this. Secondly, even though differences in DARPP-32 were shown in the culture system after

7 DIV, the number of DARPP-32 positive cells across all cultures was low owing to the fact DARPP-32 is not fully expressed until 2-3 weeks after birth (Gustafson *et al.* 1992). Future experiments will focus on what can be added to the striatal cultures to maintain survival for 14 DIV as it likely there will be an increase in DARPP-32 expression further emphasising the differences between the genotypes

However, on this occasion to look at differences in DARPP-32 expression at later developmental stages striatal cells from the three genotypes (WT, *Foxp1$^{+/-}$* and *Foxp1$^{-/-}$*) were transplanted into the QA lesioned striatum, which was discussed in Chapter 4. Grafting potentially allowed the cells to mature, differentiate and make connections with host circuitry over a 12 week period, which was unattainable using *in vitro* cultures. These studies revealed a decrease in the number of DARPP-32 positive striatal neurons irrespective of donor age (E12 or E14), in the absence of *Foxp1*, thus indirectly supporting the findings from Chapter 3. Unfortunately, in this instance, differences in mature MSNs *in vivo*, i.e. differences in DARPP-32, in the adult mouse striatum, in the absence of *Foxp1,* were not able to be directly studied in the lack of a striatal specific *Foxp1* CKO. However, in addition to expression in mature MSNs, DARPP-32 is known to be expressed in the layer V1 cortical neurons (Ouimet *et al.* 1984; Rajput *et al.* 2009; Wang *et al.* 2004b) and results from the *Foxp1* CKO showed there was a decrease in DARPP-32 staining in layer V1 of the cortex. This result therefore further suggests that in the absence of *Foxp1,* DARPP-32 is not properly expressed, irrespective of neuronal subtype. This result therefore asks further questions as to whether *Foxp1* is needed in a general step that controls the maturity of neurons or whether its role is specific to DARPP-32 development. This question is something that will be explored in future work.

These studies demonstrate that *Foxp1* is necessary for the generation of a population of DARPP-32 positive MSNs. However, they do not distinguish whether *Foxp1* is necessary for the generation of MSNs, without which they do not develop; or if they follow an aberrant differentiation pathway; or whether neurons with MSN characteristics develop, but do not express DARPP-32 (and therefore presumably do not synpase with incoming DA terminals). This questions what we really mean by a MSN. Although DARPP-32 is the "gold standard" MSN marker, its loss does not necessarily indicate absent and dysfunctional MSNs but could suggest a specific MSN feature is

lost, i.e. loss of a specific subset of DA receptors, which could lead to a disconnected striatum. In summary, it is clear that, in the absence of *Foxp1*, DARPP-32 expressing cells in both the striatum and cortex are reduced or absent. However, what this means in terms of precisely what neurons are remaining in the *Foxp1*^{-/-} striatum requires further exploration.

6.3   <u>Do *Foxp1* and *Ctip2* work together in MSN development?</u>

Ctip2 is a TF that is expressed in the developing striatum and cortex and its expression persists throughout adulthood where it has shown to co-localize with DARPP-32 and FOXP1 in the adult striatum (Arlotta *et al.* 2008), these findings are also corroborated in the Allen Brain Atlas. Additionally, it is used to label layer V cortical neurons (Arlotta *et al.* 2005). In this Thesis I used CTIP2 mainly as a marker of MSNs (Chapters 3 and 4) but also as a marker of layer V cortical neurons (Chapter 5). Our experiments showed for the first time that CTIP2 was expressed after FOXP1 in the developing striatum at E12 (Fig 3.1), and unlike FOXP1 staining, was restricted to the MZ where it appeared to co-localise fully with FOXP1 from E14 onwards in agreement with Arlotta et al (2008). These results suggest that FOXP1 is an earlier marker of MSNs than CTIP2, but that both TFs stain the same populations of MSNs from E14 in the MZ of the striatum.

In addition to *Ctip2* and *Foxp1* being expressed at comparable times and spatial location in the developing and adult mouse brain, *Ctip2* is also closely related to the *Bcl11A* gene which, like *Foxp1* is associated with types of B-cell malignancies. Both genes are also transcriptional repressors and there is a known binding site for *Foxp1* upstream of the CTIP2 promoter region thus an interaction between these two genes is very likely during striatal and/or cortical development. After 7 DIV, there were fewer CTIP2 positive cells in the differentiation cultures from *Foxp1*^{-/-} striate compared to WT cultures (Fig 3.12). This result is consistent with the loss of DARPP-32 staining after 7 DIV, supporting the idea that *Foxp1* is needed to ensure the correct development of at least a subset of MSNs, but also that *Foxp1* is upstream of *Ctip2* and is positively regulating its expression. Conversely, results from Chapter 4, although not significant, indicated after 12 weeks, the grafts that received donor tissue in the absence of *Foxp1* had an increase in the number of CTIP2 positive cells (Fig 4.10), suggesting that *Foxp1*

can also represses CTIP2. Moreover, in the adult cortex, in the absence of *Foxp1,* there was ectopic staining of CTIP2 in layers 3 and 4 (Fig 5. 17), further implying that *Foxp1* is needed upstream of CTIP2, but again, that *Foxp1* is negatively regulating CTIP2 rather than positively as the E14 data suggests. Furthermore, when CTIP2 was KO at P0, there was a decrease in FOXP1 expression in the striatum (Arlotta *et al.* 2008). Combined, these findings suggest that FOXP1 and CTIP2 may function together in a feedback loop but have different regulatory functions dependant on developmental time point. Furthermore, the data points to FOXP1 being expressed earlier than CTIP2 (Fig 3.1), and the fact that there are known FOXP1 binding sites upstream of the *Ctip2* promoter (Tang *et al.* 2012) suggests that FOXP1 can act upstream of CTIP2. As mentioned, FOXP1 staining was lost in the mouse striatum at P0 when *Ctip2* was knocked out. This suggests that *Ctip2*, at least at this age, positively regulates *Foxp1*, however whether this is the case earlier in development is unknown. The supposed interaction between *Foxp1* and *Ctip2* is shown in Figure 6.1.

To conclude, in addition to *Ctip2, Foxp1* has a functional role in MSN development and it is likely these two TFs work in synergy. However, owing to its earlier expression it is possible that *Foxp1* may have a more specific role in earlier stages of MSN development, and that CTIP2 is concerned with ensuring correct MSN organisation in the postnatal striatum (Arlotta *et al.* 2008). Additionally it has been demonstrated that during the development of a subset of cortical neurons CTIP2 and the transcriptional repressor Fezf2 interact (Chen *et al.* 2008). *Fezf2* is expressed on the same chromosome as Foxp1 in humans (3p14.2) thus these two genes may also interact and work together in aspects of cortical development although no link has been shown suggested yet.
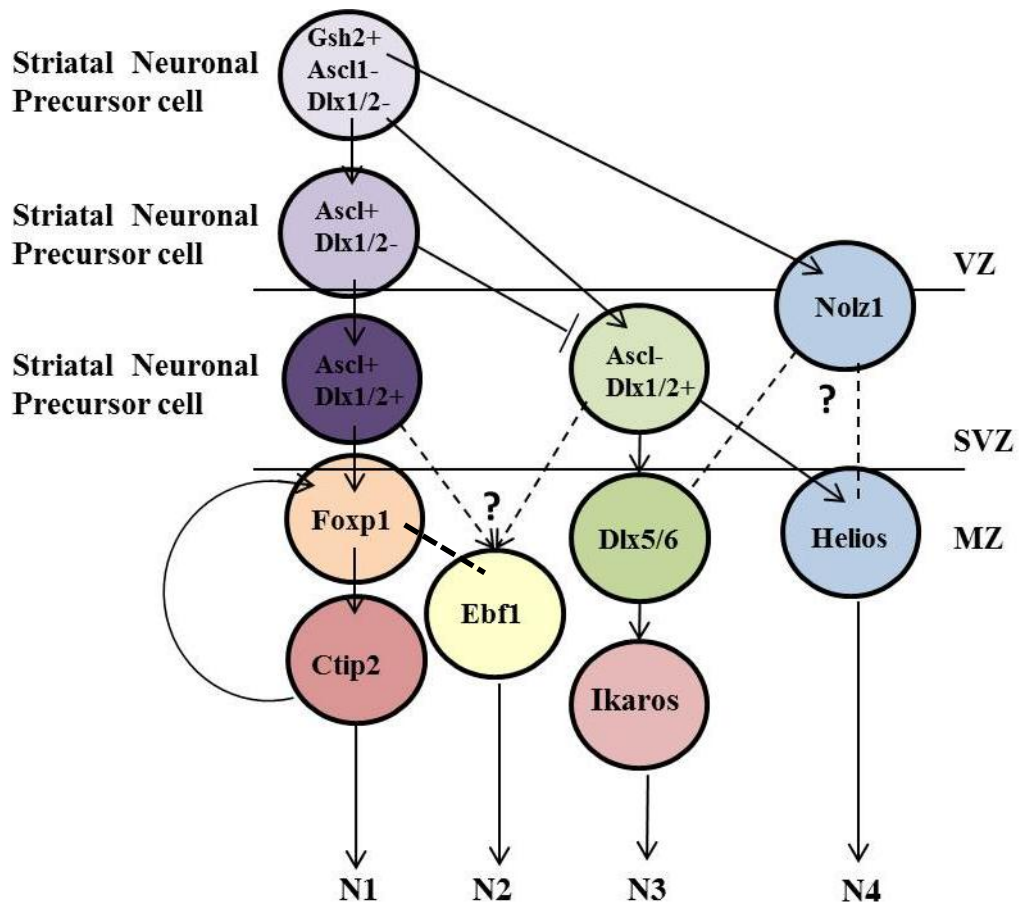
Figure 6.1 Proposed model of the different genetic lineages contributing to striatal development with an additional pathway based on work outlined in this thesis. I suggest that *Foxp1* may be implicated downstream of *Gsh2/Ascl1* and *Dlx1*/2 during striatal neurogenesis. I also propose that in the MZ of the developing striatum, *Foxp1* can regulate itself, in addition to CTIP2, for the development of striatal neurons (this could also be true for the cortical neuron development). A feedback loop between CTIP2 and FOXP1 has also been supposed. It is also possible that *Foxp1* regulates other genes, such as *Ebf1* (N1) *Abbreviations: VZ-Ventricular zone, SVZ- sub-ventricular zone, MZ-Mantle zone, N- Neuronal lineage. Dashed lines indicate possible interactions. Figure adapted from Figure 1.13 (Martin-Ibanez et al. 2012)*.

6.4   **A Foxp1 CKO model in the cortex is a new mouse model of ADHD**

In Chapter 5 we aimed to generate a conditional *Foxp1* KO in the developing striatum to study MSNs differentiation after E14 and to look at the role of *Foxp1* in the cortex. However, as a direct consequence of the timing of the hGFAP-Cre expression, *Foxp1* was completely lost in the cortex but expression in the striatum was retained. This cortical loss of *Foxp1* resulted in mice that were hyperactive and inattentive in both the home cage and in a novel environment when compared to littermate controls. Hyperactivity and lack of attention are two of the key indicators of ADHD, a disorder in which the precise aetiology is unknown, but has been suggested, at a physiological level, to be caused by the dysregulation of the catecholaminergic system leading to imbalances in the DA and NA neurotransmitter systems particularly in the prefrontal cortical regions (Arnsten 2009). Interestingly when the NA reuptake inhibitor atomoxetine was administered to the mice, the hyperactivity of the *Foxp1* CKO mice was significantly reduced with no effects on the locomotor activity of the WT animals (Fig 5.14). Taken together, this data shows that *Foxp1* CKO mice recapitulated key symptoms of a disorder (face validity) and responded to biochemical therapeutics associated with ADHD (predictive validity). Although construct validity i.e. comparable physiological differences, was not achieved, this is a difficulty accepted in the characterisation of animal models, such as those recapitulating ADHD in the absence of a known pathophysiological aetiology. However, work looking into the precise mechanisms of atomoxetine, i.e. if it is blocking alpha 1 or alpha 2 receptors, is on-going together with histology addressing whether the NA system is involved.

In support of the supposed ADHD model created in Chapter 5 is that ADHD is known to be highly heritable (concordant twin studies show it be 76% (Faraone *et al.* 2005)) and may result from several different gene mutations, together with environmental factors. Candidate gene studies have shown a number of genes, many of which relate to catecholamine function are associated with the aetiology of ADHD, however the association between gene mutation and ADHD phenotype is small stressing that the disorder is likely caused by many genes of little effect. Thus it is highly likely additional genes such as Foxp1 may be associated with ADHD and that this new model will enhance the understanding of aspects of the disease. Moreover, ADHD shares a high

degree of comorbidity and inherited factors with ASD (Lichtenstein *et al.* 2010; Ronald *et al.* 2011; Thapar *et al.* 2013). For example some ASD patients have been shown to be associated with poor attentional switching, resembling the inattention seen in ADHD patients (Polderman *et al.* 2013). Therefore as Foxp1 has been linked to several cases of ASD ((Hamdan *et al.* 2010; Horn *et al.* 2010; Palumbo *et al.* 2013) and this further strengthens the support for Foxp1 being genetically linked to ADHD.

Table 6.1 shows how this novel model fits in with three of the most studied ADHD models. The most studied ADHD model is the spontaneous hypertensive rat (SHR) originally developed in the 1960's as a model of hypertension (Okamoto and Aoki 1963). In addition to hypertension this rat model showed symptoms of hyperactivity and impulsivity that were attenuated with monoaminergic agents and thus became a valid model of ADHD (Sagvolden 2000; Sagvolden *et al.* 1993). However, the rats have increased blood pressure which has not been linked with ADHD and the control group used in the behavioural studies are known to be poor responders, thus questioning the reliability of the results (Drolet *et al.* 2002). Two other popular ADHD models are caused by genetic mutations in mice. Firstly, the DAT KO mouse causes loss of DAT in the brain leading to a decrease in DA clearance (Jones *et al.* 1998), and spontaneous hyperactivity (Gainetdinov *et al.* 1999) that is responsive to pyschostimulants. However, there are no indications that DAT is absent in ADHD. Indeed, the opposite has been reported and several studies have shown increased DAT levels in the striatum of ADHD patients (Cheon *et al.* 2004). Secondly, the thyroid hormone receptor (TR)-beta (1) TG mouse has a mutant TRβ1 gene derived from a patient diagnosed with resistance to thyroid hormone syndrome (RTH); 70% of children with this disorder are also diagnosed with ADHD (Burd *et al.* 2003). This TG mouse line has increased thyroid levels that induce impulsivity, inattention and hyperactivity in these mice and these symptoms were sensitive to Ritalin treatment (Siesser *et al.* 2006). Although predictive, construct and face validity have been achieved in this model, the role of the thyroid system in ADHD is unclear and as abnormal thyroid levels can affect brain development, this could be a direct cause of the ADHD behavioural phenotype.

In summary, the strong link between FOXP1 and the ADHD/ASD spectrum (Carr *et al.* 2010; Chien *et al.* 2013; Hamdan *et al.* 2010; Horn *et al.* 2010) and the behavioural phenotype seen in the novel *Foxp1* CKO model presented in this Thesis, make it a

realistic mouse model of ADHD. Unlike previous ADHD models, it has an obvious phenotype caused by selective loss of one gene in a specific area of the brain known to be associated with ADHD.

Prominent features evident in HD patients are signs of impulsivity with absence of forethought, difficulties in multi-tasking and inattention, which can be attributable to both striatal and cortical cell loss (Craufurd and Snowden 2002; Rosas *et al.* 2008). Additionally, on the 5-CSRTT, the TG HD Q92 mouse line showed a decrease in accuracy from their baseline performance when compared to WT mice (Trueman *et al.* 2012b). These selective HD symptoms overlap with behavioural traits apparent in patients with ASDs and thus some of the behavioural phenotypes associated with the *Foxp1* CKO model discussed in Chapter 5. Interestingly, parallels with *Foxp1* and HD have been published. *Foxp1* is known to be down regulated in the striatum of R6/1 TG mouse models of HD, which, as a direct result, leads to aberrant immune regulation and increased gliogenesis, which are associated with the disease (Tang *et al.* 2012). Specifically, mutant HTT protein can directly bind FOXP1, and as a direct result, FOXP1 is present in the nuclear aggregates in the brains of HD patients, thus preventing auto-regulation of *Foxp1* (Tang *et al.* 2012). Although the most prominent cell loss in HD is in the striatum, one of the earliest changes in the HD brain is thinning in specific regions of the cortex (Rosas *et al.* 2002; Rosas *et al.* 2008). Thus taking the cortical thinning, the nature of the behavioural changes and the loss of *Foxp1* in the cortex, there are interesting parallels between the HD and the *Foxp1*$^{-/-}$ *ADHD* model that may be deserving of further consideration in the future.

MODEL	MODIFICATION	FACE VALIDITY	PREDICITVE VALIDITY	CONSTRUCT VALIDITY	MISSING DATA/ PROBLEMS	KEY REFERENCES
Spontaneous Hypertensive Rat **(SHR)** (1963)	Bred for hypertension	Hyperactivity Impulsivity	Symptoms reduced by monoaminergic agents	Dysfunctional fronto-striatal system	Hypertension WKY rats as control group (strain known to be poor at behavioural tasks)	(Okamoto and Aoki 1963) (Sagvolden 2000) (Sagvolden *et al.* 1993)
The dopamine-transporter KO mouse **(DAT-KO)** (1996)	DA transporter gene knocked out	Hyperactivity Spatial memory deficits	Hyperacitvity reduced by pyschostimulants	Alterations in the DA system	Not shown there are reduced numbers of DAT in patients with ADHD	(Giros *et al.* 1996) (Jones *et al.* 1998)
Thyroid hormone receptor (TR)-beta(1) Tg mouse **(TRβ1-KO)** *(2006)*	Carries a mutant human Trβ1 gene	Hyperactivity Impulsivity Inattention	All symptoms reduced by Ritalin	Alterations in the DA system	Role of the thyroid system in ADHD unclear	(Siesser *et al.* 2006)
Foxp1 **CKO model** *(2013)*	Cortical knock out of a single gene - *Foxp1*	Hyperactivity Inattention	Symptoms reduced by atomoxetine	On-going work	Further impulsivity data still needed Construct validity	(Evans et al., 2013) Paper in preparation,

Table 6.1 A summary of the key animal models of ADHD

6.5 **Where Next?**

The main aim of this Thesis was to analyse the role of Foxp1 and its role in striatal MSN differentiation as well as its functional role in the adult brain. The results strongly indicated that *Foxp1* is required for the correct development of the DARPP-32 positive MSNs, as demonstrated by a decrease in DARPP-32 in *Foxp1*$^{-/-}$ striatal cultures after 7 DIV (Chapter 3), after 12 weeks following transplantation of *Foxp1*$^{-/-}$ tissue (Chapter 4), and in layer V1 cortical neurons (Chapter 5). However, a striatal specific *Foxp1* CKO would be optimum in confirming these results and is planned using the *Gsh2*-Cre line which should knock out *Foxp1* in the striatum only from ~E10. It is also appreciated that further *in vitro* experiments using the *Foxp1*$^{-/-}$ line are needed to fully confirm the suggested immaturity of the neurons in the absence of *Foxp1* and will be carried out following further rounds of breeding. Furthermore, the transplantation studies in Chapter 4 will likely be repeated following optimisation of the mouse allografting protocol, or alternatively carried out in rats (requiring daily immunosuppression).

In the absence of a known direct *Foxp1* binding region on the *Darpp-32* gene, the mechanism by which *Foxp1* could regulate DARPP-32 needs to be researched. Downstream targets of *Foxp1* have previously been studied in a striatal cell line and showed that *Foxp1* was capable of regulating its own expression, and that there are also binding sites upstream of the *Ctip2* promoter (Tang et al., 2010). In addition, downstream targets of *Foxp1* in the CNS have included *Pitx3* in midbrain DA development (Konstantoulas *et al.* 2010). *Foxp1* also binds p21, a gene needed for cell cycle exit (Jepsen *et al.* 2008), thus it is possible this interaction is also seen during striatal development. It is anticipated that results from a microarray (currently being analysed) to assess differences in gene expression between WT and *Foxp1*$^{-/-}$ E14 LGE and MGE, will be helpful in ascertaining downstream targets of *Foxp1* in the developing striatum and will form the basis of future work. Online databases such as the Allen Brain Atlas will also be very useful in seeing if any of the genes from the microarray are already associated with Foxp1 in human or mouse development and/or in the adult brain.

Moreover, there will be on-going experiments to further characterise the *Foxp1 CKO* line in order to fully establish it as a new mouse model of ADHD. Characterisation will

involve further behavioural testing using larger cohorts of mice together with more comprehensive pharmacological testing to establish specifically what NA transporters are being targeted by atomoxetine, thus establishing construct validity. Furthermore, thorough histological analysis will be attempted.

Lastly, the *Mef2c CKO* mouse line needs to be fully characterised and results from expression studies (Appendix 8) suggest that generating cultures from a later developmental time point such as E16 or E18, in addition to E14 cultures, will give a more accurate representation of differences in MSN differentiation due to the loss of *Mef2c*.

6.6 **Concluding Remarks**

I have shown that *Foxp1* is required for the development of a subset of DARPP-32 positive neurons, as in the absence of *Foxp1* there were fewer DARPP-32 positive cells in the developing striatum and in the adult cortex. The results presented throughout this Thesis, together with published data, suggest that *Foxp1* is a definitive marker of MSNs at early and late stages of mouse striatal development. The data also suggests that the functional role of *Foxp1* is likely to ensure the correct maturation of at least a subset of MSN precursors to DARPP-32 positive neurons following their exit from the cell cycle, although further work is needed to confirm this. It is anticipated that results from the on-going microarray will highlight whether there are any differences in the cell cycle genes or genes associated with MSN migration, survival and differentiation giving more specific clues about the function of *Foxp1* in striatal development.

To conclude, these findings suggest that *Foxp1* is required in aspects of MSN development and that this should be considered in the development of *in vitro* protocols aiming to direct renewable cells such as ESCs and iPSCs to functional DARPP-32 positive MSNs for their use in cell transplantation. The findings also suggest that Foxp1 is a gene that could be implicated in aspects of ADHD and that knocking it out from E14 creates a CKO model that can be used to trial novel drugs to target disease symptoms as well as to study possible pathways contributing to the disorder.

7 *References*

Abercrombie, M. (1946). Estimation of nuclear population from microtome sections. *Anat Rec* **94:**239-247.

Akhtar, M. W., Kim, M. S., Adachi, M., Morris, M. J., Qi, X., Richardson, J. A., Bassel-Duby, R. *et al.* (2012). In vivo analysis of MEF2 transcription factors in synapse regulation and neuronal survival. *PLoS One* **7:**e34863.

Anderson, K. and Reiner, A. (1991). Immunohistochemical localization of DARPP-32 in striatal projection neurons and striatal interneurons: implications for the localization of D1-like dopamine receptors on different types of striatal neurons. *Brain Research* **568:**235-243.

Anderson, R. M., Lawrence, A. R., Stottmann, R. W., Bachiller, D. and Klingensmith, J. (2002). Chordin and noggin promote organizing centers of forebrain development in the mouse. *Development* **129:**4975-4987.

Anderson, S. A., Qiu, M., Bulfone, A., Eisenstat, D. D., Meneses, J., Pedersen, R. and Rubenstein, J. L. R. (1997). Mutations of the Homeobox Genes Dlx-1 and Dlx-2 Disrupt the Striatal Subventricular Zone and Differentiation of Late Born Striatal Neurons. *Neuron* **19:**27-37.

Anthony, T. E. and Heintz, N. (2008). Genetic lineage tracing defines distinct neurogenic and gliogenic stages of ventral telencephalic radial glial development. *Neural Dev* **3:**30.

Anthony, T. E., Klein, C., Fishell, G. and Heintz, N. (2004). Radial Glia Serve as Neuronal Progenitors in All Regions of the Central Nervous System. *Neuron* **41:**881-890.

Archer, T., Fredriksson, A., Lewander, T. and Soderberg, U. (1987). Marble burying and spontaneous motor activity in mice: interactions over days and the effect of diazepam. *Scand J Psychol* **28:**242-249.

Arime, Y., Kubo, Y. and Sora, I. (2011). Animal models of attention-deficit/hyperactivity disorder. *Biol Pharm Bull* **34:**1373-1376.

Arlotta, P., Molyneaux, B. J., Chen, J., Inoue, J., Kominami, R. and Macklis, J. D. (2005). Neuronal Subtype-Specific Genes that Control Corticospinal Motor Neuron Development In Vivo. *Neuron* **45:**207-221.

Arlotta, P., Molyneaux, B. J., Jabaudon, D., Yoshida, Y. and Macklis, J. D. (2008). Ctip2 controls the differentiation of medium spiny neurons and the establishment of the cellular architecture of the striatum. *J Neurosci* **28:**622-632.

Arnsten, A. F. (2009). The Emerging Neurobiology of Attention Deficit Hyperactivity Disorder: The Key Role of the Prefrontal Association Cortex. *J Pediatr* **154:**I-s43.

Aubry, L., Bugi, A., Lefort, N., Rousseau, F., Peschanski, M. and Perrier, A. L. (2008). Striatal progenitors derived from human ES cells mature into DARPP32 neurons in vitro and in quinolinic acid-lesioned rats. *Proc Natl Acad Sci U S A* **105:**16707-16712.

Bachoud-Levi, A. C., Gaura, V., Brugieres, P., Lefaucheur, J. P., Boisse, M. F., Maison, P., Baudic, S. *et al.* (2006). Effect of fetal neural transplants in patients with Huntington's disease 6 years after surgery: a long-term follow-up study. *Lancet Neurol* **5:**303-309.

Bachoud-Levi, A. C., Remy, P., Nguyen, J. P., Brugieres, P., Lefaucheur, J. P., Bourdet, C., Baudic, S. *et al.* (2000). Motor and cognitive improvements in patients with Huntington's disease after neural transplantation. *Lancet* **356:**1975-1979.

Backman, M., Machon, O., Mygland, L., van den Bout, C. J., Zhong, W., Taketo, M. M. and Krauss, S. (2005). Effects of canonical Wnt signaling on dorso-ventral specification of the mouse telencephalon. *Dev Biol* **279:**155-168.

Bai, C. B. and Joyner, A. L. (2001). Gli1 can rescue the in vivo function of Gli2. *Development* **128:**5161-5172.

Bai, X., Saab, S., Huang, A., Hoberg, I., Kirchhoff, F. and Scheller, A. (2013). Genetic Background Affects Human Glial Fibrillary Acidic Protein Promoter Activity. *PLoS One.* **8:**e66873.

Banham, A. H., Beasley, N., Campo, E., Fernandez, P. L., Fidler, C., Gatter, K., Jones, M. *et al.* (2001). The FOXP1 winged helix transcription factor is a novel candidate tumor suppressor gene on chromosome 3p. *Cancer Res* **61:**8820-8829.

Banham, A. H., Connors, J. M., Brown, P. J., Cordell, J. L., Ott, G., Sreenivasan, G., Farinha, P. *et al.* (2005). Expression of the FOXP1 transcription factor is strongly associated with inferior survival in patients with diffuse large B-cell lymphoma. *Clin Cancer Res* **11:**1065-1072.

Barbosa, A. C., Kim, M. S., Ertunc, M., Adachi, M., Nelson, E. D., McAnally, J., Richardson, J. A. *et al.* (2008). MEF2C, a transcription factor that facilitates learning and memory by negative regulation of synapse numbers and function. *Proceedings of the National Academy of Sciences of the United States of America* **105:**9391-9396.

Beal, M., Kowall, N., Ellison, D., Mazurek, M., Swartz, K. and Martin, J. (1986). Replication of the neurochemical characteristics of Huntington's disease by quinolinic acid. *Nature* **321:**168-171.
.

Berridge, C. W., Devilbiss, D. M., Andrzejewski, M. E., Arnsten, A. F., Kelley, A. E., Schmeichel, B., Hamilton, C. *et al.* (2006). Methylphenidate preferentially increases catecholamine neurotransmission within the prefrontal cortex at low doses that enhance cognitive function. *Biol Psychiatry* **60:**1111-1120.

Biederman, J. (2005). Attention-deficit/hyperactivity disorder: a selective overview. *Biol Psychiatry* **57:**1215-1220.

Biederman, J. and Faraone, S. V. (2005). Attention-deficit hyperactivity disorder. *Lancet* **366:**237-248.

Borello, U., Cobos I, Long JE and JLR, M. C. a. R. (2008). FGF15 promotes neurogenesis and opposes FGF8 function during neocortical development. *Neural Dev* **3:**17.

Brand, N. J. (1997). Myocyte enhancer factor 2 (MEF2). *The International Journal of Biochemistry & Cell Biology* **29:**1467-1470.

Broekkamp, C. L., Rijk, H. W., Joly-Gelouin, D. and Lloyd, K. L. (1986). Major tranquillizers can be distinguished from minor tranquillizers on the basis of effects on marble burying and swim-induced grooming in mice. *Eur J Pharmacol* **126:**223-229.

Brown, P. J., Ashe, S. L., Leich, E., Burek, C., Barrans, S., Fenton, J. A., Jack, A. S. *et al.* (2008a). Potentially oncogenic B-cell activation-induced smaller isoforms of FOXP1 are highly expressed in the activated B cell-like subtype of DLBCL. *Blood* **111:**2816-2824.

Brown, P. J., Kagaya, R. and Banham, A. H. (2008b). Characterization of human FOXP1 isoform 2, using monoclonal antibody 4E3-G11, and intron retention as a tissue-specific mechanism generating a novel FOXP1 isoform. *Histopathology* **52:**632-637.

Burd, L., Klug, M. G., Coumbe, M. J. and Kerbeshian, J. (2003). Children and adolescents with attention deficit-hyperactivity disorder: 1. Prevalence and cost of care. *J Child Neurol* **18:**555-561.

Bymaster, F. P., Katner, J. S., Nelson, D. L., Hemrick-Luecke, S. K., Threlkeld, P. G., Heiligenstein, J. H., Morin, S. M. *et al.* (2002). Atomoxetine increases extracellular levels of norepinephrine and dopamine in prefrontal cortex of rat: a potential mechanism for efficacy in attention deficit/hyperactivity disorder. *Neuropsychopharmacology* **27:**699-711.

Campbell, K. (2003). Dorsal-ventral patterning in the mammalian telencephelon. *Current opinion in neurobiology* **13:**50-56.

Campbell, K., Olsson, M. and Björklund, A. (1995). Regional incorporation and site-specific differentiation of striatal precursors transplanted to the embryonic forebrain ventricle. *Neuron* **15:**1259 –1273.

Carr, C. W., Moreno-De-Luca, D., Parker, C., Zimmerman, H. H., Ledbetter, N., Martin, C. L., Dobyns, W. B. *et al.* (2010). Chiari I malformation, delayed gross motor skills, severe speech delay, and epileptiform discharges in a child with FOXP1 haploinsufficiency. *Eur J Hum Genet* **18:**1216-1220.

Carri, A. D., Onorati, M., Lelos, M. J., Castiglioni, V., Faedo, A., Menon, R., Camnasio, S. *et al.* (2013). Developmentally coordinated extrinsic signals drive human pluripotent

stem cell differentiation toward authentic DARPP-32+ medium-sized spiny neurons. *Development* **140:**301-312.

Casarosa, S., Fode, C. and Guillemot, F. (1999). Mash1 regulates neurogenesis in the ventral telencephalon. *Development* **126:**525-534.

Casper, K. B. and McCarthy, K. D. (2006). GFAP-positive progenitor cells produce neurons and oligodendrocytes throughout the CNS. *Mol Cell Neurosci* **31:**676-684.

Castro, D. S., Martynoga, B., Parras, C., Ramesh, V., Pacary, E., Johnston, C., Drechsel, D. *et al.* (2011). A novel function of the proneural factor Ascl1 in progenitor proliferation identified by genome-wide characterization of its targets. *Genes Dev* **25:**930-945.

Chamberlain, S. and Sahakian, B. (2007). The neuropsychiatry of impulsivity. *Curr Opin Psychiatry* **20:**255-261.

Chatzi, C., Brade, T. and Duester, G. (2011). Retinoic acid functions as a key GABAergic differentiation signal in the basal ganglia. *PLoS Biol* **9:**e1000609.

Chen, B., Wang, S. S., Hattox, A. M., Rayburn, H., Nelson, S. B. and McConnell, S. K. (2008). The Fezf2-Ctip2 genetic pathway regulates the fate choice of subcortical projection neurons in the developing cerebral cortex. *Proc Natl Acad Sci U S A* **105:**11382-11387.

Cheon, K. A., Ryu, Y. H., Namkoong, K., Kim, C. H., Kim, J. J. and Lee, J. D. (2004). Dopamine transporter density of the basal ganglia assessed with [123I]IPT SPECT in drug-naive children with Tourette's disorder. *Psychiatry Res* **130:**85-95.

Chiang, C., Litingtung, Y., Lee, E., Young, K. E., Corden, J. L., Westphal, H. and Beachy, P. A. (1996). Cyclopia and defective axial patterning in mice lacking Sonic hedgehog gene function. *Nature* **383:**407-413.

Chien, W. H., Gau, S. S., Chen, C. H., Tsai, W. C., Wu, Y. Y., Chen, P. H., Shang, C. Y. *et al.* (2013). Increased gene expression of FOXP1 in patients with autism spectrum disorders. *Mol Autism* **4:**23.

Cho, E. G., Zaremba, J. D., McKercher, S. R., Talantova, M., Tu, S., Masliah, E., Chan, S. F. *et al.* (2011). MEF2C enhances dopaminergic neuron differentiation of human embryonic stem cells in a parkinsonian rat model. *PLoS One* **6:**e24027.

Cholfin, J. A. and Rubenstein, J. L. (2007). Patterning of frontal cortex subdivisions by Fgf17. *Proc Natl Acad Sci U S A* **104:**7652-7657.

Cisbani, G., Saint Pierre, M. and Cicchetti, F. (2013). Single cell suspension methodology favours survival and vascularization of fetal striatal grafts in the YAC128 mouse model of Huntington's disease. *Cell Transplant*.

Cocas, L. A., Miyoshi, G., Carney, R. S., Sousa, V. H., Hirata, T., Jones, K. R., Fishell, G. *et al.* (2009). Emx1-lineage progenitors differentially contribute to neural diversity in the striatum and amygdala. *J Neurosci* **29:**15933-15946.

Collinson, J. M., Hill, R. E. and West, J. D. (2000). Different roles for Pax6 in the optic vesicle and facial epithelium mediate early morphogenesis of the murine eye. *Development* **127:**945-956.

Coolen, M., Katz, S. and Bally-Cuif, L. (2013). miR-9: a versatile regulator of neurogenesis. *Front Cell Neurosci* **7:**220.

Corbin, J. G., Gaiano, N., Machold, R. P., Langston, A. and Fishell, G. (2000). The Gsh2 homeodomain gene controls multiple aspects of telencephalic development. *Development* **127:**5007-5020.

Craufurd, D. and Snowden, J. (2002). Neuropsychological and neuropsychiatric aspects of Huntington's Disease. In: Bates, G. and Harper, P. and Jones, L. (eds.) *Huntington's Disease*. Oxford: Oxofrd University Press
pp. 62-94.

Crossley, P. H., Martinez, S., Ohkubo, Y. and Rubenstein, J. L. (2001). Coordinate expression of Fgf8, Otx2, Bmp4, and Shh in the rostral prosencephalon during development of the telencephalic and optic vesicles. *Neuroscience* **108:**183-206.

Cruz, A. P., Frei, F. and Graeff, F. G. (1994). Ethopharmacological analysis of rat behavior on the elevated plus-maze. *Pharmacol Biochem Behav* **49:**171-176.

Dai, P., Akimaru, H., Tanaka, Y., Maekawa, T., Nakafuku, M. and Ishii, S. (1999). Sonic Hedgehog-induced activation of the Gli1 promoter is mediated by GLI3. *J Biol Chem* **274:**8143-8152.

Danesin, C., Peres, J. N., Johansson, M., Snowden, V., Cording, A., Papalopulu, N. and Houart, C. (2009). Integration of telencephalic Wnt and hedgehog signaling center activities by Foxg1. *Dev Cell* **16:**576-587.

Dasen, J. S., De Camilli, A., Wang, B., Tucker, P. W. and Jessell, T. M. (2008). Hox repertoires for motor neuron diversity and connectivity gated by a single accessory factor, FoxP1. *Cell* **134:**304-316.

Dawson, G. R. and Tricklebank, M. D. (1995). Use of the elevated plus maze in the search for novel anxiolytic agents. *Trends Pharmacol Sci* **16:**33-36.

Deacon, T., Pakzaban, P. and Isacson, O. (1994). The lateral ganglionic eminence is the origin of cells committed to striatal phenotypes: neural transplantation and developmental evidence. *Brain Research* **668:**211–219.

Desplats, P. A., Kass, K. E., Gilmartin, T., Stanwood, G. D., Woodward, E. L., Head, S. R., Sutcliffe, J. G. *et al.* (2006). Selective deficits in the expression of striatal-enriched mRNAs in Huntington's disease. *J Neurochem* **96:**743-757.

Dobrossy, M., Klein, A., Janghra, N., Nikkhah, G. and Dunnett, S. B. (2011). Validating the use of M4-BAC-GFP mice as tissue donors in cell replacement therapies in a rodent model of Huntington's disease. *J Neurosci Methods* **197:**6-13.

Dobrossy, M. D. and Dunnett, S. B. (2005). Training specificity, graft development and graft-mediated functional recovery in a rodent model of Huntington's disease. *Neuroscience* **132:**543-552.

Dragatsis, I. and Zeitlin, S. (2000). CaMKIIalpha-Cre transgene expression and recombination patterns in the mouse brain. *Genesis* **26:**133-135.

Drolet, G., Proulx, K., Pearson, D., Rochford, J. and Deschepper, C. F. (2002). Comparisons of behavioral and neurochemical characteristics between WKY, WKHA, and Wistar rat strains. *Neuropsychopharmacology* **27:**400-409.

Duester, G. (2008). Retinoic acid synthesis and signaling during early organogenesis. *Cell* **134:**921-931.

Dunnett, S. (1996). Neural Transplantation *Neuromethods* **32:**55-87.

Dunnett, S. B., Carter, R. J., Watts, C., Torres, E. M., Mahal, A., Mangiarini, L., Bates, G. *et al.* (1998). Striatal transplantation in a transgenic mouse model of Huntington's disease. *Exp Neurol* **154:**31-40.

Dunnett, S. B., Kendall, A. L., Watts, C. and Torres, E. M. (1997). Neuronal cell transplantation for Parkinson's and Huntington's diseases. *Br Med Bull* **53:**757-776.

Dunnett, S. B. and Rosser, A. E. (2013). Challenges for taking primary and stem cells into clinical neurotransplantation trials for neurodegenerative disease. *Neurobiol Dis*.

Dupe, V., Matt, N., Garnier, J. M., Chambon, P., Mark, M. and Ghyselinck, N. B. (2003). A newborn lethal defect due to inactivation of retinaldehyde dehydrogenase type 3 is prevented by maternal retinoic acid treatment. *Proc Natl Acad Sci U S A* **100:**14036-14041.

Eagleson, K. L., Schlueter McFadyen-Ketchum, L. J., Ahrens, E. T., Mills, P. H., Does, M. D., Nickols, J. and Levitt, P. (2007). Disruption of Foxg1 expression by knock-in of cre recombinase: effects on the development of the mouse telencephalon. *Neuroscience* **148:**385-399.

Echelard, Y., Epstein, D., St-Jacques, B., Shen, L., Mohler, J., McMahon, J. and McMahon, A. (1993). Sonic hedgehog, a member of a family of putative signaling molecules, is implicated in the regulation of CNS polarity. *Cell* **75 (7):**1417-1430.

Ehrlich, M. E., Rosen, N. L., Kurihara, T., Shalaby, I. A. and Greengard, P. (1990). DARPP-32 development in the caudate nucleus is independent of afferent input from the substantia nigra. *Developmental Brain Research* **54:**257-263.

Epstein, J. N., Erkanli, A., Conners, C. K., Klaric, J., Costello, J. E. and Angold, A. (2003). Relations between Continuous Performance Test performance measures and ADHD behaviors. *J Abnorm Child Psychol* **31:**543-554.

Ericson, J., Muhr, J., Placzek, M., Lints, T., Jessell, T. and Edlund, T. (1995). Sonic hedgehog induces the differentiation of ventral forebrain neurons: a common signal for ventral patterning within the neural tube. *Cell* **81(5):**747-756.

Evans, A. E., Kelly, C. M., Precious, S. V. and Rosser, A. E. (2012). Molecular regulation of striatal development: a review. *Anat Res Int* **2012:**106529.

Evans, M. J. and Kaufman, M. H. (1981). Establishment in culture of pluripotential cells from mouse embryos. *Nature* **292:**154-156.

Faraone, S. V., Perlis, R. H., Doyle, A. E., Smoller, J. W., Goralnick, J. J., Holmgren, M. A. and Sklar, P. (2005). Molecular genetics of attention-deficit/hyperactivity disorder. *Biol Psychiatry* **57:**1313-1323.

Feng, X., Ippolito, G. C., Tian, L., Wiehagen, K., Oh, S., Sambandam, A., Willen, J. *et al.* (2010). Foxp1 is an essential transcriptional regulator for the generation of quiescent naive T cells during thymocyte development. *Blood* **115:**510-518.

Ferland, R. J., Cherry, T. J., Preware, P. O., Morrisey, E. E. and Walsh, C. A. (2003). Characterization of Foxp2 and Foxp1 mRNA and protein in the developing and mature brain. *J Comp Neurol* **460:**266-279.

Finlay, B. L. and Darlington, R. B. (1995). Linked regularities in the development and evolution of mammalian brains. *Science* **268:**1578-1584.

Fode, C., Ma, Q., Casarosa, S., Ang, S. L., Anderson, D. J. and Guillemot, F. (2000). A role for neural determination genes in specifying the dorsoventral identity of telencephalic neurons. *Genes Dev* **14:**67-80.

Foster, G., Schultzberg, M., Hakfelt, T., Goldstein, M., Hemmings, H., Jr.,, Ouimet, C., Walaas, S. *et al.* (1987). Development of a Dopamine- and Cyclic Adenosine 3'5Monophosphate-Regulated Phosphoprotein (DARPP-32) in the Prenatal Rat Central Nervous System, and Its Relationship to the Arrival of Presumptive Dopaminergic Innervation. *The Journal of Neuroscience* **7:**1994-2018.

Fox, S. B., Brown, P., Han, C., Ashe, S., Leek, R. D., Harris, A. L. and Banham, A. H. (2004). Expression of the forkhead transcription factor FOXP1 is associated with estrogen receptor alpha and improved survival in primary human breast carcinomas. *Clin Cancer Res* **10:**3521-3527.

Freeman, T. B., Sanberg, P. R. and Isacson, O. (1995). Development of the human striatum: implications for fetal striatal transplantation in the treatment of Huntington's disease. *Cell Transplant* **4:**539-545.

Fricker-Gates, R. A., White, A., Gates, M. A. and Dunnett, S. B. (2004). Striatal neurons in striatal grafts are derived from both post-mitotic cells and dividing progenitors. *Eur J Neurosci* **19:**513-520.

Fuccillo, M., Rallu, M., McMahon, A. P. and Fishell, G. (2004). Temporal requirement for hedgehog signaling in ventral telencephalic patterning. *Development* **131:**5031-5040.

Furuta, Y., Piston, D. W. and Hogan, B. L. (1997). Bone morphogenetic proteins (BMPs) as regulators of dorsal forebrain development. *Development* **124:**2203-2212.

Gabut, M., Samavarchi-Tehrani, P., Wang, X., Slobodeniuc, V., O'Hanlon, D., Sung, H. K., Alvarez, M. *et al.* (2011). An alternative splicing switch regulates embryonic stem cell pluripotency and reprogramming. *Cell* **147:**132-146.

Gainetdinov, R. R., Jones, S. R., Fumagalli, F., Wightman, R. M. and Caron, M. G. (1998). Re-evaluation of the role of the dopamine transporter in dopamine system homeostasis. *Brain Res Brain Res Rev* **26:**148-153.

Gainetdinov, R. R., Wetsel, W. C., Jones, S. R., Levin, E. D., Jaber, M. and Caron, M. G. (1999). Role of serotonin in the paradoxical calming effect of psychostimulants on hyperactivity. *Science* **283:**397-401.

Garel, S., Marin, F., Grosschedl, R. and Charnay, P. (1999). Ebf1 controls early cell differentiation in the embryonic striatum. *Development* **126:**5285-5294.

Gaveriaux-Ruff, C. and Kieffer, B. L. (2007). Conditional gene targeting in the mouse nervous system: Insights into brain function and diseases. *Pharmacol Ther* **113:**619-634.

Gerfen, C. (1992). The neostriatal mosaic: Multiple levels of compartmental organization. *Trends in Neuroscience* **15:**133–139.

Gerfen, C. R. (1984). The neostriatal mosaic: compartmentalization of corticostriatal input and striatonigral output systems. *Nature* **311:**461-464.

Gerfen, C. R., Baimbridge, K. G. and Miller, J. J. (1985). The neostriatal mosaic: compartmental distribution of calcium-binding protein and parvalbumin in the basal ganglia of the rat and monkey. *Proc Natl Acad Sci U S A* **82:**8780-8784.

Gerfen, C. R. and Young, W. S., 3rd. (1988). Distribution of striatonigral and striatopallidal peptidergic neurons in both patch and matrix compartments: an in situ hybridization histochemistry and fluorescent retrograde tracing study. *Brain Res* **460:**161-167.

Giatromanolaki, A., Koukourakis, M. I., Sivridis, E., Gatter, K. C., Harris, A. L. and Banham, A. H. (2006). Loss of expression and nuclear/cytoplasmic localization of the FOXP1 forkhead transcription factor are common events in early endometrial cancer: relationship with estrogen receptors and HIF-1alpha expression. *Mod Pathol* **19:**9-16.

Giros, B., Jaber, M., Jones, S. R., Wightman, R. M. and Caron, M. G. (1996). Hyperlocomotion and indifference to cocaine and amphetamine in mice lacking the dopamine transporter. *Nature* **379:**606-612.

Goatly, A., Bacon, C. M., Nakamura, S., Ye, H., Kim, I., Brown, P. J., Ruskone-Fourmestraux, A. *et al.* (2008). FOXP1 abnormalities in lymphoma: translocation breakpoint mapping reveals insights into deregulated transcriptional control. *Mod Pathol* **21:**902-911.

Golden, J. A., Bracilovic, A., McFadden, K. A., Beesley, J. S., Rubenstein, J. L. and Grinspan, J. B. (1999). Ectopic bone morphogenetic proteins 5 and 4 in the chicken forebrain lead to cyclopia and holoprosencephaly. *Proc Natl Acad Sci U S A* **96:**2439-2444.

Gong, S., Doughty, M., Harbaugh, C., Cummins, A., Hatten, M., Heintz, N. and Campbell, K. (2007). Targeting Cre Recombinase to Specific Neuron Populations with Bacterial Artificial Chromosome Constructs. *The Jounral of Neuroscience* **27(37):**9817–9823.

Gotz, M. and Huttner, W. B. (2005). The cell biology of neurogenesis. *Nat Rev Mol Cell Biol* **6:**777-788.

Graybiel, A. M., Liu, F. C. and Dunnett, S. B. (1989). Intrastriatal grafts derived from fetal striatal primordia. I. Phenotypy and modular organization. *J Neurosci* **9:**3250-3271.

Graybiel, A. M. and Ragsdale, C. W., Jr. (1978). Histochemically distinct compartments in the striatum of human, monkeys, and cat demonstrated by acetylthiocholinesterase staining. *Proc Natl Acad Sci U S A* **75:**5723-5726.

Groen, J. L., de Bie, R. M., Foncke, E. M., Roos, R. A., Leenders, K. L. and Tijssen, M. A. (2010). Late-onset Huntington disease with intermediate CAG repeats: true or false? *J Neurol Neurosurg Psychiatry* **81:**228-230.

Grove, E. A., Tole, S., Limon, J., Yip, L. and Ragsdale, C. W. (1998). The hem of the embryonic cerebral cortex is defined by the expression of multiple Wnt genes and is compromised in Gli3-deficient mice. *Development* **125:**2315-2325.

Gunhaga, L., Marklund, M., Sjodal, M., Hsieh, J. C., Jessell, T. M. and Edlund, T. (2003). Specification of dorsal telencephalic character by sequential Wnt and FGF signaling. *Nat Neurosci* **6:**701-707.

Gustafson, E. L., Ehrlich, M. E., Trivedi, P. and Greengard, P. (1992). Developmental regulation of phosphoprotein gene expression in the caudate-putamen of rat: an in situ hybridization study. *Neuroscience* **51:**65-75.

Gyertyan, I. (1995). Analysis of the marble burying response: marbles serve to measure digging rather than evoke burying. *Behav Pharmacol* **6:**24-31.

Hahn, M. K., Steele, A., Couch, R. S., Stein, M. A. and Krueger, J. J. (2009). Novel and functional norepinephrine transporter protein variants identified in attention-deficit hyperactivity disorder. *Neuropharmacology* **57:**694-701.

Hamasaki, T., Goto, S., Nishikawa, S. and Ushio, Y. (2003). Neuronal cell migration for the developmental formation of the mammalian striatum. *Brain Res Brain Res Rev* **41:**1-12.

Hamdan, F. F., Daoud, H., Rochefort, D., Piton, A., Gauthier, J., Langlois, M., Foomani, G. *et al.* (2010). De novo mutations in FOXP1 in cases with intellectual disability, autism, and language impairment. *Am J Hum Genet* **87:**671-678.

Haralambieva, E., Adam, P., Ventura, R., Katzenberger, T., Kalla, J., Holler, S., Hartmann, M. *et al.* (2006). Genetic rearrangement of FOXP1 is predominantly detected in a subset of diffuse large B-cell lymphomas with extranodal presentation. *Leukemia* **20:**1300-1303.

Harper, P. (1997). Huntgiton's Disease. WB Saunders company Ltd.

Harris, E. and Barraclough, B. (1994). Suicide as an outcome of medical disorders *Medicine(Baltimore)* **73:**281-296.

Haskell, G. T. and LaMantia, A. S. (2005). Retinoic acid signaling identifies a distinct precursor population in the developing and adult forebrain. *J Neurosci* **25:**7636-7647.

Heal, D. J., Cheetham, S. C. and Smith, S. L. (2009). The neuropharmacology of ADHD drugs in vivo: insights on efficacy and safety. *Neuropharmacology* **57:**608-618.

Hebert, J. and McConnell, S. (2000). Targeting of cre to the Foxg1 (BF-1) locus mediates loxP recombination in the telencephalon and other developing head structures. *Dev Biol* **222:**296-306.

Hebert, J. M. and Fishell, G. (2008). The genetics of early telencephalon patterning: some assembly required. *Nat Rev Neurosci* **9:**678-685.

Higginbotham, H., Guo, J., Yokota, Y., Umberger, N. L., Su, C. Y., Li, J., Verma, N. *et al.* (2013). Arl13b-regulated cilia activities are essential for polarized radial glial scaffold formation. *Nat Neurosci* 1000-1007.

Hill, R. E., Favor, J., Hogan, B. L., Ton, C. C., Saunders, G. F., Hanson, I. M., Prosser, J. *et al.* (1991). Mouse small eye results from mutations in a paired-like homeobox-containing gene. *Nature* **354:**522-525.

Hisaoka, T., Nakamura, Y., Senba, E. and Morikawa, Y. (2010). The forkhead transcription factors, Foxp1 and Foxp2, identify different subpopulations of projection neurons in the mouse cerebral cortex. *Neuroscience* **166:**551-563.

Horn, D., Kapeller, J., Rivera-Brugues, N., Moog, U., Lorenz-Depiereux, B., Eck, S., Hempel, M. *et al.* (2010). Identification of FOXP1 deletions in three unrelated patients

with mental retardation and significant speech and language deficits. *Hum Mutat* **31:**E1851-1860.

Houart, C., Caneparo, L., Heisenberg, C., Barth, K., Take-Uchi, M. and Wilson, S. (2002). Establishment of the telencephalon during gastrulation by local antagonism of Wnt signaling. *Neuron* **35:**255-265.

Hsieh-Li, H. M., Witte, D. P., Szucsik, J. C., Weinstein, M., Li, H. and Potter, S. S. (1995). Gsh-2, a murine homeobox gene expressed in the developing brain. *Mech Dev* **50:**177-186.

Hu, H., Wang, B., Borde, M., Nardone, J., Maika, S., Allred, L., Tucker, P. W. *et al.* (2006). Foxp1 is an essential transcriptional regulator of B cell development. *Nat Immunol* **7:**819-826.

Jain, M., Armstrong, R., Barker, R. and Rosser, A. (2001). Cellular and molecular aspects of striatal development. *Brain Research Bulletin* **55(4):**533-540.

Jepsen, K., Gleiberman, A. S., Shi, C., Simon, D. I. and Rosenfeld, M. G. (2008). Cooperative regulation in development by SMRT and FOXP1. *Genes Dev* **22:**740-745.

Jessell, T. (2000). Neuronal specification in the spinal cord:inductive signals and transcriptional codes. *Nature Reviews genetics* **1:**20-29.

Jimenez-Castellanos, J. and Graybiel, A. M. (1987). Subdivisions of the dopamine-containing A8-A9-A10 complex identified by their differential mesostriatal innervation of striosomes and extrastriosomal matrix. *Neuroscience* **23:**223-242.

Johann, V., Schiefer, J., Sass, C., Mey, J., Brook, G., Kruttgen, A., Schlangen, C. *et al.* (2007). Time of transplantation and cell preparation determine neural stem cell survival in a mouse model of Huntington's disease. *Exp Brain Res* **177:**458-470.

Jones, S. R., Gainetdinov, R. R., Jaber, M., Giros, B., Wightman, R. M. and Caron, M. G. (1998). Profound neuronal plasticity in response to inactivation of the dopamine transporter. *Proc Natl Acad Sci U S A* **95:**4029-4034.

Kaufmann, E. and Knochel, W. (1996). Five years on the wings of fork head. *Mech Dev* **57:**3-20.

Kelly, C., Dunnett, S. and Rosser, A. (2009). Medium Spiny neurones for transplantation in Huntington's Disease. . *Biochemical Society Transations* **37:**323-328.

Kelly, C., Precious, S., Penketh, R., Amso, N., Dunnett, S. and Rosser, A. (2007). Striatal graft projections are influenced by donor cell type and not the immunogenic background. *Brain* **130:**1317-1329.

Kelly, C. M., Precious, S. V., Torres, E. M., Harrison, A. W., Williams, D., Scherf, C., Weyrauch, U. M. *et al.* (2011). Medical terminations of pregnancy: a viable source of tissue for cell replacement therapy for neurodegenerative disorders. *Cell Transplant* **20:**503-513.

Kessaris, N., Fogarty, M., Iannarelli, P., Grist, M., Wegner, M. and Richardson, W. D. (2006). Competing waves of oligodendrocytes in the forebrain and postnatal elimination of an embryonic lineage. *Nat Neurosci* **9:**173-179.

Kimura, S., Hara, Y., Pineau, T., Fernandez-Salguero, P., Fox, C., Ward, J. and FJ, G. (1996). The T/ebp null mouse: thyroid specific enhancer-binding protein is essential for the organogenesis of the thyroid, lung, ventral forebrain, and pituitary. *Genes and Development* **10** 60-69.

Kita, H. and Kitai, S. T. (1987). Efferent projections of the subthalamic nucleus in the rat: light and electron microscopic analysis with the PHA-L method. *J Comp Neurol* **260:**435-452.

Kita, H. and Kitai, S. T. (1988). Glutamate decarboxylase immunoreactive neurons in rat neostriatum: their morphological types and populations. *Brain Res* **447:**346-352.

Koda, K., Ago, Y., Cong, Y., Kita, Y., Takuma, K. and Matsuda, T. (2010). Effects of acute and chronic administration of atomoxetine and methylphenidate on extracellular levels of noradrenaline, dopamine and serotonin in the prefrontal cortex and striatum of mice. *J Neurochem* **114:**259-270.

Kohtz, J., Baker, D., Corte, G. and Fishell, G. (1998). Regionalization within the mammalian telencephalon is mediated by changes in responsiveness to Sonic Hedgehog. *Development* **125:**5079 –5089.

Konstantoulas, C. J., Parmar, M. and Li, M. (2010). FoxP1 promotes midbrain identity in embryonic stem cell-derived dopamine neurons by regulating Pitx3. *J Neurochem* **113:**836-847.

Kremer, B., Goldberg, P., Andrew, S., Theilmann, J., Telenius, H., Zeisler, J., Squitieri, F. *et al.* (1994). A worldwide study of the Huntington's disease mutation. The sensitivity and specificity of measuring CAG repeats. *The New England journal of medicine* **330:**1401-1406.

Kuwajima, T., Nishimura, I. and Yoshikawa, K. (2006). Necdin promotes GABAergic neuron differentiation in cooperation with Dlx homeodomain proteins. *J Neurosci* **26:**5383-5392.

Lanska, D., Lanska MJ, Lavine, L. and Schoenberg, B. (1998). Conditions Associated With Huntington's Disease at Death: A Case-Control Study. *Archives Neurology* **45:**878-880.

Lee, M. K., Tuttle, J. B., Rebhun, L. I., Cleveland, D. W. and Frankfurter, A. (1990). The expression and posttranslational modification of a neuron-specific beta-tubulin isotype during chick embryogenesis. *Cell Motil Cytoskeleton* **17:**118-132.

Leifer, D., Krainc, D., Yu, Y. T., McDermott, J., Breitbart, R. E., Heng, J., Neve, R. L. *et al.* (1993). MEF2C, a MADS/MEF2-family transcription factor expressed in a laminar distribution in cerebral cortex. *Proc Natl Acad Sci U S A* **90:**1546-1550.

Lempp, T., Toennes, S. W., Wunder, C., Russe, O. Q., Moser, C. V., Kynast, K. L., Freitag, C. M. *et al.* (2013). Altered gene expression in the prefrontal cortex of young rats induced by the ADHD drug atomoxetine. *Prog Neuropsychopharmacol Biol Psychiatry* **40:**221-228.

Li, H., Radford, J. C., Ragusa, M. J., Shea, K. L., McKercher, S. R., Zaremba, J. D., Soussou, W. *et al.* (2008). Transcription factor MEF2C influences neural stem/progenitor cell differentiation and maturation in vivo. *Proc Natl Acad Sci U S A* **105:**9397-9402.

Li, S., Wang, Y., Zhang, Y., Lu, M. M., DeMayo, F. J., Dekker, J. D., Tucker, P. W. *et al.* (2012). Foxp1/4 control epithelial cell fate during lung development and regeneration through regulation of anterior gradient 2. *Development* **139:**2500-2509.

Li, S., Weidenfeld, J. and Morrisey, E. (2004). Transcriptional and DNA binding activity of the Foxp1/2/4 family is modulated by heterotypic and homotypic protein interactions. *Mol Cell Biol* **24:**809-822.

Liang, H., Hippenmeyer, S. and Ghashghaei, H. T. (2012). A Nestin-cre transgenic mouse is insufficient for recombination in early embryonic neural progenitors. *Biol Open* **1:**1200-1203.

Lichtenstein, P., Carlstrom, E., Rastam, M., Gillberg, C. and Anckarsater, H. (2010). The genetics of autism spectrum disorders and related neuropsychiatric disorders in childhood. *Am J Psychiatry* **167:**1357-1363.

Lin, Q., Schwarz, J., Bucana, C. and Olson, E. N. (1997). Control of mouse cardiac morphogenesis and myogenesis by transcription factor MEF2C. *Science* **276:**1404-1407.

Lister, R. G. (1987). The use of a plus-maze to measure anxiety in the mouse. *Psychopharmacology (Berl)* **92:**180-185.

Liu, J., Githinji, J., McLaughlin, B., Wilczek, K. and Nolta, J. (2012). Role of miRNAs in neuronal differentiation from human embryonic stem cell-derived neural stem cells. *Stem Cell Rev* **8:**1129-1137.

Liu, J. K., Ghattas, I., Liu, S., Chen, S. and Rubenstein, J. L. (1997). Dlx genes encode DNA-binding proteins that are expressed in an overlapping and sequential pattern during basal ganglia differentiation. *Dev Dyn* **210:**498-512.

Liu, L., Cavanaugh, J. E., Wang, Y., Sakagami, H., Mao, Z. and Xia, Z. (2003). ERK5 activation of MEF2-mediated gene expression plays a critical role in BDNF-promoted survival of developing but not mature cortical neurons. *Proc Natl Acad Sci USA* **100:**8532-8537.

Lobe, C. G., Koop, K. E., Kreppner, W., Lomeli, H., Gertsenstein, M. and Nagy, A. (1999). Z/AP, a double reporter for cre-mediated recombination. *Dev Biol* **208:**281-292.

Long, J. E., Garel, S., Alvarez-Dolado, M., Yoshikawa, K., Osumi, N., Alvarez-Buylla, A. and Rubenstein, J. L. (2007). Dlx-dependent and -independent regulation of olfactory bulb interneuron differentiation. *J Neurosci* **27:**3230-3243.

Long, J. E., Swan, C., Liang, W. S., Cobos, I., Potter, G. B. and Rubenstein, J. L. (2009). Dlx1&2 and Mash1 transcription factors control striatal patterning and differentiation through parallel and overlapping pathways. *J Comp Neurol* **512:**556-572.

Lyons, G. E., Micales, B. K., Schwarz, J., Martin, J. F. and Olson, E. N. (1995). Expression of mef2 genes in the mouse central nervous system suggests a role in neuronal maturation. *J Neurosci* **15:**5727-5738.

Ma, L., Hu, B., Liu, Y., Vermilyea, S. C., Liu, H., Gao, L., Sun, Y. *et al.* (2012). Human embryonic stem cell-derived GABA neurons correct locomotion deficits in quinolinic acid-lesioned mice. *Cell Stem Cell* **10:**455-464.

Malatesta, P. and Gotz, M. (2013). Radial glia - from boring cables to stem cell stars. *Development* **140:**483-486.

Malatesta, P., Hack, M. A., Hartfuss, E., Kettenmann, H., Klinkert, W., Kirchhoff, F. and Götz, M. (2003). Neuronal or Glial Progeny: Regional Differences in Radial Glia Fate. *Neuron* **37:**751-764.

Malatesta, P., Hartfuss, E. and Gotz, M. (2000). Isolation of radial glial cells by fluorescent-activated cell sorting reveals a neuronal lineage. *Development* **127:**5253-5263.

Manuel, M., Martynoga, B., Yu, T., West, J. D., Mason, J. O. and Price, D. J. (2010). The transcription factor Foxg1 regulates the competence of telencephalic cells to adopt subpallial fates in mice. *Development* **137:**487-497.

Manuel, M. N., Martynoga, B., Molinek, M. D., Quinn, J. C., Kroemmer, C., Mason, J. O. and Price, D. J. (2011). The transcription factor Foxg1 regulates telencephalic progenitor proliferation cell autonomously, in part by controlling Pax6 expression levels. *Neural Dev* **6:**9.

Mao, Z., Bonni, A., Xia, F., Nadal-Vicens, M. and Greenberg, M. E. (1999). Neuronal activity-dependent cell survival mediated by transcription factor MEF2. *Science* **286:**785-790.

Maretto, S., Cordenonsi, M., Dupont, S., Braghetta, P., Broccoli, V., Hassan, A. B., Volpin, D. *et al.* (2003). Mapping Wnt/beta-catenin signaling during mouse development and in colorectal tumors. *Proc Natl Acad Sci U S A* **100:**3299-3304.

Marigo, V., Johnson, R. L., Vortkamp, A. and Tabin, C. J. (1996). Sonic hedgehog differentially regulates expression of GLI and GLI3 during limb development. *Dev Biol* **180:**273-283.

Marin, O., Anderson, S. A. and Rubenstein, J. L. (2000). Origin and molecular specification of striatal interneurons. *J Neurosci* **20:**6063-6076.

Mark, M., Ghyselinck, N. B. and Chambon, P. (2006). Function of retinoid nuclear receptors: lessons from genetic and pharmacological dissections of the retinoic acid signaling pathway during mouse embryogenesis. *Annu Rev Pharmacol Toxicol* **46:**451-480.

Marklund, M., Sjodal, M., Beehler, B. C., Jessell, T. M., Edlund, T. and Gunhaga, L. (2004). Retinoic acid signalling specifies intermediate character in the developing telencephalon. *Development* **131:**4323-4332.

Martin-Ibanez, R., Crespo, E., Esgleas, M., Urban, N., Wang, B., Waclaw, R., Georgopoulos, K. *et al.* (2012). Helios transcription factor expression depends on Gsx2 and Dlx1&2 function in developing striatal matrix neurons. *Stem Cells Dev* **21:**2239-2251.

Martın-Ibanez, R., Crespo, E., Urban N, S, S.-T., Herranz C, M, J., Valiente M *et al.* (2010). Ikaros-1 Couples Cell Cycle Arrest of Late Striatal Precursors With Neurogenesis of Enkephalinergic Neurons. *The Journal of Comparative Neurology* **518:**329–351.

Martin, G. R. (1981). Isolation of a pluripotent cell line from early mouse embryos cultured in medium conditioned by teratocarcinoma stem cells. *Proc Natl Acad Sci USA* **78:**7634-7638.

Martynoga, B., Morrison, H., Price, D. J. and Mason, J. O. (2005). Foxg1 is required for specification of ventral telencephalon and region-specific regulation of dorsal telencephalic precursor proliferation and apoptosis. *Dev Biol* **283:**113-127.

Mason, H. A., Rakowiecki, S. M., Raftopoulou, M., Nery, S., Huang, Y., Gridley, T. and Fishell, G. (2005). Notch signaling coordinates the patterning of striatal compartments. *Development* **132:**4247-4258.

Mason, I. (2007). Initiation to end point: the multiple roles of fibroblast growth factors in neural development. *Nature Reviews Neuroscience* **8:**583-596

Molotkova, N., Molotkov, A. and Duester, G. (2007). Role of retinoic acid during forebrain development begins late when Raldh3 generates retinoic acid in the ventral subventricular zone. *Dev Biol* **303:**601-610.

Molyneaux, B. J., Arlotta, P., Menezes, J. R. and Macklis, J. D. (2007). Neuronal subtype specification in the cerebral cortex. *Nat Rev Neurosci* **8:**427-437.

Montgomery, K. (1955). The relationship between fear induced by novel stimulation and exploratory behaviour. *J. Comp. Physiol. Psychol.* **48:**254-226.

Monuki, E. S., Porter, F. D. and Walsh, C. A. (2001). Patterning of the dorsal telencephalon and cerebral cortex by a roof plate-Lhx2 pathway. *Neuron* **32:**591-604.

Nair, J., Ehimare, U., Beitman, B. D., Nair, S. S. and Lavin, A. (2006). Clinical review: evidence-based diagnosis and treatment of ADHD in children. *Mo Med* **103:**617-621.

Navarra, R., Graf, R., Huang, Y., Logue, S., Comery, T., Hughes, Z. and Day, M. (2008). Effects of atomoxetine and methylphenidate on attention and impulsivity in the 5-choice serial reaction time test. *Prog Neuropsychopharmacol Biol Psychiatry* **32:**34-41.

Nery, S., Corbin, J. G. and Fishell, G. (2003). Dlx2 progenitor migration in wild type and Nkx2.1 mutant telencephalon. *Cereb Cortex* **13:**895-903.

Nicolas, L. B., Kolb, Y. and Prinssen, E. P. (2006). A combined marble burying-locomotor activity test in mice: a practical screening test with sensitivity to different classes of anxiolytics and antidepressants. *Eur J Pharmacol* **547:**106-115.

Nicoleau, C., Varela, C., Bonnefond, C., Maury, Y., Bugi, A., Aubry, L., Viegas, P. *et al.* (2013). Embryonic stem cells neural differentiation qualifies the role of Wnt/beta-Catenin signals in human telencephalic specification and regionalization. *Stem Cells* **31:**1763-1774.

Njung'e, K. and Handley, S. L. (1991). Evaluation of marble-burying behavior as a model of anxiety. *Pharmacol Biochem Behav* **38:**63-67.

Noctor, S. C., Flint, A. C., Weissman, T. A., Wong, W. S., Clinton, B. K. and Kriegstein, A. R. (2002). Dividing precursor cells of the embryonic cortical ventricular zone have morphological and molecular characteristics of radial glia. *J Neurosci* **22:**3161-3173.

Ohkubo, Y., Chiang, C. and Rubenstein, J. (2002). Coordinate regulation and synergistic actions of BMP4, SHH and FGF8 in the rostral prosencephalon regulate morphogenesis of the telencephalic and optic vesicles. . *Neuroscience* **111:**1–17.

Okamoto, K. and Aoki, K. (1963). Development of a strain of spontaneously hypertensive rats. *Jpn Circ J* **27:**282-293.

Okamoto, S., Krainc, D., Sherman, K. and Lipton, S. A. (2000). Antiapoptotic role of the p38 mitogen-activated protein kinase-myocyte enhancer factor 2 transcription factor pathway during neuronal differentiation. *Proc Natl Acad Sci U S A* **97:**7561-7566.

Olsson, M., Bjorklund, A. and Campbell, K. (1998). Early specification of striatal projection neurons and interneuronal subtypes in the lateral and medial ganglionic eminence. *Neuroscience* **84:**867– 876

Olsson, M., Campbell, K., Wictorin, K. and Bjorklund, A. (1995). Projection neurons in fetal striatal transplants are predominantly derived from the lateral ganglionic eminence. *Neuroscience* **69:**1169-1182.

Otaegi, G., Pollock, A., Hong, J. and Sun, T. (2011). MicroRNA miR-9 modifies motor neuron columns by a tuning regulation of FoxP1 levels in developing spinal cords. *J Neurosci* **31:**809-818.

Ouimet, C. C., Miller, P. E., Hemmings, H. C., Jr., Walaas, S. I. and Greengard, P. (1984). DARPP-32, a dopamine- and adenosine 3':5'-monophosphate-regulated phosphoprotein enriched in dopamine-innervated brain regions. III. Immunocytochemical localization. *J Neurosci* **4:**111-124.

Owens, D. F., Boyce, L. H., Davis, M. B. and Kriegstein, A. R. (1996). Excitatory GABA responses in embryonic and neonatal cortical slices demonstrated by gramicidin perforated-patch recordings and calcium imaging. *J Neurosci* **16:**6414-6423.

Paek, H., Gutin, G. and JM., H. (2009). FGF signalling is strictly required to maintain early telencephalic precursor cell survival. *Development* **136:**2457-2465.

Pakzaban, P., Deacon, T. W., Burns, L. H. and Isacson, O. (1993). Increased proportion of acetylcholinesterase-rich zones and improved morphological integration in host striatum of fetal grafts derived from the lateral but not the medial ganglionic eminence. *Exp Brain Res* **97:**13-22.

Palumbo, O., D'Agruma, L., Minenna, A. F., Palumbo, P., Stallone, R., Palladino, T., Zelante, L. *et al.* (2013). 3p14.1 de novo microdeletion involving the FOXP1 gene in an adult patient with autism, severe speech delay and deficit of motor coordination. *Gene* **516:**107-113.

Park, H. L., Bai, C., Platt, K. A., Matise, M. P., Beeghly, A., Hui, C. C., Nakashima, M. *et al.* (2000). Mouse Gli1 mutants are viable but have defects in SHH signaling in combination with a Gli2 mutation. *Development* **127:**1593-1605.

Pei, Z., Wang, B., Chen, G., Nagao, M., Nakafuku, M. and Campbell, K. (2011). Homeobox genes Gsx1 and Gsx2 differentially regulate telencephalic progenitor maturation. *Proc Natl Acad Sci U S A* **108:**1675-1680.

Pellow, S., Chopin, P., File, S. E. and Briley, M. (1985). Validation of open:closed arm entries in an elevated plus-maze as a measure of anxiety in the rat. *J Neurosci Methods* **14:**149-167.

Perrier, A. and Peschanski, M. (2012). How can human pluripotent stem cells help decipher and cure Huntington's disease? *Cell Stem Cell* **11:**153-161.

Pert, C. B., Kuhar, M. J. and Snyder, S. H. (1976). Opiate receptor: autoradiographic localization in rat brain. *Proc Natl Acad Sci U S A* **73:**3729-3733.

Pliszka, S. R. (1989). Effect of anxiety on cognition, behavior, and stimulant response in ADHD. *J Am Acad Child Adolesc Psychiatry* **28:**882-887.

Polderman, T. J., Hoekstra, R. A., Vinkhuyzen, A. A., Sullivan, P. F., van der Sluis, S. and Posthuma, D. (2013). Attentional switching forms a genetic link between attention problems and autistic traits in adults. *Psychol Med* **43:**1985-1996.

Porteus, M. H., Bulfone, A., Liu, J. K., Puelles, L., Lo, L. C. and Rubenstein, J. L. (1994). DLX-2, MASH-1, and MAP-2 expression and bromodeoxyuridine incorporation define molecularly distinct cell populations in the embryonic mouse forebrain. *J Neurosci* **14:**6370-6383.

Precious, S. V. and Rosser, A. E. (2012). Producing striatal phenotypes for transplantation in Huntington's disease. *Exp Biol Med (Maywood)* **237:**343-351.

Puelles, L., Kuwan, a. E., Puelles, E., Bulfone, A., Shimamura, K., Kelehe, r. J., SmigaS *et al.* (2000). Pallial and subpallial derivatives in the embryonic chick and mouse telencephalon, traced by the expression of the genes Dlx-2, Emx-1, Nkx-2.1, Pax-6, and Tbr-1. *J. Comp. Neurol* **424:** 409–438.

Quinn, J. C., West, J. D. and Hill, R. E. (1996). Multiple functions for Pax6 in mouse eye and nasal development. *Genes Dev* **10:**435-446.

Rajput, P. S., Kharmate, G., Somvanshi, R. K. and Kumar, U. (2009). Colocalization of dopamine receptor subtypes with dopamine and cAMP-regulated phosphoprotein (DARPP-32) in rat brain. *Neurosci Res* **65:**53-63.

Rallu, M., Machold, R., Gaiano, N., Corbin, J. G., McMahon, A. P. and Fishell, G. (2002). Dorsoventral patterning is established in the telencephalon of mutants lacking both Gli3 and Hedgehog signaling. *Development* **129:**4963-4974.

Rayoo, M., Yan, M., Takano, E. A., Bates, G. J., Brown, P. J., Banham, A. H. and Fox, S. B. (2009). Expression of the forkhead box transcription factor FOXP1 is associated with oestrogen receptor alpha, oestrogen receptor beta and improved survival in familial breast cancers. *J Clin Pathol* **62:**896-902.

Robbins, T. W. (2002). The 5-choice serial reaction time task: behavioural pharmacology and functional neurochemistry. *Psychopharmacology (Berl)* **163:**362-380.

Roberton, V. H., Evans, A. E., Harrison, D. J., Precious, S. V., Dunnett, S. B., Kelly, C. M. and Rosser, A. E. (2013). Is the adult mouse striatum a hostile host for neural transplant survival? *Neuroreport* **24:**1010-1015.

Rodgers, R. J. and Johnson, N. J. (1995). Factor analysis of spatiotemporal and ethological measures in the murine elevated plus-maze test of anxiety. *Pharmacol Biochem Behav* **52:**297-303.

Roelink, H., Porter. JA, Chiang, C., Tanabe, Y., Chang, D., Beachy, P. and Jessell, T. (1995). Floor plate and motor neuron induction by different concentrations of the amino-terminal cleavage product of sonic hedgehog autoproteolysis. *Cell* **81(3):**445-455.

Ronald, A., Larsson, H., Anckarsater, H. and Lichtenstein, P. (2011). A twin study of autism symptoms in Sweden. *Mol Psychiatry* **16:**1039-1047.

Rosas, H. D., Liu, A. K., Hersch, S., Glessner, M., Ferrante, R. J., Salat, D. H., van der Kouwe, A. *et al.* (2002). Regional and progressive thinning of the cortical ribbon in Huntington's disease. *Neurology* **58:**695-701.

Rosas, H. D., Salat, D. H., Lee, S. Y., Zaleta, A. K., Pappu, V., Fischl, B., Greve, D. *et al.* (2008). Cerebral cortex and the clinical expression of Huntington's disease: complexity and heterogeneity. *Brain* **131:**1057-1068.

Rosser, A. E., Barker, R. A., Harrower, T., Watts, C., Farrington, M., Ho, A. K., Burnstein, R. M. *et al.* (2002). Unilateral transplantation of human primary fetal tissue in four patients with Huntington's disease: NEST-UK safety report ISRCTN no 36485475. *J Neurol Neurosurg Psychiatry* **73:**678-685.

Rosser, A. E. and Dunnett, S. B. (2003). Neural transplantation in patients with Huntington's disease. *CNS Drugs* **17:**853-867.

Rosser, A. E., Kelly, C. M. and Dunnett, S. B. (2011). Cell Transplantation for Huntington's Disease: Practical and Clinical Considersations. *Future Neurology* **6:**45-62.

Rousso, D. L., Gaber, Z. B., Wellik, D., Morrisey, E. E. and Novitch, B. G. (2008). Coordinated actions of the forkhead protein Foxp1 and Hox proteins in the columnar organization of spinal motor neurons. *Neuron* **59:**226-240.

Rubenstein, J., Shimamura, K., Martinez, S. and Puelles, L. (1998). Regionalization of the prosencephalic neural plate. *Annu Rev Neurosci.* 445–477.

Sagaert, X., de Paepe, P., Libbrecht, L., Vanhentenrijk, V., Verhoef, G., Thomas, J., Wlodarska, I. *et al.* (2006). Forkhead box protein P1 expression in mucosa-associated lymphoid tissue lymphomas predicts poor prognosis and transformation to diffuse large B-cell lymphoma. *J Clin Oncol* **24:**2490-2497.

Sagardoy, A., Martinez-Ferrandis, J. I., Roa, S., Bunting, K. L., Aznar, M. A., Elemento, O., Shaknovich, R. *et al.* (2013). Downregulation of FOXP1 is required during germinal center B-cell function. *Blood* **121:**4311-4320.

Sagvolden, T. (2000). Behavioral validation of the spontaneously hypertensive rat (SHR) as an animal model of attention-deficit/hyperactivity disorder (AD/HD). *Neurosci Biobehav Rev* **24:**31-39.

Sagvolden, T., Pettersen, M. B. and Larsen, M. C. (1993). Spontaneously hypertensive rats (SHR) as a putative animal model of childhood hyperkinesis: SHR behavior compared to four other rat strains. *Physiol Behav* **54:**1047-1055.

Sandau, U. S., Alderman, Z., Corfas, G., Ojeda, S. R. and Raber, J. (2012). Astrocyte-specific disruption of SynCAM1 signaling results in ADHD-like behavioral manifestations. *PLoS One* **7:**e36424.

Schackel, S., Pauly, M. C., Piroth, T., Nikkhah, G. and Dobrossy, M. D. (2013). Donor age dependent graft development and recovery in a rat model of Huntington's disease: Histological and behavioral analysis. *Behav Brain Res*.

Schneider, R. A., Hu, D., Rubenstein, J. L., Maden, M. and Helms, J. A. (2001). Local retinoid signaling coordinates forebrain and facial morphogenesis by maintaining FGF8 and SHH. *Development* **128:**2755-2767.

Schulz, R. A., Chromey, C., Lu, M. F., Zhao, B. and Olson, E. N. (1996). Expression of the D-MEF2 transcription in the Drosophila brain suggests a role in neuronal cell differentiation. *Oncogene* **12:**1827-1831.

Schuurmans, C. and Guillemot, F. (2002). Molecular mechanisms underlying cell fate specification in the developing telencephalon. *Current Opinion in Neurobiology* **12:**26-34.

Schwarcz, R. and Kohler, C. (1983). Differential vulnerability of central neurons of the rat to quinolinic acid. *Neurosci Lett* **38:**85-90.

Schwarcz, R., Whetsell, W., Jr., and Mangano, R. (1983). Quinolinic acid: an endogenous metabolite that produces axon-sparing lesions in rat braiN. *Science* **219:**316-318.

Searle, A. (1966). New mutants,. *Mouse News Letters* **2**.

Shanmugalingam, S., Houart C, Picker A, Reifers F, Macdonald R, Barth A, Griffin K *et al.* (2000). Ace/Fgf8 is required for forebrain commissure formation and patterning of the telencephalon. *Development* **127:**2549-2561.

Shi, C., Sakuma, M., Mooroka, T., Liscoe, A., Gao, H., Croce, K. J., Sharma, A. *et al.* (2008). Down-regulation of the forkhead transcription factor Foxp1 is required for monocyte differentiation and macrophage function. *Blood* **112:**4699-4711.

Shi, C., Zhang, X., Chen, Z., Sulaiman, K., Feinberg, M. W., Ballantyne, C. M., Jain, M. K. *et al.* (2004). Integrin engagement regulates monocyte differentiation through the forkhead transcription factor Foxp1. *J Clin Invest* **114:**408-418.

Shimamura, K., Hartigan, D. J., Martinez, S., Puelles, L. and Rubenstein, J. L. (1995). Longitudinal organization of the anterior neural plate and neural tube. *Development* **121:**3923-3933.

Shimamura, K. and Rubenstein, J. (1997). Inductive interactions direct early regionalization of the mouse forebrain. *Development ,* **124:**2709-2718.

Shu, W., Lu, M. M., Zhang, Y., Tucker, P. W., Zhou, D. and Morrisey, E. E. (2007). Foxp2 and Foxp1 cooperatively regulate lung and esophagus development. *Development* **134:**1991-2000.

Shu, W., Yang, H., Zhang, L., Lu, M. and Morrisey, E. (2001). Characterization of a New Subfamily of Winged-helix/Forkhead (Fox) Genes That Are Expressed in the Lung and Act as Transcriptional Repressors. *J Biol Chem.* **276:**27488–27497.

Siesser, W. B., Zhao, J., Miller, L. R., Cheng, S. Y. and McDonald, M. P. (2006). Transgenic mice expressing a human mutant beta1 thyroid receptor are hyperactive, impulsive, and inattentive. *Genes Brain Behav* **5:**282-297.

Solanto, M. V. (1998). Neuropsychopharmacological mechanisms of stimulant drug action in attention-deficit hyperactivity disorder: a review and integration. *Behav Brain Res* **94:**127-152.

Song, J., Lee, S. T., Kang, W., Park, J. E., Chu, K., Lee, S. E., Hwang, T. *et al.* (2007). Human embryonic stem cell-derived neural precursor transplants attenuate apomorphine-induced rotational behavior in rats with unilateral quinolinic acid lesions. *Neurosci Lett* **423:**58-61.

Sontag, T. A., Tucha, O., Walitza, S. and Lange, K. W. (2010). Animal models of attention deficit/hyperactivity disorder (ADHD): a critical review. *Atten Defic Hyperact Disord* **2:**1-20.

Soriano, P. (1999). Generalized lacZ expression with the ROSA26 Cre reporter strain. *Nat Genet* **21:**70-71.

Squitieri, F. and Jankovic, J. (2012). Huntington's disease: how intermediate are intermediate repeat lengths? *Mov Disord* **27:**1714-1717.

Stehling-Sun, S., Dade, J., Nutt, S. L., DeKoter, R. P. and Camargo, F. D. (2009). Regulation of lymphoid versus myeloid fate 'choice' by the transcription factor Mef2c. *Nat Immunol* **10:**289-296.

Stenman, J., Toresson, H. and Campbell, K. (2003). Identification of two distinct progenitor populations in the lateral ganglionic eminence: implications for striatal and olfactory bulb neurogenesis. *J Neurosci* **23:**167-174.

Storm, E., Garel, S., Borello U, Hebert JM, Martinez S, McConnell SK, GR, M. *et al.* (2006). Dose-dependent functions of Fgf8 in regulating telencephalic patterning centers. *Development* **133:**1831-1844.

Stoykova, A., Fritsch, R., Walther, C. and Gruss, P. (1996). Forebrain patterning defects in Small eye mutant mice. *Development* **122:**3453-3465.

Stoykova, A., Gotz, M., Gruss, P. and Price, J. (1997). Pax6-dependent regulation of adhesive patterning, R-cadherin expression and boundary formation in developing forebrain. *Development* **124:**3765-3777.

Stoykova, A. and Gruss, P. (1994). Roles of Pax-genes in developing and adult brain as suggested by expression patterns. *J Neurosci* **14:**1395-1412.

Stoykova, A., Treichel, D., Hallonet, M. and Gruss, P. (2000). Pax6 modulates the dorsoventral patterning of the mammalian telencephalon. *J Neurosci* **20:**8042-8050.

Streubel, B., Vinatzer, U., Lamprecht, A., Raderer, M. and Chott, A. (2005). T(3;14)(p14.1;q32) involving IGH and FOXP1 is a novel recurrent chromosomal aberration in MALT lymphoma. *Leukemia* **19:**652-658.

Sturrock, R. (1980). A comparative quantitative and morphological study of ageing in the mouse neostriatum, indusium griseum and anterior commissure. *Neuropathology and Applied Neurobiology* **6:**51-68.

Surmeli, G., Akay, T., Ippolito, G. C., Tucker, P. W. and Jessell, T. M. (2011). Patterns of spinal sensory-motor connectivity prescribed by a dorsoventral positional template. *Cell* **147:**653-665.

Sussel, L., Marin, O., Kimura S and JL., R. (1999). Loss of Nkx2.1 homeobox gene function results in a ventral to dorsal molecular respecification within the basal telencephalon: evidence for a transformation of the pallidum into the striatum. *Development* **126:**3359-3370.

Swanson, C. J., Perry, K. W., Koch-Krueger, S., Katner, J., Svensson, K. A. and Bymaster, F. P. (2006). Effect of the attention deficit/hyperactivity disorder drug atomoxetine on extracellular concentrations of norepinephrine and dopamine in several brain regions of the rat. *Neuropharmacology* **50:**755-760.

Szucsik, J. C., Witte, D. P., Li, H., Pixley, S. K., Small, K. M. and Potter, S. S. (1997). Altered forebrain and hindbrain development in mice mutant for the Gsh-2 homeobox gene. *Dev Biol* **191:**230-242.

Takahashi, K., Liu, F. C., Oishi, T., Mori, T., Higo, N., Hayashi, M., Hirokawa, K. *et al.* (2008). Expression of FOXP2 in the developing monkey forebrain: comparison with the expression of the genes FOXP1, PBX3, and MEIS2. *J Comp Neurol* **509:**180-189.

Takahashi, K. and Yamanaka, S. (2006). Induction of pluripotent stem cells from mouse embryonic and adult fibroblast cultures by defined factors. *Cell* **126:**663-676.

Tamura, S., Morikawa, Y., Iwanishi, H., Hisaoka, T. and Senba, E. (2003). Expression pattern of the winged-helix/forkhead transcritpion factor FOXP1 in the central nervous system. *Gene Expression Patterns* **3:**193-197.

Tamura, S., Morikawa, Y., Iwanishi, H., Hisaoka, T. and Senba, E. (2004). Foxp1 gene expression in projection neurons of the mouse striatum. *Neuroscience* **124:**261-267.

Tang, B., Becanovic, K., Desplats, P. A., Spencer, B., Hill, A. M., Connolly, C., Masliah, E. *et al.* (2012). Forkhead box protein p1 is a transcriptional repressor of immune signaling in the CNS: implications for transcriptional dysregulation in Huntington disease. *Hum Mol Genet* **21:**3097-3111.

Tao, W. and Lai, E. (1992). Telencephalon-restricted expression of BF-1, a new member of the HNF-3/fork head gene family, in the developing rat brain. *Neuron* **8:**957-966.

Tate, M. C., Shear, D. A., Hoffman, S. W., Stein, D. G., Archer, D. R. and LaPlaca, M. C. (2002). Fibronectin promotes survival and migration of primary neural stem cells transplanted into the traumatically injured mouse brain. *Cell Transplant* **11:**283-295.

Teramitsu, I., Kudo, L. C., London, S. E., Geschwind, D. H. and White, S. A. (2004). Parallel FoxP1 and FoxP2 expression in songbird and human brain predicts functional interaction. *J Neurosci* **24:**3152-3163.

Thapar, A., Cooper, M., Eyre, O. and Langley, K. (2013). What have we learnt about the causes of ADHD? *J Child Psychol Psychiatry* **54:**3-16.

Theil, T., Alvarez-Bolado, G., Walter, A. and Ruther, U. (1999). Gli3 is required for Emx gene expression during dorsal telencephalon development. *Development* **126:**3561-3571.

Thomas, A., Burant, A., Bui, N., Graham, D., Yuva-Paylor, L. A. and Paylor, R. (2009). Marble burying reflects a repetitive and perseverative behavior more than novelty-induced anxiety. *Psychopharmacology (Berl)* **204:**361-373.

Thomson, J. A., Itskovitz-Eldor, J., Shapiro, S. S., Waknitz, M. A., Swiergiel, J. J., Marshall, V. S. and Jones, J. M. (1998). Embryonic stem cell lines derived from human blastocysts. *Science* **282:**1145-1147.

Tole, S., Ragsdale, C. W. and Grove, E. A. (2000). Dorsoventral patterning of the telencephalon is disrupted in the mouse mutant extra-toes(J). *Dev Biol* **217:**254-265.

Toresson, H. and Campbell, K. (2001). A role for Gsh1 in the developing striatum and olfactory bulb of Gsh2 mutant mice. *Development* **128:**4769-4780.

Toresson, H., Mata de Urquiza, A., Charlotta, F., Perlmann, T. and Campbel, l. K. (1999). Retinoids are produced by glia in the lateral ganglionic eminence and regulate striatal neuron differentiation. *Development* **126:**1317-1326.

Toresson, H., Potter, S. S. and Campbell, K. (2000). Genetic control of dorsal-ventral identity in the telencephalon: opposing roles for Pax6 and Gsh2. *Development* **127:**4361-4371.

Tripp, G. and Wickens, J. R. (2009). Neurobiology of ADHD. *Neuropharmacology* **57:**579-589.

Tronche, F., Kellendonk, C., Kretz, O., Gass, P., Anlag, K., Orban, P. C., Bock, R. *et al.* (1999). Disruption of the glucocorticoid receptor gene in the nervous system results in reduced anxiety. *Nat Genet* **23:**99-103.

Trueman, R. C., Dunnett, S. B., Jones, L. and Brooks, S. P. (2012a). Five choice serial reaction time performance in the HdhQ92 mouse model of Huntington's disease. *Brain Res Bull* **88:**163-170.

Trueman, R. C., Jones, L., Dunnett, S. B. and Brooks, S. P. (2012b). Early onset deficits on the delayed alternation task in the Hdh(Q92) knock-in mouse model of Huntington's disease. *Brain Res Bull* **88:**156-162.

Ueno, K., Togashi, H. and Yoshioka, M. (2003). [Behavioral and pharmacological studies of juvenile stroke-prone spontaneously hypertensive rats as an animal model of

attention-deficit/hyperactivity disorder]. *Nihon Shinkei Seishin Yakurigaku Zasshi* **23:**47-55.

Umehara, M., Ago, Y., Fujita, K., Hiramatsu, N., Takuma, K. and Matsuda, T. (2013). Effects of serotonin-norepinephrine reuptake inhibitors on locomotion and prefrontal monoamine release in spontaneously hypertensive rats. *Eur J Pharmacol* **702:**250-257.

Urban, N., Martin-Ibanez, R., Herranz, C., Esgleas, M., Crespo, E., Pardo, M., Crespo-Enriquez, I. *et al.* (2010). Nolz1 promotes striatal neurogenesis through the regulation of retinoic acid signaling. *Neural Dev* **5:**21.

Valerius, M. T., Li, H., Stock, J. L., Weinstein, M., Kaur, S., Singh, G. and Potter, S. S. (1995). Gsh-1: a novel murine homeobox gene expressed in the central nervous system. *Dev Dyn* **203:**337-351.

Van der Kooy, D. and Fishell, G. (1987). Neuronal birthdate underlies the development of striatal compartments. *Brain Res* **401:**155-161.

Verma, A. K., Shoemaker, A., Simsiman, R., Denning, M. and Zachman, R. D. (1992). Expression of retinoic acid nuclear receptors and tissue transglutaminase is altered in various tissues of rats fed a vitamin A-deficient diet. *J Nutr* **122:**2144-2152.

Walker, F. O. (2007). Huntington's disease. *Lancet* **369:**218-228.

Wang, B., Fallon, J. F. and Beachy, P. A. (2000). Hedgehog-regulated processing of Gli3 produces an anterior/posterior repressor gradient in the developing vertebrate limb. *Cell* **100:**423-434.

Wang, B., Lin, D., Li, C. and Tucker, P. (2003). Multiple domains define the expression and regulatory properties of Foxp1 forkhead transcriptional repressors. *J Biol Chem* **278:**24259-24268.

Wang, B., Waclaw, R. R., Allen, Z. J., 2nd, Guillemot, F. and Campbell, K. (2009). Ascl1 is a required downstream effector of Gsx gene function in the embryonic mouse telencephalon. *Neural Dev* **4:**5.

Wang, B., Weidenfeld, J., Lu, M., Maika, S., Kuziel, W., Morrisey, E. and Tucker, P. (2004a). Foxp1 regulates cardiac outflow tract, endocardial cushion morphogenesis and myocyte proliferation and maturation. *Development* **131:**4477-4487.

Wang, W. W., Cao, R., Rao, Z. R. and Chen, L. W. (2004b). Differential expression of NMDA and AMPA receptor subunits in DARPP-32-containing neurons of the cerebral cortex, hippocampus and neostriatum of rats. *Brain Res* **998:**174-183.

Watts, C., Brasted, P. J. and Dunnett, S. B. (2000a). Embryonic donor age and dissection influences striatal graft development and functional integration in a rodent model of Huntington's disease. *Exp Neurol* **163:**85-97.

Watts, C., Brasted, P. J. and Dunnett, S. B. (2000b). The morphology, integration, and functional efficacy of striatal grafts differ between cell suspensions and tissue pieces. *Cell Transplant* **9:**395-407.

Wichterle, H., Turnbull, D., Nery, S., Fishell, G. and Alvarez-BuyllA, A. (2001). In utero fate mapping reveals distinct migratory pathways and fates of neurons born in the mammalian basal forebrain. *Development ,* **128:**3759-3771.

Wilson, S., and Rubesntein JL,. (2000). Induction and dorsoventral patterning of the telencephelon. *Neuron* **28:**641-651.

Wilson, S. W. and Houart, C. (2004). Early steps in the development of the forebrain. *Dev Cell* **6:**167-181.

Wilson, S. W. and Rubenstein, J. L. (2000). Induction and dorsoventral patterning of the telencephalon. *Neuron* **28:**641-651.

Wlodarska, I., Veyt, E., De Paepe, P., Vandenberghe, P., Nooijen, P., Theate, I., Michaux, L. *et al.* (2005). FOXP1, a gene highly expressed in a subset of diffuse large B-cell lymphoma, is recurrently targeted by genomic aberrations. *Leukemia* **19:**1299-1305.

Wu, S., Esumi, S., Watanabe, K., Chen, J., Nakamura, K. C., Nakamura, K., Kometani, K. *et al.* (2011). Tangential migration and proliferation of intermediate progenitors of GABAergic neurons in the mouse telencephalon. *Development* **138:**2499-2509.

Xu, G., Green, C. C., Fromholt, S. E. and Borchelt, D. R. (2012). Reduction of low-density lipoprotein receptor-related protein (LRP1) in hippocampal neurons does not proportionately reduce, or otherwise alter, amyloid deposition in APPswe/PS1dE9 transgenic mice. *Alzheimers Res Ther* **4:**12.

Xu, Q., Wonders, C. P. and Anderson, S. A. (2005). Sonic hedgehog maintains the identity of cortical interneuron progenitors in the ventral telencephalon. *Development* **132:**4987-4998.

Xuan, S., Baptista, C. A., Balas, G., Tao, W., Soares, V. C. and Lai, E. (1995). Winged helix transcription factor BF-1 is essential for the development of the cerebral hemispheres. *Neuron* **14:**1141-1152.

Ye, W., Shimamura K, Rubenstein JLR, MA, H. and A, R. (1998). FGF and Shh Signals Control Dopaminergic and Serotonergic Cell Fate in the Anterior Neural Plate *Cell* **93:**755-766

Young, K. M., Fogarty, M., Kessaris, N. and Richardson, W. D. (2007). Subventricular zone stem cells are heterogeneous with respect to their embryonic origins and neurogenic fates in the adult olfactory bulb. *J Neurosci* **27:**8286-8296.

Yu, W., Wang, Y., McDonnell, K., Stephen, D. and Bai, C. B. (2009). Patterning of ventral telencephalon requires positive function of Gli transcription factors. *Dev Biol* **334:**264-275.

Yun, K., Fischman, S., Johnson, J., Hrabe de Angelis, M., Weinmaster, G. and Rubenstein, J. L. (2002). Modulation of the notch signaling by Mash1 and Dlx1/2 regulates sequential specification and differentiation of progenitor cell types in the subcortical telencephalon. *Development* **129:**5029-5040.

Yun, K., Garel, S., Fischman, S. and Rubenstein, J. L. (2003). Patterning of the lateral ganglionic eminence by the Gsh1 and Gsh2 homeobox genes regulates striatal and olfactory bulb histogenesis and the growth of axons through the basal ganglia. *J Comp Neurol* **461:**151-165.

Yun, K., Potter, S. and Rubenstein, J. L. (2001). Gsh2 and Pax6 play complementary roles in dorsoventral patterning of the mammalian telencephalon. *Development* **128:**193-205.

Zhang, Y., Li, S., Yuan, L., Tian, Y., Weidenfeld, J., Yang, J., Liu, F. *et al.* (2010). Foxp1 coordinates cardiomyocyte proliferation through both cell-autonomous and nonautonomous mechanisms. *Genes Dev* **24:**1746-1757.

Zhuo, L., Theis, M., Alvarez-Maya, I., Brenner, M., Willecke, K. and Messing, A. (2001). hGFAP-cre transgenic mice for manipulation of glial and neuronal function in vivo. *Genesis* **31:**85-94.

8 <u>*The Characterisation of Mef2c in the Developing Mouse Brain*</u>

8.1 <u>Summary</u>

Mef2c is a TF involved in muscle development and has shown to be expressed in both the developing and adult brain. Mef2c was shown to be significantly up-regulated in an Affymetrix screen that used mouse WGE to detect significant differences in gene expression over peak striatal development (E12-E16). Although Mef2c has been shown to be expressed in the brain previously the specific temporal and spatial pattern of its expression during striatal development is largely unknown. Therefore the initial aim of this Chapter was to characterise Mef2c during embryonic and early post-natal development at a mRNA level using in situ hybridisation and qPCR, and at a protein level using immunohistochemistry. Following WT characterisation the functional role of Mef2c in MSN development was attempted. However as homozygous Mef2c KO mice are embryonic lethal at E9.5 it was necessary to develop a Mef2c CKO mouse line. The CKO line was achieved by crossing a Mef2c$^{+/-}$ mouse with a Nestin-Cre line (Mef2c$^{+/-}$/Nestin) and subsequent breeding to a homozygous Mef2c$^{fl/fl}$ mouse.

Results showed that peak expression of Mef2c was between E18 and P0 and expression is restricted to post-mitotic neurons residing in the MZ of the developing striatum; neurons that will populate the matrix region of the adult striatum. Preliminary results from in vitro experiments using the Mef2c CKO suggest that that in the absence of Mef2c there are no differences in apoptosis, proliferation or the number of MSNs after 24 hours or 7 DIV. However, further experiments, derived from cultures at the same age and derived from later stages of striatal development, will need to be carried out to confirm initial results and to investigate if Mef2c has the same role at later stages of development.

8.2 **Introduction**

The TF *Mef2C* was found to be significantly up regulated during peak MSN development in the screen carried out in the host lab to find gene expression changes associated with MSN development (Precious et al., 2013 submitted). Thus this increased expression during MSN neurogenesis may suggest that, like *Foxp1*, *Mef2c* has a role in MSN development and differentiation. *Mef2c* is a member of the MADS domain family of TFs, which are involved in the development of many systems, notably muscle (Brand 1997), and although all Mef2 genes (*Mef2A-D*) are expressed in the developing CNS (Lyons *et al.* 1995), *Mef2c* is the first expressed, and the most studied Mef2c gene in the CNS.

Specifically *Mef2c* is expressed in the developing telencephalon from E11.5 (Leifer *et al.* 1993; Lyons *et al.* 1995) and by E14.5 *Mef2c* expression is apparent in the cortex, amygdala, hippocampus and midbrain (Lyons *et al.* 1995). *Mef2c* expression persists to adulthood in some regions, notably the cortex (Lyons *et al.* 1995). Additionally *Mef2c* has been detected in human foetuses at 14 weeks of gestation and is present throughout the cortical plate, specifically in cell nuclei (Leifer *et al.,* 1994), but there is limited, if any, MEF2C found in the human striatum at this age (Leifer *et al.,* 1994). In rodents *Mef2c* expression is associated with post mitotic neurons (Mao *et al.* 1999) and *in vitro* experiments have implicated *Mef2c* in neuronal differentiation, and as an anti-apoptotic factor during cortical and cerebellar development (Mao *et al.* 1999). Conversely, following birth, it has been reported that *Mef2c* acts as an apoptotic factor and acts to limit neuronal number (Liu *et al.* 2003). Recently it has also been shown that over-expressing MEF2C in hESC cultures significantly increases neuronal number (Cho *et al.* 2011), specifically increasing the number of DA neurons.

Owing to the embryonic lethality associated with homozygous *Mef2c* KO mice at E9.5, attributable to cardiac defects (Lin *et al.* 1997), the above mentioned functions of *Mef2c* in neuronal development were largely identified through *in vitro* analyses. Therefore to understand more about the functional role of *Mef2c in vivo, Mef2c* CKO mice were generated. Specifically, conditional deletion of *Mef2c* in the brains of mice using the hGFAP-Cre line showed a marked increase in the number of excitatory synapses, but significant impairments in hippocampal-dependent learning and memory (Barbosa *et al.*

2008). In a separate study loss of *Mef2c* using a *Nestin*-Cre line was shown to impair neuronal differentiation, be required in the correct development and organisation of cortical layers, as well as control normal synaptic activity in the cortex (Li *et al.* 2008). Collectively the *in vivo* data suggest that *Mef2c* has an important role in learning and memory and in synaptic plasticity. Triple *Mef2A, C* and *D* KO mice have recently been created and showed that all three genes can act redundantly in neuronal survival as post natal neuronal death was not apparent in individual *Mef2* KOs. However, it was also shown that only *Mef2c* was sufficient to ensure correct hippocampal synaptic function as when either *Mef2A* or *D* were knocked out there were no differences (Akhtar *et al.* 2012) which suggests *Mef2c* is particularly important in CNS development.

Although *Mef2c* is known to be expressed in the ventral telencephalon from E11 (Lyons *et al.* 1995), a thorough characterisation of Mef2c mRNA and protein throughout development has not been reported and thus this was the aim of the initial experiments outlined in this Chapter. This analysis allowed the expression pattern of *Mef2c* to be identified, and to observe if levels of *Mef2c* were reduced, maintained or increased throughout development. *In situ* hybridisation was undertaken to analyse the spatial distribution of mRNA expression from E12-P7 and expression analysis was supported with semi-quantitative PCR (qPCR). Immunohistochemistry was used as means of looking at the presence of MEF2C protein throughout development.

While functional roles for *Mef2c* have been shown in the cortex, cerebellum and hippocampus, as mentioned, no-one has looked at the expression pattern or function of *Mef2c* during striatal development and thus a conditional mouse model was developed to selectively KO *Mef2c* in the developing striatum. The *nestin*-Cre line (Tronche *et al.* 1999), which has been fully described in Chapters 1 and 5, was chosen to drive specific Cre expression and thus KO *Mef2c* in the developing striatum. Previous reports have shown successful cortical KO of *Mef2c* with this line when it was crossed to the same *Mef2c* KO mouse lines I am using (Li *et al.* 2008). *Mef2c* cortical loss has also been reported when the hGFAP-Cre was used (Barbosa *et al.* 2008). However, as shown extensively in Chapter 5, this Cre-line only knocked out *Foxp1* in the developing cortex and it was decided it was not suitable for knocking out *Mef2c* during striatal development.

The aim of this Chapter was to use the *Mef2c* CKO line to analyse differences in MSNs using specific markers throughout development, into adulthood and ultimately to dissect the functional importance of *Mef2c* in striatal differentiation. However, I have only recently established the *Mef2c* CKO line and maintained the colony, thus only limited results are presented here. However, results do serve as an indication of what effect the loss of *Mef2c* could have on MSN differentiation. Future work will aim to increase sample numbers in order to analyse MSN development in the absence of *Mef2c*.

8.3   <u>**Experimental Procedures**</u>

<u>***In situ* hybridisation**</u>

A biotinylated RNA probe was previously designed and made by Dr R.A Jeyasingham. Briefly, probes were generated from plasmids of the gene through PCR cloned into pCRIItopo vector (*Invitrogen*). Sense and antisense probes were generated by linearization with appropriate restriction enzymes then reverse transcribed with either SP6 or T7 polymerase (*Roche*) and labelled with DIG (*Roche*). Full details are outlined in Precious et al., 2013 submitted.

<u>**Preparation**</u>

Whole heads were removed as described in 2.2.1 from E12, E14, E16, E18, P0 and P7 mouse embryos and were snap frozen in iso-pentane on dry ice and stored at -80°C. The heads were then cut on the cryostat (30 μm) onto superfrost plus slides and were left to dry at 37°C and stored at -80°C.

<u>**Day 1**</u>

Slides were fixed in 4% PFA at RT for 20 minutes. Slides were then washed in 1 X PBS for 1 minute before carbethoxylation (0.1% Diethyl pyrocarbonate (DEPC) (*Sigma*) in 1 X PBS) was carried out for 10 minutes at RT. The slides were then washed again in 1 X PBS for 1 minute and then twice in 2 X SSC, each wash for 2 minutes (Appendix 4). Pre-hybridisation of the slides then took place in boxes lined with 50% formamide (*Fisher*) and 5 X SSC. 300μl of pre-hybridisation buffer (Appendix 4) was added per slide for 3 hours at 56ºC. Approximately 10 minutes before the end of the incubation period the probes were denatured for 5 minutes at 95°C and either the sense (control) or anti-sense probe (both 1:100) was added separately to 200 μl of hybridisation buffer on ice. The buffer-probe mix was then added to the individual slides and these were covered with parafilm and incubated O/N at 56°C in wetted boxes.

<u>**Day 2**</u>

Slides underwent the following washes at 56°C on a rocker, 5 X SSC for 2 minutes, 5 X SSC for 5 minutes, 2 X SSC for 5 minutes, 0.2 X SSC for 5 minutes, 50%

formamide/0.2 X SSC for 20 minutes, followed by 0.2 X SSC wash for 5 minutes at RT, and finally by 2 x 5 minute washes in 1 X TBS-T at RT. Next, slides were blocked in 3% milk solution (dried carnation milk powder) in 1 X TBS-T for 1 hour. During the blocking step, the antibody binding solution was prepared; anti-DIG-AP (*Roche*) (1:5000) was added to1 X blocking factor. Following blocking 500 µl of antibody solution was applied per slide. When blocking was complete the slides went through further washes at RT; 1 X TBS-T for 2 minutes and 1 X TBS-T for 15 minutes twice. Slides were then equilibrated in alkaline phosphatise (AP) buffer with $MgCl_2$ (2.5% MgCl/ml of AP) for 5 minutes at RT. During equilibration, the development solution was prepared. To 5 ml of AP buffer the colour solutions were added, 17 µl of NBT (100mg/ml) (Roche) and 18 µl of BCIP (50mg/ml) (Roche). 500 µl of this solution was added per slide, covered with parafilm and left to develop O/N at RT.

Day 3

Upon colour developing, slides were subjected to 2 washes in 1 X TE buffer for 10 minutes. Slides were then left to dry O/N and dehydrated through decreasing concentrations of ethanol (75%, 95% and 100%), 5 minutes per concentration. Slides were then placed in xylene and cover slipped using DPX mounting medium. Staining was visualised using a Leica DRMBE microscope. Analysis was qualitative to look at where and when expression took place.

qPCR

For cDNA synthesis please see Chapter 2.3. For the qPCR reactions the fluorescent probe SYBER Green (*Finzymes*) was used. For each cDNA sample analysed, 3 replicate wells were prepared with 1 µl of cDNA (diluted 1:20), 10 pmol of each of the oligo pairs (primers used in qPCR are outlined in Appendix 5), 10 µl SYBER green master-mix and water (*Sigma*) to give a final 20 µl volume. Opticom Monitor 3 software was used for qPCR analysis. For all primers amplification conditions used were 95˚C for 15 minutes followed by 40 cycles of 95˚C for 30 seconds, 60˚C for 30 seconds and 72˚C for 30 seconds on an Opticon 2 (MG research) machine. Melt curves were generated from readings every 0.5˚C between 53˚C and 95˚. Amplification of the target transcript sequence was quantified using relative quantification, where the ratio between the Ct

value of the target transcript and that of GAPDH was determined using the $2^{-\Delta\Delta}C_{\mathrm{T}}$ Method (Livak and Schmittgen, 2002).

Breeding Strategy of the *Mef2c* CKO Line

To establish the line, initial breeding pairs were set up to generate *Mef2c$^{+/-}$/Nestin$^{+/-}$* mice. Subsequent to this, time mating's were set up between *Mef2c$^{+/-}$/Nestin$^{+/-}$* positive mice and homozygous *Mef2c* floxed mice (*Mef2c$^{fl/fl}$*) (a gift from Professor Olson) to ensure thorough genetic knock down. Females were checked daily for a vaginal plug, the day of plug discovery was recorded as E0. Pregnant dams were sacrificed at E14 and embryos were dissected from the uterine horn as outlined in Chapter 2. Embryos were either snap frozen for use in immunohistochemistry or individual striate were dissected and individually cultured. Due to time restraints for this line, animals were genotyped at Laragen, California using the tail biopsies taken during dissections.

Cell culture

Primary Cell Suspensions

For WT analysis individual striatae from CD1 E14 pups were dissected, pooled and then cultured. For *Mef2c* CKO experiments each pair of striate from E14 pups were cultured separately. For both experiments the cells were triturated to produce single cell suspensions and cell counts were performed as described fully in Chapter 2. Cells were plated down at a density of 100,000 per coverslip and fixed with fresh 4% PFA following 24 hours, or 7 DIV.

Immunocytochemistry

Fluorescent immunocytochemistry was undertaken according to the protocol detailed in Chapter 2. Primary antibodies used were anti-NESTIN (1:400), anti-BRDU (1:200) anti-FOXP1 (1:500), anti-CTIP2 (1:500), anti TUJ1 (1:2000), anti-GFAP (1:2000) anti DARPP-32 (S.Cruz) (1:200) and anti MEF2C (1:4000) (gift from McrDermott lab) (for full antibody details see Appendix 2).

Proliferation Assays

BrdU was added to the cells the day before fixation at a concentration of 2 µg/µl. Immunohistochemistry was carried out according to the protocol outlined in Chapter 2.

Statistical Analysis

Statistical analysis was performed using a one-factor ANOVA with Tukey-Kramer *post-hoc* comparisons when appropriate. The alpha level for significant F-ratios was set at 0.05 for all analyses.

8.4 **Results**

The WT expression pattern of *Mef2c* between E12 and P0

In situ hybridisation was carried out on coronal mouse brain sections from E12-P7, the left hemisphere was used as the control (using a sense probe) and the right hemisphere had the *Mef2c* specific probe applied to it. Results showed that at E12 there was limited *Mef2c* expression in the MGE and LGE of the developing striatum (Figure 8.1A). At E14 expression was evident in the MZ of the striatum and no staining was shown in the proliferative VZ or SVZ (Figure 8.1B). At E16 *Mef2c* expression was apparent in the MZ, and by E18 the same spatial expression pattern was evident but was stronger (Figure 8.1C, D). Expression was apparent along a dorso-medial to ventral-lateral gradient. At P0 *Mef2c* was still expressed in the MZ but expression was weaker than that at E18, and by P7 expression had decreased further (Figure 8.1E-F). In addition to striatal expression *Mef2C* was expressed in the developing cortex from E14 through to P7 where expression was clearly seen in all cortical layers, but strongest expression was apparent in the outer layers (Figure 8.1).
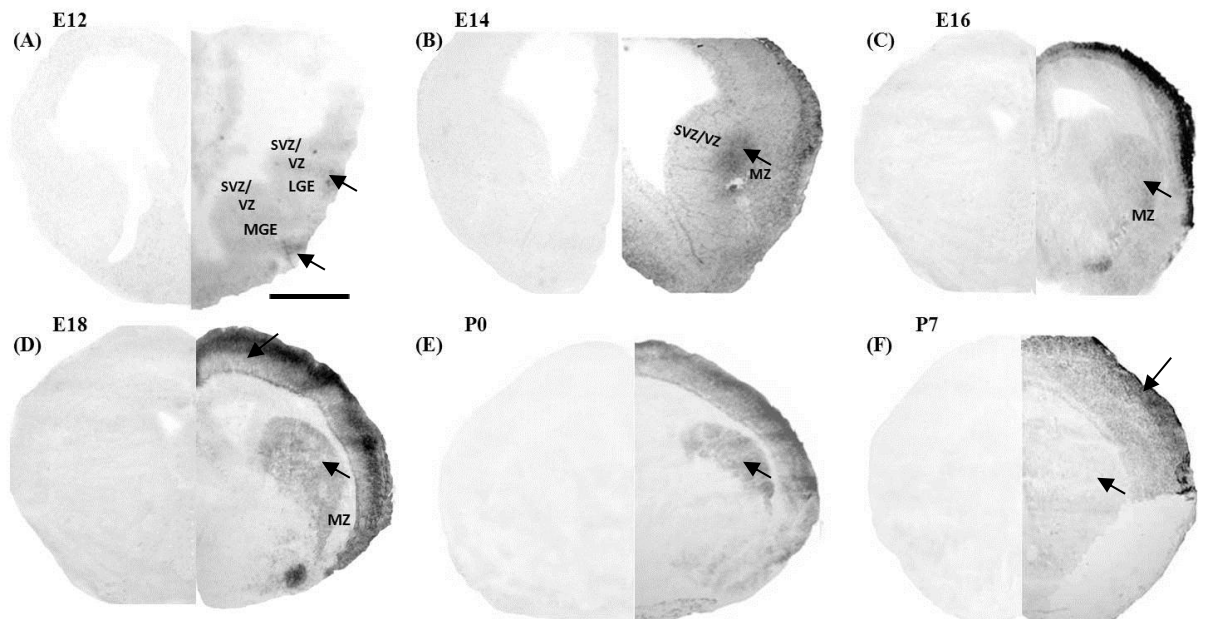

Figure 8.1 mRNA analysis of *Mef2c* using *in situ* hybridisation in WT brains from E12-P7. The left hemisphere is the control hemisphere (sense probe added) and the right hemisphere is the experimental hemisphere (had the specific probe added) **(A)** At E12 there is weak *Mef2c* expression in the MGE and LGE. **(B)** At E14 *Mef2c* expression is shown in the MZ and not in the SVZ or VZ. **(C)** At E16 expression is seen throughout the MZ. **(D)** At E18 *Mef2c* is expressed strongly in the MZ. **(E-F)** Post natally *Mef2*c expression begins to decrease compared to staining at E18. Arrows identify regions of expression *Scale bar =500μM.*

qPCR analysis of *Mef2c* in WT brains

To complement the mRNA expression levels apparent in the *in situ* hybridisation qPCR analysis was carried out using cDNA generated from E12-P7 striatal tissue of WT embryos/pups. After normalisation to the house keeling gene GAPDH results showed that there was a significant increase in *Mef2c* expression across development ($F_{5,\ 17}$ = 6.60, p<0.01) (Figure 8.2). *Post Hoc* tests showed that there was a significant difference in *Mef2c* expression from E12-E18, and from E12-P0 (P< 0.05, 0.01 respectively), and between E14 and P0, and E16 and P0 (P≤0.01, p<0.05, respectively).
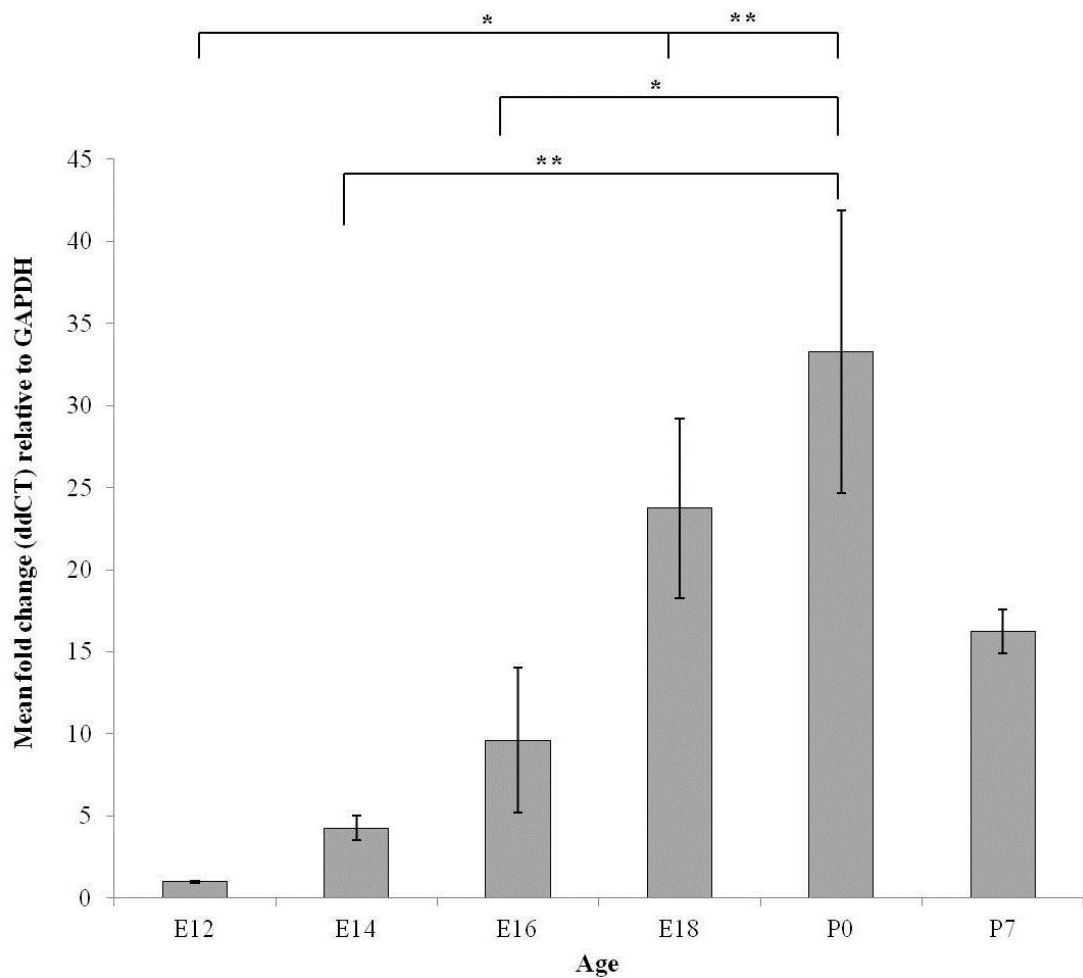

Figure 8.2 Expression of *Mef2c* was analysed using semi quantitative RT-PCR on cDNA prepared from WT striatal tissue from E12-P7 embryos/pups. Gene expression shown is relative to GAPDH. Each bar on the graph represents a mean of 3 different samples. *Significant post hoc tests are indicated with brackets (* p<0.05, **≤0.01.)*

The expression of MEF2C from E12 to adulthood

To analyse the presence and distribution of MEF2C protein during development, immunohistochemistry was undertaken on coronal mouse brain sections from E12-P7 and staining was retrieved using DAB where relative intensity of staining was assessed subjectively and validated by additional assessors, but quantification was not performed. At E12 there was no detectable protein in the striatum (Figure 8.3A), but starting at E14 through to P0, MEF2C staining became more intense in the MZ of the striatum with levels peaking at P0 (Figure 8.3B-E). At P7 MEF2C intensity in the striatum was reduced compared to E16, E18 and P0. MEF2C was also evident in the cortex from E12 and expression continued throughout development (Figure 8.3A-F). MEF2C protein was also assessed in the adult striatum and cortex. There was no MEF2C staining in the adult striatum (Figure 8.3Gi,ii) but strong expression was evident in the adult cortex, with the strongest staining seen in the outer layers (Figure 8.3Giii).
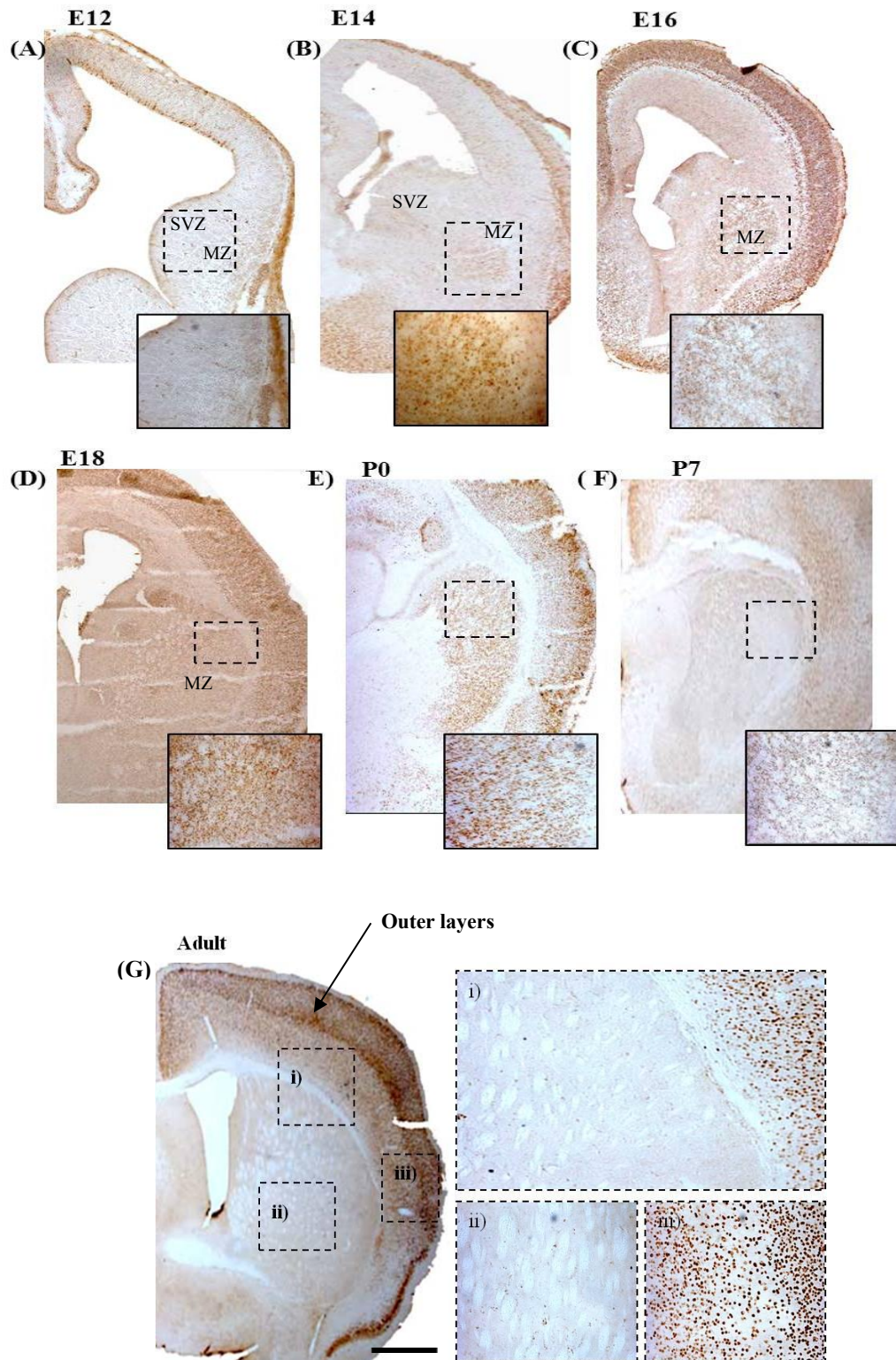
Figure 8.3 Immunohistochemistry showing MEF2C in WT brains from E12-Adult.(A) At E12 there is no MEF2C evident in the developing striatum. **(B-E)** From E14-P7 MEF2C levels increased in the striatum and expression was highest at P7. **(F)** MEF2C levels in the striatum were reduced compared to E16 onwards. **(G)(i, ii)** There was no MEF2C in the adult striatum. **(G) (iii)** MEF2C expression remained in the adult cortex with highest levels evident in the outer layers, indicated with arrows. The dotted boxes indicated staining in the striatum. Abbreviations, SVZ= Sub ventricular zone, MZ= Mantle zone *Scale bars: = 500µm, high power images= 50 µm.*

It was hoped lineage analysis of MEF2C co-localisation with DARPP-32 and CTIP2 could be carried out as was the case for FOXP1 staining in Chapter 3. Unfortunately when using a commercial Mef2c antibody no MEF2C staining was obtained despite using several different fluorescent protocols, both in the host lab or in the lab of Professor Canals at the University of Barcelona with the exception of one age, P3 (Figure 8.4). Thus co-localisation of MEF2C with striatal markers throughout MSN development could not be performed in this instance. In the developing striatum patch neurons are born before matrix neurons and subsequently will mature, and be recognisable by the neuronal marker NEUN earlier (Martin-Ibanez *et al.* 2012). Therefore at late developmental/early postnatal ages it is likely NEUN is identifying the earlier born patch neurons only. Results showed that at P3 MEF2C did not co-localise with NEUN (Figure 8.4) suggesting MEF2C is associated with later born matrix neurons at this time point.
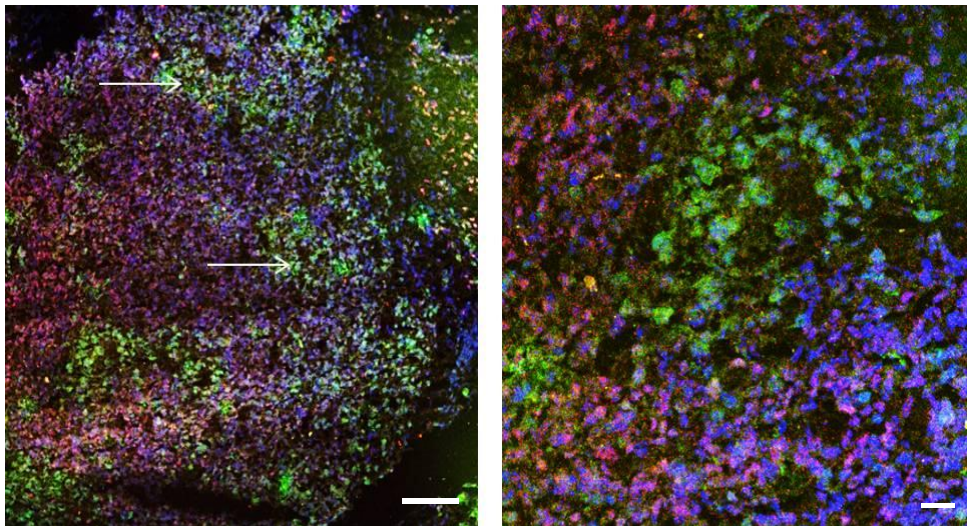

Figure 8.4 Photomicrographs showing MEF2C (Red) and NEUN (Green) and the nuclear marker DAPI at P3. These two stains do not co-localise. Arrows show examples of NEUN selectively staining the patches in the striatum at this age. *Scale bars = 50μm and 20 μm at the higher magnification.*

***In vitro* analysis of MEF2C in WT striatal differentiation cultures after 7 DIV**

As cell culture is a useful tool for analysing differences in MSNs in the absence of *Mef2c* (presented later) it was important to understand what type of cell *Mef2c* co-localised with in WT animals. As discussed previously, the commercial Mef2c antibody would not work in fluorescent protocols. However a small aliquot of an "in house" developed antibody was acquired as a gift from the McDermott lab and was used in the subsequent fluorescent immunocytochemistry. Following 7 DIV MEF2C co-localised with the neuronal marker TUJ1 but not the neuronal precursor marker NESTIN or the astrocyte marker GFAP (Figure 8.5).
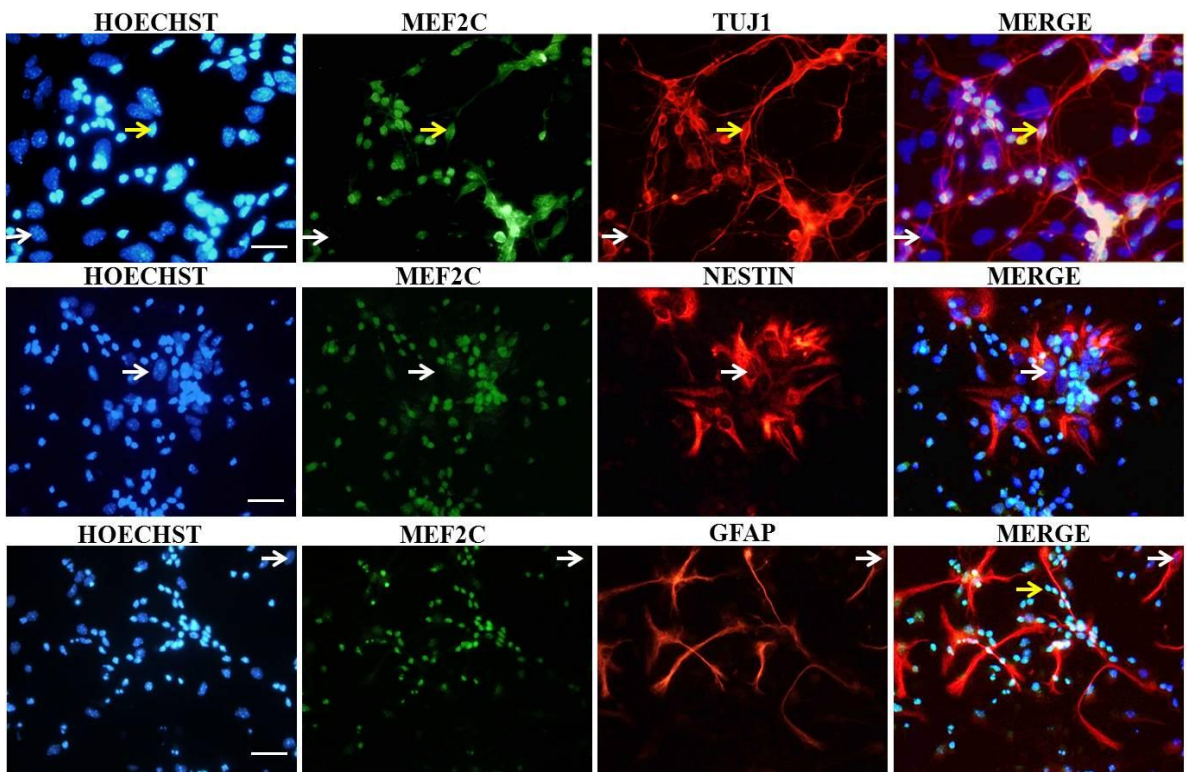

Figure 8.5 *In vitro* analysis of MEF2C after 7 DIV. WT E14 mouse WGE cultures were left to differentiate for 7 DIV. Following fixation cells were double labelled for MEF2C (Green) and either TUJ1, NESTIN or GFAP (Red) and the nuclear stain Hoechst (Blue). The fourth column is a merged image of the first three photomicrographs. Yellow arrows indicate where MEF2C co-localises with TUJ1. White arrows indicate where MEF2C does not co-localise with NESTIN or GFAP and shows there are TUJ1postive/MEF2C negative neurons. *Scale bars = 50μm.*

In vitro **analysis of striatal differentiation cultures derived from Mef2c CKO embryos**

Pairs of E14 striate (WGE) from individual pups of WT and Nestin/*Mef2c*$^{+/-}$/*Mef2c*$^{+/fl}$ (*Mef2c* CKO) mice were separately cultured in differentiation medium (1% FCS, 2% BSA) for either 24 hours, or 7 DIV, and were then stained with the neuronal marker TUJ1, and the MSN specific markers CTIP2, DARPP-32 and FOXP1.

<u>**24 hour analyses**</u>

After 24 hours there were no differences in the total number of Hoechst positive cells between the groups (Mean; WT = 456±19, *Mef2c* CKO 463±290) ($F_{1, 18}$ = 0.37, p=n.s.). There was no difference in the total number of FOXP1 (WT, 19±2.36, *Mef2c* CKO 19±2.65) or TUJ1 (WT, 61±3.72; *Mef2c* CKO 64±0.41) positive neurons between the two genotypes ($F_{1, 7}$ =0.001, 0.71 respectively, p=n.s.) Figure 8.6. Representative photomicrographs are shown in Figure 8.7. Similarly there were no differences in the number of FOXP1 cells when calculated as a percentage of total TUJ1 positive cells after 24 hours (WT, 26±3.45, *Mef2c* CKO 27±3.70 ($F_{1, 7}$ = 0.77, p=n.s.) (data not shown). There was no significant difference in the number of CTIP2 positive cells between the groups (WT, 68±6.27; *Mef2c* CKO 82±3.21) ($F_{1, 5}$ =1.21, p=n.s.) (Figure 8.6). As expected, at this very early differentiation time point, there was no DARPP-32 staining in cultures from either group. Representative photomicrographs are shown in Figure 8.7.
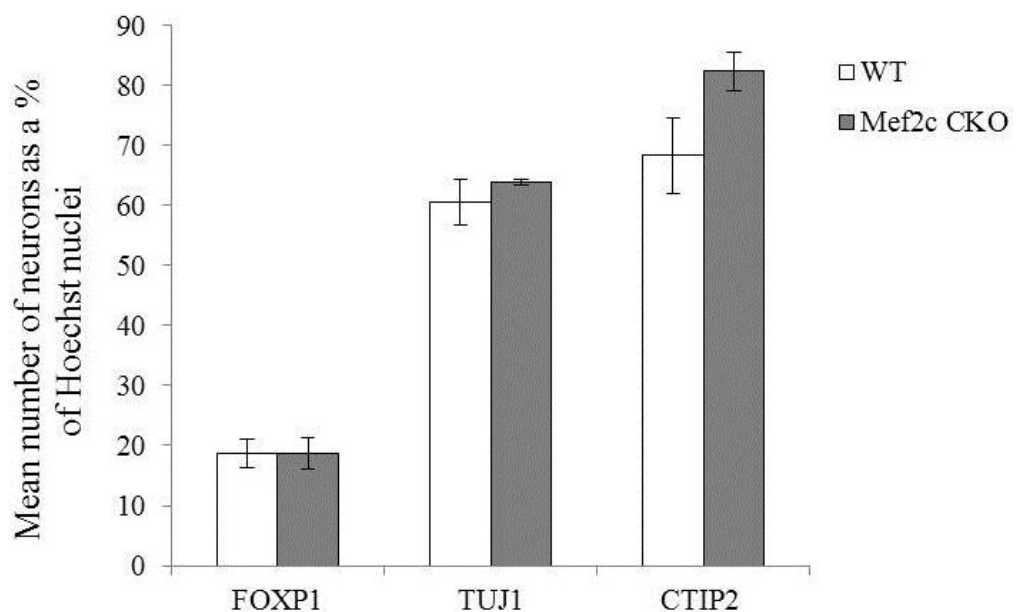
Figure 8.6 *In vitro* cell counts at 24hours. Cultures were generated and cultured individually from WT and *Mef2c* CKO striate and fixed after 24 hours *in vitro.* **(A)** FOXP1, TUJ1 and CTIP positive cells were counted and are represented as a percentage of total Hoechst positive nuclei. Each bar on the graph represents a mean of at least 2 different cultures. *Error bars are SEM*

Figure 8.7 *(overleaf) In vitro* analysis at 24 hours. E14 mouse WGE cultures from both genotypes were plated down and left to differentiate for 24 hours *in vitro.* Following fixation cells were labelled for **(A)** FOXP1 (Red) and TUJ1 (Green) or **(B)** CTIP2 (Red) and DARPP-32 (Green) and the nuclear stain Hoechst (Blue). The fourth column is a merged image of FOXP1, TUJ1 and Hoechst. Arrows represent examples of co-localised cells. *Scale bars = 50μm.*
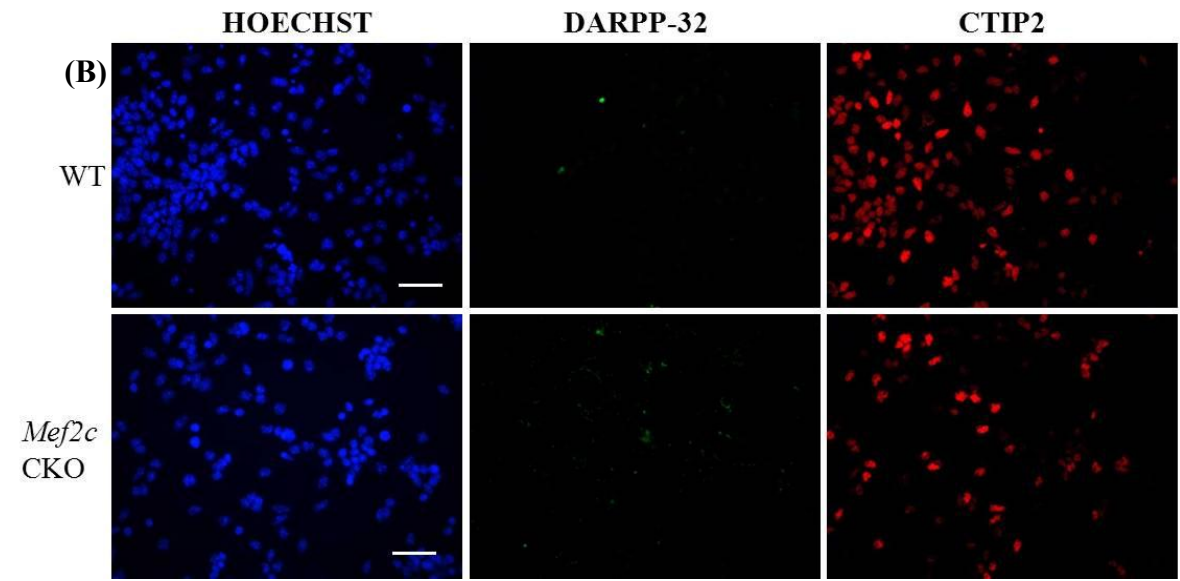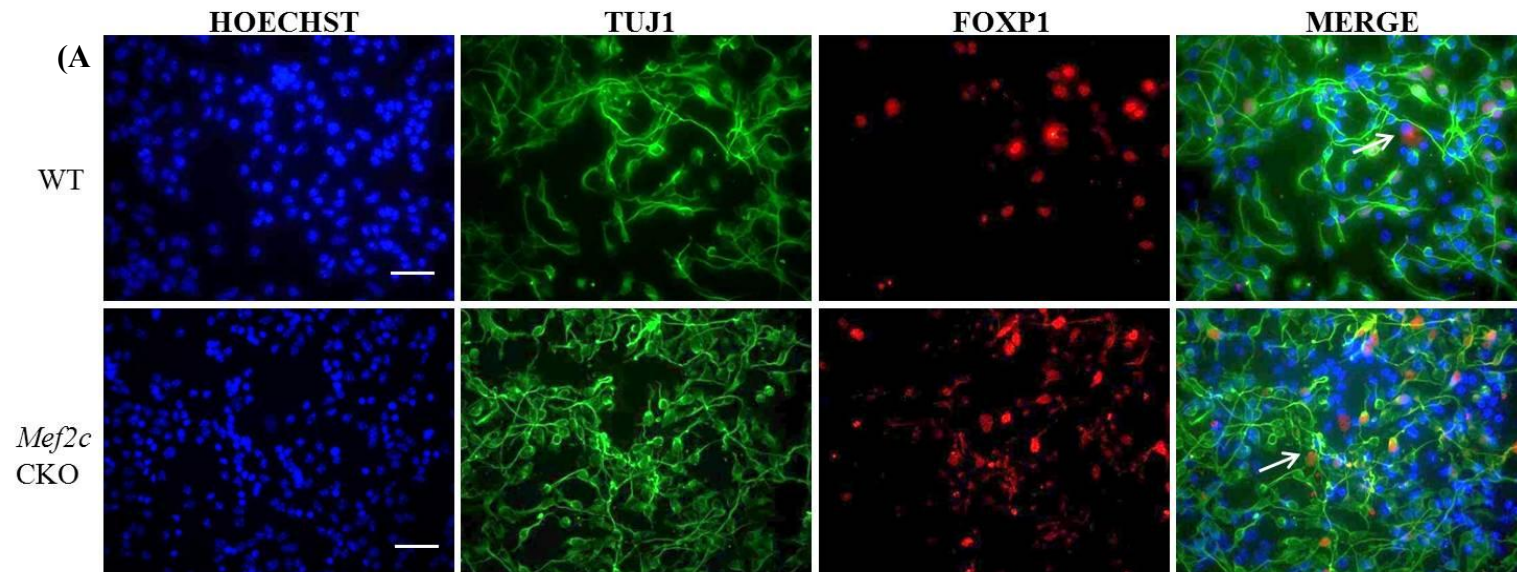
7 DIV Analyses

There were no differences after 7 DIV in the number of total Hoechst positive nuclei between the groups ($F_{1, 13}$ = 2.27, p=n.s.). There was no difference in the number of FOXP1 (WT, 36±1.84; *Mef2c* CKO 35±2.69), or TUJ1 (WT, 65±1.27; *Mef2c* CKO 51±1.58) positive cells between the genotypes ($F_{1\ 3}$ = 0.00, 2.63, respectively, p =n.s.) (Figure 8.8). Representative photomicrographs of the cultures are shown in Figure 8.9A. There were no significant genotypic difference in the number of FOXP1 positive cells when calculated as a percentage of total TUJ1 positive cells ($F_{1,\ 3}$= 0.471, p= n.s.) (data not shown). DARPP-32 staining was seen but there were no differences as a percentage of total Hoechst positive cells between the two groups (WT, 8± 1.09; *Mef2c* CKO, 9±1.84) ($F_{1,\ 9}$ = 0.77, p= n.s.) (Figure 8.8). Representative photomicrographs of the cultures are shown in Figure 8.9B. Additionally after 24 hours or after 7 DIV there were no obvious differences in neuronal morphology as determined by TUJ1 or signs of cell death, identifiable by fragmented nuclei in the Hoechst staining, in the absence of *Mef2c*.
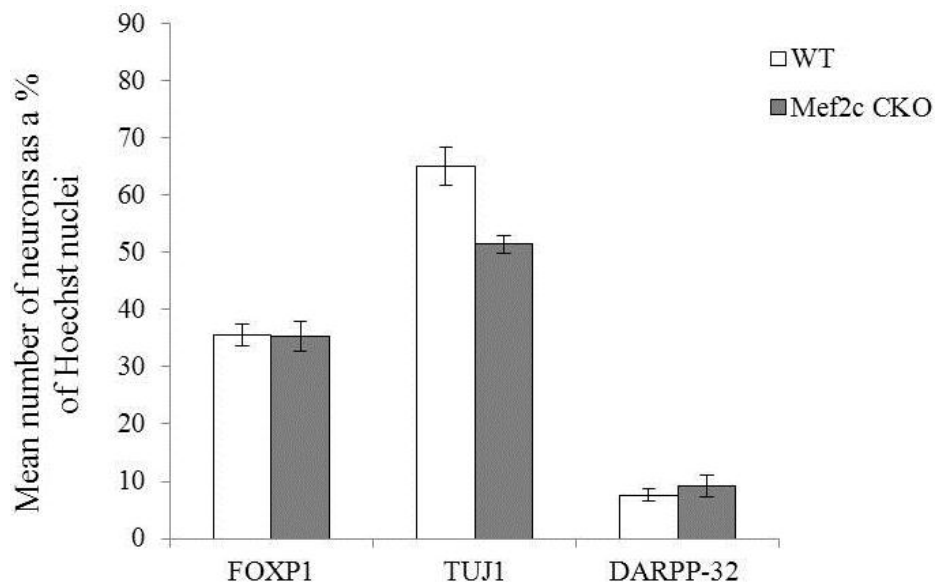
Figure 8.8 *In vitro* **cell counts at 7 DIV.** Cultures were generated and cultured individually from WT and *Mef2c* CKO striate and fixed after 7 DIV. **(A)** FOXP1, TUJ1, and DARPP-32 positive cells were counted and are represented as a percentage of total Hoechst positive nuclei. Each bar on the graph represents a mean of at least 2 different cultures. *Error bars are SEM.*
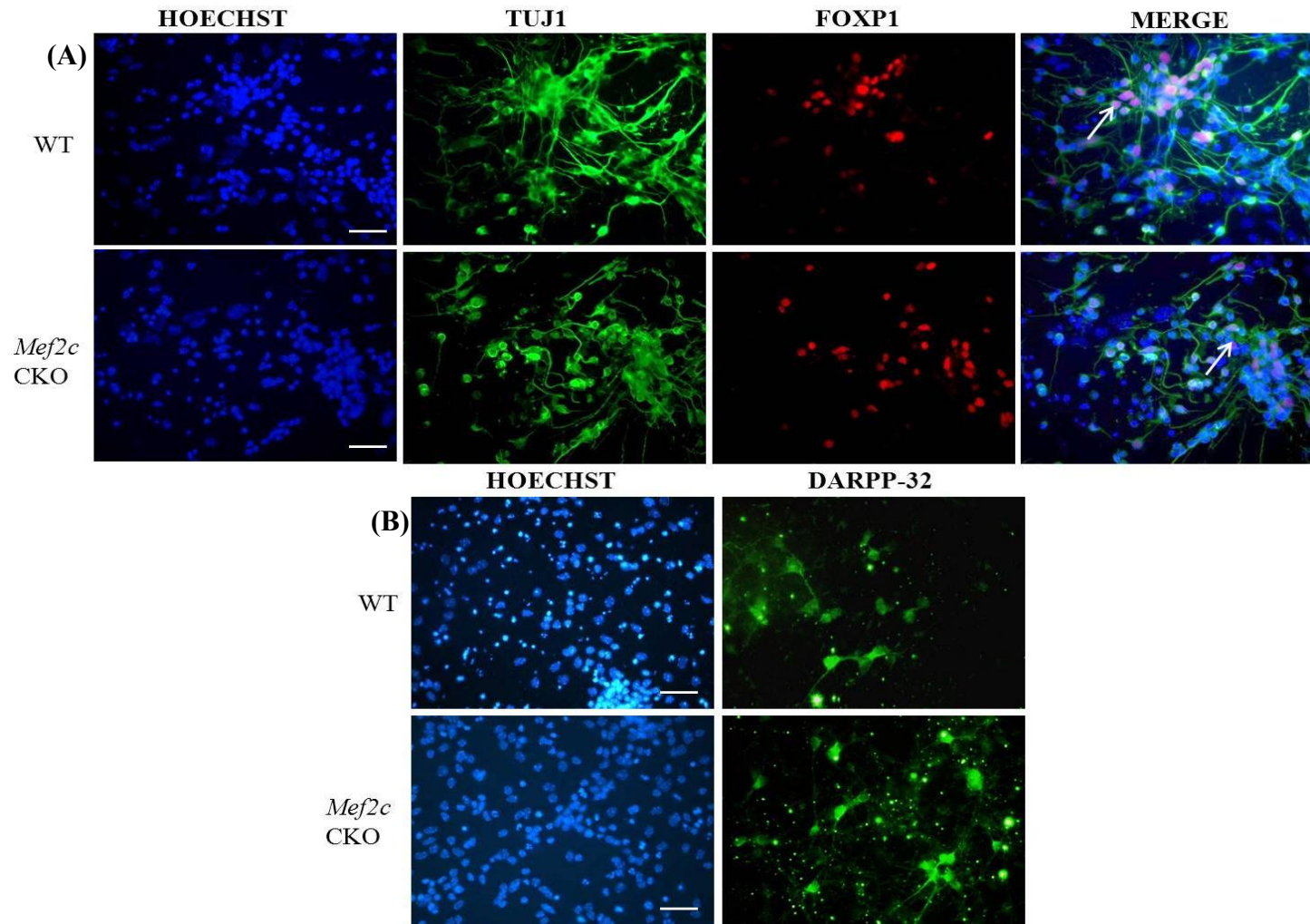
Figure 8.9 *In vitro* analysis at 7 DIV. E14 mouse WGE cultures from both genotypes were plated down and left to differentiate. Following fixation cells were **(A)** Double labelled for FOXP1 (Red) and TUJ1 (Green) and the nuclear stain Hoechst. The fourth column is a merged image of the first three photomicrographs **(B)** Single stained for DARPP-32 (Green) and the nuclear stain Hoechst (Blue). Arrows represent examples of co-localised cells. *Scale bars = 50μm.*

Does the absence of Mef2c effect proliferation in the developing striatum?

BrdU was added to the differentiation media 24 hours before fixation. After 24 hours there was no difference in the number of TUJ1 positive cells ($F_{1, 13}$= 0.47, p=n.s.) or the number of BrdU positive cells ($F_{1, 13}$= 1.18, p=n.s.) as a percentage of Hoechst positive nuclei (Figure 8.10A). When analysed at 7 DIV there was again no significant difference between the number of TUJ1 cells as a percentage of Hoechst positive nuclei ($F_{1, 14}$ = 0.69, p=n.s.), or between the numbers of BRDU positive cells as a percentage of Hoechst between genotypes ($F_{1, 14}$ =2.14, p= n.s.) (Figure 8.10B). BRDU positive cells were not seen to co-localize with TUJ1 positive cells at 24 hours or 7 DIV and only limited co-localisation was seen with GFAP (1%; data not shown) and thus further experiments are needed to determine what these proliferating cells are co-localising with. Representative photomicrographs are shown in Figure 8.10C and D.
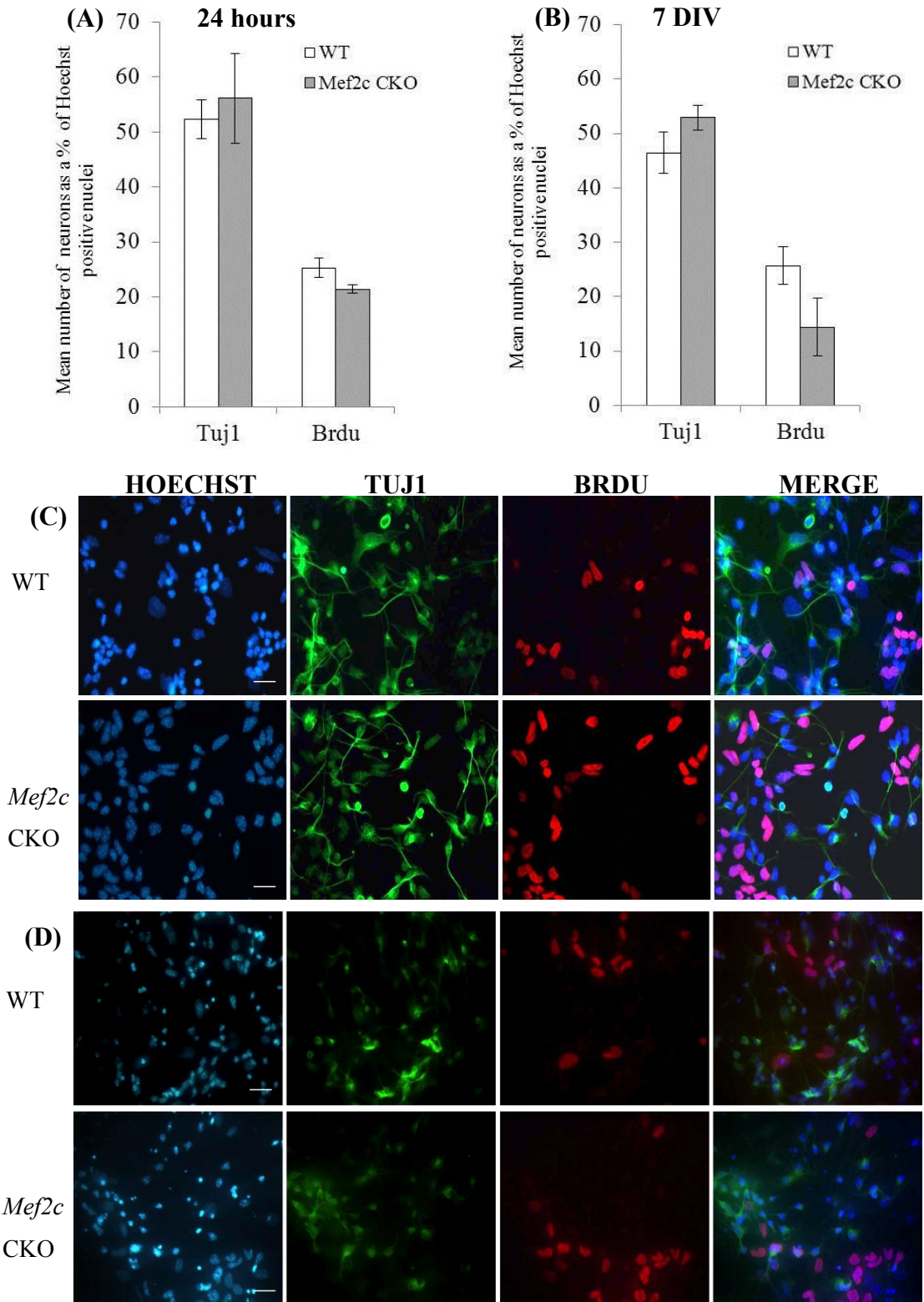
Figure 8.10 (A and B) TUJ1 and BRDU positive cells were counted and are represented as a percentage of total Hoechst positive nuclei after 24 hours and 7 DIV respectively. Each bar on the graph represents a mean of at least 3 different cultures. *Error bars are SEM*. **(C and D)** Representative photomicrographs of cultures that were double labelled for BRDU (Red) and TUJ1 (Green) and the nuclear stain Hoechst (Blue) after 24 hours and 7 DIV respectively. The fourth column is a merged image of the first three photomicrographs. *Scale bars = 50μm.*

8.5 **Discussion**

Mef2c has a peak window of expression during striatal development

In vertebrates, all MEF2 isoforms are expressed at variable levels in distinct but overlapping patterns in the embryonic and adult CNS (Lyons *et al.* 1995). It is known that the temporal and spatial expression pattern of the *Mef2* genes changes during embryogenesis, specifically increasing during neuronal maturation and withdraw from the cell cycle (Schulz *et al.* 1996). *Mef2c* expression has been studied in some areas of the CNS but specific expression during striatal development has not. Thus *in situ* hybridisation and immunohistochemistry was used to characterise the presence of Mef2c mRNA and protein respective*ly,* in WT mice during development.

At E12.5 small patches of *Mef2c* expression were apparent along the lateral edge of the developing LGE and MGE, but expression was weak and there was no protein evident at this stage, likely because translation of mRNA is not always immediate (Ferland *et al.* 2003). In the MZ of the developing striatum at E14 and E16 there was a gradual increase in mRNA expression, and also in the intensity of the immunohistochemical signal suggesting an increase in protein, there was no staining apparent in the proliferative VZ or SVZ. These results are consistent with what was shown by previously by our lab (Vinh *et al.,* unpublished). Between E18 and P0 MEF2C mRNA expression and corresponding immunohistochemical staining increased with a strong signal in the striatal MZ coinciding with neuronal maturation (Schulz *et al.* 1996). qPCR confirmed that there was a significant increase in expression at E18 and P0 compared to E12, and a significant increase from E14 and E16 compared to P0. However, these results could not confirm the spatial expression of *Mef2c* shown in the *in situ* hybridisation. These results suggest that between E18 and P0 there is a peak window of *Mef2c* expression in the developing striatum as by P7 expression has started to decrease and in the adult striatum it is no longer evident. These results are consistent with *Mef2c* peak expression during cortical neurogenesis in the rat. Peak expression was evident in the cortical plate between E18 and E21, the area associated with post-mitotic, differentiating neurons with no expression evident in the VZ (Mao *et al.* 1999) .

***Mef2c* expression is coincident with the second wave of neurogenesis in the developing striatum**

There are two waves of peak neurogenesis in striatal development. Striatal neurons born between E12 and E13 populate the patches (Mason *et al.* 2005), whereas those born later, between E13-E16, reside in the matrix of the adult striatum (Mason *et al.* 2005; Van der Kooy and Fishell 1987). It is believed that the neurons that populate the patch and matrix transiently mix in the MZ of the striatum, and it is not until E18, through differential gene expression, that segregation is apparent (Mason *et al.* 2005). Therefore the later, peak expression of *Mef2c* could suggest that it is associated with matrix, rather than patch born neurons. However although I have shown that MEF2C co-localises with neurons (Fig 6.5), I was unable to show whether MEF2C co-stained with MSN markers or, if it co-stained with interneurons, and thus further immunohistochemistry needs to be carried out to answer these questions.

Between E16 and P0 *Mef2c* expression was apparent along a dorso-medial to vental-lateral gradient, similar to that of the TF *Ikaros,* a modulator of cell cycle exit for a subset of neuronal precursor cells that promotes neurogenesis of Enkephelin positive, matrix neurons (Martin-Ibanez *et al.* 2012). Ikaros is expressed from E14.5, peaks at E18.5 and has disappeared by P15, comparable to what we have shown for *Mef2c* expression. Additionally like *Mef2, Ikaro*s is expressed in neurons of the MZ, does not co-localise with Nestin or GFAP and is not expressed in the VZ or SVZ of the developing striatum (Martin-Ibanez *et al.* 2012). Furthermore we have shown that the complementary pattern of expression between MEF2C and NEUN (which has shown to be used as a patch marker at P3 (Martin-Ibanez *et al.* 2012)) is comparable to the expression pattern shown by IKAROS and DARPP-32 at E18 (which has shown to be used as a patch marker at E18 (Martın-Ibanez *et al.* 2010)). Taken together these results are consistent with *Mef2c* being associated in the development of matrix born neurons and the possibility of *Mef2c* and *Ikaros* functioning in the same genetic pathways implicated in later born striatal neurons.

Dlx1/2 are two genes also associated with the development of later born striatal neurons (Anderson et al., 1997, Yun et al., 2002) and in the *Dlx1/2* double knock-out mouse, expression of both *Mef2c* and *Ikaros* was lost from the MZ of the striatum (Long *et al.* 2009). Moreover when *Mef2c* is knocked out from multipotent progenitors derived from

hematopoietic stem cells, lymphocytes do not develop properly and the expression of *Ikaros*, which is essential in lymphoid development, is decreased (Stehling-Sun *et al.* 2009). However, when *Ikaros* was knocked out in the same multipotent progenitor cells *Mef2c* expression was maintained (Stehling-Sun *et al.* 2009), suggesting that *Mef2c* is functioning upstream of *Ikaros.* It was attempted to look at differences in MEF2C in the *Ikaros*^-/- coronal brain sections. However as discussed earlier, despite using several different fluorescent protocols the commercial Mef2c antibody would not routinely work on sections, with the exception of at P3 for unknown reasons. Nevertheless, if the role of *Mef2c* and *Ikaros* in lymphocyte development is similar in striatal neurogenesis it is possible that no differences would have been seen in *Mef2c* expression in the *Ikaros*^-/- brain sections had the protocol worked (although the experiment will be repeated). An important experiment, and one I will perform, will be to look at differences in Ikaros in the developing striatum of the *Mef2c* CKO line.

No differences in cell death or proliferation were seen following the loss of *Mef2c* in E14 cultures

The *Mef2c* CKO line differed to the *Foxp1* CKO line as it had one null *Mef2c* allele, and one allele conditionally knocked out using the Nestin-Cre line, comparable to the *Mef2c* CKO generated by Li and colleagues (Li *et al.* 2008). I have undertaken only limited *in vitro* experiments on *Mef2c* function. *Mef2c* has strongly been implicated as an anti-apoptotic factor during embryonic development (Mao *et al.* 1999; Okamoto *et al.* 2000) and thus differences in cell death, looking at differences in fragmented nuclei using Hoechst were looked for in cultures. Preliminary data showed that there were no obvious differences in cell death between WT and *Mef2c* CKO mice in E14 differentiation cultures, consistent with previous experiments previously reported (Mao *et al.* 1999). Specifically, when a dominant negative (DN) plasmid (a plasmid that expressed a dominant negative version of the *Mef2c* gene) was added to rat E14 primary cortical cultures to reduce MEF2C levels, there were no differences in apoptosis. However when these *in vitro* experiments were carried out at a later age i.e. E17, there were increases in apoptosis as determined by the number of fragmented nuclei and disintegrated cell bodies (Mao *et al.* 1999). These results suggest *Mef2c* does not have an anti-apoptotic role until later in development when levels are higher (Mao *et al.* 1999). BrdU incorporation also showed no differences in proliferation at 24 hours or 7 DIV, suggesting that *Mef2c* is operating at later stages of MSN development once the

cells have excited the cell cycle and completed mitosis. This is in agreement with cultured cortical neurons (Mao *et al.* 1999) which did not co-loclasie with Nestin or BrdU. Future work will need to include more specific apoptotic tests such as TUNEL analysis and in addition to repeating analyses at E14, culturing cells at later developmental time points, such as E16 or E18 which may be more representative of *Mef2c* function in striatal development.

Similar to the discussed work in cortical neurons *in vitro* experiments using DN plasmids to knock-down *Mef2c* expression in WT E14 striatal cultures was trialled during the course of this thesis. However, as discussed in Chapter 4, and shown in Appendix 7, successful transfection of plasmids into primary striatal cells that would allow comparisons on a population rather than of single cell basis was attempted using several strategies without success. Unfortunately the transfection method or efficiency was not disclosed in the work carried out by Mao et al and therefore comparisons in methods could not be made. Thus, knocking down/out *Mef2c* depended upon the generation of *Mef2c* CKO mice.

The loss of *Mef2c* in E14 striatal cultures did not affect the number of cells positively staining for MSN markers

The number of MSNs in cultures generated from E14 WT and *Mef2c* CKO mice was assessed using the markers CTIP2 and DARPP-32. In addition, building on the results in Chapters 3 and 4, FOXP1 was also used and considered as a new and robust marker of MSNs. Preliminary results show that there were no differences in the number of MSNs after 24 hours or 7 DIV although no results were obtained for CTIP2 at 7 DIV. Increased sample numbers are needed to validate these results and cultures generated from later born striatal neurons (E16 or E18), when *Mef2c* expression has shown to peak may give a more accurate representation *Mef2c* function.

It has been shown that *Mef2c* can form heterodimers with the bHLH factors *Ascl1* and E-12, to synergistically regulate target gene expression, and thus transcription in neuronal cells (Black et al., 1996; Black et al., 2000). It was shown that at a protein level both *Mef2c* and *Ascl1* can activate each other and only one of these TFs needs to bind directly to DNA to regulate gene expression (Black et al., 1996). As *Ascl1* is needed to control the differentiation of at least one lineage of MSNs, it is possible that

Mef2c is also working up or downstream of this gene, in addition to *Ikaros* in conjunction with other genes, in later aspects MSN development.

8.6   **Conclusion**

WT expression of *Mef2c* during striatal development is apparent from E12, peaks between E18 and P0 and by adulthood is lost in the mouse striatum but retained in the cortex. This peak in expression corresponds with that of the TF *Ikaros*, which is implicated in promoting neurogenesis in the later born matrix neurons. Additionally, at P3 MEF2C does not co-localise with NEUN, which at this time is a marker of patch neurons, further suggesting that *Mef2c* is associated with post-mitotic matrix neurons. Preliminary data from the *Mef2c* CKO mice suggests that there are no differences in apoptosis, proliferation or MSN number in the absence of *Mef2c,* but an increase in the number of biological replicates is needed to confirm this. Moreover as results presented in this Chapter have suggested that peak *Mef2c* expression in the developing striatum is apparent later than E14, it is likely that striatal cultures will need to be generated from embryos at later time points i.e. E16 or E18, to obtain more specific and representative results of the role of *Mef2c* in striatal development.

9 *Appendices*

9.1 **Appendix 1**

Cell Culture Solutions

PLL:

1mg/kg dissolved in distilled 0.1 % DEPC H_2O

Trypsin Solution:

Mix 0.1% Trypsin with 0.05% DNase in HBSS.

DNase solution:

Mix 0.05% DNase into Hanks Balanced Solution (HBSS)

Differentiation Media:

Basic DMEM-12 with the addition of 1% Foetal calf serum (FCS) and 2% B27

4% PFA:

For 50ml, 5.4ml of Paraformaldehyde and 2.5 ml of 20X PBS made up in with 0.1 % DEPC H_2O

Immunocytochemistry Solutions

20X Phosphate Buffered Saline (PBS) (pH 7.4):

Sodium Chloride- 160g

*Potassium Chloride-*4g,

Di-hydrogen sodium phosphate (NaH_2PO_4) - 28.84g,

Di-sodium hydrogen phosphate (Na_2HPO_4) - 4.14 g

Distilled Water – Up to 1L *(+ 0.01% DEPC (diethyl pyrocarbonate); over night on stirrer; autoclave for 45 min at 120 °C if used for in situ Hybridisation)*

(Dilute in distilled water for 10X and 1X PBS)

PBS- T

1X PBSTriton- Add 0.5% Triton[*] and let dissolve on a shaker. (* advisable to make in a glass bottle even if only small amounts needed)

Appendix 1- Immunocytochemistry Antibodies

Primary Antibody	Species	Supplier	Dilution	Secondary Antibody	Protocol
FOXP1	Mouse	Abcam-	1:500	Goat-Anti mouse	Protocol B
β111-Tubulin (Tuj1)	Mouse	Sigma	1:2000	Goat-Anti mouse	Protocol A/B
		Sigma	1:2000	Goat Anti-rabbit	
NESTIN	Mouse	BD Pharm	1:400	Goat-Anti mouse	Protocol A
GFAP	Rabbit	DAKO	1:2000	Goat-Anti rabbit	Protocol A
CTIP2	Rat	Abcam	1:200	Goat-Anti rat	Protocol A/B
DARPP-32	Rabbit	Santa Cruz	1:200	Goat-Anti rabbit	Protocol B
BrdU	Rat	Oxford Bio	1:200	Goat-Anti rat	Protocol C
Mef2c	Rabbit	Gift from McDermott (USA)	1:4000	Goat-Anti rabbit	Protocol A

AlexFluor 594 was preferred for Anti-rat and AlexFluor 488 was preferred for Anti rabbit

9.2 <u>**Appendix 2**</u>

Soltuion	Supplier	Concentration
Extracellular Solution **(ECM)**	NA	NaCl – 135mM KCl - 5mM HEPES - 5mM Glucose -10mM $MgCl_2$ 1.2mM $CaCl_2$ 1.25mM
N-Methyl-D-aspartic acid **(NMDA)**	Sigma	Stock:100 mM in H2O Dose used 50μM
γ-Aminobutyric acid **(GABA)**	Sigma	Stock 300 mM in H2O Dose used 50μM
α-Amino-3-hydroxy-5 methylisoxazole-4-propionic acid hydrate **(AMPA):**	Sigma	Stock:10 mM in H2O Dose used 50μM
Kainic acid monohydrate **(Kainate):**	Sigma	Stock:10 mM in H2O Dose used 50μM

d

9.3 **Appendix 3**

Immunohistochemistry –Embryonic Sections

Citrate Buffer (pH6)

Citric Acid (Sigma) - 1.92g

Distilled Water - Up to 1000ml and then add 1 ml of Tween20 (Sigma),

PBS- T

1X PBS

Triton - Add either 0.1 or 0.3% Triton[*] and let dissolve on a shaker.

(* advisable to make in a glass bottle even if only small amounts needed)

Appendix 3 Antibodies used on embryonic mouse sections

Primary Antibody	Species	Supplier	Normal Serum	Dilution	Secondary Antiboy	Dilution
FOXP1	Mouse	Abcam	Horse Horse	1:500	Horse-Anti mouse Goat-Anti mouse (α488/ α594)	1:200 1:200
FOXP1	Rabbit	Abcam	Goat Goat	1:4000	Goat-Anti Rabbit Goat-Anti Rabbit (α488/ α594)	1:200 1:200
MEF2C	Goat	Santa Cruz	Horse	1:1000	Horse-Anti Goat	1:200
CTIP2	Rat	Abcam	Goat	1:500	Goat-Anti Rat Goat-Anti Rat (α594)	1:200 1:200
DARPP-32	Mouse Mouse	Santa Cruz BD transduction Lab	Goat	1:200	Goat-Anti Rabbit (α594/ α 488) Goat-Anti Mouse (α 488)	1:200 1:500
NEUN	Mouse	Abcam	Goat	1:200	Goat-Anti Mouse (α 594)	1:200

9.4 **Appendix 4**

Molecular Solutions

***In situ* Solutions**

20X SSC (pH 7)

Sodium Chloride -175g ,

Tri-sodium citrate dehydrate - 88.3g

0.01% DEPC Water – Up to 1L (O/N on stirrer at RT; autoclave for 45 min 120 °C)

10x TE   (pH8) 1 litre

Tris-base – 12.1g

EDTA - 3.72g

0.01% DEPC Water – Up to 1L

50x Denhardt solution

1 %   Ficoll

1 %   BSA (non-acetylated)

1 %   PVP (polyvinylpyrrolidone)

Pre-hybridisation/hybridisation buffer

50% Formamide,

 0.25% yeast total RNA/ml,

0.5% herring sperm DNA/m,

2.5% 5XSSC/ml,

1% / ml of 5X Denhardts/ml in 10ml of distilled water

Genotyping

Lysis Buffer (50ml)

10% Tris HCL (pH8.4) (*Fisher*),

1% 0.5M EDTA (*Sigma*),

4% 5M NaCl (*Fisher*),

1% SDS (20%) (*Sigma*),

2.5 % PK (20mg/ml) (*Roche*)

In distilled water

20 X TAE (500ml)

121 g Tris Base

285.5 ml HCL

50 ml EDTA (pH8)

9.5 **Appendix 5**

Process	Primers	PCR cycle/programme	Other notes.
cDNA Synthesis	Random Primers (Invitrogen)	65˚C for 5 mins (Q65-5) Chill on ice ~ 2mins 25˚C for 2 mins (Q25-2) 25˚C for 10 minutes 42 C for 50 minutes 70˚C for 15 minutes	Dilute the cNDA to 1:20 dilution,take 20ul and add 30ul of water
GAPDH RT-PCR	TCCACCACCCTGTTGCTGTA ACCACAGTCCATGCCATCAC	**PCR machine programme name Q55-25** Master Mix: 1.5 mM Mg ; Initial Denaturation- 95ºC- 1 minute **Cycle Denaturation - 95ºC for 45 seconds** **Annealing temp- 60˚C for 1 minute** **Extension time- 72 ºC 1 minute** Final extension of 72 ºC for 1 minute Cycle Number-32 3% Agarose Gel	100bp ladder, 1% gel
Foxp1-RT-PCR	GCAGCAGCTCTGGAAAGAAG GCAGACTTGGAGAGGGTGAC	**PCR machine programme name Q60-32** Master Mix: 1.5 mM Mg ; Initial Denaturation- 95ºC- 1 minute **Cycle Denaturation - 95ºC for 45 seconds** **Annealing temp- 60˚C for 1 minute** **Extension time- 72 ºC 1 minute** Final extension of 72 ºC for 1 minute Cycle Number-32 3% Agarose Gel	

Name	Primers (Genotyping)	PCR cycle/programme
12F 10R (recognise floxed allele)	(F)CCA GGG ATC AGA GAT TAC TGT AGC (R)CAC CCT CTC CAA GTC TGC CTC AG	**PRC machine programme name: Q60-32** Master Mix: 1.5 mM Mg Initial Denaturation- 95ºC- 1 minute **Cycle Denaturation - 95ºC for 45 seconds** **Annealing temp- 60˚C** **Extension time- 1 minute** Cycle Number-32 3% Agarose Gel
BIN10 BIN12 (to recognise WT allele)	(F)CCT CTG GCG ATG AAC CTA GTG GTT C (R)AGC CAC ACT TTC TCT CAG GAT GTC C	**PRC machine programme name Q60-35** Master Mix: 1.5 mM Mg **Initial Denaturation- 95ºC- 1 minute** **Cycle Denaturation - 95ºC for 45 seconds** **Annealing temp - 60˚C** Extension time- 30 sec Cycle Number -35 3% Agarose gel
BIN1 B1N10	AGC GCA TGC TCC AGA CTG CCT TG As above	As above
hGFAP	(F) ACT CCT TCA TAA AGC CCT (R) ATC ACT CGT TGC ATC GAC CG	**PRC machine programme name h31-35** Master Mix: 1.5 mM Mg **Initial Denaturation- 95ºC- 1 minute** **Cycle Denaturation - 95ºC for 45 seconds** **Annealing temp- 51** Extension time – 1 minute Cycle number – 35 3% Agarose gel

| Nestin | GCG GTC TGG CAG TAA AAA CTA TC
GTG AAA CAG CAT TGC TGT CAC T

CTA GGC CAC AGA ATT GAA AGA TCT
GTA GGT GGA AAT TCT AGC ATC ATC C | **PRC machine programme nameQ51-35**
Master Mix: 2.0mM MgCl2
Initial Denaturation- 95ºC- 1 minute
Cycle Denaturation - 95ºC for 45 seconds
Annealing temp- 51.7
Extension time – 1 minute
Cycle number 35 |

1 qPCR reaction		**PCR conditions**
10ul of master mix 1ul primer A 1 ul of primer B 7ul water 1ul cDNA (put in first) **20ul total**		Initial Denaturation- 95ºC- 15 minutes Cycle Denaturation - 95ºC for 30 seconds Annealing temp- 60˚C for 30 seconds Extension time- 72 ºC 30 seconds Cycle Number-40
qPCR Primer	**Forward Sequence**	**Reverse Sequence**
Mef2c	AGGACAAGGAATGGGAGGAT	GCAGTGTTGAAGCCAGACAG
GAPDH	GTTCCTACCCCCAATGTGTC	CTGCTTCACCACCTTCTTGA

9.6 **Appendix 6-**

Perfusion and Immunohistochemistry

Prewash Buffer (1L)

Di-sodium hydrogen phosphate (Na_2HPO_4) - 18g

Sodium Chloride -9g

Distilled Water -Up to 1L

pH to 7.3 with orthophosphoric acid

Fixative (1% Paraformaedehyde) 1L)

PFA- 15g (weighed out in fume hood)

Up to 1L with pre-wash buffer

Heat for ~ 3 hours to dissolve on stirrer (do not let boil)

 pH, to pH 7.3 with sodium hydroxide/orthophosphoric acid

Sucrose (pH7.3)

Sucrose **-**25g

TBS **-** make up to 1000ml

TBS-T 10X solution:

Tris-Hydrochloric Acid – 100 ml

Sodium Chloride- 87.7g

Tween 20 - 10ml

Distilled water – Up to a 1L

Anti-Freeze (800ml)

Di-hydrogen sodium phosphate (NaH_2PO_4) – 1.256

Di-sodium hydrogen phosphate (Na_2HPO_4) - 4.36

Distilled Water – Up to 320 ml

Dissolve fully and then add 240 ml ethylene glycol (Sigma E-9129) and 240ml Glycerol (Sigma G-7893)

TBZ

0.02% Sodium Azide in 1 X TBS

Cresyl Violet

Cresyl Violet Acetate (*Sigma*)- 7g

Sodium Acetate (anhydrous)- 5g

Distilled water- up to 600ml

Acid Alcohol

Add 5 ml of Glacial Acetic Acid to 200ml of 95% alcohol

4X Tris Buffered Saline (TBS)

TRIS base – 96g

Sodium Chloride – 72g

Distilled Water – Up to 1000ml

Adjust to pH7.4 with conc HCL (~50ml)

Working solution is 250 ml of 4X + 750 ml of distilled water, check pH

TxTBS

Add 0.2% Triton to TBS

Once dissolved pH to 7.4 with HCl

TNS (pH7.4)

Trizma Base (Sigma) – 6g

Distilled water- Up to 1L,
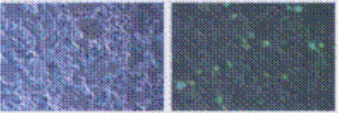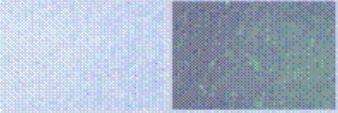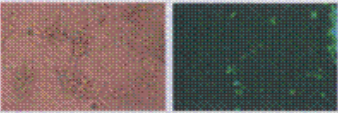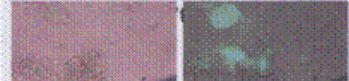

DAB

DAB (5%) – 2ml

TNS - 40ml

H_2O_2 - 12 µl

Appendix 6 (Cont.) Antibodies used for Immunohistochemistry in adult brains (Free-Floating sections)

Primary Antibody	Species in which antibody was raised	Manufacturer	Normal Serum	Dilution	Secondary Antibody	Dilution
FOXP1	Mouse	Abcam	Horse Horse	1:500	Horse-Anti mouse Goat-Anti mouse (α488/ α594)	1:200 1:200
FOXP1	Rabbit	Abcam	Goat Goat	1:4000	Goat-Anti Rabbit Goat-Anti Rabbit (α488/ α594)	1:200 1:200
Mef2c	Goat	Santa Cruz	Horse	1:1000	Horse-Anti Goat	1:200
CTIP2	Rat	Abcam	Goat	1:200	Goat-Anti Rat	1:200 1:200
DARPP-32	Mouse	Cornell University	Goat	1:10000	Horse Anti-Mouse	1:200
FOXP2	Rabbit	Abcam	Goat	1:500	Goat-Anti mouse (α488/ α594)	1:200
NeuN	Mouse	Abcam	Horse	1:2000	Horse-Anti mouse	1:200
Trb1	Rabbit	Abcam	Goat	1:500	Goat Anti Rabbit	1:200

9.7   **Appendix 7**

Transfection type	Transfection efficiency	Clumping	Cell death for control	Comments
Normal	NA	Only when there are high cell densities > 100,000	A few straight after that havn't sat down, < 1%	NA
Lipofectamine (1:3 ratio) ★ Best ratio	AV- 29% (with YFP)	Doesn't occur when plate down 100,000	In the optimum conditions get cell death after ~ 72hrs	The toxicity is the factor that is the problem but again it is fine up to 72 hrs.
Neon Transfection (1500,10,3)	Av- 22% (with YFP)	Only if excessive cell numbers used. > 100,000	Variable- The majority of the time the cells had to be fixed ~ 4 DIV due to infection problems causing cell death, however on some other times was ok.	Perhaps worth trying in paralell with the Nanofection if they are getting the siRNA for us as I have more experience now? However, a lot of optimisation would be required (concentrations etc) and when we tried the small amount from Alun Davies lab there was no expression.
Nanofection	Av ≤10% (after retransfection)	A lot of clumping when there were 120,000 cells but none with 60,000 cells.	Cell death afer ~ 48 hours in the best transfected conditons. In the poorest transfection condtions there was much better viabilty. However, At 2 weeks when looked at the cells	Try the siRNA, 2 different flurophores to see if transfecting 2 things makes a difference to the cell death. Also need to look at 7 days to see if the GFP is neuronal by then or is just in the cytoplasm.